UNIVERSIDADE DE BRASÍLIA

INSTITUTO DE CIÊNCIAS BIOLÓGICAS

DEPARTAMENTO DE BIOLOGIA CELULAR

PÓS-GRADUAÇÃO EM BIOLOGIA MOLECULAR

Integrando o silenciamento gênico dos efetores *Minc03328* e *Minc16803* à superexpressão da proteína *Germin-like protein 10*: Potencial abordagem para o controle de *Meloidogyne incognita*

Valdeir Junio Vaz Moreira

Brasília – Distrito Federal

Novembro de 2024

Autor - Valdeir Moreira da exposição científica-artística intitulada "BIOTRÓFICOS". Exposição composta por imagens de microscopia de campo ótico de galhas induzidas pelo fitonematoide *Meloidogyne incognita* em raízes de soja. A exibição, que tem como objetivo a divulgação da ciência, foi submetida ao XIII Prêmio Fotografia-Ciência & Arte (2024) promovida pelo Conselho Nacional de Desenvolvimento Científico e Tecnológico (CNPq).

UNIVERSIDADE DE BRASÍLIA

INSTITUTO DE CIÊNCIAS BIOLÓGICAS

DEPARTAMENTO DE BIOLOGIA CELULAR

PÓS-GRADUAÇÃO EM BIOLOGIA MOLECULAR

Integrando o silenciamento gênico dos efetores *Minc03328* e *Minc16803* à superexpressão da proteína *Germin-like protein 10*: Potencial abordagem para o controle de *Meloidogyne incognita*

Valdeir Junio Vaz Moreira

Orientadora: Prof[a]. Dr[a]. Maria Fátima Grossi de Sá

Tese apresentada ao Programa de Pós-Graduação em Biologia Molecular como requisito para obtenção do grau de Doutor em Biologia Molecular.

Orientadora: Dra. Maria Fátima Grossi de Sá
Coorientadora: Dra. Janice de Almeida Engler

Brasília – Distrito Federal

Novembro de 2024

BANCA EXAMINADORA

Dr. Antônio Vargas de Oliveira Figueira

Universidade de São Paulo (USP)

Dra. Elizabeth Pacheco Batista Fontes

Universidade Federal de Viçosa (UFV)

Dr. Elibio Leopoldo Rech Filho

Universidade de Brasília (UnB)

Dra. Maria Fátima Grossi de Sá (Orientadora)

Embrapa Recursos Genéticos e Biotecnologia (CENARGEN)

Dra. Maria Cristina Mattar da Silva (Suplente)

Embrapa Recursos Genéticos e Biotecnologia (CENARGEN)

Brasília – Distrito Federal

Novembro de 2024

Aos meus amados pais, Ângela Vaz e João Moreira,
às minhas irmãs, Geralda Aparecida e Vileide Moreira,
e aos meus queridos sobrinhos, Aylla e Ayllon,

DEDICO.

AGRADECIMENTOS

A Deus, por Seu infinito amor, graça e bondade, que me capacitaram e sustentaram até aqui.

Aos meus pais, Ângela Vaz e João Moreira, pelo apoio emocional incondicional durante toda a minha caminhada, pelos conselhos sábios e pela constante presença em minha vida.

À minha orientadora, Fátima Grossi, pela orientação firme e confiança depositada em mim. Pelos ensinamentos preciosos e pelas inúmeras oportunidades de aprendizado oferecidas ao longo dos sete anos que passei em seu grupo de pesquisa. Agradeço pela chance de desenvolver este projeto e por me permitir dar os primeiros passos na ciência em seu laboratório.

À minha coorientadora, Janice Engler, pela generosidade em compartilhar seu conhecimento e por sua disposição em auxiliar-me nas análises de microscopia essenciais para este trabalho. Meu sincero agradecimento também à Dra. Diana Fernandez (IRD-França), por me abrir as portas para a ciência em nível internacional.

Às instituições Embrapa Recursos Genéticos e Biotecnologia e à Universidade de Brasília, por fornecerem a infraestrutura e a oportunidade indispensáveis para a execução deste trabalho.

Aos colegas do Laboratório de Interação Molecular Planta-Praga I (LIMPP-I), que compartilharam comigo essa jornada da pós-graduação. Um agradecimento especial à Daniela Pinheiro, cuja parceria tornou essa caminhada mais leve e prazerosa.

Aos relatores desta tese, “Rachel” Sampaio e Cristina Mattar, pela análise criteriosa e contribuições valiosas.

Aos membros internos e externos do Programa de Biologia Molecular — Dra. Alice Nagata, Dra. Angela Mehta, Dr. Marcelo Brígido, Dr. Antônio Figueira, Dr. Elíbio Rech e Dra. Elizabeth Fontes — pelos valiosos *inputs* científicos, que contribuíram significativamente para tornar esta obra ainda mais completa.

À comissão de acompanhamento, Dr. Georgios Pappas e Dr. João Alexandre, pela orientação ao longo do percurso.

Aos funcionários do Prédio da Biotecnologia, especialmente Darcilene e Dona Isabel, por sua dedicação e apoio nos momentos necessários.

Às agências de fomento CAPES-COFECUB (Sv.622/18), CNPq, FAP-DF e INCT PlantStress Biotech, pelo financiamento que tornou possível o desenvolvimento deste projeto de pesquisa.

E, por fim, a todos aqueles que torceram por mim ao longo desta jornada e que, de forma direta ou indireta, contribuíram para a realização deste trabalho. Meu sincero agradecimento a todos.

ÍNDICE

RESUMO

O gênero *Meloidogyne* (NEMATODA: HETERODERIDAE) consiste em 98 espécies sendo o nematoide *Meloidogyne incognita* o maior representante patogênico endêmico nas Américas. Sua atividade cosmopolita de interação com múltiplas plantas é atualmente justificada no uso de proteínas efetoras para a indução de sítios de alimentação em hospedeiros compatíveis resultando na perda da produtividade de importantes culturas no campo. Entender as bases desse sinergismo direciona para uma nova perspectiva centrada nos aspectos da intervenção gênica via RNA de interferência (RNAi) contra transcritos envolvidos na tradução dessas proteínas, além da prospecção de genes associadas à resistência de hospedeiros incompatíveis ser também utilizada como segunda medida visando à evolução de plantas superiores. Neste presente trabalho, dividido em quatro capítulos, identificamos os genes efetores *Minc03328* e *Minc16803* de *M. incognita* e o gene *Germin-like protein subfamily 1 member 10* do genótipo de soja PI 595099 como candidatos promissores para engenharia genética de resistência em plantas. Por meio do novo levantamento bibliográfico elaborado no capítulo 1 desta tese, concluímos os papéis-chave de efetores de *M. incognita* majoritariamente voltados para inibição de redes imunes de plantas bem como na formação e manutenção de células gigantes. Esse indicativo pode ser novamente constatado com a seleção dos alvos efetores *Minc03328* e *Minc16803*, onde seus silenciamentos – via RNAi – foram capazes de reduzir a susceptibilidade de linhagens transgênicas de *Arabidopsis thaliana*. O resultado de nossas análises culminou na publicação de dois artigos, integrando os Capítulos 2 e 3 deste documento. O capítulo final deste trabalho integra um terceiro elemento validado denominado *Germin-like protein subfamily 1 member 10*, sendo o seu envolvimento na resistência contra *M. incognita* confirmado de forma heteróloga em planta modelo. Dentre outras análises, certificamos um modo de atuação extrínseco para sua resistência sendo o incremento da sua atividade na geração de peróxido de hidrogênio mensurados a níveis transcricionais para importantes marcadores gênicos relacionados às vias de fitormônios e respostas de hipersensibilidade. Esses dados contribuem para uma nova medida adotada na proteção de soja contra nematoides, sendo a piramidação gênica dos elementos aqui validados, a estratégia delineada na salvaguarda desse e outros importantes cultivos de relevância agronômica.

PALAVRAS-CHAVE: *Meloidogyne incognita*, RNA de interferência, genes efetores, Germin-like protein, proteção *in planta*.

ABSTRACT

The genus *Meloidogyne* (NEMATODA: HETERODERIDAE) comprises 98 species, with *Meloidogyne incognita* being the most prominent endemic pathogenic representative in the Americas. Its cosmopolitan ability to interact with a wide range of plant species is attributed to the use of effector proteins, which facilitate the induction of feeding sites in compatible hosts, ultimately leading to significant yield losses in economically important crops. Understanding the mechanisms underlying this interaction opens new perspectives, including gene intervention via RNA interference (RNAi) targeting transcripts involved in the production of these proteins. Additionally, the identification and use of resistance-associated genes from incompatible hosts represent a complementary approach to fostering the evolution of higher plants with enhanced defenses. In this study, divided into four chapters, we identify the effector genes *Minc03328* and *Minc16803* from *M. incognita* and the *Germin-like protein subfamily 1 member 10* gene (*GmGLP10*) from the resistant soybean genotype PI 595099 as critical components in plant defense against *M. incognita*. A comprehensive literature review in Chapter 1 highlights the pivotal roles of these genes, primarily in inhibiting plant immune responses and enabling the formation and maintenance of giant cells. The significance of these findings is demonstrated by the selection and silencing of the effector targets *Minc03328* and *Minc16803* through RNAi, which successfully reduced the susceptibility of transgenic *Arabidopsis thaliana* lines. These results are detailed in two published articles, comprising Chapters 2 and 3 of this thesis. Chapter 4 introduces a third validated component, *GmGLP10*, whose involvement in resistance against *M. incognita* was confirmed through heterologous expression in a model plant. Our analyses reveal an extrinsic mode of action, where increased activity of *GmGLP10* leads to elevated hydrogen peroxide production, as measured by transcriptional changes in key gene markers associated with phytohormone pathways and hypersensitivity responses. These findings provide a new avenue for soybean protection, with gene pyramiding of the validated elements presented here emerging as a promising strategy to safeguard soybeans and other crops of agronomic importance.

KEYWORDS: *Meloidogyne incognita*, RNA interference, effector genes, Germin-like proteins, protection *in planta*.

INTRODUÇÃO GERAL

Nematoides parasitas de plantas (NPP) são considerados um dos principais patógenos agrícolas capazes de impor severas restrições na proteção de importantes cultivos de interesses comerciais no mundo (Decraemer & Geraert, 2006a, b). No Brasil, um dos maiores problemas é a infestação de solos por nematoides formadores de galhas (NFG), que acometem as raízes de culturas de grande relevância agronômica, como por exemplo a soja. Dentre eles, destacam-se as espécies do gênero *Meloidogyne*, sendo os NFG *Meloidogyne incognita*, *M. javanica* e *M. enterolobii* responsáveis por perdas de US$ 6.5 bilhões por ano no mercado da soja, integrando a faixa estimada de 10 a 14% dos danos causados por NPP na agricultura mundial (Barros *et al.*, 2022).

Para solucionar esse problema, nosso grupo de pesquisa busca, por meio da engenharia genética de plantas, desenvolver cultivares superiores como uma alternativa promissora, priorizando o mínimo impacto no equilíbrio ambiental (Basso *et al.,* 2024). Tecnologias como o RNA de interferência (RNAi) e a expressão de proteínas recombinantes antinematoides têm se mostrado, ao longo dos últimos 18 anos de estudos (2005–2023), ferramentas moleculares cruciais para o controle de espécies do gênero *Meloidogyne* (**Fig. 1**). Essas estratégias não apenas contribuem para a redução significativa dos danos às culturas agrícolas, mas também promovem maior produtividade de forma sustentável, oferecendo uma alternativa ao uso indiscriminado de agroquímicos e atendendo às demandas globais por práticas agrícolas mais equilibradas e ecologicamente responsáveis (Vashisth *et al.,* 2024).

Nesse contexto, a aplicação de ferramentas ômicas tem ampliado o entendimento das interações moleculares entre plantas e nematoides, revelando as principais estratégias evolutivas envolvidas tanto em interações compatíveis quanto incompatíveis (Ibrahim *et al.,* 2019). Estudos como os de Bellafiore *et al.* (2008), que identificaram cerca de 486 proteínas efetoras no secretoma de *M. incognita*, destacam a complexidade das táticas empregadas por esses NPP para se estabelecerem em mais de 3.000 espécies de plantas vasculares (Jones *et al.,* 2013). Essas proteínas têm sido exploradas como alvos para a tecnologia de RNAi, inicialmente em estudos de prova de conceito em plantas modelo e, mais recentemente, em culturas comerciais, reforçando o potencial protetivo dessa abordagem (Lisei-de-Sá *et al.,* 2021).

Recentemente, nosso grupo de pesquisa identificou a existência dos genes efetores *Minc03328* e *Minc16803* como importantes alvos específicos pela tecnologia do RNA de interferência *in planta* (Moreira *et al.,* 2022, 2023). Esses dados, reunidos nos capítulos 2 e 3

desta tese, revelaram altos níveis na redução da susceptibilidade de linhagens transgênicas de *Arabidopsis thaliana* desafiadas contra o NFG *M. incógnita*. Além do silenciamento gênico pós-transcricional determinados, via análises de PCR em tempo real (RT-qPCR), confirmamos seus usos para indução e manutenção das células gigantes (CG) em plantas terrestres. Enquanto a regulação negativa de *Minc03328* foi capaz de infringir a estabilidade do citoplasma das CG averiguadas (Moreira *et al.,* 2022), *Minc16803* revelou este mesmo fenótipo acompanhado da malformação de fêmeas adultas, em relação ao controle experimental (Moreira *et al.,* 2023). Com base nesses resultados, uma nova medida visando à proteção de cultivos de soja foi adotada, sendo a utilização dos mesmos cassetes gênicos atualmente utilizados em provas de conceito em plantas de interesse comerciais (estudos em andamento).

De forma semelhante, a expressão heteróloga do gene *Germin-like protein subfamily 1 member 10* (*GmGLP10*) foi também validada para este último fim atestando para uma redução significativa na reprodução de *M. incógnita*, em mais de 49% em raízes de tabaco transgênico. Estudos prévios realizados em nosso grupo de pesquisa já levantava indícios da superexpressão de *GmGLP10* como uma medida a ser investigada em provas de conceito *in planta*, devido a sua alta expressão diferencial constatada tanto a níveis de transcritos, quanto proteicos no genótipo resistente de soja PI 595099 (Arraes *et al.,* 2022). Além do seu envolvimento na proteção de plantas, a atividade de GmGLP10 foi mensurada via análises de RT-qPCR para vários marcadores gênicos de planta, sensitivos ao incremento do peróxido de hidrogênio no espaço citoplasmático. Esses dados reunidos no capítulo 4 desta tese permitiram identificar os principais elementos a jusante, intricados com as vias do ácido salicílico e jasmônico, etileno, espécies reativas de oxigênio (ERO) e respostas de hipersensibilidade, como os principais agentes capazes de intervir no desbalanço homeostático de CG.

Deste modo, a presente investigação teve como principal objetivo conhecer os principais elementos-chaves explorados em ambos contextos coevolutivo de interação com a finalidade de elaborar novas medidas de controle por meio da intervenção genética. Assim como o uso do RNAi mediando o silenciamento de *Minc03328* e *Minc16803* – terem nos mostrado os melhores resultados –, a superexpressão de $GmGLP10^{OE}$ foi vislumbrada como uma terceira alternativa a ser integrada em cassetes gênicos de transformação, em cultivares elites. Para tanto, novos estudos estão sendo executados a fim de validar se os efeitos antagônicos combinados dos três elementos aqui averiguados, podem ser utilizados como nova medida protetiva em cultivares transgênicos de soja e algodão.

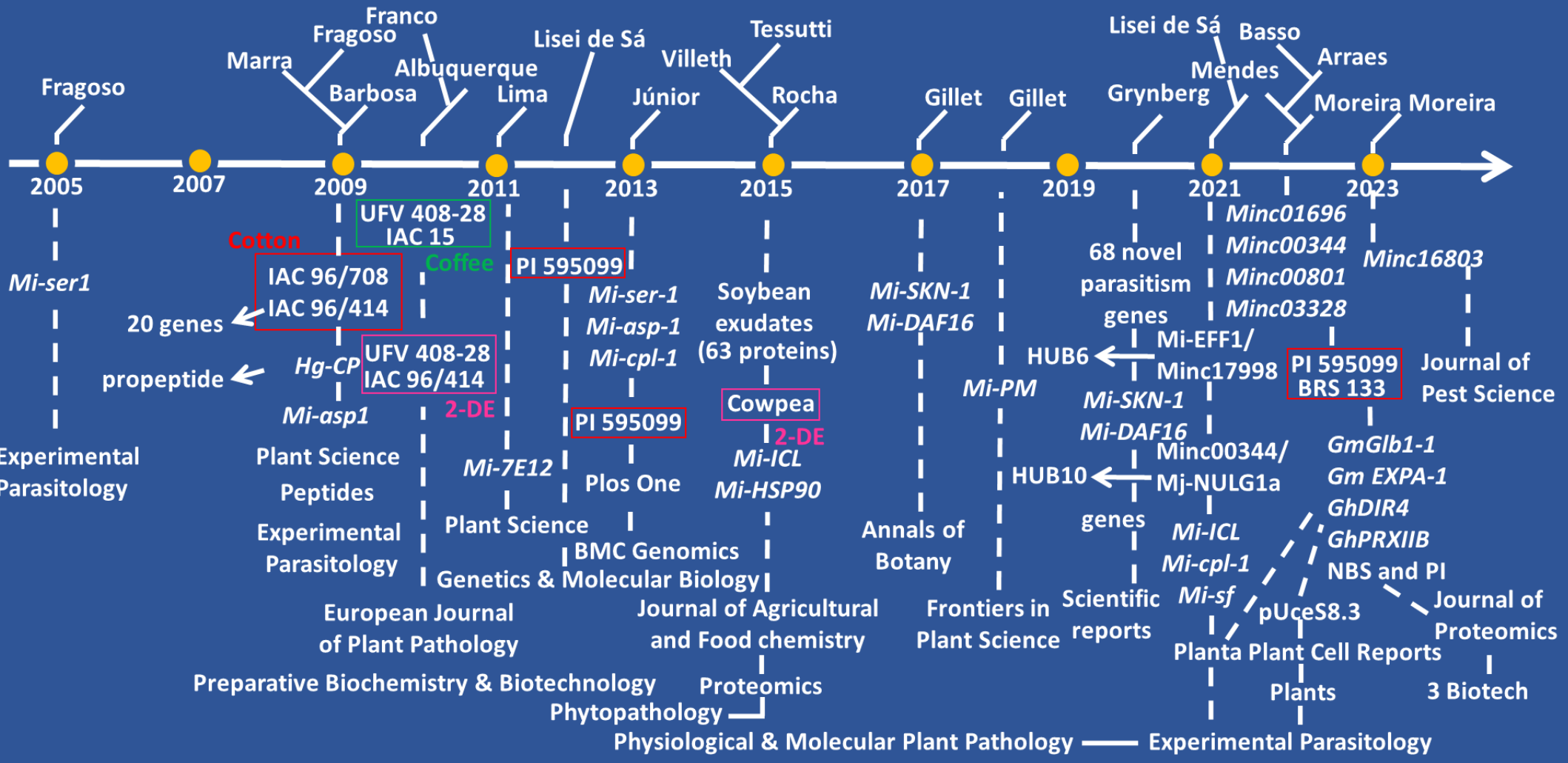

Figura 1: Validação de moléculas antinematoides. Nos últimos 18 anos, nosso grupo de pesquisa identificou dezenas de genes de *M. incognita* como potenciais alvos para a tecnologia de RNA de interferência (RNAi), resultando na publicação de estudos significativos sobre os melhores candidatos atualmente investigados em plantas de interesse comercial, como soja e algodão. Por meio de tecnologias ômicas (proteômica, transcriptômica e genômica), genótipos resistentes, como a soja PI 595099, foram analisados, revelando traços gênicos relacionados à resistência ao nematoide das galhas (NFG) e ao nematoide de cisto da soja (NFC). Esta linha do tempo destaca os genes que apresentaram maior eficácia quando validados em plantas modelo. Em particular, os genes *Minc03328* e *Minc16803* de *M. incógnita* e a proteína *Germin-like protein subfamily 1 member 10* (*GmGLP10*), proveniente da soja PI 595099, estão sendo avaliados em cultivares comerciais de soja e algodão como potenciais ferramentas protetivas para cultivares geneticamente modificadas. Dados preliminares indicam que o uso de RNAi contra *Minc03328* e *Minc16803* reduziu a susceptibilidade em plantas modelo em mais de 85%, enquanto a expressão heteróloga de *GmGLP10* em tabaco reduziu a reprodução do patógeno em mais de 49%.

CAPÍTULO I

REVISÃO DE LITERATURA

O ciclo parasítico das espécies do gênero *Meloidogyne*

As espécies de *Meloidogyne*, conhecidas como formadoras de galhas, têm destaque científico e econômico devido aos prejuízos causados à agricultura. De acordo com a revista *Molecular Plant Pathology*, elas figuram entre os dez principais nematoides agrícolas (Jones *et al.*, 2013). Até o momento, são identificadas 98 espécies, com *M. incognita* sendo o principal representante nas Américas. No Brasil, *M. incognita*, *M. javanica* e *M. enterolobii* causam perdas anuais de US$ 6,5 bilhões na produção de soja, representando de 10 a 14% dos danos globais por nematoides parasitas (Barros *et al.*, 2022).

Embora o sinergismo entre *Meloidogyne* e plantas ainda seja pouco compreendido, os genomas de *M. incognita* e *M. hapla* já foram sequenciados, revelando diferenças significativas no tamanho genômico: 183 Mb e 43.718 genes em *M. incognita*, contra 53,6 Mb e 14.207 genes em *M. hapla* (Abad *et al.*, 2008; Blanc-Mathieu *et al.*, 2017). Apesar disso, ambas as espécies compartilham o mesmo ciclo infeccioso, que se completa em 3 a 8 semanas a 28°C (**Fig. 2A**; Favery *et al.*, 2016). Mudanças climáticas, como o aumento da temperatura, aceleram o desenvolvimento embrionário e a infecção em raízes (Velloso *et al.*, 2022).

Juvenis pré-parasíticos (*ppJ2*) são atraídos por compostos liberados pelas raízes, como o salicilato de metila e o dissacarídeo L-Gal(α1-3)-L-Rha, detectados por órgãos sensoriais cefálicos chamados anfídeos (**Fig. 2A - C**; Čepulytė *et al.*, 2018; Kihika *et al.*, 2017). Os juvenis perfuram a parede celular das raízes com o estilete e secretam efetores moleculares para superar barreiras físicas e imunológicas de plantas, facilitando o parasitismo (Escobar *et al.*, 2015; Sato *et al.*, 2019).

Durante a fase migratória, os juvenis percorrem a raiz até o cilindro vascular, onde desdiferenciam células para criar sítios de alimentação, conhecidos como células gigantes **(Fig. 2A, D)**. Essas células são hipertrofiadas e multinucleadas, apresentando intensa atividade metabólica, enquanto as adjacentes sofrem hiperplasia, formando as galhas características (Kyndt *et al.*, 2013; de Almeida Engler *et al.*, 2013).

Após a instalação, os juvenis avançam para as fases J3 e J4, tornando-se sedentários **(Fig. 2A)**. Em hospedeiros incompatíveis, podem regredir para machos e retornar à rizosfera (Castagnone-Sereno *et al.*, 2013; Goverse & Smant, 2014). Fêmeas maduras produzem centenas de ovos por partenogênese, liberados em uma matriz glicoproteica (**Fig. 2E**; Castagnone-Sereno, 2006). Temperaturas elevadas podem acelerar o ciclo, promovendo a eclosão precoce de juvenis e aumentando a capacidade infecciosa (Calderón-Urrea *et al.*, 2016; Oota *et al.*, 2020).

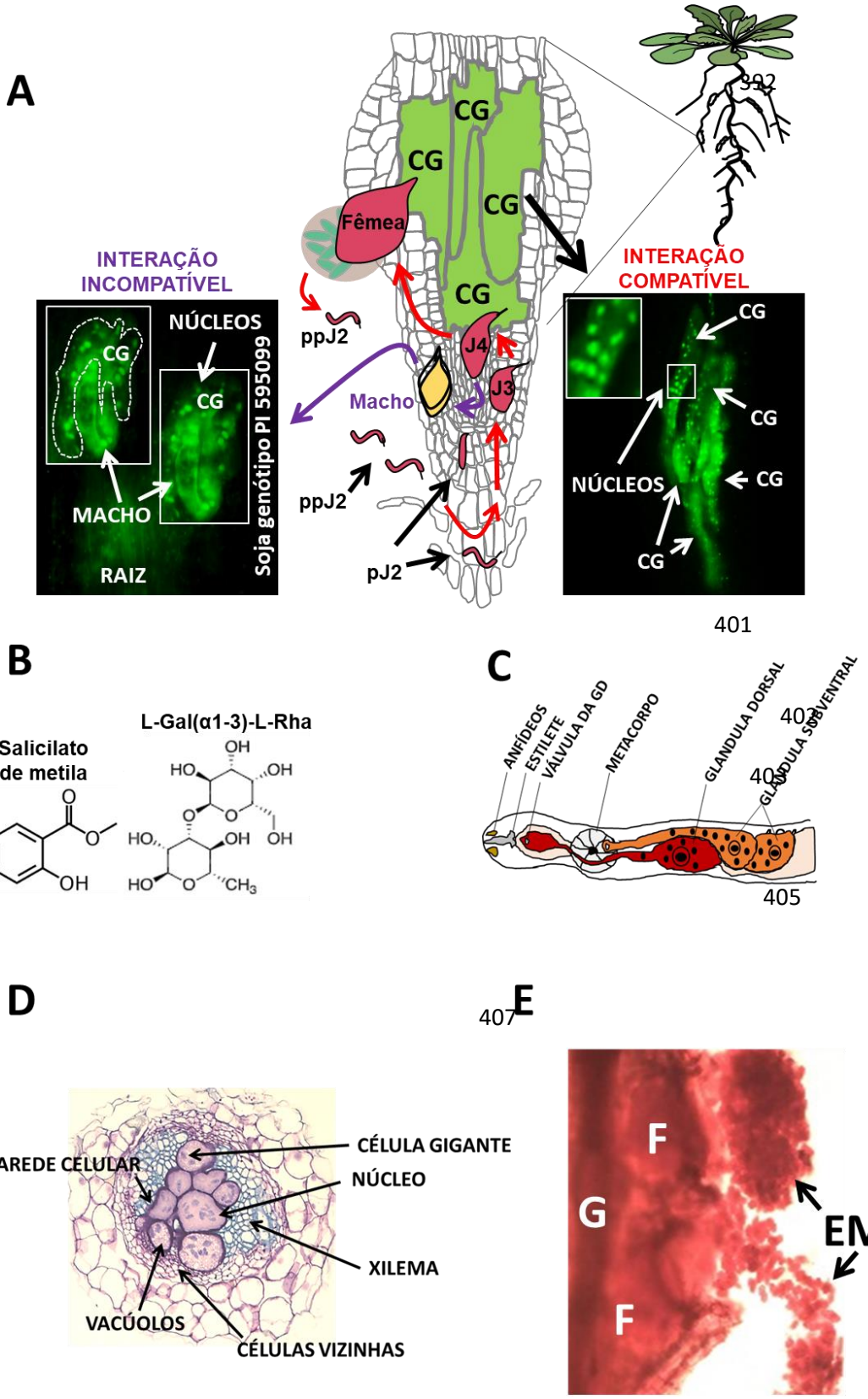

Figura 2: Ciclo do desenvolvimento de *M. incógnita* em plantas terrestres. (**A**) O ciclo de vida de *M. incógnita* é composto por seis estádios de desenvolvimento: ovos, ppJ2 (juvenis de segundo estádio pré-parasítico), pJ2 (juvenis em estádio parasítico), J3 (juvenis em estádio 3), J4 (juvenis em estádio 4, que não se alimentam) e fêmeas adultas. Durante o ciclo endocítico,

pJ2s migram através das camadas de células epidérmicas e corticais até as células do parênquima cortical, onde as desdiferenciarão em CG que comporão o seu sítio de alimentação (setas vermelhas). Como característica, observa-se nas interações compatíveis que as CG apresentam citoplasma bastante proeminentes contendo vários núcleos os quais se dividem de maneira acitocinética (Imagem BABB à direita). Em relações incompatíveis (seta lilás), estádio J4 diferenciam-se em macho abandonando o hospedeiro (Imagem BABB à esquerda). (**B**) Estruturas moleculares de Salicilato de metila e ramnogalacturonanos: principais metabólitos atrativos para interação de *M. incógnita* em raízes de plantas. (**C**) Representação esquemática anatômica de *M. incógnita*. (**D**) Representação da análise histopatológica de uma galha, após coloração com azul de toluidina. (**E**) Imagem de galha (G) corada com fucsina ácida evidenciando estádio de fêmea adulta desenvolvida (F) e massa de ovos (EM).

Mecanismos de patogenicidade de *Meloidogyne* spp., em plantas terrestres

O aparelho bucal (estilete) e as glândulas esofágicas (duas subventrais e uma dorsal) são os principais mecanismos adaptativos de *Meloidogyne* spp., permitindo sua sobrevivência em mais de 3.000 espécies de plantas vasculares (**Fig. 2C**, Jones *et al.,* 2013; Mitchum *et al.,* 2013). O estilete é essencial para superar barreiras físicas, como a parede celular rica em celulose e lignina e a estria de Caspary, enquanto as glândulas secretam efetores catalíticos que degradam polissacarídeos da célula vegetal (Quentin *et al.,* 2013; Cosgrove *et al.,* 2005).

Estudos sugerem que genes de origem bacteriana foram incorporados ao genoma ancestral dos nematoides. O sequenciamento de *M. incognita* revelou cerca de 60 proteínas relacionadas a seis famílias de enzimas de origem bacteriana, como celulases (EC 3.2.1.4), pectato liases (EC 4.2.2.2) e expansinas, que desempenham papéis na degradação e modificação das paredes celulares das plantas (**Fig. 3A**, Abad *et al.,* 2008; Danchin *et al.,* 2010).

Durante as fases migratória e sedentária, *Meloidogyne* spp. secreta efetores via estilete, dos quais cerca de 87% suprimem a imunidade das plantas, e 23% induzem a formação e manutenção de células gigantes nos sítios de alimentação (**Fig. 3B**, Bellafiore *et al.,* 2008; Molloy *et al.,* 2023). Essas células hipertrofiadas são metabolicamente ativas e recebem nutrientes transportados pela vascularização ao redor, garantindo o suprimento necessário para o desenvolvimento do nematoide (**Fig. 4A**, Hoth *et al.,* 2005).

As glândulas esofágicas têm papel central na produção de efetores. Nas fases iniciais, as glândulas subventrais são altamente ativas, com intensa transcrição e secreção de proteínas como Mi-CRT, MiMSP40 e Minc03328, importantes para o parasitismo (Jaubert *et al.*, 2005; Niu *et al.*, 2016). Em estágios mais avançados, a glândula dorsal assume maior relevância, sustentando o ciclo sedentário (Hussey & Mims, 1990).

Embora a maior parte dos efetores seja produzida pelas glândulas esofágicas, outros tecidos, como anfídeos, glândulas retais e hipoderme, também participam da secreção de moléculas essenciais durante o parasitismo (Rutter *et al.*, 2014; Zhao *et al.*, 2019). Estudos recentes identificaram novos genes associados a esses órgãos, ampliando o entendimento sobre os mecanismos de interação de *Meloidogyne* spp. com plantas (Moreira *et al.*, 2022).

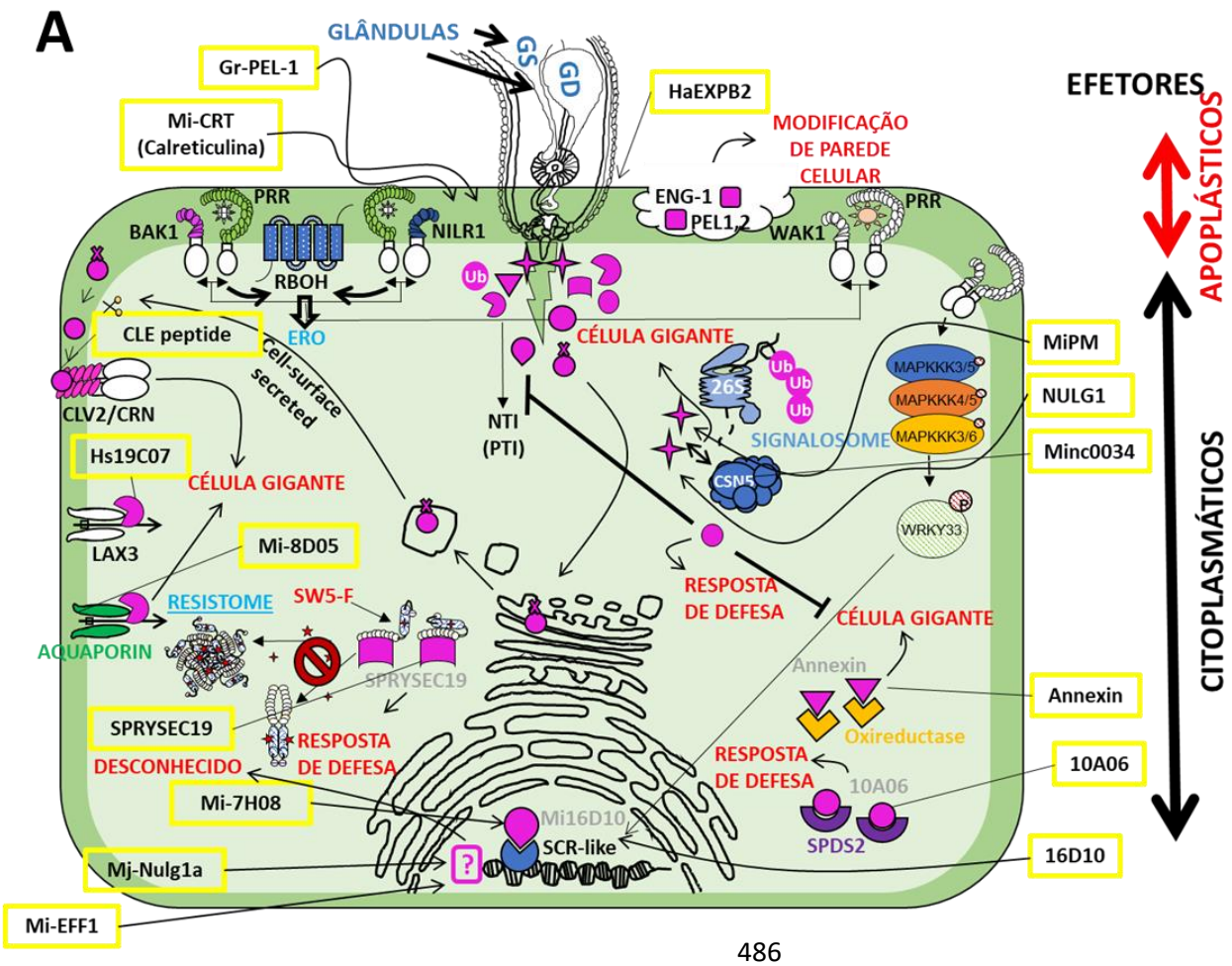

486

487

B

488

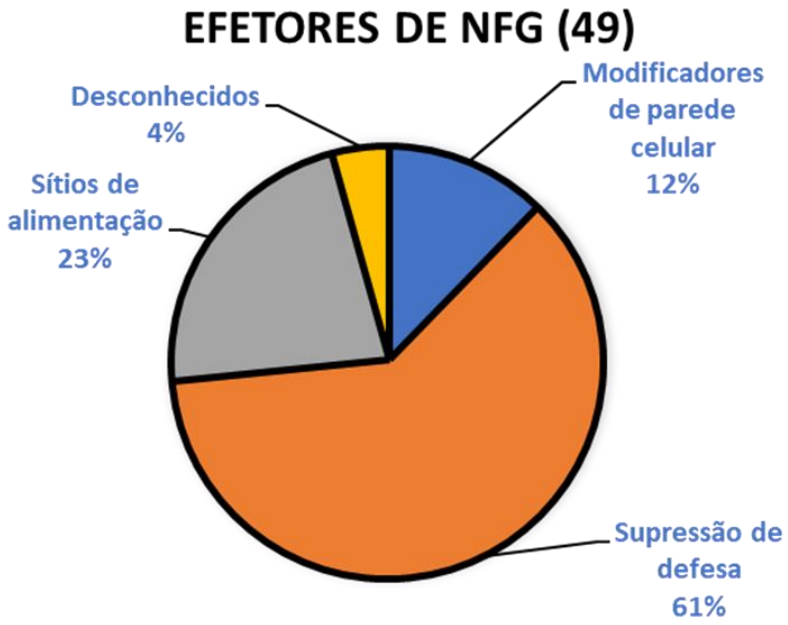

489

490

491

492

493

494

495

496

497

Figura 3: Intersecção dos efetores de *M. incógnita* no desenvolvimento e fisiologia de células vegetais. (**A**) Representação esquemática dos principais efetores de *M. incógnita* (em caixas amarelas) bem como seus alvos *in planta* por meio de análises de interatomas proteína-proteína (PPI). Segundo Sato *et al.*, (2019), os modos de ação de proteínas efetoras podem ser classificados aos níveis apoplásticos e citoplasmáticos em células vegetais. No primeiro nível se enquadram efetores catalíticos e miméticos de plantas, enquanto no segundo englobam uma diversidade efetora sumariamente envolvida na inibição de resposta de defesa da planta e na formação e manutenção de CG. (**B**) Gráfico de pizza representando os 49 efetores de *M. incógnita* com funções determinadas em plantas. Segundo Molloy *et al.*, (2023), suas funções encontram-se reclusas em processos de plantas cujos efeitos permitem intervir na supressão de redes imunes de defesa (PTI e ETI), estabelecimento de CG e degradação da parede celular. Desse número, apenas 4% permanecem desconhecidos suas classificações quanto a esses processos, embora seus alvos de plantas sejam compreendidos pelas técnicas de PPI. (Figura adaptada, Molloy *et al.*, 2023)

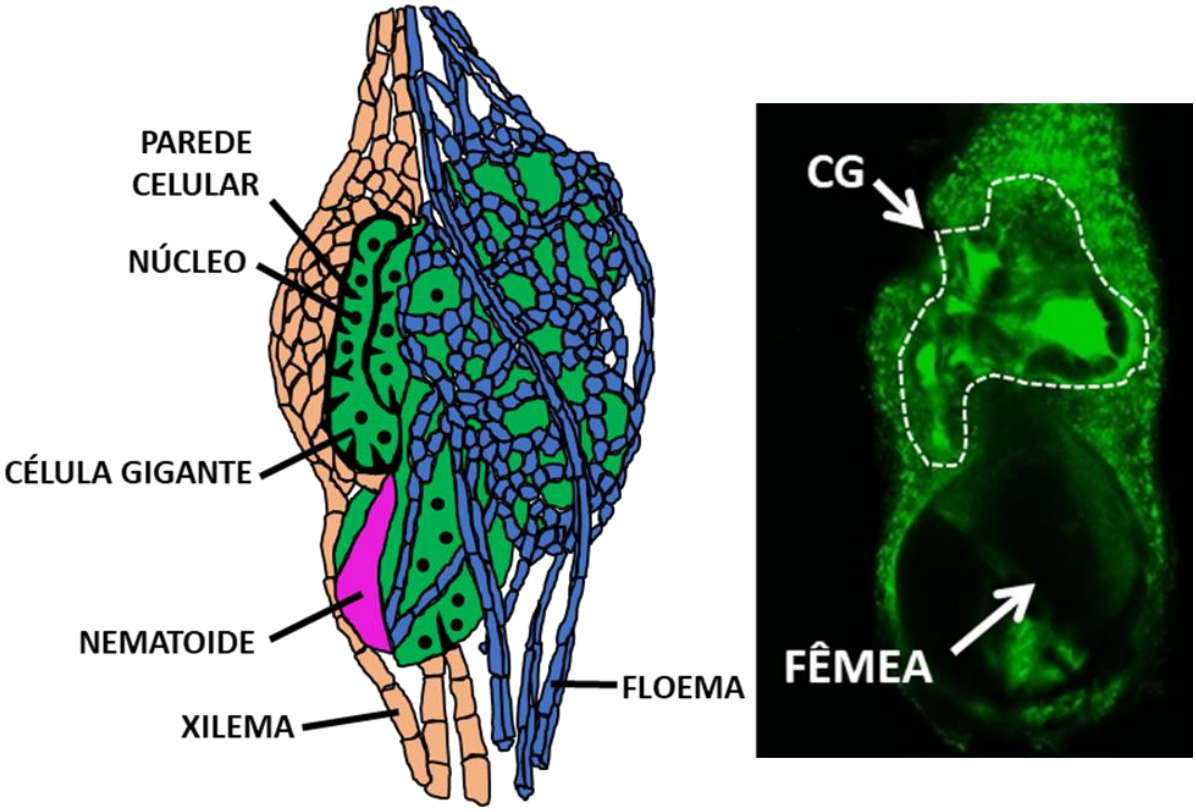

Figura 4: Vascularização dos tecidos vasculares como medida importante de aquisição de nutrientes. À esquerda, representação esquemática: sítios de alimentação (em verde) circundado pelo xilema (na cor bege) e floema (em azul) como mecanismo de obtenção de nutrientes por meio do extravasamento apoplástico. À direita, imagem de galha induzida em

raiz de *A. thaliana* obtida por análise de BABB. CG encontra-se delimitada por linhas tracejadas. (Figura adaptada, Bartlem *et al.*, 2014)

Efetores de nematoides formadores de galhas

Entre as várias definições propostas para efetores de patógenos de plantas, Bird *et al.* (2015) foram pioneiros ao defini-los como "qualquer molécula do nematoide parasita capaz de suprimir as defesas do hospedeiro ou manipulá-lo para garantir um fornecimento constante de alimento". Com base nos resultados do genoma de *M. incognita*, essa definição destacou a transferência horizontal de genes como um dos principais fatores que sustentam o sucesso do parasitismo de nematoides formadores de galhas (NFG) (Abad *et al.*, 2008; Opperman *et al.*, 2008; Haegeman *et al.*, 2011). Avanços na genômica funcional permitiram a classificação sistemática de efetores em apoplásticos e citoplasmáticos, de acordo com sua ação no núcleo e em outros compartimentos celulares da célula vegetal (**Fig. 3A**; Jaouannet & Rosso, 2013; Gardner *et al.*, 2015).

Embora esse tema tenha evoluído recentemente, Gheysen & Fenoll (2002) já haviam apontado indícios da hiperplasia de organelas como consequência direta dessa ação (**Fig. 5**). Alterações como fragmentação do vacúolo e proliferação de organelas, como retículo endoplasmático rugoso, ribossomos, mitocôndrias e plastídios, foram associadas a uma ontogenia celular diversificada (**Fig. 5C**; Molloy *et al.*, 2023). Essas mudanças foram inicialmente interpretadas como respostas de defesa do hospedeiro, resultando na formação de tecido *de novo* para reparar danos causados pelo patógeno (Harris & Pitzschke, 2020; Ribeiro *et al.*, 2023). Repetidos ciclos de divisão celular indicaram potencial regenerativo nas células lesionadas, resultando na formação de "calos" (Kyndt *et al.*, 2013; Ribeiro *et al.*, 2023).

Embora essa hipótese ainda esteja em investigação, o foco recente tem sido a habilidade dos efetores em manipular redes de sinalização do hospedeiro, causando desequilíbrios homeostáticos. O efetor MjMCM2, por exemplo, é o primeiro identificado a induzir hiperplasia nuclear em células gigantes (CG). Quando superexpresso em raízes de tomateiro, Fitoussi *et al.* (2022) demonstraram sua capacidade de promover replicação excessiva de DNA, levando à multiplicação e clusterização de núcleos nas CG (**Fig. 5A**). Esse efeito foi relacionado à semelhança de sequência entre MjMCM2 e a subunidade MCM2 do complexo MCM2-7,

envolvido na fase S do ciclo celular eucariótico (Bochman & Schwacha, 2009; Fitoussi *et al.*, 2022).

Efetores como *chorismate mutase 1* (MjCM-1) e *isocorismatase 1* (Mi-ISC-1) também foram validados em *Meloidogyne spp.* Essas proteínas, quando superexpressas, causaram uma redução significativa nos níveis de auxina e ácido salicílico, demonstrando que o desbalanço hormonal é um mecanismo de ação crucial para os NFG (Bauters *et al.*, 2020; Doyle & Lambert, 2003; Qin *et al.*, 2022). Adicionalmente, efetores miméticos de hormônios vegetais podem interagir com receptores da família CEP (peptídeos codificados na extremidade C-terminal), IDA (*inflorescence deficient in abscission*) e RALF (*rapid alkalization factors*), induzindo a proliferação e diferenciação celular em tecidos do procâmbio e xilema, essenciais para o transporte de nutrientes às CG (Mitchum & Liu, 2022).

Com base nesses avanços, uma nova classificação dos efetores foi proposta, considerando seu modo de ação (apoplástico ou intracelular), os aspectos da biologia vegetal que alteram e sua função como fatores de virulência que beneficiam o parasitismo ao longo do ciclo de vida dos nematoides (Molloy *et al.*, 2023). Estudos recentes identificaram 49 efetores de NFG e 45 de nematoides formadores de cisto (NFC), destacando seu envolvimento em processos como supressão da defesa imune, modificação da parede celular e manutenção das CG (**Fig. 3B**; Molloy *et al.*, 2023). No entanto, 4% a 9% desses efetores ainda têm funções desconhecidas, embora seus alvos vegetais já tenham sido identificados.

Há evidências de que a evolução dos efetores contribuiu para inibir redes de defesa imune do hospedeiro, facilitando a coevolução dos NFG em plantas terrestres (**Fig. 3 e 6**; Molloy *et al.*, 2023; Bali & Gleason, 2023). Mais da metade dos efetores analisados demonstraram a capacidade de bloquear a resposta de hipersensibilidade (HR) do hospedeiro. Por exemplo, Kumar *et al.* (2023) relataram que o efetor MjShKT, quando coinfiltrado com os marcadores MAPKKKα e Gpa2/RBP-1, foi capaz de suprimir HR em folhas de *Nicotiana benthamiana*. Além disso, outros efetores têm sido associados à interferência em vias de transdução de sinais mediados por cinases, fatores de transcrição, hormônios de defesa e espécies reativas de oxigênio (Haegeman *et al.*, 2012; Goverse & Mitchum, 2022).

Finalmente, a ausência de plasmodesmatas nas CG sugere um mecanismo alternativo de fornecimento de nutrientes, mediado pelo extravasamento de elementos do tubo crivado para o apoplasto (Hoth *et al.*, 2008). Apesar do isolamento dessas estruturas, efetores desempenham papel crítico ao promover a permeabilidade de transportadores simplásticos, garantindo a

absorção de micronutrientes e macromoléculas pelas CG recém-formadas (Hoth *et al.*, 2005; 2008).

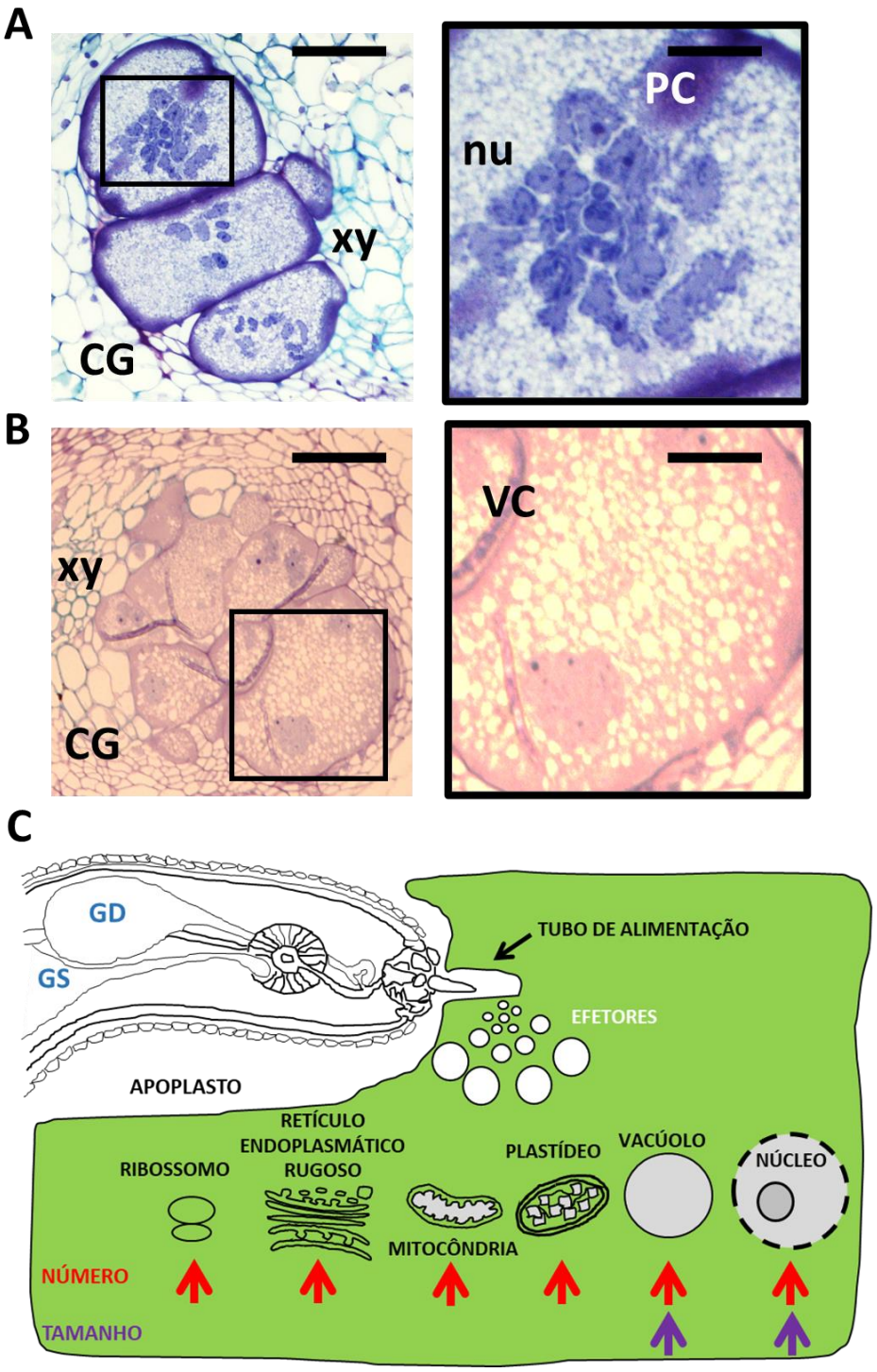

Figure 5: Hiperplasia de organelas na CG. Análise de seções de galhas coradas com azul de toluidina indicando os (**A**) Cluster de núcleos derivados do processo mitose celular acitocinético e a (**B**) fragmentação do vacúolo celular. xy, xilema; nu, núcleo; PC, parede celular; VC, vacúolo; GD, glândula dorsal; GS, glândula subventral. (**C**) Entre outras mudanças previstas

nas CG destacam-se a proliferação de ribossomos, retículo endoplasmático, mitocôndrias e plastídeos. Setas vermelhas simbolizam o incremento do número de organelas em CG, enquanto seta roxa representam o incremento de seus tamanhos.

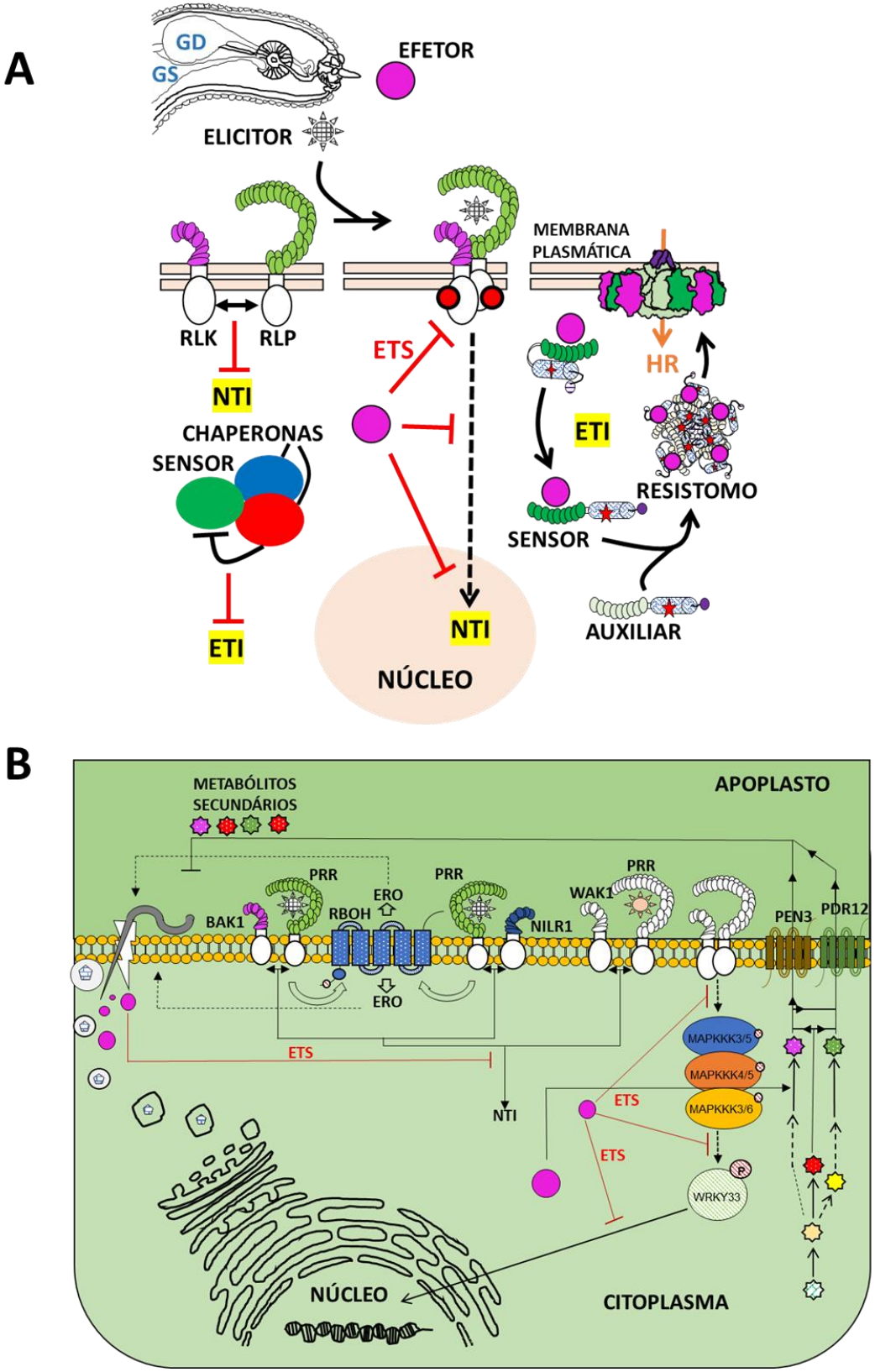

Figura 6: Redes imunes de plantas. (**A**) O reconhecimento de elicitores de nematoide pelos receptores de reconhecimento de padrão RLP (receptors-like proteins) permitem suas heterodimerizações com correceptores do tipo RLK (receptor-like kinases) determinando a primeira via de defesa designada NTI (Nematode – Triggered Immunity). A fosforilação do domínio citoplasmático (círculos vermelhos) representa o passo subsequente determinando a mobilização de outros fatores a jusante para o núcleo da célula vegetal. Durante a coevolução, a aquisição e neofuncionalização de efetores no genoma de NFG deram a possibilidade de inibir essa primeira rede de defesa dando origem à susceptibilidade desencadeada pelo efetor (ETS). Por outro lado, plantas fazem uso de proteínas da família NLR que possuem a habilidade no reconhecimento direto de efetores (NBS sensores) e induzem a formação dos anéis pentaméricos denominados "resistossomos" em associação com proteínas auxiliares da família NBS. Este resultado permitirá a formação de poros da membrana plasmática da célula vegetal dando origem à resposta de hipersensibilidade (HR). (**B**) Principais vias de sinalização relacionadas à via NTI, descobertas nos últimos anos.

Coevolução nas interações *Meloidogyne* spp-hospedeiros: intersecção de efetores na rede imune

Durante o curso coevolutivo entre nematoides e plantas hospedeiras, ambos os lados desenvolveram mecanismos sofisticados que garantem a coexistência dessas espécies (Williamson & Kumar, 2006). As plantas possuem um arsenal genético composto por receptores que codificam proteínas envolvidas na imunidade desencadeada por nematoides (NTI) e na imunidade desencadeada por efetores (ETI) (**Fig. 6**; Kaloshian & Teixeira, 2019; Ngou *et al.*, 2022). Esse sistema de defesa possibilita que os vegetais permaneçam saudáveis e férteis em ambientes terrestres, adotando estratégias de reconhecimento direto e indireto de padrões moleculares associados a patógenos de plantas (NPP), mediados por receptores de reconhecimento de padrão (PRR), que acionam respostas imunológicas multifacetadas (Mitchum *et al.*, 2013; Kaloshian & Teixeira, 2019).

O reconhecimento de padrões moleculares associados a nematoides (NAMP) e efetores desencadeia respostas de defesa dramáticas, que incluem a ativação de MAPK e a indução de morte celular programada (**Fig. 6, 7**; Kaloshian & Teixeira, 2019). Diferentemente dos efetores apoplásticos, que são frequentemente adquiridos via transferência lateral de genes (TLG), os efetores citoplasmáticos são mais diversificados nos genomas de nematoides formadores de

676 galhas (NFG) e apresentam modos de ação versáteis (Danchin *et al.*, 2010; Kikuchi *et al.*, 2017).
677 Um exemplo notável é o efetor citoplasmático chorismate mutase (MjCM-1), cuja origem, via
678 TLG, é atribuída às plantas; a origem dos demais efetores citoplasmáticos ainda é pouco
679 compreendida (Doyle & Lambert, 2003). Estudos sugerem que a diversidade dos efetores nos
680 genomas de *Meloidogyne* spp. resulta de múltiplos eventos de duplicação gênica e
681 diversificação das cópias parálogas, um processo conhecido como neofuncionalização (Lilley
682 *et al.*, 2018).

683 Embora a maioria dos efetores citoplasmáticos tenha funções ainda indefinidas, estudos
684 de interatomas revelaram importantes alvos moleculares *in planta*. Por exemplo, as proteínas
685 transthyretin-like (MjTTL5) e lectina do tipo C (MiCTL1) reduzem o conteúdo de peróxido de
686 hidrogênio em células vegetais, inibindo as atividades da redutase ferroredoxina:tiorredoxina
687 (AtFTRc) e catalases, respectivamente (**Fig. 6B**; Lin *et al.*, 2016; Zhao *et al.*, 2021). De forma
688 semelhante, o efetor MgMO237 de *Meloidogyne graminicola* interage com proteínas como 1,3-
689 β-glucan synthase (OsGSC), cysteine-rich repeat secretory protein 55 (OsCRRSP55) e
690 pathogenesis-related BetvI family protein (OsBetvI), modulando o equilíbrio redox nas células
691 vegetais (Chen *et al.*, 2018). Essas interações envolvem vias canônicas de imunidade disparadas
692 pelo reconhecimento de NAMP por PRRs, levando à expressão de genes de defesa e à produção
693 de espécies reativas de oxigênio (ERO) (Kaloshian & Teixeira, 2019).

694 Na via ETI, o reconhecimento de efetores por genes da família NBS-LRR é crucial para
695 a execução da morte celular programada como parte da resposta de hipersensibilidade (HR) em
696 plantas não hospedeiras (**Fig. 7**; Rhodes *et al.*, 2022). Essa resposta, mais duradoura e drástica
697 que a PTI, tem efeitos localizados nos sítios de infecção. Exemplos bem estudados incluem
698 tomateiros (*Lycopersicon peruvianum*) e batateiras (*Solanum bulbocastanum*), cujos genomas
699 servem como base para programas de melhoramento genético visando resistência a espécies de
700 *Meloidogyne* e outros patógenos (Williamson & Hussey, 1996; Williamson & Kumar, 2006).

701 Após décadas de pesquisa, o gene *Mi-1.2*, proveniente do locus *Mi* da variedade
702 resistente de tomateiros (*L. esculentum Mill* × *L. peruvianum*), foi clonado, representando um
703 dos principais elementos dessa segunda rede de defesa (Smith, 1944). A superexpressão de *Mi-*
704 *1.2* conferiu alta resistência em linhagens transgênicas de berinjela (*S. melongena*), reduzindo
705 sua suscetibilidade a *M. javanica* em mais de 80% (Goggin *et al.*, 2006). Resultados similares
706 foram obtidos para *M. incognita* e outros patógenos, indicando que Mi-1.2 atua de forma
707 conservada, reconhecendo efetores e desencadeando HR (**Fig. 7**, Nombela *et al.*, 2003).

Avanços em microscopia sugerem que Mi-1.2 interage com a proteína auxiliadora NRC4 de solanáceas, participando da montagem do resistossomo e da indução de HR (Fig. 7; Lüdke *et al.*, 2023). Apesar de o efetor de *Meloidogyne* reconhecido por Mi-1.2 ainda não ter sido identificado, sua coexpressão com NRC4 em *N. benthamiana* induziu HR local mesmo na ausência do efetor (Wu *et al.*, 2017). A superexpressão de Mi-1.2 mostrou-se segura, sem evidências de respostas autoimunes (Goggin *et al.*, 2006).

Entretanto, o uso de cultivos geneticamente modificados, como os que contêm *Mi-1.2*, deve ser alternado com outras práticas agrícolas para evitar a superação da resistência por novos isolados. Casos de resistência vencida já foram relatados em tomateiros resistentes a NFG na América do Norte, sul da Europa e África (El-Sappah *et al.*, 2019). Além disso, fatores como monocultivo e aumento da temperatura global, provocados por atividades humanas, contribuem significativamente para a perda funcional da família gênica *Mi* (Dropkin, 1969a, b). Essa pressão antrópica tem favorecido a adaptação dos NFG, destacando a necessidade de desenvolver novas estratégias de controle.

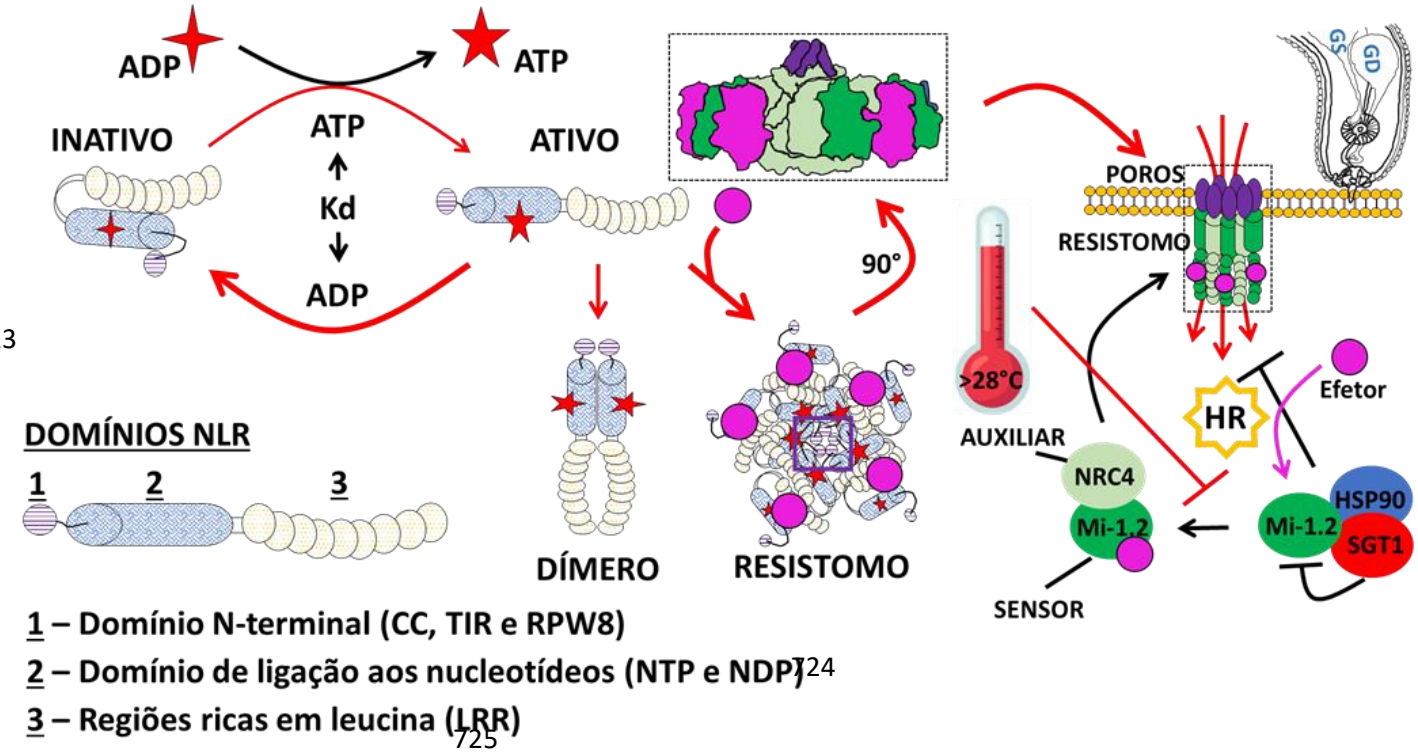

Figura 7: Mecanismo de acionamento de proteínas NLR e indução da formação de resistomos. (**A**) O estádio inativo de NLR é estável (Kd baixa), sendo o seu acionamento dependente do reconhecimento direto do efetor cognato pelo sítio LRR (3). Neste ponto é concebido a troca de ADP por ATP no domínio NBS (2) de NLR tornando-a passível à interação

com a proteína NLR auxiliar. O resultado desse processo é a formação de resistomo, sendo a exposição do domínio N-terminal (1) capaz de induzir a formação de poros na membrana plasmática da célula vegetal no complexo ativo. Particularmente a NLR sensora Mi-1.2 (figura à direita), instável a temperaturas superiores a 28°C, sabe-se do seu apoio síncrono à NRC4 de tomateiros, embora permaneça elusivo o efetor cognato à Mi-1.2. Para evitar sua autoativação, Mi-1.2 são estabilizados, a níveis pós-traducionais, pelas chaperonas SGT1 e HSP90, sendo o seu acionamento dependente do reconhecimento direto ao efetor.

Efetores para a manutenção dos sítios de alimentação

Ao contrário dos sincícios, que estão conectados aos elementos de tubo crivado enucleados por meio de plasmodesmatas secundários (PD) induzidos por nematoides formadores de cisto (NFC), as células gigantes (CG) são isoladas simplasticamente, recebendo nutrientes das células de tubo crivado nucleadas, desprovidas das células companheiras (CC) (**Fig. 8A**; Hoth *et al.,* 2005, 2008). Inicialmente, estudos de microscopia eletrônica evidenciaram uma espessura elevada da parede celular na interface dessas células, destacando a ausência de PD como indicativo do isolamento funcional dos sítios de alimentação (**Fig. 8B**; Jones & Northcote, 1972; Jones & Dropkin, 1976). Devido às semelhanças morfológicas entre CG e células de transferência de plantas, Hammes *et al.* (2005) hipotetizaram que a abundância de transportadores em CG poderia ser uma compensação pela desconexão com os tecidos vasculares adjacentes (**Fig. 8A**; Rodiuc *et al.,* 2014).

Essa hipótese foi corroborada pela identificação de transportadores, como AtSUC2, H+-ATPase e a aquaporina TobRB7, que mostraram expressão restrita aos sítios de alimentação (Opperman *et al.,* 1994; Bird & Wilson, 1994; Juergensen *et al.,* 2003). Além disso, análises de microarranjo revelaram a regulação positiva de pelo menos 26 transportadores em CG induzidas por *Meloidogyne incognita*, destacando as famílias MOP (multidrug/oligosaccharidyl-lipid/polysaccharide flippase), AAAP (auxin amino acid permease) e ABC (ATP-binding cassette transporters) como as mais representativas (**Fig. 8A**; Hammes *et al.,* 2005).

Durante o processo de infecção por nematoides formadores de galha (NFG), observa-se a perda funcional das CC nos tecidos vasculares e a proliferação de elementos de tubo crivado nucleados (Hoth *et al.,* 2005, 2008). Como as CC são responsáveis por recuperar a sacarose perdida no floema, sua ausência redireciona o fluxo de fotoassimilados para o apoplasto que

circunda as CG (**Fig. 8A**). Hoth *et al.* (2008) indicaram que o extravasamento apoplástico, auxiliado por transportadores altamente expressos, é o principal mecanismo de importação de nutrientes. Por exemplo, o gene *AtSUC1*, com expressão exclusiva em CC, demonstrou alta atividade em sítios de alimentação de *M. incognita* (Hammes *et al.*, 2005).

Outros genes, como *AtLHT4*, *AtAAP-3*, -6, -7, *AtAUX4*, *AtACA8* e *AtPIP2.5*, também exibiram altos níveis de expressão transcricional em CG, sugerindo que a reprogramação gênica é mediada direta ou indiretamente por efetores de nematoides (Hammes *et al.*, 2005). No entanto, as identidades desses fatores de virulência ainda permanecem desconhecidas. Apesar disso, alguns efetores foram identificados como reguladores da atividade dos transportadores. Por exemplo, o efetor 8D05 de *M. incognita* interage com a aquaporina TIP-2, promovendo sua permeabilidade para transporte de água, ureia, amônia e compostos nitrogenados, essenciais para a manutenção metabólica das CG (Xue *et al.*, 2013; Leitão *et al.*, 2012).

A interação entre nematoides formadores de cisto (NFC) e plantas também revela diferenças significativas. Enquanto os NFC utilizam PD para o transporte simplástico em sincícios, os NFG dependem de alterações na polaridade de carreadores de efluxo de auxina, como PIN-3 e -4, para manter o abastecimento nos sítios de alimentação. A deleção de *pin-1* em *Arabidopsis thaliana* resultou em uma redução de 40% na reprodução de *Heterodera schachtii*, destacando a importância do transporte de auxina no desenvolvimento dos sincícios (Grunewald *et al.*, 2009).

Assim, os nematoides parasitas de plantas (NPP) manipulam o transporte de metabólitos para estabelecer e manter seus sítios de alimentação. A interação entre efetores e transportadores ativos destaca a adaptação evolutiva dos NFG e NFC, evidenciando estratégias funcionais similares, apesar de diferenças em seus alvos moleculares *in planta* (Abril-Urias *et al.*, 2023).

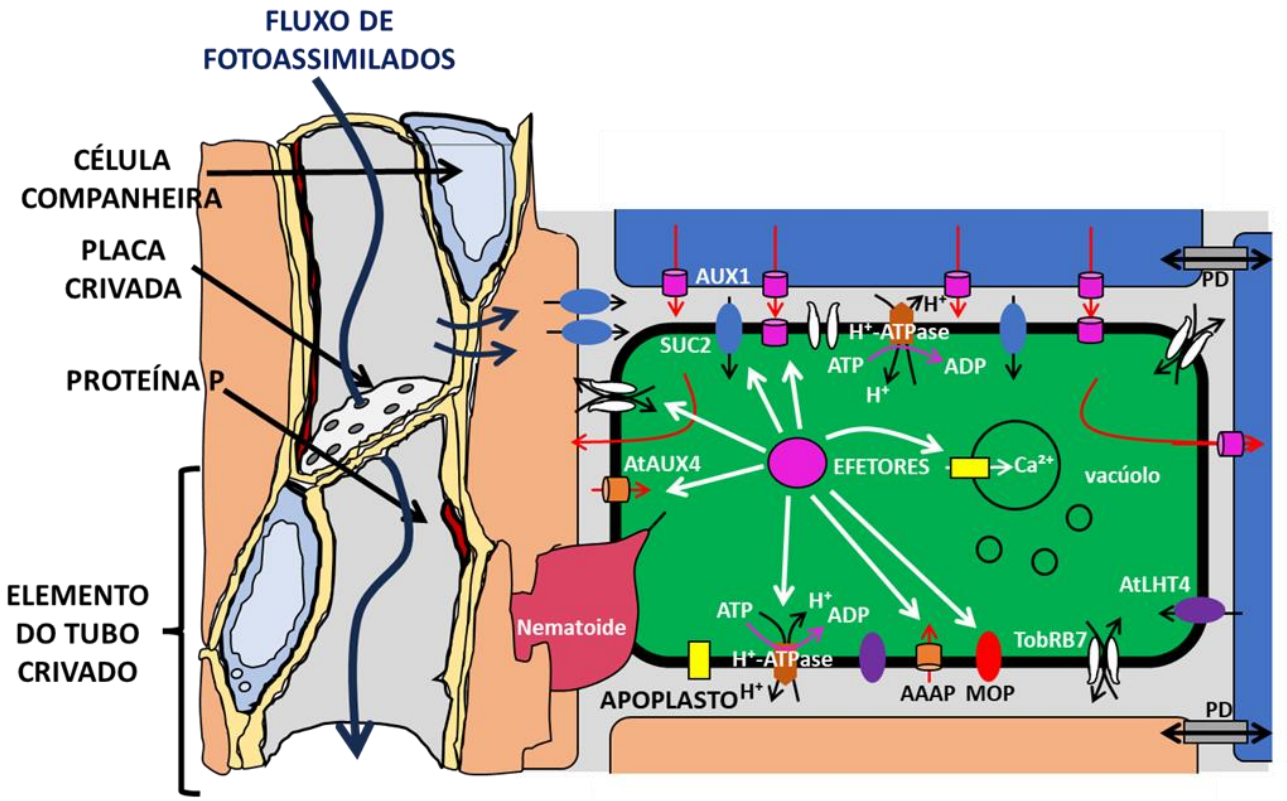
A
FLUXO DE FOTOASSIMILADOS
CÉLULA COMPANHEIRA
PLACA CRIVADA
PROTEÍNA P
ELEMENTO DO TUBO CRIVADO
AUX1
PD
SUC2
H+-ATPase
ATP
ADP
H+
AtAUX4
EFETORES
Ca2+
vacúolo
AtLHT4
Nematoide
TobRB7
APOPLASTO
AAAP
MOP

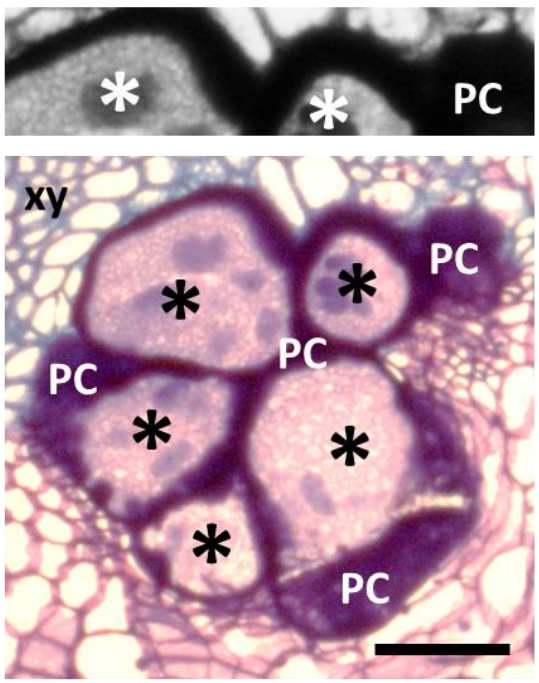
B
PC
xy
PC
PC
PC
PC

Figura 8: Intersecção dos efetores de *M. incógnita* na atividade de transportadores de CG. (**A**) Representação esquemática da obtenção de fotoassimilados por meio da violação da atividade de transportadores. Entre eles, destacam-se os transportadores de sacarose (AtSUC1), aquaporinas (TobRB7), aminoácidos histidina e lisina (AtLHT4), permeasse e influxo de auxina (AAAP e AUX-1, -4), flipases de lipídeos e sacarídeos (MOP) e influxos de prótons (ABC). (**B**) Análise histopatológica de seção de galha corada com azul de toluidina. A coloração escura da imagem representa a elevada espessura da CG como medida física do isolamento dos sítios de alimentação com as células adjacentes. (*) células gigantes, PC parede celular, PD plasmodesmos e xy xilema.

Base molecular da resistência não-hospedeira contra nematoides parasitas de plantas

A resistência não-hospedeira (NHR) é definida como a capacidade de todos os genótipos de uma planta resistirem a uma espécie de patógeno, impedindo seu ciclo reprodutivo (Panstruga & Moscou, 2020). Essa forma de defesa é resultado da interação entre barreiras físicas e químicas pré-formadas e o sistema imune inato da planta. Algumas espécies da família *Solanaceae*, como o tomateiro (*Lycopersicon peruvianum*) e a soja (*Glycine max*), têm sido amplamente estudadas nesse contexto, contribuindo para o desenvolvimento de cultivares resistentes e para a conservação de germoplasma em bancos genéticos (Smith, 1944; El-Sappah *et al.*, 2019).

O tomateiro foi uma das primeiras espécies a apresentar evidências genéticas de resistência a nematoides, com a descoberta do alelo dominante *Mi*, localizado no cromossomo 6. Esse gene mostrou eficácia contra *M. incognita*, promovendo redução de 71% na formação de galhas e aumento de necrose em 88% nas cultivares resistentes (Dropkin *et al.*, 1969). A introdução do gene *Mi* em cultivares comerciais, por meio de programas de melhoramento genético, resultou em diversas linhagens híbridas. Posteriormente, avanços em técnicas de mapeamento genético, como RAPD e RFLP, levaram à identificação do gene *Mi-1.2*, responsável pela resistência, codificando uma proteína NLR (Nucleotide-binding Leucine-rich Repeat) da classe CNL (CC-NB-LRR) (Milligan *et al.*, 1998). Essa proteína requer a estabilização por chaperonas como SlHSP90-1 e SlSGT1, ativando-se apenas na presença de efetores do nematoide, o que evita respostas imunes indevidas (**Fig. 7**, Bhattarai *et al.*, 2007).

Apesar de sua ampla utilização, o gene *Mi* apresenta limitações, como instabilidade a temperaturas acima de 28°C, o que motivou a busca por homólogos termoestáveis. Genes como *Mi-9* e *Mi-HT* demonstraram maior resistência, inclusive em temperaturas de até 32°C, ampliando o espectro de ação contra *Meloidogyne spp.* Outros genes, como *Mi-2*, *Mi-3* e *Mi-6*, também mostraram potencial termoestável, embora sua aplicação em cultivares comerciais ainda seja limitada (Sanchez-Puerta & Masuelli, 2011; Devran *et al.*, 2023).

Na soja, a resistência a nematoides do cisto (*Heterodera glycines*) é atribuída aos lócus *rhg1* e *Rhg4*, predominantes nas cultivares Peking e PI 88788. Genes como *GmSNAP18*, *GmAAT* e *GmWI12* são componentes-chave nesse processo, contribuindo para a estabilidade dos sincícios e limitando o estabelecimento do nematoide (Cook *et al.*, 2012). Variantes do gene *GmSNAP18*, por exemplo, afetam sua interação com a proteína NSF, gerando instabilidade no complexo 20S e induzindo citotoxicidade nos sítios de alimentação, o que prejudica o ciclo de vida do patógeno (Bayless *et al.*, 2016).

Embora os mecanismos de resistência em tomateiros e soja apresentem diferenças, ambos demonstram o papel central de fatores genéticos e proteicos na defesa contra nematoides. A compreensão dessas interações moleculares abre perspectivas para o desenvolvimento de novas estratégias de controle, seja pelo melhoramento genético tradicional ou por meio de ferramentas biotecnológicas como a edição genômica. A identificação de genes termoestáveis e a exploração de complexos imunológicos, como os resistossomos observados em plantas, oferecem caminhos promissores para ampliar a resistência a nematoides e melhorar a produtividade agrícola (Ngou *et al.*, 2022; Wang *et al.*, 2019).

Abordagens ômicas aplicadas à prospecção de genes associados à resposta de defesa no genótipo de soja PI 595099

Avanços em tecnologias de sequenciamento têm destacado as abordagens ômicas como ferramentas-chave para identificar genes de defesa nos genótipos PI 437654 e PI 595099, resistentes a nematoides de cisto (NFC) e galha (NFG), respectivamente. PI 437654 se destaca pela interrupção completa do desenvolvimento de fêmeas de *Heterodera glycines* (tipo 1.2.5.7), com análises de RNA-seq identificando 63 genes diferencialmente expressos (DEG) em 5 dias após a infecção (DAI) e 39 em 10 DAI. Esses genes estão associados a fortalecimento da parede celular, enzimas oxidativas e sinalização de cálcio, consolidando o papel desse genótipo na resistência não-hospedeira (NHR) a NFC (Torabi *et al.*, 2023).

Em contrapartida, PI 595099 apresenta resistência significativa contra NFC e NFG. Ensaios recentes confirmaram sua eficiência contra *M. incognita* (raça 1), detectada em São Paulo, reforçando seu potencial no desenvolvimento de cultivares superiores. Estudos anteriores já haviam demonstrado a riqueza de genes relacionados à regulação hormonal, transdução de sinais e defesa celular em galhas induzidas por *M. javanica*, com termos funcionais associados à resistência sistêmica mediada por ácido jasmônico e etileno identificados (Lisei-de-Sá *et al.,* 2012; Beneventi *et al.,* 2013).

Análises mais recentes com *M. incognita* (raça 1) identificaram 66 termos funcionais enriquecidos nos níveis transcricionais e 26 nos níveis proteicos, destacando processos de oxidação-redução, replicação e morfologia celular. Entre os genes validados, *GmBetV* (PR-10) apresentou redução superior a 60% na reprodução de *M. incognita*. Contudo, devido ao seu potencial alergênico em humanos, modificações mutagênicas foram propostas para minimizar riscos (Arraes *et al.,* 2022; Führer *et al.,* 2022).

Outro gene destacado foi *Glyma.20G220800* (*GmGLP-10*), escolhido por sua alta expressão em análises ômicas. Estudos prévios demonstraram o papel da família GLP na resistência contra fungos como *Sclerotinia sclerotiorum* e *Rhizoctonia solani* e na defesa contra patógenos em arroz e tabaco, devido à geração de íons peróxidos e ativação de genes de defesa como PR-1 e PR-5 (Beracochea *et al.,* 2015; Zhang *et al.,* 2018). Esses achados reforçam o potencial do genótipo PI 595099 na proteção contra nematoides e sua relevância para estratégias de melhoramento genético.

Desvendando novos papéis das proteínas Germin e Germin-like proteins (GLP) em plantas terrestres

Além de seu papel de defesa, amplamente documentado em relação à superexpressão contra diversos fitopatógenos, as proteínas Germin e GLP são onipresentes nos genomas das plantas (**Fig. 9A**). O primeiro relato de Germin foi feito em estudos sobre embriões de trigo, por Thompson e Lane (1980), no contexto de germinação. Contudo, a verdadeira função dessas proteínas era difícil de entender, levando à busca pelo seu ortólogo. Assim, as proteínas esferulina-A (57,3%) e -B (57,5%) do protista *Physarum polycephalum*, envolvidas no encistamento sob déficit hídrico, foram as primeiras a serem registradas como homólogas (Lane *et al.,* 1991). Outro indício importante surgiu com a proteína Germin-like de

Mesembryanthemum crystallinum, que, com 75,7% de similaridade, foi associada ao equilíbrio osmótico em plantas halófitas adaptadas à salinidade (Andolfatto *et al.,* 1994).

Com os avanços no sequenciamento de proteínas, Lane *et al.* (1993) descobriram que a proteína Germin compartilhava o domínio Cupin-1, que é também encontrado nas enzimas oxalato oxidases (OXO; EC 1.2.3.4) de *Hordeum vulgare* (**Fig. 9A-B**). Esse domínio se mostrou crucial para o melhoramento da cevada contra fungos, por sua capacidade de catalisar a conversão de ácido oxálico em CO_2 e peróxido de hidrogênio (H_2O_2) no apoplasto das células vegetais (Hu *et al.,* 2003). Ambas as proteínas Germin e GLP desempenham papéis importantes em processos como oxidação de oxalato e dismutação de superóxido, embora também estejam envolvidas em outras funções, como polifenol oxidase e pirofosfatase, além de atuarem como receptores de plantas, como as ricadesinas, que têm papel no estabelecimento de simbióticos (**Fig. 9A**, Swart *et al.,* 1994; Fan *et al.,* 2005; Cheng *et al.,* 2014; Pei *et al.,* 2019).

O H_2O_2 gerado por essas proteínas é considerado um fator chave na regulação de múltiplas funções fisiológicas, incluindo defesa, desenvolvimento e autofagia. Segundo Podgórska *et al.* (2017), a associação de Germin e GLP com outras oxidases apoplásticas resulta em uma produção basal de H_2O_2 de 10–25 pmol·g−1 em condições normais. No entanto, em situações de estresse, esse nível pode aumentar significativamente. O H_2O_2 é essencial para o controle redox no citoplasma, afetando a translocação de NPR1 (Non-Expressor of PR-1) para o núcleo, onde interage com o fator de transcrição TGA para induzir a expressão de genes PR (Pathogenesis-Related) relacionados à resistência contra patógenos (**Fig. 9A**, Chi *et al.,* 2013; Castro *et al.,* 2021).

A evolução de Germin e GLP em plantas terrestres tem sido marcada pela adaptação extrema de suas atividades, com estruturas estabilizadas por pontes de dissulfeto e glicosilações antes de serem exportadas para o apoplasto (Ilyas *et al.*, 2023). Além do peptídeo sinal na região N-terminal, suas funções estão associadas ao domínio Cupin_1, cujos motivos BOX-A (QDFCVAD), -B (G--P-H-HPRATEXXXX-G) e -C (GXXHFQ-N-G) são essenciais para sua catálise (**Fig. 9B**, Bernier & Berna, 2001). A presença de resíduos como o glutamato, que coordena íons de cobre e manganês, facilita a atividade do cluster de histidina, fundamental para a atividade oxalato-oxidase (Dunwell *et al.*, 2008; Freitas *et al.*, 2017). Além disso, essas proteínas podem formar oligômeros para maximizar sua atividade catalítica, o que as torna mais resistentes ao ambiente redutor gerado no apoplasto, bem como a condições extremas como calor ou presença de proteases (Dumas *et al.,* 1993; Carter & Thornburg, 1999).

O excesso de H_2O_2 no apoplasto também está envolvido na atividade de peroxidases, que catalisam a conversão de monolignóis em ligninas, resultando em uma parede celular recalcitrante (**Fig. 9A**). Esse processo tem sido associado à resistência de plantas como o algodão (*Gossypium barbadense*) ao fungo *Verticillium dahliae* e à soja (*Glycine max*) à *Meloidogyne incognita*, onde a via de fenilpropanoides é fortemente expressa (Xu *et al.*, 2011; Arraes *et al.*, 2022).

Germin e GLP podem atuar de maneira anterógrada na defesa das plantas, sendo limitados pelo ácido oxálico proveniente de patógenos ou do metabolismo secundário das plantas (Kumar *et al.*, 2019). A ausência desse ácido no metabolismo de plantas tem sido associada ao desequilíbrio de suas vias biossintéticas. Li *et al.* (2022) sugerem que as vias de glioxalato e ascorbato podem ser responsáveis pela produção de ácido oxálico, com seus metabolitos intermediários como o succinato e ácido acético atuando como marcadores de resistência em genótipos de tomateiro resistentes a *Meloidogyne spp.* (Afifah *et al.*, 2019).

Chavan *et al.* (2023) observaram que a aplicação exógena de dehidroascorbato (20 mM) em arroz aumentou a resistência ao nematoide *M. graminicola*, gerando uma resposta rápida de H_2O_2 e ativando genes da rota do ácido salicílico, como os genes *PR1-a, -b* e *WRKY45*. Isso também ativou a fenilalanina amônia-liase, fortalecendo a via de fenilpropanoides (Chavan *et al.*, 2022; Singh *et al.*, 2021). Esses achados são importantes no contexto do nosso estudo, onde a superexpressão de GmGLP10 em tabaco resultou em um aumento na expressão da ascorbato peroxidase (NtAPX), facilitando a geração de ácido oxálico e a resistência ao nematoide *M. incognita* (Li *et al.*, 2022).

Em resumo, as proteínas Germin e GLP têm papéis fundamentais na defesa das plantas contra patógenos, atuando em várias frentes, incluindo a geração de H_2O_2, a modulação de vias antioxidantes e de fenilpropanoides, e a resistência a nematoides, com a superexpressão dessas proteínas abrindo novas perspectivas para o manejo biotecnológico de cultivos resistentes a doenças.

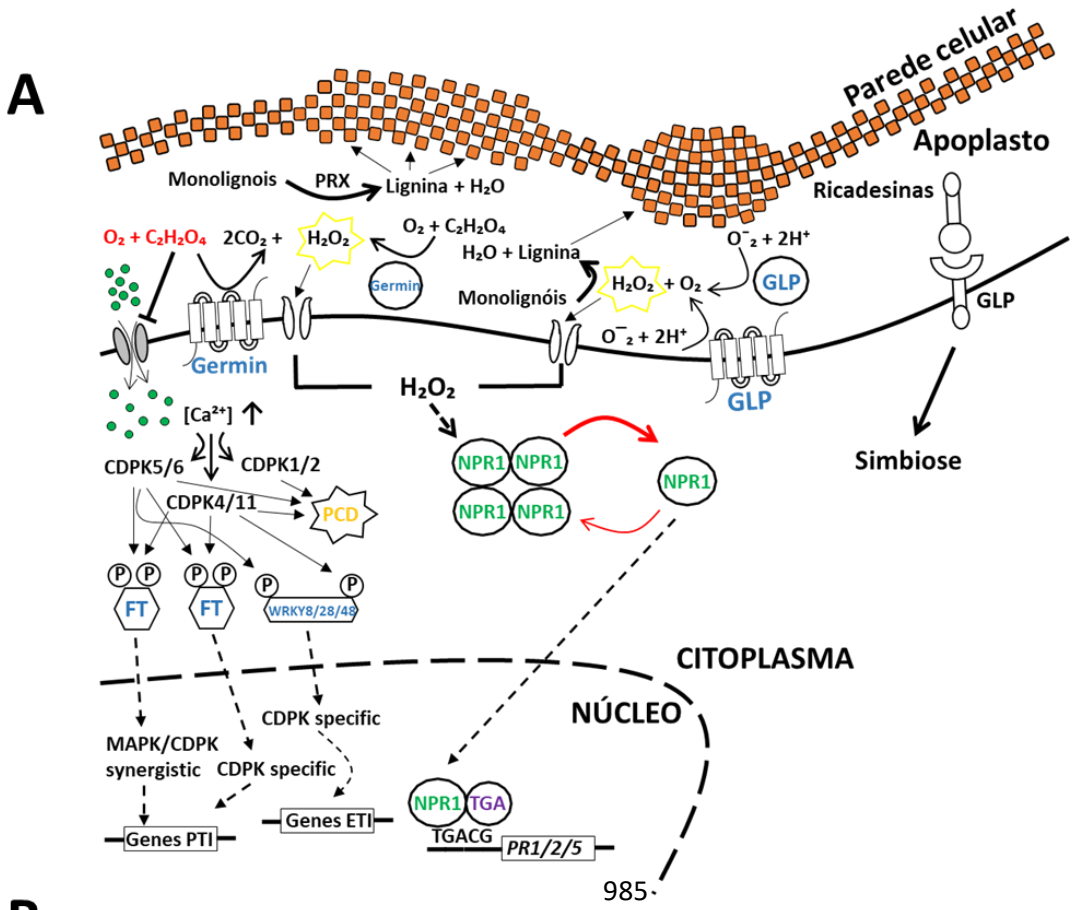
A
Parede celular
Apoplasto
Monolignois
PRX
Lignina + H2O
Ricadesinas
O2 + C2H2O4
2CO2 +
H2O2
O2 + C2H2O4
H2O + Lignina
O2− + 2H+
Germin
Monolignóis
H2O2 + O2
GLP
GLP
Germin
O2− + 2H+
H2O2
GLP
[Ca2+]
Simbiose
CDPK5/6
CDPK1/2
CDPK4/11
PCD
NPR1
NPR1
NPR1
NPR1
NPR1
FT
FT
WRKY8/28/48
CITOPLASMA
NÚCLEO
CDPK specific
MAPK/CDPK
synergistic
CDPK specific
NPR1
TGA
TGACG
PR1/2/5
Genes ETI
Genes PTI

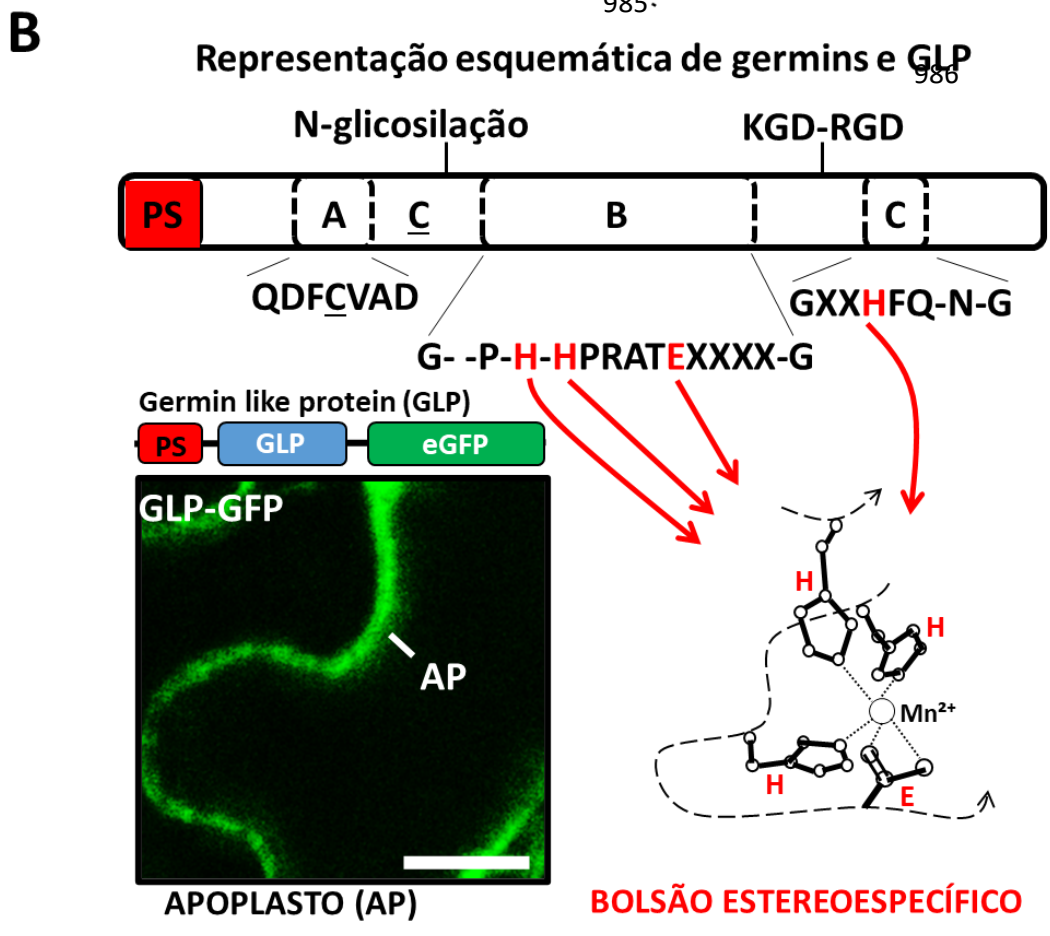
B
Representação esquemática de germins e GLP
N-glicosilação
KGD-RGD
PS
A
C
B
C
QDFCVAD
GXXHFQ-N-G
G- -P-H-HPRATEXXXX-G
Germin like protein (GLP)
PS
GLP
eGFP
GLP-GFP
AP
APOPLASTO (AP)
H
H
Mn2+
H
E
BOLSÃO ESTEREOESPECÍFICO

Figura 9: Mecanismos de ação das proteínas Germin e Germin-like proteins (GLP). (**A**) Germin e Germin-like proteins são dois grupos de proteínas com atividades catalíticas de conversão do ácido oxálico (substrato) em peróxido de hidrogênio. O desbalanço homeostático gerado pelo incremento deste último produto fará com que parte do peróxido de hidrogênio seja utilizado por peroxidases (PRX) no apoplasto (AP) para a polimerização de ligninas, enquanto demais excedentes seja mobilizado para o citoplasma do citosol, via aquaporinas. Seu excesso neste compartimento promoverá uma mudança no potencial redox do coativador transcricional NPR1 (inicialmente oligomerizado) para sua forma monomérica que, por sua vez, será translocado para o núcleo vegetal. Essa mobilização representa um precedente importante para a resistência de plantas contra *M. incognita*, já que o módulo NPR1/TGA estará disponível para a ativação transcricional dos genes de defesa relacionadas às vias de fitormônios de defesa validadas neste estudo. (**B**) Representação esquemática da GLP. Além do peptídeo sinal (PS) que a auxilia para o AP, a proteína GLP possui o domínio Cupin_1 (representado pelos motivos BOX-A, -B e -C) responsável pela conversão de radicais superóxido em oxigênio e peróxido de hidrogênio. Presença dos resíduos de histidina (H) e glutamato (E) a auxilia na coordenação do íon manganês (Mn^{2+}) para o estabelecimento do bolsão estereoespecífico da enzima ao radical superóxido. Imagem à esquerda mostra a localização da proteína GLP10 fusionada à proteína GFP no AP de células de *N. benthamiana*.

Referências bibliográficas

Abad, P., Gouzy, J., Aury, J.M., Castagnone-Sereno, P., Danchin, E.G.J., *et al.*, (2008). Genome sequence of the metazoan plant-parasitic nematode *Meloidogyne incognita*. **Nature. Biotechnology**. 26, 909–915

Abril-Urias P, Ruiz-Ferrer V, Cabrera J, Olmo R, Silva AC, Díaz-Manzano FE, Domínguez-Figueroa J, Martínez-Gómez Á, Gómez-Rojas A, Moreno-Risueno MÁ, Fenoll C, Escobar C. (2023). Divergent regulation of auxin responsive genes in root-knot and cyst nematodes feeding sites formed in Arabidopsis. **Frontiers in Plant Science**. Feb 15; 14:1024815. doi: 10.3389/fpls.2023.1024815.

Afifah EN, Murti RH, Nuringtyas TR. (2019). Metabolomics Approach for the Analysis of Resistance of Four Tomato Genotypes (*Solanum Lycopersicum* L.) to Root-Knot Nematodes

(*Meloidogyne incognita*) **Open Life Sciences**. Apr 6; 14:141-149. doi: 10.1515/biol-2019-0016.

Andolfatto P., Bornhouser A., Bohnert H.J., Thomas J.T., (1994). Transformed hairy roots of *Mesembryanthemum crystallinum*: gene expression patterns upon salt stress. **Physiologia Plantarum**. 90: 708–714.

Arraes FBM, Vasquez DDN, Tahir M, Pinheiro DH, Faheem M, Freitas-Alves NS, Moreira-Pinto CE, Moreira VJV, Paes-de-Melo B, Lisei-de-Sa ME, Morgante CV, Mota APZ, Lourenço-Tessutti IT, Togawa RC, Grynberg P, Fragoso RR, de Almeida-Engler J, Larsen MR, Grossi-de-Sa MF. (2022). Integrated Omic Approaches Reveal Molecular Mechanisms of Tolerance during Soybean and *Meloidogyne incognita* Interactions. **Plants (Basel)**. Oct 17; 11(20):2744. doi: 10.3390/plants11202744.

Bali S, Gleason C. (2023). Unveiling the diversity: Plant parasitic nematode effectors and their plant interaction partners. **Molecular Plant-Microbe Interactions**. Oct 23. doi: 10.1094/MPMI-09-23-0124-FI.

Barros FMDR, Pedrinho A, Mendes LW, Freitas CCG, Andreote FD. (2022). Interactions between Soil Bacterial Diversity and Plant-Parasitic Nematodes in Soybean Plants. **Applied and Environmental Microbiology**. Sep 13; 88(17):e0096322. doi: 10.1128/aem.00963-22.

Bartlem DG, Jones MG, Hammes UZ. (2014). Vascularization and nutrient delivery at root-knot nematode feeding sites in host roots. **Journal of Experimental Botany**. Apr; 65(7):1789-98. doi: 10.1093/jxb/ert415.

Basso MF, Neves MF, Grossi-de-Sá MF. (2024). Agriculture evolution, sustainability and trends, focusing on Brazilian agribusiness: a review. **Frontiers in Sustainable Food Systems**. Jan 11; 7:1296337. doi: 10.3389/fsufs.2023.1296337

Bauters L, Kyndt T, De Meyer T, Morreel K, Boerjan W, Lefevere H, Gheysen G. (2020). Chorismate mutase and isochorismatase, two potential effectors of the migratory nematode *Hirschmanniella oryzae*, increase host susceptibility by manipulating secondary metabolite content of rice. **Molecular Plant Pathology**. Dec; 21(12):1634-1646. doi: 10.1111/mpp.13003.

Bayless AM, Smith JM, Song J, McMinn PH, Teillet A, August BK, Bent AF. (2016). Disease resistance through impairment of α-SNAP-NSF interaction and vesicular trafficking by soybean *Rhg1*. **Proceedings of the National Academy of Sciences of the United States of America**. Nov 22; 113(47):E7375-E7382. doi: 10.1073/pnas.1610150113.

Bellafiore S, Shen Z, Rosso MN, Abad P, Shih P, Briggs SP. (2008). Direct identification of the *Meloidogyne incognita* secretome reveals proteins with host cell reprogramming potential. **PLoS Pathogens**. Oct; 4(10):e1000192. doi: 10.1371/journal.ppat.1000192.

Beneventi MA, da Silva OB Jr, de Sá ME, Firmino AA, de Amorim RM, Albuquerque EV, da Silva MC, da Silva JP, Campos Mde A, Lopes MJ, Togawa RC, Pappas GJ Jr, Grossi-de-Sa MF. (2013). Transcription profile of soybean-root-knot nematode interaction reveals a key role of phythormones in the resistance reaction. **BMC Genomics**. May 10; 14:322. doi: 10.1186/1471-2164-14-322.

Bernier F. O., Berna A. (2001). Germins and germin-like proteins: plant do-all proteins. But what do they do exactly? **Plant Physiology and Biochemistry**. 39; 545–554. doi: 10.1016/s0981-9428(01)01285-2

Bhattarai KK, Li Q, Liu Y, Dinesh-Kumar SP, Kaloshian I. (2007). The MI-1-mediated pest resistance requires Hsp90 and Sgt1. **Plant Physiology**. May; 144(1):312-23. doi: 10.1104/pp.107.097246.

Bird DM, Jones JT, Opperman CH, Kikuchi T, Danchin EG. (2015). Signatures of adaptation to plant parasitism in nematode genomes. **Parasitology**. Feb; 142 Suppl 1(Suppl 1):S71-84. doi: 10.1017/S0031182013002163.

Bird DM, Wilson MA. (1994). DNA sequence and expression analysis of root-knot nematode-elicited giant cell transcripts. **Molecular Plant-Microbe Interactions**. May-Jun; 7(3):419-24. doi: 10.1094/mpmi-7-0419.

Blanc-Mathieu R, Perfus-Barbeoch L, Aury JM, Da Rocha M, Gouzy J, Sallet E, Martin-Jimenez C, Bailly-Bechet M, Castagnone-Sereno P, Flot JF, Kozlowski DK, Cazareth J, Couloux A, Da Silva C, Guy J, Kim-Jo YJ, Rancurel C, Schiex T, Abad P, Wincker P, Danchin EGJ. (2017). Hybridization and polyploidy enable genomic plasticity without sex in the most devastating plant-parasitic nematodes. **PLoS Genetics**. Jun 8; 13(6):e1006777. doi: 10.1371/journal.pgen.1006777.

Bochman ML, Schwacha A. (2009). The Mcm complex: unwinding the mechanism of a replicative helicase. **Microbiology and Molecular Biology Reviews**. Dec; 73(4):652-83. doi: 10.1128/MMBR.00019-09.

Calderón-Urrea A, Vanholme B, Vangestel S, Kane SM, Bahaji A, Pha K, Garcia M, Snider A, Gheysen G. (2016). Early development of the root-knot nematode *Meloidogyne incognita*. **BMC Developmental Biology**. Apr 28; 16:10. doi: 10.1186/s12861-016-0109-x.

Carter C, Thornburg RW. (1999). Germin-like proteins: structure, phylogeny, and function. **Journal of Plant Biology**. 42, 97–108.

Castagnone-Sereno P. (2006). Genetic variability and adaptive evolution in parthenogenetic root-knot nematodes. **Heredity (Edinb)**. Apr; 96(4):282-9. doi: 10.1038/sj.hdy.6800794.

Castagnone-Sereno, P., Danchin, E. G., Perfus-Barbeoch, L. & Abad, P. (2013). Diversity and evolution of root-knot nematodes, genus *Meloidogyne*: new insights from the genomic era. **Annual Review of Phytopathology**. 51, 203–220.

Castro B, Citterico M, Kimura S, Stevens DM, Wrzaczek M, Coaker G. (2021). Stress-induced reactive oxygen species compartmentalization, perception and signaling. **Nature Plants**. Apr; 7(4):403-412. doi: 10.1038/s41477-021-00887-0.

Čepulytė R, Danquah WB, Bruening G, Williamson VM. (2018). Potent Attractant for Root-Knot Nematodes in Exudates from Seedling Root Tips of Two Host Species. **Scientific Reports**. Jul 18; 8(1):10847. doi: 10.1038/s41598-018-29165-4.

Chavan SN, De Kesel J, Desmedt W, Degroote E, Singh RR, Nguyen GT, Demeestere K, De Meyer T, Kyndt T. (2022). Dehydroascorbate induces plant resistance in rice against root-knot nematode *Meloidogyne graminicola*. **Molecular Plant Pathology**. Sep; 23(9):1303-1319. doi: 10.1111/mpp.13230.

Chavan SN, Tumpa FH, Khokon MAR, Kyndt T. (2023). Potential of Exogenous Treatment with Dehydroascorbate to Control Root-knot Nematode Infection in Rice. **Rice**. Jun 29; 16(1):29. doi: 10.1186/s12284-023-00644-1.

Chen J, Hu L, Sun L, Lin B, Huang K, Zhuo K, Liao J. (2018). A novel *Meloidogyne graminicola* effector, MgMO237, interacts with multiple host defence-related proteins to manipulate plant basal immunity and promote parasitism. **Molecular Plant Pathology**. Feb 27; 19(8):1942–55. doi: 10.1111/mpp.12671.

Cheng X, Huang X, Liu S, Tang M, Hu W, Pan S. (2014). Characterization of germin-like protein with polyphenol oxidase activity from *Satsuma mandarine*. **Biochemical and Biophysical Research Communications**. Jul 4; 449(3):313-8. doi: 10.1016/j.bbrc.2014.05.027.

Chi YH, Paeng SK, Kim MJ, Hwang GY, Melencion SM, Oh HT, Lee SY. (2013). Redox-dependent functional switching of plant proteins accompanying with their structural changes. **Frontiers in Plant Science**. Jul 26; 4:277. doi: 10.3389/fpls.2013.00277.

Cook DE, Lee TG, Guo X, Melito S, Wang K, Bayless AM, Wang J, Hughes TJ, Willis DK, Clemente TE, Diers BW, Jiang J, Hudson ME, Bent AF. (2012). Copy number variation of multiple genes at *Rhg1* mediates nematode resistance in soybean. **Science**. Nov 30; 338(6111):1206-9. doi: 10.1126/science.1228746.

Cosgrove DJ. (2005). Growth of the plant cell wall. **Nature Reviews Molecular Cell Biology**. Nov; 6(11):850-61. doi: 10.1038/nrm1746.

Danchin EG, Rosso MN, Vieira P, de Almeida-Engler J, Coutinho PM, Henrissat B, Abad P. (2010). Multiple lateral gene transfers and duplications have promoted plant parasitism ability in nematodes. **Proceedings of the National Academy of Sciences of the United States of America**. Oct 12; 107(41):17651-6. doi: 10.1073/pnas.1008486107.

de Almeida Engler J, Gheysen G. (2013). Nematode-induced endoreduplication in plant host cells: why and how? **Molecular Plant-Microbe Interactions**. Jan; 26(1):17-24. doi: 10.1094/MPMI-05-12-0128-CR.

Decraemer, W. and Geraert, E. (2006a). Ectoparasitic nematodes. In: Plant Nematology (Perry, R.N. and Moens, M., eds). **Wallingford, Oxfordshire: CAB International**. pp. 153–184.

Decraemer, W. and Hunt, D.J. (2006b). Structure and classification. In: Plant Nematology (Perry, R.N. and Moens, M., eds). **Wallingford, Oxfordshire: CAB International**. pp. 3–32.

Devran Z, Özalp T, Studholme DJ, Tör M. (2023). Mapping of the gene in tomato conferring resistance to root-knot nematodes at high soil temperature. **Frontiers in Plant Science**. Oct 10; 14:1267399. doi: 10.3389/fpls.2023.1267399.

Dropkin, V. (1969a). The necrotic reaction of tomatoes and other hosts resistant to *Meloidogyne*: Reversal by temperature. **Phytopathology**. 59, 1632–1637.

Dropkin VH, Helgeson JP, Upper CD. (1969b). The Hypersensitivity Reaction of Tomatoes Resistant to *Meloidogyne incognita*: Reversal by Cytokinins. **Journal of Nematology**. Jan; 1(1):55-61.

Dumas B, Sailland A, Cheviet JP, Freyssinet G, Pallett K. (1993). Identification of barley oxalate oxidase as a germin-like protein. **Comptes Rendus de l'Académie des Sciences - Series III**. 316:793-798

Dunwell JM, Gibbings JG, Mahmood T, Naqvi SMS. (2008). Germin and germin-like proteins: evolution, structure, and function. **Critical Reviews in Plant Sciences**. 27:342–375.

Fitoussi N, de Almeida Engler J, Sichov N, Bucki P, Sela N, Harel A, Belausuv E, Kumar A, Brown Miyara S. (2022). The Minichromosome Maintenance Complex Component 2 (MjMCM2) of *Meloidogyne javanica* is a potential effector regulating the cell cycle in nematode-induced galls. **Scientific Reports**. Jun 2; 12(1):9196. doi: 10.1038/s41598-022-13020-8.

Führer S, Unterhauser J, Zeindl R, Eidelpes R, Fernández-Quintero ML, Liedl KR, Tollinger M. (2022). The Structural Flexibility of PR-10 Food Allergens. **International Journal of Molecular Sciences**. Jul 26; 23(15):8252. doi: 10.3390/ijms23158252.

Doyle EA, Lambert KN. (2003). *Meloidogyne javanica* chorismate mutase 1 alters plant cell development. **Molecular Plant-Microbe Interactions**. Feb; 16(2):123-31. doi: 10.1094/MPMI.2003.16.2.123.

El-Sappah AH, M M I, H El-Awady H, Yan S, Qi S, Liu J, Cheng GT, Liang Y. (2019). Tomato Natural Resistance Genes in Controlling the Root-Knot Nematode. **Genes (Basel)**. Nov 14; 10(11):925. doi: 10.3390/genes10110925.

Escobar C, Barcala M, Cabrera J, Fenoll C. (2015). Overview of root-knot nematodes and giant cells. **Advances in Botanical Research**. 73: 1–32

Fan Z, Gu H, Chen X, Song H, Wang Q, Liu M, Qu LJ, Chen Z. (2005). Cloning and expression analysis of *Zmglp1*, a new germin-like protein gene in maize. **Biochemical and Biophysical Research Communications**. Jun 17; 331(4):1257-63. doi: 10.1016/j.bbrc.2005.04.045.

Favery B, Quentin M, Jaubert-Possamai S, Abad P. (2016). Gall-forming root-knot nematodes hijack key plant cellular functions to induce multinucleate and hypertrophied feeding cells. **Journal of Insect Physiology**. Jan; 84:60-69. doi: 10.1016/j.jinsphys.2015.07.013.

Freitas CDT, Freitas DC, Cruz WT, Porfírio CTMN, Silva MZR, Oliveira JS, Carvalho CPS, Ramos MV. (2017). Identification and characterization of two germin-like proteins with oxalate oxidase activity from *Calotropis procera* latex. **International Journal of Biological Macromolecules**. Dec; 105(Pt 1):1051-1061. doi: 10.1016/j.ijbiomac.2017.07.133.

Gardner, M., Verma, A., and Mitchum, M. G. (2015). Emerging roles of cyst nematode effectors in exploiting plant cellular processes. **Advances in Botanical Research**. 73, 259–291. doi: 10.1016/bs.abr.2014.12.009

1183 Gheysen G, Fenoll C. (2002). Gene expression in nematode feeding sites. **Annual Review of**
1184 **Phytopathology**. 40:191-219. doi: 10.1146/annurev.phyto.40.121201.093719.

1185 Goggin FL, Jia L, Shah G, Hebert S, Williamson VM, Ullman DE. (2006). Heterologous
1186 expression of the *Mi-1.2* gene from tomato confers resistance against nematodes but not aphids
1187 in eggplant. **Molecular Plant-Microbe Interactions**. Apr; 19(4):383-8. doi: 10.1094/MPMI-
1188 19-0383.

1189 Goverse A, Mitchum MG. (2022). At the molecular plant-nematode interface: New players and
1190 emerging paradigms. **Current Opinion in Plant Biology**. Jun; 67:102225. doi:
1191 10.1016/j.pbi.2022.102225.

1192 Goverse A, Smant G. (2014). The activation and suppression of plant innate immunity by
1193 parasitic nematodes. **Annual Review of Phytopathology**. 52:243-65. doi: 10.1146/annurev-
1194 phyto-102313-050118.

1195 Grunewald W, Cannoot B, Friml J, Gheysen G. (2009). Parasitic nematodes modulate PIN-
1196 mediated auxin transport to facilitate infection. **PLoS Pathogens**. Jan; 5(1):e1000266. doi:
1197 10.1371/journal.ppat.1000266.

1198 Haegeman A, Jones JT, Danchin EG. (2011). Horizontal gene transfer in nematodes: a catalyst
1199 for plant parasitism? **Molecular Plant-Microbe Interactions**. Aug; 24(8):879-87. doi:
1200 10.1094/MPMI-03-11-0055.

1201 Haegeman A, Mantelin S, Jones JT, Gheysen G. (2012). Functional roles of effectors of plant-
1202 parasitic nematodes. **Gene**. Jan 15; 492(1):19-31. doi: 10.1016/j.gene.2011.10.040.

1203 Hammes UZ, Schachtman DP, Berg RH, Nielsen E, Koch W, McIntyre LM, Taylor CG. (2005).
1204 Nematode-induced changes of transporter gene expression in Arabidopsis roots. **Molecular**
1205 **Plant-Microbe Interactions**. Dec; 18(12):1247-57. doi: 10.1094/MPMI-18-1247.

1206 Harris MO, Pitzschke A. (2020). Plants make galls to accommodate foreigners: some are
1207 friends, most are foes. **New Phytologist**. Mar; 225(5):1852-1872. doi: 10.1111/nph.16340.

1208 Hoth S, Schneidereit A, Lauterbach C, Scholz-Starke J, Sauer N. (2005). Nematode infection
1209 triggers the *de novo* formation of unloading phloem that allows macromolecular trafficking of
1210 green fluorescent protein into syncytia. **Plant Physiology**. May; 138(1):383-92. doi:
1211 10.1104/pp.104.058800.

Hoth S, Stadler R, Sauer N, Hammes UZ. (2008). Differential vascularization of nematode-induced feeding sites. **Proceedings of the National Academy of Sciences of the United States of America**. Aug 26; 105(34):12617-22. doi: 10.1073/pnas.0803835105.

Hu X, Bidney DL, Yalpani N, Duvick JP, Crasta O, Folkerts O, Lu G. (2003). Overexpression of a gene encoding hydrogen peroxide-generating oxalate oxidase evokes defense responses in sunflower. **Plant Physiology**. Sep; 133(1):170-81. doi: 10.1104/pp.103.024026.

Hussey, R. S., and Mims, C. W. (1990). Ultrastructure of esophageal glands and their secretory granules in the root-knot nematode *Meloidogyne incognita*. **Protoplasma**. 156:9-18.

Ibrahim HMM, Ahmad EM, Martínez-Medina A, Aly MAM. (2019). Effective approaches to study the plant-root knot nematode interaction. **Plant Physiology and Biochemistry**. Aug; 141:332-342. doi: 10.1016/j.plaphy.2019.06.009.

Ilyas M, Ali I, Nasser Binjawhar D, Ullah S, Eldin SM, Ali B, Iqbal R, Bokhari SHA, Mahmood T. (2023). Molecular Characterization of Germin-like Protein Genes in *Zea mays* (ZmGLPs) Using Various *In Silico* Approaches. **ACS Omega**. Apr 26; 8(18):16327-16344. doi: 10.1021/acsomega.3c01104.

Jaouannet M, Rosso MN. (2013). Effectors of root sedentary nematodes target diverse plant cell compartments to manipulate plant functions and promote infection. **Plant Signaling & Behavior**. Sep; 8(9):e25507. doi: 10.4161/psb.25507.

Jaubert S, Milac AL, Petrescu AJ, de Almeida-Engler J, Abad P, Rosso MN. (2005). *In planta* secretion of a calreticulin by migratory and sedentary stages of root-knot nematode. **Molecular Plant-Microbe Interactions**. 18:1277-1284. https://doi.org/10.1094/MPMI-18-1277

Jones JT, Haegeman A, Danchin EG, Gaur HS, Helder J, Jones MG, Kikuchi T, Manzanilla-López R, Palomares-Rius JE, Wesemael WM, Perry RN. (2013). Top 10 plant-parasitic nematodes in molecular plant pathology. **Molecular Plant Pathology**. Dec; 14(9):946-61. doi: 10.1111/mpp.12057.

Jones MGK, Northcote DH. (1972). Multinucleate Transfer Cells Induced in Coleus Roots by the Root-Knot Nematode, *Meloidogyne arenaria*. **Protoplasma**. 75:381–395.

Jones MG, Dropkin VH. (1976). Scanning electron microscopy in nematode-induced giant transfer cells. **Cytobios**. 15:149 –161.

Juergensen K, Scholz-Starke J, Sauer N, Hess P, van Bel AJ, Grundler FM. (2003). The companion cell-specific Arabidopsis disaccharide carrier AtSUC2 is expressed in nematode-induced syncytia. **Plant Physiology**. Jan; 131(1):61-9. doi: 10.1104/pp.008037.

Kaloshian I, Teixeira M. (2019). Advances in Plant-Nematode Interactions with Emphasis on the Notorious Nematode Genus *Meloidogyne*. **Phytopathology**. Dec; 109(12):1988-1996. doi: 10.1094/PHYTO-05-19-0163-IA.

Kikuchi T, Eves-van den Akker S, Jones JT. (2017). Genome Evolution of Plant-Parasitic Nematodes. **Annual Review of Phytopathology**. Aug 4; 55:333-354. doi: 10.1146/annurev-phyto-080516-035434.

Kihika R, Murungi LK, Coyne D, Nganga M, Hassanali A, Teal PEA, Torto B. (2017). Parasitic nematode *Meloidogyne incognita* interactions with different *Capsicum annum* cultivars reveal the chemical constituents modulating root herbivory. **Scientific Reports**. Jun 6; 7(1):2903. doi: 10.1038/s41598-017-02379-8.

Kumar A, Fitoussi N, Sanadhya P, Sichov N, Bucki P, Bornstein M, Belausuv E, Brown Miyara S. (2023). Two Candidate *Meloidogyne javanica* Effector Genes, *MjShKT* and *MjPUT3*: A Functional Investigation of Their Roles in Regulating Nematode Parasitism. **Molecular Plant-Microbe Interactions**. Feb; 36(2):79-94. doi: 10.1094/MPMI-10-22-0212-R.

Kumar V, Irfan M, Datta A. (2019). Manipulation of oxalate metabolism in plants for improving food quality and productivity. **Phytochemistry**. Feb; 158:103-109. doi: 10.1016/j.phytochem.2018.10.029.

Kyndt T, Vieira P, Gheysen G, de Almeida-Engler J. (2013). Nematode feeding sites: unique organs in plant roots. **Planta**. Nov; 238(5):807-18. doi: 10.1007/s00425-013-1923-z.

Lane BG, Bernier F, Dratewka-Kos E, Shafai R, Kennedy TD, Pyne C, Munro JR, Vaughan T, Walters D, Altomare F. (1991). Homologies between members of the germin gene family in hexaploid wheat and similarities between these wheat germins and certain *Physarum spherulins*. **Journal of Biological Chemistry**. Jun 5; 266(16):10461-9.

Lane BG, Dunwell JM, Ray JA, Schmitt MR, Cuming AC. (1993). Germin, a protein marker of early plant development, is an oxalate oxidase. **Journal of Biological Chemistry**. Jun 15; 268(17):12239-42.

Leitão L, Prista C, Moura TF, Loureiro-Dias MC, Soveral G. (2012). Grapevine aquaporins: gating of a tonoplast intrinsic protein (TIP2;1) by cytosolic pH. **PLoS One**. 7(3):e33219. doi: 10.1371/journal.pone.0033219.

Li P, Liu C, Luo Y, Shi H, Li Q, PinChu C, Li X, Yang J, Fan W. (2022). Oxalate in Plants: Metabolism, Function, Regulation, and Application. **Journal of Agricultural and Food Chemistry**. Dec 28; 70(51):16037-16049. doi: 10.1021/acs.jafc.2c04787.

Lilley CJ, Maqbool A, Wu D, Yusup HB, Jones LM, Birch PRJ, Banfield MJ, Urwin PE, Eves-van den Akker S. (2018). Effector gene birth in plant parasitic nematodes: Neofunctionalization of a housekeeping glutathione synthetase gene. **PLoS Genetics**. Apr 11; 14(4):e1007310. doi: 10.1371/journal.pgen.1007310.

Lin B, Zhuo K, Chen S, Hu L, Sun L, Wang X, Zhang LH, Liao J. (2016). A novel nematode effector suppresses plant immunity by activating host reactive oxygen species-scavenging system. **New Phytologist**. Feb; 209(3):1159-73. doi: 10.1111/nph.13701.

Lisei-de-Sá ME, Rodrigues-Silva PL, Morgante CV, de Melo BP, Lourenço-Tessutti IT, Arraes FBM, Sousa JPA, Galbieri R, Amorim RMS, de Lins CBJ, Macedo LLP, Moreira VJ, Ferreira GF, Ribeiro TP, Fragoso RR, Silva MCM, de Almeida-Engler J, Grossi-de-Sa MF. (2021). Pyramiding dsRNAs increases phytonematode tolerance in cotton plants. **Planta**. Nov 15; 254(6):121. doi: 10.1007/s00425-021-03776-0

Lisei-de-Sá ME, Conceição Lopes MJ, de Araújo Campos M, Paiva LV, Dos Santos RM, Beneventi MA, Firmino AA, de Sá MF. (2012). Transcriptome analysis of resistant soybean roots infected by *Meloidogyne javanica*. **Genetics and Molecular Biology**. Jun; 35(1 (suppl)):272-82. doi: 10.1590/S1415-47572012000200008.

Lüdke D, Sakai T, Kourelis J, Toghani A, Adachi H, Posbeyikian A, Frijters R, Pai H, Harant A, Ernst K, Ganal M, Verhage A, Wu C and Kamoun S. (2023). A root-specific NLR network confers resistance to plant parasitic nematodes. **bioRxiv**: doi.org/10.1101/2023.12.14.571630

Milligan SB, Bodeau J, Yaghoobi J, Kaloshian I, Zabel P, Williamson VM. (1998). The root knot nematode resistance gene Mi from tomato is a member of the leucine zipper, nucleotide binding, leucine-rich repeat family of plant genes. **The Plant Cell**. Aug; 10(8):1307-19. doi: 10.1105/tpc.10.8.1307.

Mitchum MG, Hussey RS, Baum TJ, Wang X, Elling AA, Wubben M, Davis EL. (2013). Nematode effector proteins: an emerging paradigm of parasitism. **New Phytologist**. Sep; 199(4):879-894. doi: 10.1111/nph.12323.

Mitchum MG, Liu X. (2022). Peptide Effectors in Phytonematode Parasitism and Beyond. **Annual Review of Phytopathology**. Aug 26; 60:97-119. doi: 10.1146/annurev-phyto-021621-115932.

Molloy B, Baum T, Eves-van den Akker S. (2023). Unlocking the development- and physiology-altering 'effector toolbox' of plant-parasitic nematodes. **Trends in Parasitology**. Sep; 39(9):732-738. doi: 10.1016/j.pt.2023.06.005.

Moreira VJV, Lourenço-Tessutti IT, Basso MF, *et al.*, (2022). Minc03328 effector gene downregulation severely affects *Meloidogyne incognita* parasitism in transgenic *Arabidopsis thaliana*. **Planta**. 255:1–16. https://doi.org/10.1007/S00425-022-03823-4

Moreira VJV, Pinheiro DH, Lourenço-Tessutti IT, Basso MF, Lisei-deSa ME, Silva MCM, Danchin EGJ, Guimaraes PM, Grynberg P, Brasileiro ACM, Macedo LLP, Morgante CV, Almeida-Engler J, Grossi-de-Sa MF. (2023). *In planta* RNAi targeting *Meloidogyne incognita* Minc16803 gene perturbs nematode parasitism and reduces plant susceptibility. **Journal of Pest Science**. https://doi.org/10.1007/ s10340-023-01623-7

Ngou BPM, Ding P, Jones JDG. (2022). Thirty years of resistance: Zig-zag through the plant immune system. **The Plant Cell**. Apr 26; 34(5):1447-1478. doi: 10.1093/plcell/koac041.

Niu J, Liu P, Liu Q, Chen C, Guo Q, Yin J, Yang G, Jian H. (2016). Msp40 effector of root-knot nematode manipulates plant immunity to facilitate parasitism. **Scientific Reports**. 6:19443. https://doi.org/10.1038/srep19443

Nombela G, Williamson VM, Muñiz M. (2003). The root-knot nematode resistance gene Mi-1.2 of tomato is responsible for resistance against the whitefly *Bemisia tabaci*. **Molecular Plant-Microbe Interactions**. Jul; 16(7):645-9. doi: 10.1094/MPMI.2003.16.7.645.

Oota M, Tsai AY, Aoki D, Matsushita Y, Toyoda S, Fukushima K, Saeki K, Toda K, Perfus-Barbeoch L, Favery B, Ishikawa H, Sawa S. (2020). Identification of Naturally Occurring Polyamines as Root-Knot Nematode Attractants. **Molecular Plant**. Apr 6; 13(4):658-665. doi: 10.1016/j.molp.2019.12.010.

Opperman CH, Bird DM, Williamson VM, Rokhsar DS, Burke M, Cohn J, Cromer J, Diener S, Gajan J, Graham S, Houfek TD, Liu Q, Mitros T, Schaff J, Schaffer R, Scholl E, Sosinski

BR, Thomas VP, Windham E. (2008). Sequence and genetic map of *Meloidogyne hapla*: A compact nematode genome for plant parasitism. **Proceedings of the National Academy of Sciences of the United States of America**. Sep 30; 105(39):14802-7. doi: 10.1073/pnas.0805946105.

Opperman CH, Taylor CG, Conkling MA. (1994). Root-knot nematode-directed expression of a plant root-specific gene. **Science**. Jan 14; 263(5144):221-3. doi: 10.1126/science.263.5144.221.

Panstruga R, Moscou MJ. (2020). What is the Molecular Basis of Nonhost Resistance? **Molecular Plant-Microbe Interactions**. Nov; 33(11):1253-1264. doi: 10.1094/MPMI-06-20-0161-CR.

Pei Y, Li X, Zhu Y, Ge X, Sun Y, Liu N, Jia Y, Li F, Hou Y. (2019). GhABP19, a Novel Germin-Like Protein From *Gossypium hirsutum*, Plays an Important Role in the Regulation of Resistance to *Verticillium* and *Fusarium* Wilt Pathogens. **Frontiers in Plant Science**. May 8; 10:583. doi: 10.3389/fpls.2019.00583.

Podgórska A, Burian M, Szal B. (2017). Extra-Cellular But Extra-Ordinarily Important for Cells: Apoplastic Reactive Oxygen Species Metabolism. **Frontiers in Plant Science**. Aug 22; 8:1353. doi: 10.3389/fpls.2017.01353.

Qin X, Xue B, Tian H, Fang C, Yu J, Chen C, Xue Q, Jones J, Wang X. (2022). An unconventionally secreted effector from the root-knot nematode *Meloidogyne incognita*, Mi-ISC-1, promotes parasitism by disrupting salicylic acid biosynthesis in host plants. **Molecular Plant Pathology**. Apr; 23(4):516-529. doi: 10.1111/mpp.13175.

Quentin, M., Abad, P., and Favery, B. (2013). Plant parasitic nematode effectors target host defense and nuclear functions to establish feeding cells. **Frontiers in Plant Science**. 4:53

Rhodes J, Zipfel C, Jones JDG, Ngou BPM. (2022). Concerted actions of PRR- and NLR-mediated immunity. **Essays in Biochemistry**. Sep 30; 66(5):501-511. doi: 10.1042/EBC20220067.

Ribeiro C, de Melo BP, Lourenço-Tessutti IT, Ballesteros HF, Ribeiro KVG, Menuet K, Heyman J, Hemerly A, de Sá MFG, De Veylder L, de Almeida Engler J. (2024). The regeneration conferring transcription factor complex ERF115-PAT1 coordinates a wound-induced response in root-knot nematode induced galls. **New Phytologist**. Jan; 241(2):878-895. doi: 10.1111/nph.19399.

Rodiuc N, Vieira P, Banora MY, de Almeida Engler J. (2014). On the track of transfer cell formation by specialized plant-parasitic nematodes. **Frontiers in Plant Science**. May 5; 5:160. doi: 10.3389/fpls.2014.00160.

Rutter WB, Franco J, Gleason C. (2022). Rooting Out the Mechanisms of Root-Knot Nematode-Plant Interactions. **Annual Review of Phytopathology**. 60: 43–76.

Sanchez-Puerta MV, Masuelli RW. (2011). Evolution of nematode-resistant Mi-1 gene homologs in three species of *Solanum*. **Molecular Genetics and Genomics**. Mar; 285(3):207-18. doi: 10.1007/s00438-010-0596-6.

Sato K, Kadota Y, Shirasu K. (2019). Plant Immune Responses to Parasitic Nematodes. **Frontiers in Plant Science**. Sep 26; 10:1165. doi: 10.3389/fpls.2019.01165.

Singh RR, Pajar JA, Audenaert K, Kyndt T. (2021). Induced Resistance by Ascorbate Oxidation Involves Potentiating of the Phenylpropanoid Pathway and Improved Rice Tolerance to Parasitic Nematodes. **Frontiers in Plant Science**. Aug 11; 12:713870. doi: 10.3389/fpls.2021.713870.

Smith PG. (1944). Embryo culture of a tomato species hybrid. **Proceedings of the American Society for Horticultural Science**. 44:413-416

Swart S, Logman TJ, Smit G, Lugtenberg BJ, Kijne JW. (1994). Purification and partial characterization of a glycoprotein from pea (*Pisum sativum*) with receptor activity for rhicadhesin, an attachment protein of *Rhizobiaceae*. **Plant Molecular Biology**. Jan; 24(1):171-83. doi: 10.1007/BF00040583.

Thompson EW, Lane BG. (1980). Relation of protein synthesis in imbibing wheat embryos to the cell-free translational capacities of bulk mRNA from dry and imbibing embryos. **Journal of Biological Chemistry**. Jun 25; 255(12):5965-70.

Torabi S, Seifi S, Geddes-McAlister J, Tenuta A, Wally O, Torkamaneh D, Eskandari M. (2023). Soybean-SCN Battle: Novel Insight into Soybean's Defense Strategies against *Heterodera glycines*. **International Journal of Molecular Sciences**. Nov 12; 24(22):16232. doi: 10.3390/ijms242216232.

Vashisth S, Kumar P, Chandel VGS, Kumar R, Verma SC, Chandel RS. (2024). Unraveling the enigma of root-knot nematodes: from origins to advanced management strategies in agriculture. **Planta**. Jun 26; 260(2):36. doi: 10.1007/s00425-024-04464-5.

Velloso JA, Maquilan MAD, Campos VP, Brito JA, Dickson DW. (2022). Temperature Effects on Development of *Meloidogyne Enterolobii* and *M. Floridensis*. **Journal of Nematology**. Jun 10; 54(1):20220013. doi: 10.2478/jofnem-2022-0013.

Xu L, Zhu L, Tu L, Liu L, Yuan D, Jin L, Long L, Zhang X. (2011). Lignin metabolism has a central role in the resistance of cotton to the wilt fungus *Verticillium dahliae* as revealed by RNA-Seq-dependent transcriptional analysis and histochemistry. **Journal of Experimental Botany**. Nov; 62(15):5607-21. doi: 10.1093/jxb/err245.

Xue B, Hamamouch N, Li C, Huang G, Hussey RS, Baum TJ, Davis EL. (2013). The 8D05 parasitism gene of *Meloidogyne incognita* is required for successful infection of host roots. **Phytopathology**. Feb; 103(2):175-81. doi: 10.1094/PHYTO-07-12-0173-R.

Wang J, Hu M, Wang J, Qi J, Han Z, Wang G, Qi Y, Wang HW, Zhou JM, Chai J. (2019). Reconstitution and structure of a plant NLR resistosome conferring immunity. **Science**. Apr 5; 364(6435):eaav5870. doi: 10.1126/science.aav5870.

Williamson VM, Hussey RS. (1996). Nematode pathogenesis and resistance in plants. **The Plant Cell**. Oct; 8(10):1735-45. doi: 10.1105/tpc.8.10.1735.

Williamson VM, Kumar A. (2006). Nematode resistance in plants: the battle underground. **Trends in Genetics**. Jul; 22(7):396-403. doi: 10.1016/j.tig.2006.05.003.

Wu CH, Abd-El-Haliem A, Bozkurt TO, Belhaj K, Terauchi R, Vossen JH, Kamoun S. (2017). NLR network mediates immunity to diverse plant pathogens. **Proceedings of the National Academy of Sciences of the United States of America**. Jul 25; 114(30):8113-8118. doi: 10.1073/pnas.1702041114.

Zhang Y, Wang X, Chang X, Sun M, Zhang Y, Li W, Li Y. (2018). Overexpression of *germin-like protein GmGLP10* enhances resistance to *Sclerotinia sclerotiorum* in transgenic tobacco. **Biochemical and Biophysical Research Communications**. Feb 26; 497(1):160-166. doi: 10.1016/j.bbrc.2018.02.046.

Zhao J, Li L, Liu Q, *et al.*, (2019). A MIF-like effector suppresses plant immunity and facilitates nematode parasitism by interacting with plant annexins. **Journal of Experimental Botany**. 70:5943–5958. https://doi.org/10.1093/jxb/erz348

Zhao J, Sun Q, Quentin M, Ling J, Abad P, Zhang X, Li Y, Yang Y, Favery B, Mao Z, Xie B. (2021). A *Meloidogyne incognita* C-type lectin effector targets plant catalases to promote parasitism. **New Phytologist**. Dec; 232(5):2124-2137. doi: 10.1111/nph.17690.

OBJETIVO GERAL

Analisar funcionalmente os papéis de genes efetores de *M. incógnita* e do genótipo de soja PI 595099 visando o desenvolvimento de novas estratégias a serem aplicadas em plantas de soja e algodão.

OBJETIVOS ESPECÍFICOS

- ✓ Validação do silenciamento gênico pós-transcricional, via RNAi, do gene efetor *Minc03328* de *M. incognita* em linhagens transgênicas de *Arabidopsis thaliana*;

- ✓ Validação do silenciamento gênico pós-transcricional, via RNAi, do putativo gene efetor *Minc16803* de *M. incognita* em linhagens transgênicas de *Arabidopsis thaliana*;

- ✓ Validação e caracterização molecular do gene *Germin-like protein subfamily 1 member 10*, proveniente do genótipo resistente de soja PI 595099, em planta modelo.

1451

INFOGRÁFICO DOS CAPÍTULOS II E III

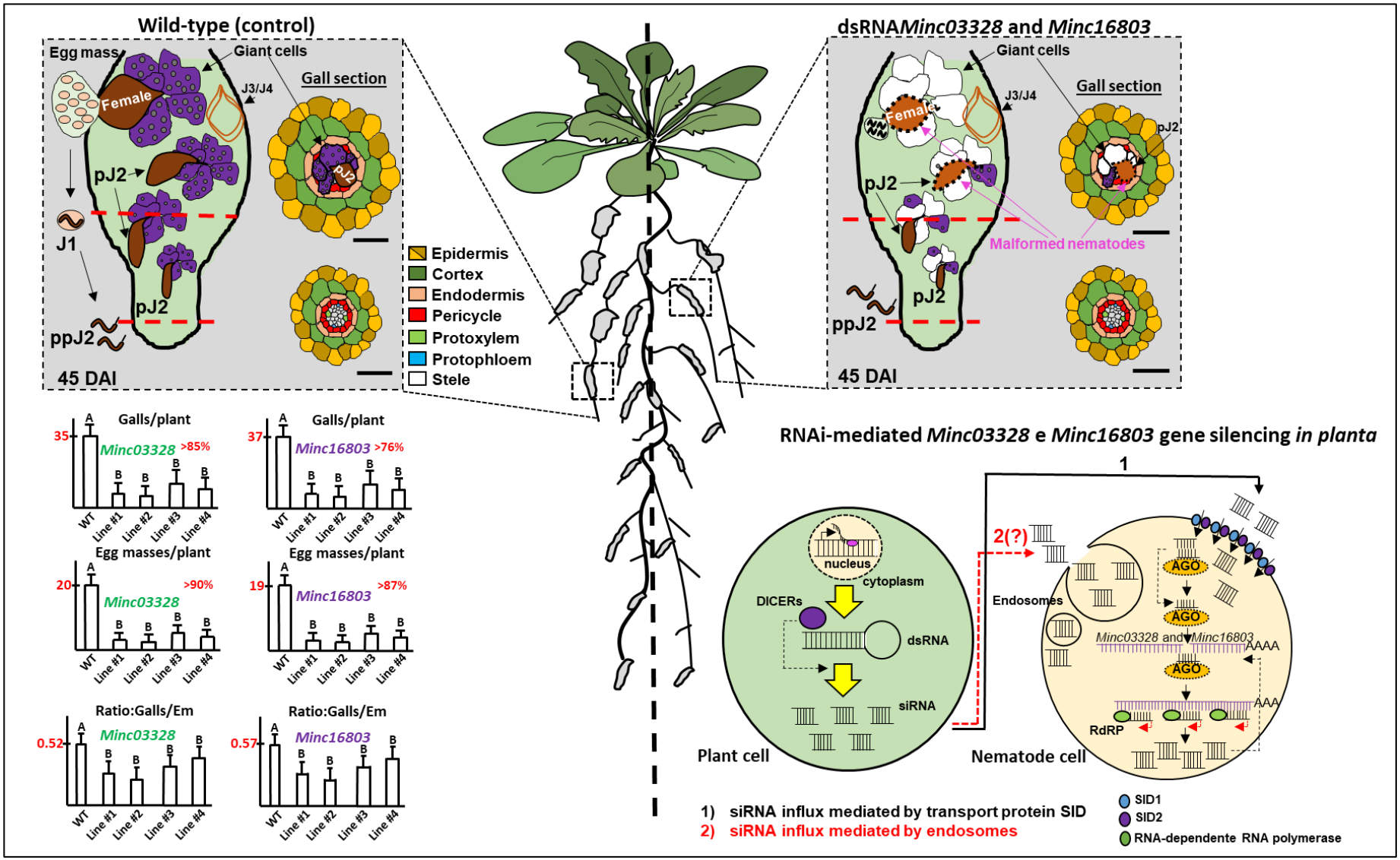

Para os estudos que integram os capítulos II e III desta tese, descrevemos os genes *Minc03328* e *Minc16803* de *M. incógnita* como importantes e promissores alvos gênicos pela tecnologia do RNA de interferência. Linhagens transgênicas de *A. thaliana* expressando duplas-fitas de RNA (dsRNA), contra ambos alvos, demonstraram uma redução de suas susceptibilidades em mais de 90% para *Minc03328*, enquanto o silenciamento de *Minc16803* mostrou uma redução em mais 87% em termos do parâmetro reprodutivo. Interessante, constatamos que ambos produtos gênicos podem estar implicados na manutenção de CG, uma vez que seus silenciamentos foram capazes de infringir na integridade dos sítios de alimentação. Por meio dos exames histopatológicos, confirmamos ainda outros efeitos diretos na morfologia do nematoides (hipodermes e massas de ovos), bem como nos tecidos vasculares de plantas (em destaque ao xilema). Apesar da atividade das proteínas DICERs de plantas intervirem no endereçamento estável de longos dsRNAs *in planta*, pequenos siRNAs gerados em células vegetais podem ser absorvidos via transportadores semelhantes a SID1 e SID2 de nematoides, tornando parte do complexo RISC (*RNA-induced silencing complex* - composto pelas proteínas Argonaute) e desencadear a clivagem do transcrito alvo compatível a fita guia do siRNA incorporado no complexo RISC. Ademais, RNA polimerases dependentes de RNA (RdRP) auxiliam na amplificação de novas moléculas de dsRNA em células do nematoide gerando novos fragmentos de siRNA, que serão disseminados de forma sistêmicas.

CAPÍTULO II

Minc03328 EFFECTOR GENE DOWNREGULATION SEVERELY AFFECTS *Meloidogyne incognita* PARASITISM IN TRANSGENIC *ARABIDOPSIS THALIANA*

Published article

Valdeir Junio Vaz Moreira, Isabela Tristan Lourenço-Tessutti, Marcos Fernando Basso, Maria Eugênia Lisei-de-Sá, Carolina Vianna Morgante, Bruno Paes-de-Melo, Fabrício Barbosa Monteiro Arraes, Diogo Martins-de-Sá, Maria Cristina Mattar Silva, Janice de Almeida-Engler, Maria Fatima Grossi-de-Sa. (2022). *Minc03328* effector gene downregulation severely affects *Meloidogyne incognita* parasitism in transgenic *Arabidopsis thaliana*. **PLANTA**. 255:44. doi.org/10.1007/s00425-022-03823-4

Pages 58 to 73

ABSTRACT

Meloidogyne incognita is the most economically important species of root-knot nematodes (RKN) and causes severe damage to crops worldwide. *M. incognita* secretes several effector proteins to suppress the host plant defense response, and manipulate the plant cell cycle and other plant processes facilitating its parasitism. Different secreted effector proteins have already been identified in *M. incognita*, but not all have been characterized or have had the confirmation of their involvement in nematode parasitism in their host plants. Herein, we characterized the *Minc03328* (*Minc3s00020g01299*) effector gene, confirmed its higher expression in the early stages of *M. incognita* parasitism in plants, as well as the accumulation of the Minc03328 effector protein in subventral glands and its secretion. We also discuss the potential for simultaneous downregulation of its paralogue *Minc3s00083g03984* gene. Using the *in planta* RNA interference strategy, *Arabidopsis thaliana* plants overexpressing double-stranded RNA (dsRNA) were generated to specifically targeting and downregulating the *Minc03328* gene during nematode parasitism. Transgenic *Minc03328-dsRNA* lines that significantly downregulated *Minc03328* gene expression during *M. incognita* parasitism were significantly less susceptible. The number of galls, egg masses, and [galls/ egg masses] ratio were reduced in these transgenic lines by up to 85%, 90%, and 87%, respectively. Transgenic *Minc03328-dsRNA* lines showed the presence of fewer and smaller galls, indicating that parasitism was hindered. Overall, data herein strongly suggest that Minc03328 effector protein is important for *M. incognita* parasitism establishment. As well, the *in planta Minc03328-dsRNA* strategy demonstrated high biotechnological potential for developing crop species that could efficiently control RKN in the field.

RESUMO

Meloidogyne incognita é a espécie economicamente mais importante dos nematoides formadores de galhas (NFGs), causando graves danos às culturas em todo o mundo. *M. incognita* secreta diversas proteínas efetoras para suprimir a resposta de defesa da planta hospedeira e manipular o ciclo celular da planta e outros processos da planta facilitando seu parasitismo. Diferentes proteínas efetoras secretadas já foram identificadas em *M. incognita*, mas nem todas foram caracterizadas ou tiveram a confirmação de seu envolvimento no parasitismo de nematoides em suas plantas hospedeiras. Aqui, caracterizamos o gene efetor *Minc03328* (*Minc3s00020g01299*), confirmamos sua maior expressão nos estádios iniciais do parasitismo de *M. incognita* em plantas, bem como o acúmulo da proteína efetora Minc03328 nas glândulas subventrais e sua secreção. Também discutimos o potencial de regulação negativa simultânea de seu gene parálogo *Minc3s00083g03984*. Usando a estratégia de interferência de RNA *in planta*, linhagens de *Arabidopsis thaliana* superexpressando RNA de fita dupla (dsRNA) foram geradas para direcionar e regular negativamente o gene *Minc03328* durante o parasitismo de nematoides. As linhas transgênicas *Minc03328-dsRNA* que reduziram significativamente a expressão do gene *Minc03328* durante o parasitismo por *M. incognita* foram significativamente menos suscetíveis. O número de galhas, massas de ovos e proporção [galhas/massas de ovos] foram reduzidos nessas linhagens transgênicas em até 85%, 90% e 87%, respectivamente. As linhas transgênicas *Minc03328-dsRNA* a presença de menos galhas e menores, indicando que o parasitismo foi prejudicado. No geral, os dados aqui sugerem fortemente que a proteína efetora Minc03328 é importante para o estabelecimento do parasitismo por *M. incognita*. Além disso, a estratégia *Minc03328-dsRNA in planta* demonstrou alto potencial biotecnológico para o desenvolvimento de espécies agrícolas que poderiam controlar eficientemente o NFG no campo.

Planta (2022) 255:44
https://doi.org/10.1007/s00425-022-03823-4

ORIGINAL ARTICLE

Minc03328 effector gene downregulation severely affects *Meloidogyne incognita* parasitism in transgenic *Arabidopsis thaliana*

Valdeir Junio Vaz Moreira[1,2,3] · Isabela Tristan Lourenço-Tessutti[1,4] · Marcos Fernando Basso[1,4] · Maria Eugênia Lisei-de-Sa[1,3,5] · Carolina Vianna Morgante[1,4,6] · Bruno Paes-de-Melo[1,7] · Fabrício Barbosa Monteiro Arraes[1,2,4] · Diogo Martins-de-Sa[1,3] · Maria Cristina Mattar Silva[1,4] · Janice de Almeida Engler[4,8] · Maria Fatima Grossi-de-Sa[1,4,9]

Received: 30 October 2021 / Accepted: 4 January 2022 / Published online: 20 January 2022

Abstract

Main conclusion ***Minc03328* effector gene downregulation triggered by *in planta* RNAi strategy strongly reduced plant susceptibility to *Meloidogyne incognita* and suggests that *Minc03328* gene is a promising target for the development of genetically engineered crops to improve plant tolerance to *M. incognita*.**

Abstract *Meloidogyne incognita* is the most economically important species of root-knot nematodes (RKN) and causes severe damage to crops worldwide. *M. incognita* secretes several effector proteins to suppress the host plant defense response, and manipulate the plant cell cycle and other plant processes facilitating its parasitism. Different secreted effector proteins have already been identified in *M. incognita*, but not all have been characterized or have had the confirmation of their involvement in nematode parasitism in their host plants. Herein, we characterized the *Minc03328* (*Minc3s00020g01299*) effector gene, confirmed its higher expression in the early stages of *M. incognita* parasitism in plants, as well as the accumulation of the Minc03328 effector protein in subventral glands and its secretion. We also discuss the potential for simultaneous downregulation of its paralogue *Minc3s00083g03984* gene. Using the *in planta* RNA interference strategy, *Arabidopsis thaliana* plants overexpressing double-stranded RNA (dsRNA) were generated to specifically targeting and downregulating the *Minc03328* gene during nematode parasitism. Transgenic Minc03328-dsRNA lines that significantly downregulated *Minc03328* gene expression during *M. incognita* parasitism were significantly less susceptible. The number of galls, egg masses, and [galls/egg masses] ratio were reduced in these transgenic lines by up to 85%, 90%, and 87%, respectively. Transgenic Minc03328-dsRNA lines showed the presence of fewer and smaller galls, indicating that parasitism was hindered. Overall, data herein strongly suggest that Minc03328 effector protein is important for *M. incognita* parasitism establishment. As well, the *in planta* Minc03328-dsRNA strategy demonstrated high biotechnological potential for developing crop species that could efficiently control RKN in the field.

Keywords Crop protection · Effector protein · *In planta* RNAi · New biotechnological tools · Plant–nematode interaction · Root-knot nematode

Abbreviations

DAI	Days after inoculation
eGFP	Enhanced green fluorescent protein
pJ2	Parasitic second-stage juvenile
ppJ2	Pre-parasitic second-stage juvenile
RKN	Root-knot nematode

Introduction

Plant–parasitic nematodes (PPNs) are one of the major agricultural pathogens in several crops, causing annually significant economic losses worldwide (Bernard et al. 2017). Among them, root-knot nematodes (RKN) comprises several obligate sedentary endoparasites from the genus

Communicated by Dorothea Bartels.

✉ Maria Fatima Grossi-de-Sa
fatima.grossi@embrapa.br

Extended author information available on the last page of the article

Meloidogyne spp. (Trudgill and Blok 2001). *Meloidogyne incognita* is the most reported species infecting several economically important crops such as cotton, eggplant, and soybean (Abad et al. 2008). Its life cycle consists of the following stages: egg, ppJ2 (pre-parasitic second-stage juveniles), pJ2 (parasitic second-stage juveniles), J3, and J4 non-feeding juveniles, and females. The pJ2, J3, and J4 parasitic stages, and females are typically sedentary endophytes, while eggs and ppJ2 are exophytes (Triantaphyllou and Hirschmann 1960; Castagnone-Sereno et al. 2013). During a compatible interaction, RKNs disrupt root cells by hyper activating their cell cycle, increasing the parasitized cells size called giant-feeding cells, causing surrounding vascular cell hyperproliferation, forming feeding sites within root swellings named-galls (Engler et al. 2012; Shukla et al. 2018). Consequently, these nematode-infected roots are disrupted on water, and nutrient uptake and, consequently, plants reduced growth and yield (Melakeberhan et al. 1987; Carneiro et al. 2002; Lu et al. 2014).

For successful parasitism, *M. incognita* secrete a cocktail of effector proteins that act in *trans* to manipulate different biological processes and defense responses of the host plants (Nguyen et al. 2018; Grossi-de-Sa et al. 2019; Zhao et al. 2019). Genome data mining and secretome analyses from *M. incognita* pJ2s allowed the identification of several candidate effector proteins (Huang et al. 2003; Bellafiore et al. 2008; Rutter et al. 2014). For example, Bournaud et al. (2018) showed that the MiPM effector protein interacts with the soybean CSN5 subunit of the COP9 signalosome protein to facilitate *M. incognita* penetration and parasitism in host plants. Mendes et al. (2021b) reported that MiEFF1/Minc17998 effector protein interacts with soybean GmHub6 protein to promote *M. incognita* parasitism in host plants. Truong et al. (2021) demonstrated that the MiEFF1 effector protein also interacts with *Arabidopsis thaliana* cytosolic glyceraldehyde-3-phosphate dehydrogenase proteins promoting *M. incognita* parasitism in plants. Mendes et al. (2021a) verified that the Minc00344 and Mj-NULG1a effector proteins interact with GmHub10 protein to promote the *M. incognita* and *M. javanica* parasitism in soybean. Interestingly, the downregulation of the *Minc01696*, *Minc00344*, or *Minc00801* effector genes using *in planta* RNAi (RNAi, host induced gene silencing) strategy in stable transgenic tobacco and soybean hairy roots strongly disturbed *M. incognita* parasitism (unpublished data). Rutter et al. (2014) revealed that the *Minc03328* effector gene expression was significantly upregulated during *M. incognita* parasitism in plants, ranging from 3 to 14 days after inoculation (DAI), followed by a strong post-transcriptional regulation at 21 DAI. In addition, Rutter et al. (2014) also indicated that *Minc03328* effector transcript specifically accumulated into *M. incognita* subventral glands (SvG) of pJ2 and J3 stages. Despite this interesting preliminary information, the importance of the Minc03328 effector protein for successful parasitism of *M. incognita* in host plants has been not yet further investigated.

Herein, we applied *in planta* RNAi strategy for the production of double-stranded RNA (dsRNA) to target and downregulate *Minc03328* effector transcripts in *M. incognita* during plant parasitism. We then evaluated the importance of this effector for *M. incognita* parasitism in these transgenic plants. Stable transgenic *A. thaliana* lines, overexpressing a dsRNA capable of producing siRNAs molecules targeting and posttranscriptionally regulating *Minc03328* gene were successfully generated, and the susceptibility level of these transgenic Minc03328-dsRNA lines to *M. incognita* was assessed. Morphological analyzes illustrated that downregulation of *Minc03328* affected nematode as well as gall morphology, and immunocytochemical analysis localized Minc03328 protein in the nematode SvG and its secretion *in planta*. Thus, the importance of the Minc03328 effector protein in the *M. incognita versus* host plant interaction and its potential biotechnological use via *in planta* RNAi strategy in economically important crops are herein discussed.

Materials and methods

Sequence features

Minc03328 effector gene, its paralogue *Minc3s00083g03984* gene, and their orthologous genes were retrieved from BioProject ID PRJEB8714 (sample: ERS1696677) (Blanc-Mathieu et al. 2017) from WormBase Parasite Database version WBPS13 (Lee et al. 2017). Subsequently, conserved domains were identified using CDD Database from NCBI (Marchler-Bauer et al. 2015), PFAM Database from EMBL-EBI (El-Gebali et al. 2018), and InterPro Scan (Blum et al. 2020), while nuclear export signal (NES) was predicted with cutoff 0.5 using NetNES 1.1 Server (la Cour et al. 2004), and nuclear localization signal (NLS) was predicted with cutoff 0.5 using NLStradamus online tool (Nguyen Ba et al. 2009). The secretory proteins were predicted using MatureP tool (http://www.stepdb.eu/MatureP.php) (Orfanoudaki et al. 2017). For inferring potential orthologous and paralogous genes corresponding to each effector studied here, comparative genomic trees were generated from BioProject PRJEB8714 (Blanc-Mathieu et al. 2017) by the WormBase ParaSite Database using the Ensembl Compara tools implemented in this database (Vilella et al. 2009) and using default parameters.

Minc03328 in silico expression level

The expression levels of the *Minc03328* effector gene and its paralogue *Minc3s00083g03984* gene in different *M.*

incognita life stages were determined using transcriptome datasets from BioProject number: PRJNA390559 (Choi et al. 2017) retrieved of the BioSample database (NCBI). Particularly, 15 transcriptome libraries from *M. incognita* egg, J2, pJ2/J3, J4, and female stages were generated by Choi et al. (2017) using Truseq RNA Sample Prep Kit (Illumina), and mRNAs were paired-end sequenced (2 × 101 nucleotides) using Illumina HiSeq 2000 technology. The raw data (fastq files) were downloaded from NCBI using the following accession numbers: egg stage: SRR5684407, SRR5684403, and SRR5684417; J2 stage: SRR5684416, SRR5684412, and SRR5684414; pJ2/J3 stage: SRR5684413, SRR5684415, and SRR5684404; J4 stage: SRR5684408, SRR5684406, and SRR5684405; and female stage: SRR5684410, SRR5684409, and SRR5684411. Fastq files were trimmed using Trimmomatic version 0.39 (Bolger et al. 2014). The quantification was performed by the Kallisto program version 0.43.0 (Bray et al. 2016) using a genome reference retrieved from WormBase Parasite Database (BioProject ID PRJEB8714) (Szitenberg et al. 2017). The target gene expression in different nematode life stages was estimated as transcript per million (TPM) by the Kallisto program.

Histopathological analysis of *Nicotiana tabacum* roots infected with *M. incognita*

N. tabacum var. SR1 Petit Havana plants were inoculated with 1.000 *M. incognita* ppJ2 and maintained under greenhouse conditions. Infected root tips were harvested during nematode parasitism at 0, 5, 10, 15, and 22 DAI, washed in water, slightly dried with a paper towel, and stained with acid fuchsin, according to Bybd et al. (1983). Then, root samples were immersed in 2.5% (*v/v*) sodium hypochlorite solution for clarification and washed with water for 10 min. Finally, roots were completely immersed in acid fuchsin solution (1.25 g acid fuchsin solubilized in 1:3 v/v glacial acetic acid and distilled water). For improved root staining, samples were gently heated in a microwave for 1 min. After staining, acid fuchsin solution was discarded, and roots were rinsed and transferred to acidified glycerol solution (24:1 glycerol and hydrochloric acid, v/v). Histopathological analyses were performed by bright-field microscopy and images were generated by a Zeiss AxioCam MR.

Minc03328 expression profile during *M. incognita* parasitism in *N. tabacum*

Total RNA was extracted using Quick-RNA™ Plant Miniprep kit (Zymo Research, Irvine, CA, USA) from *M. incognita* eggs, ppJ2, and infected *N. tabacum* galls at 5, 10, 15, and 22 DAI. The RNA concentration was estimated using a spectrophotometer (NanoDrop 2000, Thermo Scientific, Waltham, MA, USA), and integrity was evaluated with 1% agarose gel electrophoresis. RNA samples were treated with RNase-free RQ1 DNase I (Promega, Madison, WI, USA), according to the manufacturer's instructions. DNase-treated RNA was used as template for cDNA synthesis using Oligo-$(dT)_{20}$ primer (100 µM), random hexamers (50 µM), and SuperScript III RT (Life Technologies, Carlsbad, CA, USA), according to the manufacturer's instructions. After synthesis, cDNA samples were diluted at 1:10 with nuclease-free water. RT-qPCR assays were performed in Applied Biosystems 7500 Fast Real-Time PCR System (Applied Biosystems, Foster City, CA, USA) using 2 µl cDNA, 0.2 µM gene-specific primer (Suppl. Table S1), and GoTaq® qPCR Master Mix (Promega, Madison,WI, USA). Gene expression level was normalized using *Mi18S* and *MiGAPDH* as endogenous reference genes. Three biological replicates were used for each treatment, composed of four plants that totaled at least 50 galls. All cDNA samples were carried out in technical triplicate, while primer efficiencies were previously determined and target-specific amplification was confirmed by a single and distinct peak in the melting curve analysis. The relative expression level was calculated using 2^-ΔCT method (Schmittgen and Livak 2008). The data were subjected by variance analysis (ANOVA) and, when significant, means were compared using Tukey test at 5% significance level using SASM-Agri statistical package (Canteri et al. 2001).

Minc03328 effector protein immunolocalization in *M. incognita*

M. incognita-infected galls at 1, 5, and 10 DAI from wild-type *A. thaliana* plants and uninfected roots were collected and fixed in 4% (v/v) formaldehyde in 50 mM PIPES buffer pH 6.9 (Sigma-Aldrich, St. Louis, MO, USA). Then, these galls were dehydrated and embedded in butyl methylmethacrylate essentially as described by Kronenberger et al. (1993) and Vieira et al. (2012). A primary anti-Minc03328 polyclonal antibody was produced in rabbits by GenScript (Leiden, The Netherlands) for use in this study, where a short amino acid sequence (14 aa length) with low sequence identity to other *M. incognita* or plant proteins was selected (Suppl. File S1). The anti-Minc03328 antibody and a commercial secondary antibody goat anti-rabbit IgG conjugated with Alexa 488 (Molecular Probes, Eugene, OR, USA) were diluted 20- and 300-fold, respectively, in blocking solution (1% w/v bovine serum albumin in 50 mM PIPES buffer pH 6.9 (Sigma-Aldrich, St. Louis, MO, USA), and 0.2% v/v DMSO). As a negative control, the primary antibody was omitted in some slides. Galls sections (5 µm) were incubated for 30 min in acetone, and adhered tissues were rehydrated in decreasing absolute ethanol concentrations. Slides were then washed twice for 15 min in PIPES buffer pH 6.9 (Sigma-Aldrich) and blocked with blocking buffer (2% w/v bovine

serum albumin in PIPES buffer, pH 6.9) for 3 h incubating at room temperature. Sections were then incubated overnight with primary antibody at 4 °C and then 1 h at 37 °C. Next, a 2 h incubation at 37 °C was performed with a secondary antibody. DNA was stained with 1 µg/mL 4',6-diamidino-2-phenylindole (Sigma-Aldrich) in water. Finally, slides were quickly washed in distilled water to remove salts and gently coverslipped in 90% (*v*/*v*) glycerol for observation under an Axioplan (Zeiss, Jena, Germany) equipped for epifluorescence microscopy. Images were acquired with an Axiocam digital camera (Zeiss).

Agrobacterium-mediated genetic transformation of *A. thaliana* to generate Minc03328-dsRNA lines

The binary vector (named GS62658-4 virMinc03328) was synthesized and assembled by Epoch Life Science (Missouri, TX, USA), and subsequently transfected into *A. tumefaciens* strain GV3101. A 200 bp fragment from *Minc03328* encoding sequence was chosen as dsRNA template to activate *in planta* RNAi strategy (Suppl. Table S2). BLASTp and BLASTn analyses from NCBI and WormBase databases were performed to evaluate sequence similarity to other metazoans and *A. thaliana* genes to minimize off-target silencing. Then, this 200 bp fragment was cloned in sense and antisense strands separated by the *pdk intron* and under control of constitutive *pUceS8.3* promoter (Grossi-de-Sa et al. 2013) (Fig. 2a). The *hptII* gene (hygromycin resistance) was used as a selection marker gene under control of the *pUbi3* promoter, while enhanced *green fluorescent protein* (*eGFP*) gene was used as molecular marker protein in transgenic Minc03328-dsRNA lines (Fig. 2a). The *A. thaliana* ecotype Col-0 inflorescences were genetically transformed by the floral dip method (Clough and Bent 1998). Then, seeds from *A. thaliana* lines were screened in vitro using 15 mg/L hygromycin B (Invitrogen, Carlsbad, CA, USA) according to Harrison et al. (2006). Subsequently, hygromycin-resistant plants were acclimated in pots containing commercial substrate and maintained in a growth room (22 °C, 70–75% relative humidity, and ~ 100 µmol photons m^{-2} s^{-1} light intensity with a 16/8 h photoperiod). Acclimated plants were screened by PCR using specific primers targeting *eGFP* gene (Suppl. Table S1) and GoTaq® DNA Polymerase mix (Promega, Madison, WI, USA). Total DNA was purified from *A. thaliana* leaves according to Doyle and Doyle method (1987). Amplicons were analyzed in 1% agarose gel electrophoresis stained with ethidium bromide. In addition, GFP protein accumulation in transgenic lines was confirmed under a Zeiss inverted LSM510 META laser scanning microscope using 488-nm excitation line and 500–530-nm band-pass filter (Zeiss). Finally, several independent transgenic lines were generated, T_1-to-T_3 generations were advanced, and four homozygous T_3 transgenic Minc03328-dsRNA lines were selected for bioassays with *M. incognita* race 3.

Minc03328-dsRNA transgenic plants' inoculation and susceptibility assessment

M. incognita ppJ2 race 3 were obtained from tomato plants (*Solanum lycopersicum* cv. Santa Clara) inoculated and maintained for 2 or 3 months under greenhouse conditions (25–37 °C, 12–16 h light, ~ 70% humidity). The infected 60–90-day-old roots were washed and ground using a blender after treatment with 0.5% sodium hypochlorite. Eggs were harvested, rinsed with tap water, and subsequently separated from root debris using 100–550 µm sieves (Hussey and Barker 1973). The eggs were then hatched under aerobic conditions incubating at 28 °C, and ppJ2 were harvested every 2 days, gently decanted at 4 °C, and quantified under a microscope using counting chambers. *A. thaliana* plants from four transgenic Minc03328-dsRNA lines ($n = 5$–20 plants) additional to wild-type control plants were inoculated with 500 M. *incognita* ppJ2 race 3 suspended in distilled water. Plant susceptibility level to *M. incognita* was evaluated at 60 DAI measuring number of galls per plant, number of egg masses per plant and, then, calculating [galls/egg masses number] ratio. Then, data were subjected to ANOVA analysis, and when significant, means were compared by the Tukey test at 5% significance level using SASM-Agri statistical package (Canteri et al. 2001).

The transgene expression and *Minc03328* gene downregulation

Total RNA was extracted from transgenic and wild-type galls at 5 DAI using TRIzol (Life Technologies, Carlsbad, CA, USA), according to the manufacturer's recommendations. The transgene expression in transgenic *A. thaliana* lines was confirmed by RT-qPCR analysis using specific primers to target *pdk intron* sequence. The relative expression values of the transgene were normalized using *AtActin 2*, *AtGAPDH*, and *AtEF1* as reference endogenous genes (Suppl. Table S1). In another hand, *Minc03328* gene downregulation in *M. incognita* during its parasitism in transgenic *A. thaliana* lines was confirmed by RT-qPCR analysis using *MiGAPDH*, *MiActin,* and *Miβ-tubulin* as reference endogenous genes (Suppl. Table S1). All Ct values were corrected according to primer's efficiencies using the Miner tool (http://www.miner.ewindup.info), and relative gene expression was calculated using 2^-ΔCT method (Schmittgen and Livak 2008) as described above. Normalized expression data obtained from *A. thaliana* and *M. incognita* reference genes were generated using geNorm software (St-Pierre et al. 2017) with *M-values* assigned between 0.4 and 0.7. Each

treatment was composed of three biological replicates, while each biological replicate included three plants. All samples were evaluated in technical triplicates.

Gall morphology analysis of Minc03328-dsRNA transgenic *A. thaliana*

The *M. incognita*-induced galls in *A. thaliana* transgenic line #1 and wild-type control plants were excised from 45 DAI plants and fixed in 2% (*v*/*v*) glutaraldehyde in 50 mM PIPES buffer pH 6.9 (Sigma-Aldrich) for 1 week. Fixed galls were then dehydrated using an ethanol gradient (10, 30, 50, 70, 90, and 100%; *v*/*v*) and embedded in Technovit 7100 resin (Kulzer, Friedrichsdorf, Germany), according to the manufacturer's recommendations. Then, galls sections (5 µm) were stained in 0.05% (*w*/*v*) toluidine blue in 100 mM sodium phosphate buffer (pH 5.5) and rinsed in distilled water. Slides were mounted with Depex (Sigma-Aldrich, St. Louis, MO, USA). Stained sections were observed under bright-field light microscopy, and images were obtained with a digital AxioCamHRc camera for morphological analyses (Carl Zeiss, Oberkochen, Germany). At least 20 galls were analyzed for gall and nematode morphology observations.

Results

In silico sequence analysis of *Minc03328* effector gene

The *Minc03328* (ID: *Minc3s00020g01299*) gene sequence has 2.06 kb length organized in 6 exons and 5 intron sequences, flanked by 5′- and 3′-UTR sequences. Its CDS sequence has 1428 nucleotides length, encoding a 475 amino acid protein with a predicted 6.67 isoelectric point and 54.99 kDa molecular weight (Table 1; Suppl. Table S2). In addition, two start codons were identified in the 5'-UTR or beginning of CDS 5' region. Blanc-Mathieu et al. (2017) have suggested that *Minc03328* translation starts from this second start codon (Suppl. Table S2). The Minc03328 effector protein has a predicted non-cytoplasmatic domain, nuclear exportation signal, nuclear localization signal, secretory signal peptide located in the N-terminal (amino acids at +1 to +22 position), and absence of an internal transmembrane domain (Table 1; Suppl. Table S2). The absence of a transmembrane domain and presence of a secretion signal peptide suggest as features needed to address Minc03328 effector protein to vesicles in the exocytic-secretory pathway and subsequent secretion of the mature protein during *M. incognita* parasitism in plants.

The comparative genomic tree generated from *Minc03328* gene showed that the *Minc3s00083g03984* gene can be consistently considered as its paralogue gene, while *scf7180000417668.g1585* (*M. floridensis*), *tig00000829.g51954* (*M. arenaria*), *scaffold1253_cov168.g2771* (*M. javanica*), *NXFT01001574.1.4100_g* (*M. graminicola*), and *scaffold8370_cov173.g11786* (*M. enterolobii*) can be considered as their orthologous genes in other *Meloidogyne* species (Suppl. Fig. S1). Pairwise comparisons of nucleotide sequences showed that *Minc03328* effector gene has 50–70% identity with other effector genes present in *Meloidogyne* sp. (Suppl. Fig. S2), whereas it has 60–99% identity with its paralogue and orthologous genes (Fig. 1a). A phylogenetic tree generated from nucleotide sequences showed that *Minc03328* effector gene is more closely related to *tig00000829.g51954* (*M. arenaria*) and *scf7180000417668.g1585* (*M. floridensis*) genes (Fig. 1b). All these collective data from in silico sequence analysis suggest that the *Minc03328* effector gene is distant at the sequence and phylogenetic levels from other *Meloidogyne* effector genes, but has remarkable characteristics closely associated with *M. incognita* parasitism in plants.

Minc03328 gene expression and protein immunolocalization in *M. incognita*

From transcriptome data mining, it was possible to identify *Minc03328* gene expression profile, as well as its paralogue *Minc3s00083g03984* gene, in different *M. incognita* life stages (egg, pJ2, ppJ2/J3, J4, and female) during nematode parasitism in plants (Fig. 1c). The highest expression level of these two genes was observed in the pJ2/J3 stage followed by the J4 stage, which coincides with onset of the *M. incognita* parasitism in plants (Fig. 1c). These in silico gene expression data were confirmed by real-time RT-qPCR analysis. The RT-qPCR analysis indicated that *Minc03328* gene is overexpressed during *M. incognita* parasitism in *N. tabacum* specifically at 5 DAI, confirming its expression modulation at the beginning of the parasitic process and suggesting its specific association during the plant–nematode interaction (Fig. 1d and e). In accordance, fuchsin-stained *N. tabacum* roots showed that *M. incognita* pJ2s at 5 DAI are fully established in infected roots, while at 10 and 15 DAI was verified that *M. incognita* J3 and J3/J4 induced successful feeding sites, and progressively developed into females at 22 DAI (Fig. 1d). Subsequently, the Minc03328 effector protein was immunolocalized and showed to accumulate in subventral glands during *M. incognita* parasitism in *N. tabacum* at 5 to 10 DAI (Fig. 1f). Punctually localized green fluorescence was observed close to the nematode head and strongly suggested *in planta* secretion of the Minc03328 effector protein during early *M. incognita* parasitism. It is expected that this signal to be very weak and localized, since this is one (or two) proteins embedded in a cocktail of a number of other nematode secreted molecules. Particularly, a significant fluorescence signal was also observed in some giant cells near

Table 1 Features of the *Minc03328* effector gene, its paralogue *Minc3s00083g03984* gene, and their orthologous genes in other *Meloidogyne* sp.

Gene	Gene ID	Gene description	Nucleotide (bp)	Amino acid	Expression	Immunolocalization	CDD domain	PFAM domain	NES motif	NLS motif	Secretory protein
M. incognita	*Minc3s00020g01299 Minc03328*	Effector involved in nematode parasitism	1428	475	3, 7, and 14 DAI/pJ2 to J4	Subventral gland cells	No	Non-cytoplasmatic domain	Yes	Yes	Yes
M. incognita	*Minc3s00083g03984*	Paralogue gene of the *Minc03328*	1452	482	pJ2 to J4	Undefined	No	Non-cytoplasmatic domain	Yes	No	Yes
M. floridensis	*scf7180000417668.g1585*	Orthologue gene of the *Minc03328*	531	176	Undefined	Undefined	No	Non-cytoplasmatic domain	No	No	Yes
M. floridensis	*scf7180000418513.g2509*	Orthologue gene of the *Minc03328*	1296	431	Undefined	Undefined	no	Non-cytoplasmatic domain	Yes	Yes	Yes
M. arenaria	*tig00000829.g51954*	Orthologue gene of the *Minc03328*	1458	485	Undefined	Undefined	No	Non-cytoplasmatic domain	Yes	Yes	Yes
M. arenaria	*tig00003009.g30158*	Orthologue gene of the *Minc03328*	1425	474	Undefined	Undefined	No	Non-cytoplasmatic domain	Yes	Yes	Yes
M. arenaria	*tig00000677.g45944*	Orthologue gene of the *Minc03328*	1470	489	Undefined	Undefined	No	Non-cytoplasmatic domain	Yes	No	Yes
M. javanica	*scaffold1170_cov195.g2611*	Orthologue gene of the *Minc03328*	1227	408	Undefined	Undefined	No	Non-cytoplasmatic domain	Yes	No	Yes
M. javanica	*scaffold1253_cov168.g2771*	Orthologue gene of the *Minc03328*	1227	408	Undefined	Undefined	No	Non-cytoplasmatic domain	Yes	No	Yes
M. graminicola	*NXFT01001574.1.4100_g*	Orthologue gene of the *Minc03328*	1347	448	Undefined	Undefined	No	Non-cytoplasmatic domain	No	Yes	Yes
M. enterolobii	*scaffold8370_cov173.g11786*	Orthologue gene of the *Minc03328*	1476	491	Undefined	Undefined	No	Non-cytoplasmatic domain	Yes	Yes	Yes
M. enterolobii	*scaffold23549_cov323.g21895*	Orthologue gene of the *Minc03328*	1175	391	Undefined	Undefined	DUF4954	cl28804	Yes	Yes	
M. enterolobii	*scaffold41831_cov389.g26027*	Orthologue gene of the *Minc03328*	333	110	Undefined	Undefined	No	Non-cytoplasmatic domain	Yes	No	Yes

Table 1 (continued)

Gene	Gene ID	Gene description	Nucleotide (bp)	Amino acid	Expression	Immunolocalization	CDD domain	PFAM domain	NES motif	NLS motif	Secretory protein
M. incognita	*Minc3s00036g02098* *Minc01696**	Effector involved in nematode parasitism	2020	573	3 dpi/J2	Subventral gland cells	smart00220 cl31127	Pkinase (CL0016)	Yes	No	Yes

The gene sequences were retrieved of BioProject PRJEB8714 (2017) from WormBase database version WBPS14 (Lee et al. 2017)

DUF4954 or cl28804 domain of unknown function; *smart00220* serine/threonine protein kinases, catalytic domain; *CL0016* protein kinase superfamily

*Outgroup used in the sequence analysis

the head tip of nematode (Fig. 1g, letters i and ii), while in some galls, a strong fluorescence signal was observed along the cell wall suggesting the presence of Minc03328 protein, but we cannot totally exclude that eventual unspecific staining from remaining sticking antibody in some tissue might occur (Fig. 1g, letters iii). No fluorescence signal was observed in late J2/J3/J4 stages ranging from 15 to 22 DAI (Fig. 1h, letters i and ii). In addition, absence of the fluorescence signal also was observed in females and egg masses at 22 to 45 DAI (Fig. 1i, letter i and ii), but interestingly, some punctual fluorescence signals were visualized within eggs possibly already containing ppJ2 that will hatch (Fig. 1i, letter ii and iii). Thus, these data collectively showed that *Minc03328* effector gene is expressed in infective juveniles (pJ2 and J3 stages) and during early stages of *M. incognita* parasitism in plants (5 DAI). As well, that the encoded effector protein accumulates in subventral glands of ppJ2 and pJ2, is visibly secreted and might be present in giant cells, suggesting that this effector may be involved in promoting *M. incognita* parasitism in plants.

Plant genetic transformation and susceptibility level assessment

A 200 bp length fragment was selected from *Minc03328* effector gene to apply the *in planta* RNAi strategy (Suppl. Table S2). It is plausible to consider that the RNAi strategy generated for *Minc03328* gene downregulation may have also downregulated the *Minc3s00083g03984* paralogue gene due to high sequence identity (Suppl. File S2). In addition, this 200-bp sequence from *Minc03328* effector gene used did not show any significant hits in the *A. thaliana* transcriptome after pairwise sequence comparison, indicating a reduced probability of potential off-target effects in these transgenic plants. The 200-bp DNA fragment was cloned into sense and antisense orientation separated by the *pdk intron,* while its expression was triggered by the constitutive *pUceS8.3* promoter (Fig. 2a). To provide more evidence that the Minc03328 effector protein is directly linked to *M. incognita* parasitism in plants, we successfully generated 12 stable transgenic *A. thaliana* lines using *A. tumefaciens*-mediated delivery system (floral dip). Transgenic Minc03328-dsRNA lines were systematically screened in vitro under hygromycin selection (Suppl. Fig. S3). After advancing to T_3 generation, four transgenic lines (Line #1 to #4) were selected to compare their susceptibility level to *M. incognita* with wild-type control plants. PCR analyses using specific primers targeting *eGFP* gene confirmed transgene insertion in all transgenic lines (Fig. 2b). Transgene expression was checked in all transgenic Minc03328-dsRNA lines by detecting the GFP fluorescent protein accumulation through confocal microscopy (Fig. 2c). Next, 15–20 plants from each transgenic line and wild-type control plants were individually transferred to

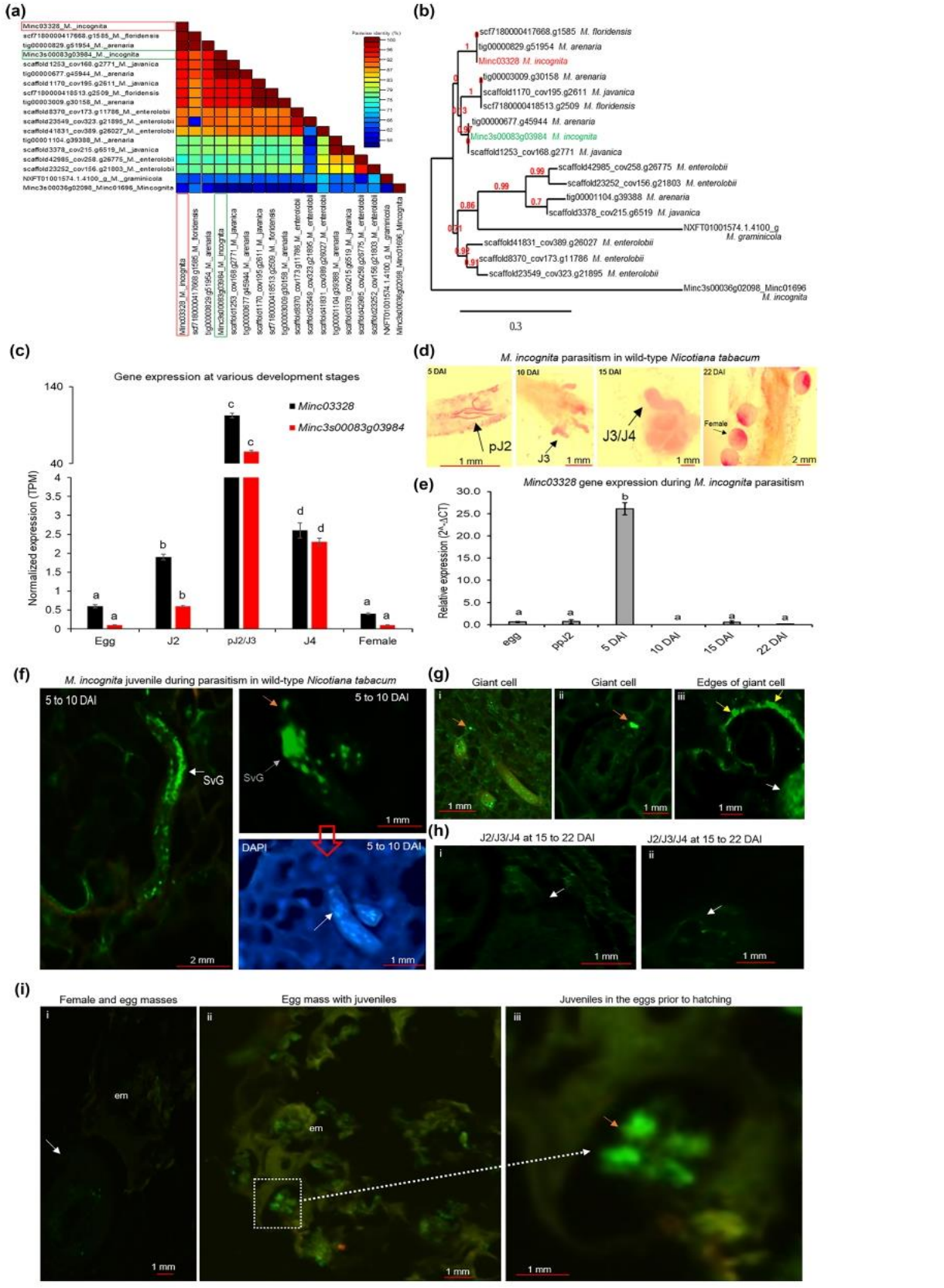
(a)
(b)
(c)
Gene expression at various development stages
Minc03328
Minc3s00083g03984
Normalized expression (TPM)
Egg
J2
pJ2/J3
J4
Female
(d)
M. incognita parasitism in wild-type Nicotiana tabacum
5 DAI
10 DAI
15 DAI
22 DAI
pJ2
J3
J3/J4
Female
(e)
Minc03328 gene expression during M. incognita parasitism
Relative expression (2^-ΔCT)
egg
ppJ2
5 DAI
10 DAI
15 DAI
22 DAI
(f)
M. incognita juvenile during parasitism in wild-type Nicotiana tabacum
5 to 10 DAI
SvG
DAPI
(g)
Giant cell
Giant cell
Edges of giant cell
(h)
J2/J3/J4 at 15 to 22 DAI
J2/J3/J4 at 15 to 22 DAI
(i)
Female and egg masses
Egg mass with juveniles
Juveniles in the eggs prior to hatching
em

◂**Fig. 1** In silico sequence analysis of the *M. incognita* effector genes, *Minc03328* effector gene expression, and Minc03328 effector protein immunolocalization in *M. incognita*. **a** Pairwise sequence identity matrices of nucleotide sequences generated using Sequence Demarcation Tool version 1.2 software. **b** Evolutionary analysis of nucleotide sequences generated by the Phylogeny.fr web service. Highlighted in red and green boxes or letters are, respectively, *Minc03328* gene studied in this work and its paralogue gene. The gene sequences were retrieved from WormBase Parasite Database version WBPS13. **c** *Minc03328* and *Minc3s00083g03984* gene expression profile in different *M. incognita* life stages: egg, pJ2, J3, J4, and female, from transcriptome datasets under BioProject number: PRJNA390559 (Choi et al. 2017), retrieved from BioSample database (NCBI). Error bars represent confidence intervals corresponding to three libraries per nematode life stage. **d** Histopathological images of *M. incognita* pJ2, J3, J3/J4, and female in *N. tabacum* roots stained with acid fuchsin at 5, 10, 15, and 22 days after inoculation (DAI). **e** *Minc03328* gene expression profile measured by real-time RT-qPCR analysis in different *M. incognita* race 3 life stages (egg, ppJ2, and pJ2 to female) during its parasitism in *N. tabacum*. Relative expression levels were normalized with *Mi18S* and *MiGAPDH* as endogenous reference genes (Suppl. Table S1). Error bars represent confidence intervals corresponding to three biological replicates. Different letters on bars indicate significant differences based on Tukey's test at 5% significance level. **f** Minc03328 effector protein immunolocalization in *M. incognita* pJ2 during its parasitism in wild-type *N. tabacum* plants. Minc03328 protein (bright green fluorescence signal) was localized in subventral glands (SvG) (white arrow) and at the head tip (orange arrow) of *M. incognita* pJ2s during its parasitism in *N. tabacum* roots at 5 to 10 DAI. **g** A significant fluorescence signal was observed in giant cells near the head tip of nematode (i and ii; indicate by orange arrows), while in some galls, a strong fluorescence signal was observed at the edges of giant cells (iii; yellow arrows); white arrow indicates the nematode. **h** No detected fluorescence signal was observed in J3/J4 at 15–22 DAI (i and ii; white arrows). **i** No detected fluorescence signal was observed in females (i; white arrow) and egg masses (ii; indicates by "em") at 22–45 DAI, but a powerful fluorescence signal was visible within juveniles (iii; orange arrow) in the eggs before hatching. The immunolocalization experiments were performed using a primary anti-Minc03328 antibody and a secondary anti-rabbit ALEXA-488-conjugated antibody. Fluorescence images represent longitudinal sections of a butyl-methyl methacrylate mixture embedded pJ2 during its parasitism in *N. tabacum*. Weak green color is autofluorescence of the fixed tissues

pots containing sterile substrate/sand mixture (1:1, *v/v*) and inoculated with *M. incognita* ppJ2s. At 5 DAI, the transgene and *Minc03328* effector gene expression were evaluated by RT-qPCR analysis. The RT-qPCR analysis revealed a high RNAi transgene expression level in *M. incognita*-infected galls of all four transgenic *A. thaliana* lines (Fig. 2d). Consistent with this, the *Minc03328* effector gene expression in *M. incognita* pJ2 to J3 fed on transgenic roots at 5 DAI was strongly decreased in all four transgenic lines compared to wild-type control plants (Fig. 2e). At 60 DAI, gall and egg mass number, and their ratio [gall/egg masses number] were assessed to estimate plant susceptibility to *M. incognita*. All four transgenic lines carrying the RNAi construct downregulating the *Minc03328* effector gene showed reduced susceptibility to *M. incognita* compared to wild-type control plants. The number of galls per plant was reduced up to 85% (Fig. 2f), egg masses were reduced up to 90% (Fig. 2g), and the [gall/egg masses number] ratio was reduced up to 87% (Fig. 2h) in transgenic lines. Collectively, these data confirmed that a reduced percentage of the *M. incognita* ppJ2s inoculated in these transgenic Minc03328-dsRNA lines successfully reached the final infection cycle. In accordance, the development and reproductive cycle of at least 64% of inoculated ppJ2s were disturbed by *in planta Minc03328* gene downregulation. Consistently with these previous data, [galls/egg masses number] ratio suggests that *Minc03328* effector gene downregulation significantly affected *M. incognita* parasitism in plants and delayed pJ2, J3, and J4 development in adult females, reflecting negatively on production of egg masses.

To investigate gall and nematode development during parasitism in plants, we analyzed gall morphology at 45 DAI from a selected transgenic line compared to wild type. Histopathological morphology analysis was focused only on Line #1, because it showed identical susceptibility levels to Minc03328-dsRNA Line #2, #3, and #4 (Fig. 2e–h). Wild-type *A. thaliana* roots showed clearly higher number and more prominent *M. incognita*-induced galls (Fig. 3a) compared with roots from transgenic *A. thaliana* line, which showed fewer and smaller galls (Fig. 3b). Interestingly, galls from wild-type control plants showed the presence of well-developed nematodes (Fig. 3c) compared with the delayed development of nematode in transgenic plants (Fig. 3d). In addition, galls from wild-type plants showed typical giant cells with high cytoplasmic content (Fig. 3c, e, and g), whereas galls induced in transgenic plants showed fewer cytoplasm content and presented cell-wall stubs suggesting attempted cell wall formation (Fig. 3d, f, and h). Neighboring cells from transgenic plants showed xylem, giant cells, and neighboring cells with irregular sizes and shapes suggesting altered gall ontogenesis (Fig. 3d and f; Suppl. Fig. S4) compared with galls and neighboring cells from wild type plants, which showed better cellular organization (Fig. 3c and e; Suppl. Fig. S4). Another notable feature was that nematodes in wild-type apparently developed faster and presented a more defined cuticle (Fig. 3c, e, and g), whereas a delayed nematode development was apparent in transgenic plants (Fig. 3d, f, and h; Suppl. Fig. S4). In addition, mature female cuticle during nematode parasitism in wild-type plants was well defined and perfectly visible (Fig. 3c, e, and g). In contrast, cuticle of nematodes in transgenic lines were not well defined and clearly disturbed presenting an undefined morphology and were weakly staining during nematode parasitism in Minc03328-dsRNA transgenic plants (Fig. 3d, f, and h; Suppl. Fig. S4). Thus, the gall morphology in transgenic *A. thaliana* illustrated the consequence of the *Minc03328* gene downregulation during *M. incognita* infection, feeding sites induction, and giant cell ontogenesis, leading to important deleterious effects on

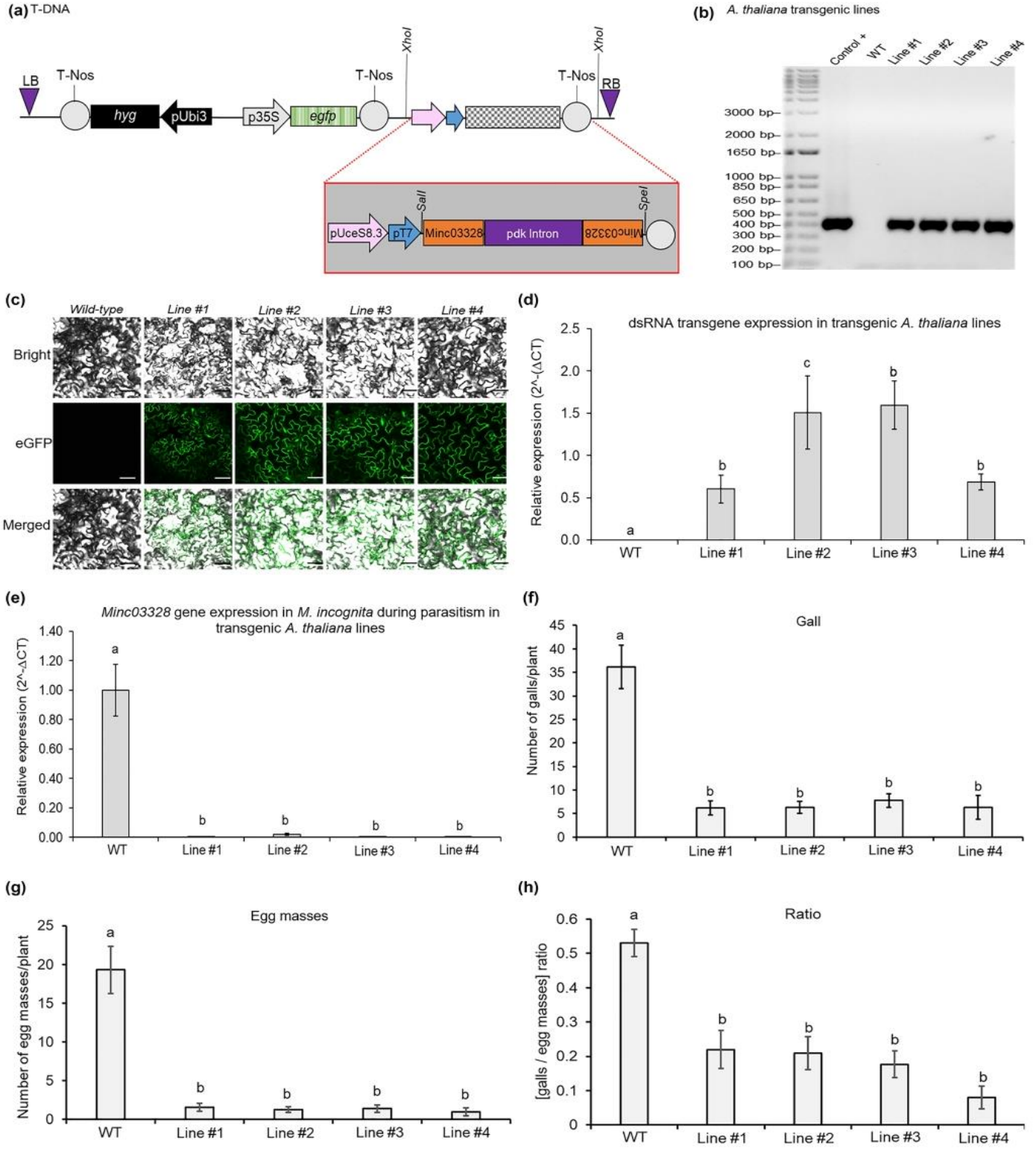
(a) T-DNA
LB
T-Nos
hyg
pUbi3
p35S
egfp
T-Nos
XhoI
T-Nos
XhoI
RB
pUceS8.3
pT7
SalI
Minc03328
pdk Intron
Minc03328
SpeI
(b) A. thaliana transgenic lines
Control +
WT
Line #1
Line #2
Line #3
Line #4
3000 bp
2000 bp
1650 bp
1000 bp
850 bp
650 bp
500 bp
400 bp
300 bp
200 bp
100 bp
(c)
Wild-type
Line #1
Line #2
Line #3
Line #4
Bright
eGFP
Merged
(d)
dsRNA transgene expression in transgenic A. thaliana lines
Relative expression (2^-(ΔCT)
WT
Line #1
Line #2
Line #3
Line #4
(e)
Minc03328 gene expression in M. incognita during parasitism in transgenic A. thaliana lines
Relative expression (2^-ΔCT)
(f)
Gall
Number of galls/plant
(g)
Egg masses
Number of egg masses/plant
(h)
Ratio
[galls / egg masses] ratio

◂**Fig. 2** *Agrobacterium*-mediated *A. thaliana* genetic transformation, dsRNA transgene expression in transgenic Minc03328-dsRNA lines, *Minc03328* effector gene expression in *M. incognita* during its parasitism in transgenic lines, and susceptibility level of transgenic *A. thaliana* lines for *M. incognita* race 3. **a** Overview of the vector-DNA used for genetic transformation of *A. thaliana* plants, targeting downregulation of the nematode *Minc03328* effector transcript by the *in planta* RNAi strategy. **b** PCR detection of the dsRNA transgene in *A. thaliana* lines indicating 400-bp expected size amplificon. Marker: 1.0-kb DNA ladder (Invitrogen, Cat. #10787018); Positive control: water-diluted binary vector; WT: non-transgenic line used as a negative control for PCR and bioassays. **c** Fluorescence detection of GFP protein in transgenic lines under a Zeiss inverted LSM510 META laser scanning microscope using 488-nm excitation line and the 500–530-nm band-pass filter (Carl Zeiss). Scale bars: 10 mm. **d** dsRNA transgene expression level in *M. incognita*-infected galls of transgenic *A. thaliana* lines. The relative expression was calculated with 2^-ΔCT formula using *AtActin 2*, *AtGAPDH*, and *AtEF1* as endogenous reference genes (Suppl. Table S1). Error bars represent confidence intervals corresponding to three biological replicates. Different letters on bars indicate statistically significant differences between transgenic Minc03328-dsRNA lines compared to wild-type control plants, according to Tukey's test at 5% significance level. **e** *Minc03328* gene expression in *M. incognita* during its parasitism in wild-type plants and transgenic lines. The relative expression was calculated with 2^-ΔCT formula using *MiGAPDH*, *MiActin,* and *Miβ-tubulin* as endogenous reference genes (Suppl. Table S1). Error bars represent confidence intervals corresponding to three biological replicates. Different letters on bars indicate statistically significant differences between *M. incognita* fed in transgenic lines compared to *M. incognita* fed in wild-type control plants, according to Tukey's test at 5% significance level. **f** Gall number per plant, **g** egg masses number per plant, and **h** [galls/egg masses] ratio in transgenic *A. thaliana* lines at 60 DAI. Error bars represent confidence intervals corresponding to 12–15 plants per line. Different letters on bars indicate statistically significant differences between transgenic lines compared to wild-type control plants, according to Tukey's test at 5% significance level

gall and nematode development. Therefore, considering that *Minc03328* gene expression is highest in early stages of *M. incognita* parasitism, our data suggest that *Minc03328* effector gene downregulation within nematodes during parasitism might negatively affect nematode infection, feeding site formation, gall genesis, and nematode development. Overall, our data strongly suggest the importance of *Minc03328* as an effector protein during *M. incognita* parasitism in host plants.

Discussion

Plant–parasitic nematodes are important phytopathogens that interfere in complex pathways of the plant hosts allowing the promotion of parasitism in numerous plant species (Quentin et al. 2013). In contrast, beyond preformed and basal defenses, higher plants exhibit another arsenal of pathogen-activated molecules (Vieira and Engler 2017; Sato et al. 2019; Cabral et al. 2020). First, root damage caused by nematode infection produces and accumulates

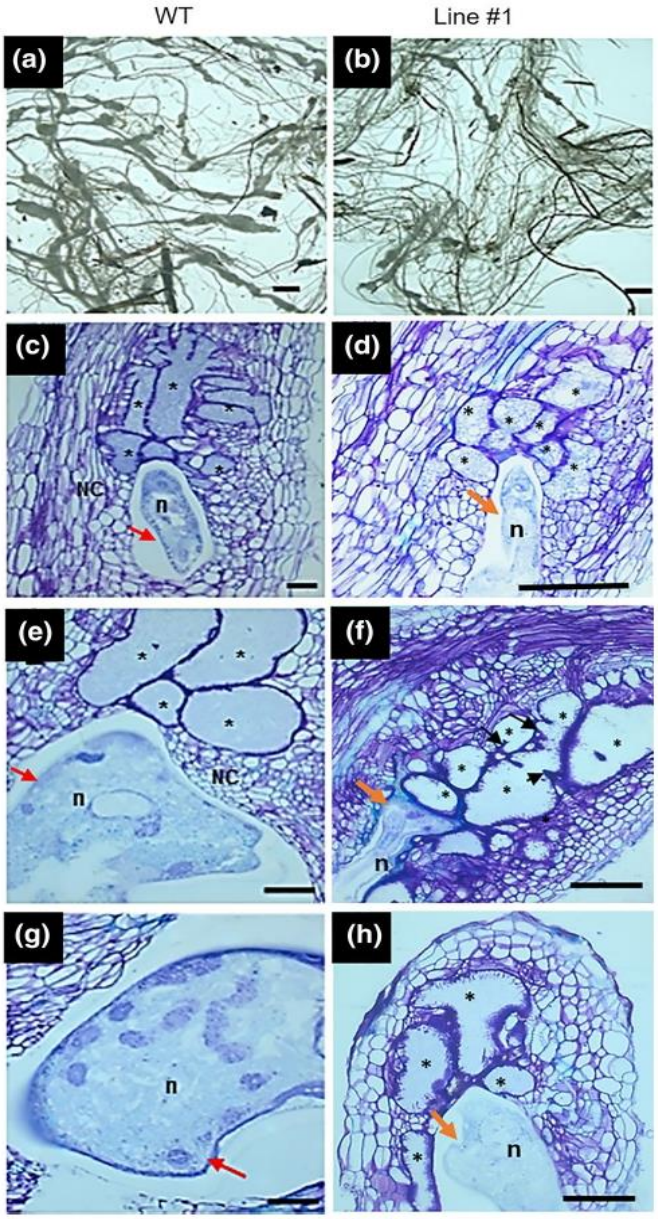

Fig. 3 Histopathological morphology of *M. incognita*-induced galls in transgenic Minc03328-dsRNA *A. thaliana* lines. Plants from transgenic Line #1 and wild-type control plants were submitted to *M. incognita* infection, and gall and nematode morphology were evaluated at 45 DAI. Sectioned galls were stained with toluidine blue. **a** and **b** Transgenic *A. thaliana* roots showed fewer and smaller galls compared to wild-type control plants. **c**–**f** Galls from wild-type control plants showed development of multiple feeding sites, giant cells filled with cytoplasm, and presented fastly maturing nematodes (identified by letter "n"). In contrast, galls from transgenic plants showed giant cells with a few cytoplasmic contents (identified by *) and often containing cell-wall stubs (black arrows). Similarly, galls and neighboring cells from transgenic lines showed a higher organization, while wild-type control plants showed xylem, galls, and neighboring cells with irregular sizes and shapes, suggesting altered giant cell ontogenesis. In the images **g**–**h**, the nematode cuticle was apparently disintegrated during *M. incognita* parasitism in transgenic *A. thaliana* plants compared to perfectly visible mature female cuticle during *M. incognita* parasitism in wild-type control plants (red arrows). This analysis demonstrated that *Minc03328* silencing caused a direct effect on nematode morphology as well indirectly in gall structure. Asterisks, giant cell; NC, neighboring cells; n, nematode. Scale bars = 50 µm

molecules that act *in trans* as damage-associated molecular patterns (DAMPs) that, consequently, activate pattern-triggered immunity (PTI). In addition, nematode-associated molecular patterns (NAMPs) enhance plant basal defense (NAMPs triggered immunity) (Ali et al. 2018). The second level of plant defense responses against nematodes is related to effector-triggered immunity (ETI) (Holbein et al. 2016). In contrast, PPNs secrete several effector proteins during host plant–nematode interaction to overcome these defense mechanisms and promote its parasitism in host plants (Vieira and Gleason 2019). More specifically, these nematode effector proteins act by disrupting the plant defense response and modulating the plant cell cycle and cellular development (Vieira and Gleason 2019). Interestingly, many nematode effectors interact with host plant proteins, individually or collectively suppressing host defense signaling or preventing PTI and ETI activation (Manosalva et al. 2015; Zhao et al. 2019; Mendes et al. 2021a, b). At the same time, other effectors can act by interacting and destabilizing host plant proteins involved in specific biological processes to make them suitable for nematode infection.

RKN (*Meloidogyne* spp.) are major crop pathogen worldwide, and limited range of available control agents or resistant/tolerant cultivars has significantly limited the effectiveness of its control and management (Seo and Kim 2014; Bernard et al. 2017). The low effectiveness of control measures in the field and the emergence of resistant or tolerant RKN populations have led to the use of genetically engineered cultivars to overcome these drawbacks. Following the sequencing and evaluation of the *M. incognita* genome (Abad et al. 2008; Blanc-Mathieu et al. 2017), several candidate effector proteins have been identified. However, the information about their biological functions after secretion in host plants or their action mode in plant cells is still poorly understood (Bellafiore et al. 2008; Lin et al. 2013; Rutter et al. 2014; Mejias et al. 2019).

In this study, the *Minc03328* gene and its effector protein were characterized and their involvement in *M. incognita* parasitism in plants was successfully confirmed. Sequence analysis showed the absence of cytoplasmic and transmembrane domains and the presence of a secretory signal peptide. In addition, orthologous or paralogous genes for *Minc03328* were also identified in other species from *Meloidogyne* sp. genus, suggesting that this effector pathway can be functionally conserved in other *Meloidogyne* species, mainly in *M. arenaria* and *M. floridensis*. In contrast, low sequence identity of *Minc03328* was observed with other already well-characterized effector genes, indicating that this particular effector might act in a specific pathway during parasitism. At the same time, its paralogue gene showed high sequence identity to *Minc03328*, being 93% (1342/1444) for nucleotide and 88% (424/481) for amino acid sequences. These observations based on sequence analysis suggest that both genes can act in a common particular effector pathway and might present redundant functions. The *Minc03328* gene expression analysis showed higher expression at onset of parasitism, and the immunocytochemical analysis proved that Minc03328 protein was accumulated in subventral glands and was observably secreted and possibly accumulated in giant cells. These collective data support that Minc03328 can be considered an effector protein closely involved during *M. incognita* parasitism in host plants. In addition, our data are in accordance with Rutter et al. (2014), which showed that *Minc03328* effector gene expression was upregulated in *M. incognita* at 3–14 DAI and showed that *Minc03328* transcript accumulated specifically in subventral glands.

Herein, we found that downregulation of this effector gene using *in planta* RNAi strategy in transgenic Minc03328-dsRNA *A. thaliana* lines consistently attenuated the parasitic capacity of *M. incognita*. Remarkably, overexpression of the dsRNA transgene in Arabidopsis lines caused a significant reduction in number of galls and egg masses, and [galls/egg masses] ratio compared with wild-type control plants. These data indicate that *Minc03328* can be in fact an effector gene with highlighted importance in plant parasitism by *M. incognita*. Since dsRNA sequence used as RNAi in this study can target both *Minc03328* and its paralogue gene, these phenotypic data, which reduced plant susceptibility to nematodes observed in the transgenic plants, indicate that this effector pathway, which could be controlled by the effector Minc03328 itself, and possibly also by its paralogue gene, might be significantly affected or compromised in some way.

Morphological analyses of *M. incognita*-induced galls showed that pJ2s fed on Minc03328 downregulated lines struggle to induce and establish feeding sites, and inhibit the progression of gall development. Since *Minc03328* effector gene expression was upregulated at 5 DAI in J2/J3s, these morphological analyses supported that its knockdown somehow strongly impaired giant cells metabolic activity and development. Giant cells displayed few cytoplasm contents and cell-wall stubs added to the observation that nematode cuticle appears to lose its structure likely hampering nematode parasitism in transgenic plants. These morphological results fully support that *Minc03328*-dsRNA overexpression downregulates *Minc03328* gene activity reducing plant susceptibility to nematodes.

Similar to previous results with other effectors, the knockdown of a single effector gene can be sufficient to impair nematode parasitism (unpublished data). Thus, data obtained in this present study collectively confirm that the *Minc03328* gene acts as a potent effector protein important for the successful parasitism of *M. incognita* in host plants. It was once again demonstrated that *in planta* RNAi

strategy is highly effective in downregulating *M. incognita* effector genes. To date, several *M. incognita* effector genes or other nematode genes have been characterized and validated using *in planta* RNAi strategy (Suppl. Table S3) (Basso et al. 2020). Similarly, the downregulation of any of the three effector genes *Minc01696*, *Minc00344*, and *Minc00801* was shown to be sufficient to strongly disturb *M. incognita* parasitism in plants (unpublished data). Data presented here, together with those in the literature, have shown that although *M. incognita* has dozens of effector proteins acting in the modulation of its parasitism in plants, the disruption of one or some of these genes can significantly compromise the infectious process of the nematode (Mejias et al. 2019; Mendes et al. 2021a, b). Thus, using *in planta* RNAi strategy to downregulate *Minc03328* effector gene in economically important crops such as cotton and soybean is an interesting biotechnological approach to decrease plant susceptibility to *M. incognita*. Recently, Lisei-de-Sa et al. (2021), using a similar strategy, showed that triple downregulation of *cysteine protease*, *isocitrate lyase*, and *splicing factor* genes significantly impaired *M. incognita* parasitism in transgenic cotton lines. Understanding the action mode of this effector when secreted in plant cells will provide further evidence in the plant–nematode interaction. Previous studies reported by Mukhtar et al. (2011), Consortium (2011), and Wessling et al. (2014) showed that different and diverse pathogen effectors could target the same hub protein of the host plant during its parasitism.

In conclusion, we have here explored the *Minc03328* gene function during parasitism, confirming that Minc03328 protein acts as a powerful effector of substantial importance for successful *M. incognita* parasitism in plants. Since the dsRNA sequence used in this study possibly downregulated not only *Minc03328* but also its paralogue *Minc3s00083g03984* gene, the complete disruption of this effector pathway likely contributed to the reduced susceptibility observed in transgenic Minc03328-dsRNA lines. Finally, our findings demonstrated that the *Minc03328* effector gene and, possibly, its paralogue gene could be powerful targets for biotechnological approaches like *in planta* RNAi technology for *M. incognita* control and management in economically important crops.

Author contribution statement MFGS was the major investigator on this project. MFGS, ITLT, and VJVM designed all experiments. VJVM, FBMA, and DMS performed PCR experiments, plant generation advancements, bioassays, and fuchsin staining, and wrote first draft of the manuscript. MFB performed sequence analyses, produced transgenic *A. thaliana* lines and, helped by MFGS, elaborated final version of the manuscript. MELS provided *M. incognita* inoculum and assisted with bioassays. ITLT and JAE carried out Minc03328 protein immunolocalization and performed *M. incognita*-infected galls histological examination. VJVM, ITLT, and BPM performed real-time RT-qPCR analysis. CVM held with statistical analysis. MFGS, MCMS, and JAE analyzed data, provided intellectual inputs, and amended the manuscript. All authors read and approved the final version of the manuscript.

Supplementary Information The online version contains supplementary material available at https://doi.org/10.1007/s00425-022-03823-4.

Acknowledgements The authors are grateful to EMBRAPA, UCB, CNPq, INCT PlantStress Biotech, CAPES, and FAP-DF for the scientific and financial support.

Funding This work was supported by grants from INCT PlantStress Biotech, UCB, CNPq, CAPES, FAP-DF, INRAE, and EMBRAPA. MFB is grateful to CNPq for a postdoctoral research fellowship (PDJ 150936/2018-4). MFGS is grateful to CAPES/Cofecub project for financial support in the researcher and students' exchange program between institutions.

Declarations

Conflict of interest The authors declare no conflict of interest.

References

Abad P, Gouzy J, Aury J-M, Castagnone-Sereno P et al (2008) Genome sequence of the metazoan plant-parasitic nematode *Meloidogyne incognita*. Nature Biotechnol 26:909. https://doi.org/10.1038/nbt.1482

Ali MA, Anjam MS, Nawaz MA, Lam H-M, Chung G (2018) Signal transduction in plant-nematode interactions. Intern J Mol Sci 19(6):1648. https://doi.org/10.3390/ijms19061648

Basso MF, Lourenço-Tessutti IT, Mendes RAG, Pinto CEM, Bournaud C, Gillet F-X, Togawa RC, de Macedo LLP, de Almeida EJ, Grossi-de-Sa MF (2020) *MiDaf16-like* and *MiSkn1-like* gene families are reliable targets to develop biotechnological tools for the control and management of *Meloidogyne incognita*. Sci Rep 10(1):6991. https://doi.org/10.1038/s41598-020-63968-8

Bellafiore S, Shen Z, Rosso MN, Abad P, Shih P, Briggs SP (2008) Direct identification of the *Meloidogyne incognita* secretome reveals proteins with host cell reprogramming potential. PLoS Pathog 4(10):e1000192. https://doi.org/10.1371/journal.ppat.1000192

Bernard GC, Egnin M, Bonsi C (2017) The impact of plant-parasitic nematodes on agriculture and methods of control. In: Shah MM, Mahamood M (eds) Nematology-concepts, diagnosis and control. Intech, London. https://doi.org/10.5772/intechopen.68958

Blanc-Mathieu R, Perfus-Barbeoch L, Aury J-M, Da Rocha M, Gouzy J, Sallet E, Martin-Jimenez C, Bailly-Bechet M, Castagnone-Sereno P, Flot J-F, Kozlowski DK, Cazareth J, Couloux A, Da Silva C, Guy J, Kim-Jo Y-J, Rancurel C, Schiex T, Abad P, Wincker P, Danchin EGJ (2017) Hybridization and polyploidy enable genomic plasticity without sex in the most devastating plant-parasitic nematodes. PLoS Genet 13(6):e1006777. https://doi.org/10.1371/journal.pgen.1006777

Blum M, Chang H-Y, Chuguransky S, Grego T, Kandasaamy S et al (2020) The InterPro protein families and domains database: 20

years on. Nucleic Acids Res 49(D1):D344–D354. https://doi.org/10.1093/nar/gkaa977

Bolger AM, Lohse M, Usadel B (2014) Trimmomatic: a flexible trimmer for Illumina sequence data. Bioinformatics 30(15):2114–2120. https://doi.org/10.1093/bioinformatics/btu170

Bournaud C, Gillet F-X, Murad AM, Bresso E, Albuquerque EVS, Grossi-de-Sa MF (2018) *Meloidogyne incognita PASSE-MURAILLE* (*MiPM*) gene encodes a cell-penetrating protein that interacts with the CSN5 subunit of the COP9 signalosome. Front Plant Sci 9:904. https://doi.org/10.3389/fpls.2018.00904

Bray NL, Pimentel H, Melsted P, Pachter L (2016) Near-optimal probabilistic RNA-seq quantification. Nat Biotechnol 34(5):525–527. https://doi.org/10.1038/nbt.3519

Bybd DW, Kirkpatrick T, Barker KR (1983) An improved technique for clearing and staining plant tissues for detection of nematodes. J Nematol 15(1):142–143

Cabral D, Banora MY, Antonino JD, Rodiuc N, Vieira P, Coelho RR, Chevalier C, Eekhout T, Engler G, De Veylder L, Grossi-de-Sa MF, de Almeida EJ (2020) The plant WEE1 kinase is involved in checkpoint control activation in nematode-induced galls. New Phytol 225(1):430–447. https://doi.org/10.1111/nph.16185

Canteri MG, Althaus RA, Virgens Filho JS, Giglioti EA, Godoy CV (2001) SASM-Agri : sistema para análise e separação de médias em experimentos agrícolas pelos métodos Scoft-Knott, Tukey e Duncan. Rev Bras De Agrocomputação 1(2):18–24

Carneiro RG, Mazzafera P, Ferraz LCCB, Muraoka T, Trivelin PCO (2002) Uptake and translocation of nitrogen, phosphorus and calcium in soybean infected with *Meloidogyne incognita* and *M. javanica*. Fitopatol Bras 27:141–150

Castagnone-Sereno P, Danchin EGJ, Perfus-Barbeoch L, Abad P (2013) Diversity and evolution of root-knot nematodes, genus *Meloidogyne*: new insights from the genomic Era. Annu Rev Phytopathol 51(1):203–220. https://doi.org/10.1146/annurev-phyto-082712-102300

Choi I, Subramanian P, Shim D, Oh B-J, Hahn B-S (2017) RNA-Seq of plant-parasitic nematode *Meloidogyne incognita* at various stages of its development. Front Genet 8:190–190. https://doi.org/10.3389/fgene.2017.00190

Clough SJ, Bent AF (1998) Floral dip: a simplified method for *Agrobacterium*-mediated transformation of *Arabidopsis thaliana*. Plant J 16(6):735–743. https://doi.org/10.1046/j.1365-313x.1998.00343.x

Consortium AIM (2011) Evidence for network evolution in an *Arabidopsis* interactome map. Science 333(6042):601–607. https://doi.org/10.1126/science.1203877

de Engler EJ, Kyndt T, Vieira P, Van Cappelle E, Boudolf V, Sanchez V, Escobar C, De Veylder L, Engler G, Abad P, Gheysen G (2012) *CCS52* and *DEL1* genes are key components of the endocycle in nematode-induced feeding sites. Plant J 72(2):185–198. https://doi.org/10.1111/j.1365-313X.2012.05054.x

Doyle JJ, Doyle JL (1987) A rapid DNA isolation procedure for small quantities of fresh leaf tissue. Phytochem Bull 19:11–15

El-Gebali S, Mistry J, Bateman A, Eddy SR, Luciani A, Potter SC, Qureshi M, Richardson LJ, Salazar GA, Smart A, EL Sonnhammer L, Hirsh L, Paladin L, Piovesan D, Tosatto SCE, Finn RD (2018) The Pfam protein families database in 2019. Nucleic Acids Res 47(D1):D427–D432. https://doi.org/10.1093/nar/gky995

Grossi-de-Sa MF, Guimaraes LM, Batista JAN, Viana AAB, da Rocha Fragoso R, da Silva MCM (2013) Compositions and methods for modifying gene expression using the promoter of ubiquitin conjugating protein coding gene of soybean plants. Patent US-201313770867-A

Grossi-de-Sa M, Petitot A-S, Xavier DA, Sá MEL, Mezzalira I, Beneventi MA, Martins NF, Baimey HK, Albuquerque EVS, Grossi-de-Sa MF, Fernandez D (2019) Rice susceptibility to root-knot nematodes is enhanced by the *Meloidogyne incognita MSP18* effector gene. Planta 250(4):1215–1227. https://doi.org/10.1007/s00425-019-03205-3

Harrison SJ, Mott EK, Parsley K, Aspinall S, Gray JC, Cottage A (2006) A rapid and robust method of identifying transformed *Arabidopsis thaliana* seedlings following floral dip transformation. Plant Method 2(1):19. https://doi.org/10.1186/1746-4811-2-19

Holbein J, Grundler FMW, Siddique S (2016) Plant basal resistance to nematodes: an update. J Exp Bot 67(7):2049–2061. https://doi.org/10.1093/jxb/erw005

Huang G, Gao B, Maier T, Allen R, Davis EL, Baum TJ, Hussey RS (2003) A profile of putative parasitism genes expressed in the esophageal gland cells of the root-knot nematode *Meloidogyne incognita*. Mol Plant-Microbe Interact 16(5):376–381. https://doi.org/10.1094/mpmi.2003.16.5.376

Hussey RS, Barker KR (1973) A comparison of methods of collecting inocula of *Meloidogyne* spp., including a new technique. Plant Dis Rep 57:1025–1028

Kronenberger J, Desprez T, Höfte H, Caboche M, Traas J (1993) A methacrylate embedding procedure developed for immunolocalization on plant tissues is also compatible with in situ hybridization. J Histochem Cytochem 17(11):1013–1021. https://doi.org/10.1006/cbir.1993.1031

la Cour T, Kiemer L, Molgaard A, Gupta R, Skriver K, Brunak S (2004) Analysis and prediction of leucine-rich nuclear export signals. Protein Eng Des Sel 17(6):527–536. https://doi.org/10.1093/protein/gzh062

Lee RYN, Howe KL, Harris TW, Arnaboldi V, Cain S et al (2017) WormBase 2017: molting into a new stage. Nucleic Acids Res 46(D1):D869–D874. https://doi.org/10.1093/nar/gkx998

Lin B, Zhuo K, Wu P, Cui R, Zhang L-H, Liao J (2013) A novel effector protein, Mj-NULG1a, targeted to giant cell nuclei plays a role in *Meloidogyne javanica* parasitism. Mol Plant-Microbe Interact 26(1):55–66. https://doi.org/10.1094/mpmi-05-12-0114-fi

Lisei-de-Sá ME, Rodrigues-Silva PL, Morgante CV, de Melo BP, Lourenço-Tessutti IT, Arraes FBM, Sousa JPA, Galbieri R, Amorim RMS, de Lins CBJ, Macedo LLP, Moreira VJ, Ferreira GF, Ribeiro TP, Fragoso RR, Silva MCM, de Almeida-Engler J, Grossi-de-Sa MF (2021) Pyramiding dsRNAs increases phytonematode tolerance in cotton plants. Planta 254(6):121. https://doi.org/10.1007/s00425-021-03776-0

Lu P, Davis RF, Kemerait RC, van Iersel MW, Scherm H (2014) Physiological effects of *Meloidogyne incognita* infection on cotton genotypes with differing levels of resistance in the greenhouse. J Nematol 46(4):352–359

Manosalva P, Manohar M, von Reuss SH, Chen S, Koch A, Kaplan F, Choe A, Micikas RJ, Wang X, Kogel K-H, Sternberg PW, Williamson VM, Schroeder FC, Klessig DF (2015) Conserved nematode signalling molecules elicit plant defenses and pathogen resistance. Nature Commun 6:7795. https://doi.org/10.1038/ncomms8795

Marchler-Bauer A, Derbyshire MK, Gonzales NR, Lu S, Chitsaz F, Geer LY, Geer RC, He J, Gwadz M, Hurwitz DI, Lanczycki CJ, Lu F, Marchler GH, Song JS, Thanki N, Wang Z, Yamashita RA, Zhang D, Zheng C, Bryant SH (2015) CDD: NCBI's conserved domain database. Nucleic Acids Res 43(Database issue):222–226. https://doi.org/10.1093/nar/gku1221

Mejias J, Truong NM, Abad P, Favery B, Quentin M (2019) Plant proteins and processes targeted by parasitic nematode effectors. Front Plant Sci 10:970. https://doi.org/10.3389/fpls.2019.00970

Melakeberhan H, Webster JM, Brooke RC, D'Auria JM, Cackette M (1987) Effect of *Meloidogyne incognita* on plant nutrient concentration and its influence on the physiology of beans. J Nematol 19(3):324–330

Mendes RA, Basso MF, Fernandes de Araújo J, Paes de Melo B, Lima RN, Ribeiro TP, da Silva MV, Saliba Albuquerque EV,

Grossi-de-Sa M, Dessaune Tameirao SN, da Rocha FR, Mattar da Silva MC, Vignols F, Fernandez D, Grossi-de-Sa MF (2021a) Minc00344 and Mj-NULG1a effectors interact with GmHub10 protein to promote the soybean parasitism by *Meloidogyne incognita* and *M. javanica*. Exp Parasitol 229:108153. https://doi.org/10.1016/j.exppara.2021.108153

Mendes RA, Basso MF, Paes de Melo B, Ribeiro TP, Lima RN, Fernandes de Araújo J, Grossi-de-Sa M, da Silva MV, Togawa RC, Saliba Albuquerque ÉV, Lisei-de-Sa ME, Mattar da Silva MC, Pepino Macedo LL, da Rocha FR, Fernandez D, Vignols F, Grossi-de-Sa MF (2021b) The Mi-EFF1/Minc17998 effector interacts with the soybean GmHub6 protein to promote host–plant parasitism by *Meloidogyne incognita*. Physiol Mol Plant Pathol 114:101630. https://doi.org/10.1016/j.pmpp.2021.101630

Mukhtar MS, Carvunis AR, Dreze M, Epple P, Steinbrenner J, Moore J, Tasan M, Galli M, Hao T, Nishimura MT, Pevzner SJ, Donovan SE, Ghamsari L, Santhanam B, Romero V, Poulin MM, Gebreab F, Gutierrez BJ, Tam S, Monachello D, Boxem M, Harbort CJ, McDonald N, Gai L, Chen H, He Y, Vandenhaute J, Roth FP, Hill DE, Ecker JR, Vidal M, Beynon J, Braun P, Dangl JL (2011) Independently evolved virulence effectors converge onto hubs in a plant immune system network. Science 333(6042):596–601. https://doi.org/10.1126/science.1203659

Nguyen CN, Perfus-Barbeoch L, Quentin M, Zhao J, Magliano M, Marteu N, Da Rocha M, Nottet N, Abad P, Favery B (2018) A root-knot nematode small glycine and cysteine-rich secreted effector, MiSGCR1, is involved in plant parasitism. New Phytol 217(2):687–699. https://doi.org/10.1111/nph.14837

Nguyen Ba AN, Pogoutse A, Provart N, Moses AM (2009) NLStradamus: a simple Hidden Markov Model for nuclear localization signal prediction. BMC Bioinform 10:202. https://doi.org/10.1186/1471-2105-10-202

Orfanoudaki G, Markaki M, Chatzi K, Tsamardinos I, Economou A (2017) MatureP: prediction of secreted proteins with exclusive information from their mature regions. Sci Rep 7(1):3263. https://doi.org/10.1038/s41598-017-03557-4

Quentin M, Abad P, Favery B (2013) Plant parasitic nematode effectors target host defense and nuclear functions to establish feeding cells. Front Plant Sci 4:53. https://doi.org/10.3389/fpls.2013.00053

Rutter WB, Hewezi T, Abubucker S, Maier TR, Huang G, Mitreva M, Hussey RS, Baum TJ (2014) Mining novel effector proteins from the esophageal gland cells of *Meloidogyne incognita*. Mol Plant-Microbe Interact 27(9):965–974. https://doi.org/10.1094/mpmi-03-14-0076-r

Sato K, Kadota Y, Shirasu K (2019) Plant immune responses to parasitic nematodes. Front Plant Sci 10:1165. https://doi.org/10.3389/fpls.2019.01165

Schmittgen TD, Livak KJ (2008) Analyzing real-time PCR data by the comparative CT method. Nature Protoc 3:1101. https://doi.org/10.1038/nprot.2008.73

Seo Y, Kim YH (2014) Control of *Meloidogyne incognita* using mixtures of organic acids. Plant Pathol J 30(4):450–455. https://doi.org/10.5423/PPJ.NT.07.2014.0062

Shukla N, Yadav R, Kaur P, Rasmussen S, Goel S, Agarwal M, Jagannath A, Gupta R, Kumar A (2018) Transcriptome analysis of root-knot nematode (*Meloidogyne incognita*)-infected tomato (*Solanum lycopersicum*) roots reveals complex gene expression profiles and metabolic networks of both host and nematode during susceptible and resistance responses. Mol Plant Pathol 19(3):615–633. https://doi.org/10.1111/mpp.12547

St-Pierre J, Grégoire J-C, Vaillancourt C (2017) A simple method to assess group difference in RT-qPCR reference gene selection using GeNorm: the case of the placental sex. Sci Rep 7(1):16923. https://doi.org/10.1038/s41598-017-16916-y

Szitenberg A, Salazar-Jaramillo L, Blok VC, Laetsch DR, Joseph S, Williamson VM, Blaxter ML, Lunt DH (2017) Comparative genomics of apomictic root-knot nematodes: hybridization, ploidy, and dynamic genome change. Genome Biol Evol 9(10):2844–2861. https://doi.org/10.1093/gbe/evx201

Triantaphyllou A, Hirschmann H (1960) Post infection development of *Meloidogyne incognita* Chitwood 1949 (Nematoda-Heteroderidae). Ann De L'institut Phytopathologique Benaki 1:1–11

Trudgill DL, Blok VC (2001) Apomictic, polyphagous root-knot nematodes: exceptionally successful and damaging biotrophic root pathogens. Annu Rev Phytopathol 39:53–77. https://doi.org/10.1146/annurev.phyto.39.1.53

Truong NM, Chen Y, Mejias J, Soulé S, Mulet K, Jaouannet M, Jaubert-Possamai S, Sawa S, Abad P, Favery B, Quentin M (2021) The *Meloidogyne incognita* nuclear effector MiEFF1 interacts with arabidopsis cytosolic glyceraldehyde-3-phosphate dehydrogenases to promote parasitism. Front Plant Sci 12:633. https://doi.org/10.3389/fpls.2021.641480

Vieira P, de Engler A (2017) Plant cyclin-dependent kinase inhibitors of the KRP family: Potent inhibitors of root-knot nematode feeding sites in plant roots. Front Plant Sci 8:1514. https://doi.org/10.3389/fpls.2017.01514

Vieira P, Gleason C (2019) Plant–parasitic nematode effectors; insights into their diversity and new tools for their identification. Curr Opin Plant Biol 50:37–43. https://doi.org/10.1016/j.pbi.2019.02.007

Vieira P, Engler G, de Almeida EJ (2012) Whole-mount confocal imaging of nuclei in giant feeding cells induced by root-knot nematodes in Arabidopsis. New Phytol 195(2):488–496. https://doi.org/10.1111/j.1469-8137.2012.04175.x

Vilella AJ, Severin J, Ureta-Vidal A, Heng L, Durbin R, Birney E (2009) Ensembl Compara GeneTrees: complete, duplication-aware phylogenetic trees in vertebrates. Genome Res 19(2):327–335. https://doi.org/10.1101/gr.073585.107

Wessling R, Epple P, Altmann S, He Y, Yang L, Henz SR, McDonald N, Wiley K, Bader KC, Glasser C, Mukhtar MS, Haigis S, Ghamsari L, Stephens AE, Ecker JR, Vidal M, Jones JD, Mayer KF, Loren V, van Themaat E, Weigel D, Schulze-Lefert P, Dangl JL, Panstruga R, Braun P (2014) Convergent targeting of a common host protein-network by pathogen effectors from three kingdoms of life. Cell Host Microbe 16(3):364–375. https://doi.org/10.1016/j.chom.2014.08.004

Zhao J, Li L, Liu Q, Liu P, Li S, Yang D, Chen Y, Pagnotta S, Favery B, Abad P, Jian H (2019) A MIF-like effector suppresses plant immunity and facilitates nematode parasitism by interacting with plant annexins. J Exp Bot 70(20):5943–5958. https://doi.org/10.1093/jxb/erz348

Authors and Affiliations

Valdeir Junio Vaz Moreira[1,2,3] · Isabela Tristan Lourenço-Tessutti[1,4] · Marcos Fernando Basso[1,4] · Maria Eugênia Lisei-de-Sa[1,3,5] · Carolina Vianna Morgante[1,4,6] · Bruno Paes-de-Melo[1,7] · Fabrício Barbosa Monteiro Arraes[1,2,4] · Diogo Martins-de-Sa[1,3] · Maria Cristina Mattar Silva[1,4] · Janice de Almeida Engler[4,8] · Maria Fatima Grossi-de-Sa[1,4,9]

1 Embrapa Genetic Resources and Biotechnology, Brasilia, DF 70770-917, Brazil

2 Biotechnology Center, PPGBCM, UFRGS, Porto Alegre, RS 90040-060, Brazil

3 Federal University of Brasilia, UNB, Brasilia, DF 70910-900, Brazil

4 National Institute of Science and Technology, INCT PlantStress Biotech, Embrapa 70297-400, Brazil

5 Agriculture Research Company of Minas Gerais State, Uberaba, MG 31170-495, Brazil

6 Embrapa Semiarid, Petrolina, PE 56302-970, Brazil

7 Federal University of Viçosa, Viçosa, MG 36570-900, Brazil

8 INRAE, Université Côte d'Azur, CNRS, ISA, 06903 Sophia Antipolis, France

9 Catholic University of Brasilia, Brasilia, DF 71966-700, Brazil

CAPÍTULO III

IN PLANTA RNAi TARGETING *Meloidogyne incognita* Minc16803 GENE PERTURBS NEMATODE PARASITISM AND REDUCES PLANT SUSCEPTIBILITY

Published article

Valdeir Junio Vaz Moreira, Daniele Heloísa Pinheiro, Isabela Tristan Lourenço-Tessutti, Marcos Fernando Basso, Maria E. Lisei-de-Sa, Maria C. M. Silva, Etienne G. J. Danchin, Patrícia M. Guimarães, Priscila Grynberg, Ana C. M. Brasileiro, Leonardo L. P. Macedo, Carolina V. Morgante, Janice de Almeida Engler, Maria Fatima Grossi-de-Sa. (2023). *In planta* RNAi targeting *Meloidogyne incognita* Minc16803 gene perturbs nematode parasitism and reduces plant susceptibility. **Journal of Pest Science**. doi.org/10.1007/s10340-023-01623-7

Pages 77 to 93

ABSTRACT

Meloidogyne incognita is one of the most important plant-parasitic nematodes (PPNs) causing severe crop losses worldwide. Plants have evolved complex defense mechanisms to respond to PPNs attacks. Conversely, PPNs have evolved infection mechanisms that involve the secretion of effector proteins into host plants to suppress immune responses and facilitate parasitism. Therefore, effector genes are attractive targets for the genetic improvement of plant resistance to *M. incognita*. In this study, we functionally characterized the *Minc16803* (*Minc3s00746g16803*) putative effector gene to evaluate its role during plant-nematode interactions. First, we found that the *Minc16803* gene is expressed in all nematode life stages and encodes a protein with an N-terminal signal peptide for secretion, a motif characteristic of effector proteins and with the absence of transmembrane domain. In addition, our data demonstrated that transgenic *Arabidopsis thaliana* lines overexpressing a *Minc16803-dsRNA* efficiently downregulated the *Minc16803* transcripts in infecting nematodes. Furthermore, transgenic lines were significantly less susceptible to *M. incognita* compared to wild-type control plants. The number of galls per plant was reduced by up to 84%, while the number of egg masses per plant decreased by up to 93.3%. Moreover, galls and feeding sites in the roots of transgenic lines were smaller than those in the control plants. Histological analysis revealed giant cells without cytoplasm, disordered neighboring cells, and malformed maturing nematodes in transgenic galls. Curiously, numerous hatching ppJ2 juveniles were often observed near the female body within the transgenic root tissues before egg mass extrusion. All findings strongly suggest that *Minc16803* gene is a promising target to engineer agricultural crops for *M. incognita* resistance through host-induced gene silencing.

RESUMO

Meloidogyne incognita é um dos mais importantes nematoides parasitas de plantas (NPPs), causando graves perdas de colheitas em todo o mundo. As plantas desenvolveram mecanismos de defesa complexos para responder aos ataques de NPPs. Por outro lado, os NPPs desenvolveram mecanismos de infecção que envolvem a secreção de proteínas efetoras nas plantas hospedeiras para suprimir as respostas imunes e facilitar o parasitismo. Portanto, genes efetores são alvos atrativos para o melhoramento genético da resistência de plantas à *M. incognita*. Neste estudo, caracterizamos funcionalmente o suposto gene efetor *Minc16803* (*Minc3s00746g16803*) para avaliar seu papel durante as interações planta-nematoide. Primeiramente, descobrimos que o gene *Minc16803* é expresso em todos os estádios de vida do nematoide e codifica uma proteína com um peptídeo sinal N-terminal para secreção, um motivo característico de proteínas efetoras e com ausência de domínio transmembrana. Além disso, nossos dados demonstraram que linhas transgênicas de *Arabidopsis thaliana* superexpressando *Minc16803-dsRNA* regulam negativamente eficientemente os transcritos de *Minc16803* na infecção de nematoides. Além disso, as linhas transgênicas foram significativamente menos susceptíveis a *M. incognita* em comparação com as plantas do controle do tipo selvagem. O número de galhas por planta foi reduzido em até 84%, enquanto o número de massas de ovos por planta diminuiu em até 93,3%. Além disso, as galhas e os locais de alimentação nas raízes das linhagens transgênicas eram menores do que nas plantas controle. A análise histológica revelou células gigantes sem citoplasma, células vizinhas desordenadas e nematoides em maturação malformados em galhas transgênicas. Curiosamente, numerosos juvenis de ppJ2 eclodidos foram frequentemente observados perto do corpo feminino dentro dos tecidos radiculares transgênicos antes da extrusão da massa de ovos. Todas as descobertas sugerem fortemente que *Minc16803* é um alvo promissor para engenharia de culturas agrícolas visando à resistência contra *M. incognita* através do silenciamento genético induzido pelo hospedeiro.

Journal of Pest Science (2024) 97:411–427
https://doi.org/10.1007/s10340-023-01623-7

ORIGINAL PAPER

In planta RNAi targeting *Meloidogyne incognita Minc16803* gene perturbs nematode parasitism and reduces plant susceptibility

Valdeir Junio Vaz Moreira[1,2,3] · Daniele Heloísa Pinheiro[1,4] · Isabela Tristan Lourenço-Tessutti[1,4] · Marcos Fernando Basso[1,4] · Maria E. Lisei-de-Sa[1,4,5] · Maria C. M. Silva[1,4] · Etienne G. J. Danchin[4,7] · Patrícia M. Guimarães[1,4] · Priscila Grynberg[1,4] · Ana C. M. Brasileiro[1,4] · Leonardo L. P. Macedo[1,4] · Carolina V. Morgante[1,4,6] · Janice de Almeida Engler[6,4] · Maria Fatima Grossi-de-Sa[1,4,8]

Received: 1 November 2022 / Revised: 22 February 2023 / Accepted: 13 April 2023 / Published online: 13 May 2023

Abstract

Meloidogyne incognita is one of the most important plant-parasitic nematodes (PPNs) causing severe crop losses worldwide. Plants have evolved complex defense mechanisms to respond to PPNs attacks. Conversely, PPNs have evolved infection mechanisms that involve the secretion of effector proteins into host plants to suppress immune responses and facilitate parasitism. Therefore, effector genes are attractive targets for the genetic improvement of plant resistance to *M. incognita*. In this study, we functionally characterized the *Minc16803* (*Minc3s00746g16803*) putative effector gene to evaluate its role during plant-nematode interactions. First, we found that the *Minc16803* gene is expressed in all nematode life stages and encodes a protein with an N-terminal signal peptide for secretion, a motif characteristic of effector proteins and with the absence of transmembrane domain. In addition, our data demonstrated that transgenic *Arabidopsis thaliana* lines overexpressing a *Minc16803*-dsRNA efficiently downregulated the *Minc16803* transcripts in infecting nematodes. Furthermore, transgenic lines were significantly less susceptible to *M. incognita* compared to wild-type control plants. The number of galls per plant was reduced by up to 84%, while the number of egg masses per plant decreased by up to 93.3%. Moreover, galls and feeding sites in the roots of transgenic lines were smaller than those in the control plants. Histological analysis revealed giant cells without cytoplasm, disordered neighboring cells, and malformed maturing nematodes in transgenic galls. Curiously, numerous hatching ppJ2 juveniles were often observed near the female body within the transgenic root tissues before egg mass extrusion. All findings strongly suggest that *Minc16803* gene is a promising target to engineer agricultural crops for *M. incognita* resistance through host-induced gene silencing.

Keywords Host-induced gene silencing · dsRNA · Plant-nematode interactions · Root-knot nematode

Communicated by Aurelio Ciancio.

Valdeir Junio Vaz Moreira, Daniele Heloísa Pinheiro have contributed equally to this work.

✉ Maria Fatima Grossi-de-Sa
fatima.grossi@embrapa.br

[1] Embrapa Genetic Resources and Biotechnology (Cenargen), PqEB Final, W5 Norte, PO Box 02372, Brasília, DF, Brazil

[2] Biotechnology Center, PPGBCM, UFRGS, Porto Alegre, RS, Brazil

[3] Federal University of Brasília, UNB, Brasília, DF, Brazil

[4] National Institute of Science and Technology, INCT PlantStress Biotech, Embrapa-Brazil, Brasília, DF, Brazil

[5] Agricultural Research Agency of Minas Gerais (EPAMIG), Uberaba, MG, Brazil

[6] Embrapa Semiarid, Petrolina, PE, Brazil

[7] INRAE, CNRS, Université Côte d'Azur, ISA, Sophia-Antipolis, Nice, France

[8] Catholic University of Brasília, Brasília, DF, Brazil

Introduction

The co-evolutionary interactions between pathogens and their host plants have driven the development of complex mechanisms of pathogen infection and plant immune defense (Zhang et al. 2020). Plant-parasitic nematodes (PPNs) have evolved a striking diversity of mechanisms to overcome plant defenses. One of the mechanisms used by PPNs for successful infection involves the secretion of several effector proteins produced by esophageal glands into plant root cells through their stylet (Jagdale et al. 2021). Nematode effectors generally impair plant immune responses by interfering with different host metabolic and physiological processes, such as hormone-dependent defense pathways (Habash et al. 2017), secondary metabolite pathways (Bauters et al. 2020), actin filaments organization (Leelarasamee et al. 2018), cell cycle onset and progression (Coke et al. 2021), protein ubiquitination, and gene expression regulation (Diaz-Granados et al. 2020).

The root-knot nematode (RKN) *Meloidogyne incognita* attacks a wide range of agronomically important crops and seriously threatens crop production worldwide (Bernard et al. 2017). The *M. incognita* life cycle includes six stages, egg, ppJ2 (pre-parasitic second-stage juveniles), pJ2 (parasitic second-stage juveniles), J3, J4 non-feeding juveniles, and adult females (Triantaphyllou and Hirschmann 1960; Castagnone-Sereno et al. 2013). The *M. incognita* pJ2s secrete several effector proteins that trigger the differentiation of root vascular parenchymal cells into 5–7 specialized, multinucleate, and hypertrophied feeding cells, named giant cells, which are formed by successive nuclear divisions without cytokinesis (Kyndt et al. 2013). The galls formed in host roots are the typical symptoms of *M. incognita* infection and result from the proliferation of the tissue around the nematode and giant cells. The feeding cells exhibit high metabolic activity and provide all nutrients required for nematodes to complete their life cycle (Siddique and Grundler 2018). Studies have revealed that *M. incognita* secretes an arsenal of effector proteins into host plant root cells that can interact with different target proteins of parasitized plants. The interaction between nematode effectors and targeted plant proteins triggers molecular, physiological, and morphological changes that culminate in the formation of permanent feeding sites (Jagdale et al. 2021). For instance, the *M. incognita* MIF-like effector facilitates nematode parasitism by interacting with plant Annexin 1 and Annexin 4, and subsequently suppressing host signal transduction and immune responses (Zhao et al. 2019). The *M. incognita* Mi-ISC-1 effector suppresses plant salicylic acid biosynthesis (Qin et al. 2021), and Mj2G02 effector from *Meloidogyne javanica* impairs cell death by disrupting jasmonic acid-mediated signaling to promote parasitism (Song et al. 2021). Similarly, the *M. incognita* effector MiEFF1 targets *A. thaliana* cytosolic glyceraldehyde-3-phosphate dehydrogenases and universal stress proteins, which are involved in the regulation of salicylic acid and jasmonic defense-related genes expression (Truong et al. 2021). Mendes et al. (2021a) showed that the Minc00344 and Mj-NULG1a effector proteins interact with GmHub10 soybean protein to promote *M. incognita* and *M. javanica* parasitism, respectively. Mendes et al. 2021b also reported that MiEFF1/Minc17998 effector protein interacts with GmHub6 protein to promote *M. incognita* parasitism in soybean plants.

Host-induced gene silencing (HIGS) provides a promising strategy toward increased plant resistance to nematodes (Basso et al. 2020; Lisei-de-Sá et al. 2021). A number of studies have demonstrated that transgenic plants expressing engineered dsRNAs can efficiently trigger the silencing of essential genes or parasitism genes of nematodes (Huang et al. 2006; Sindhu et al. 2009; Souza Júnior et al. 2013; Lourenço-Tessutti et al. 2015). Since effectors can contribute substantially to nematode pathogenicity, their silencing is expected to impair nematode infection. Therefore, effector genes are attractive targets for developing RNAi-based transgenic plants with reduced susceptibility to PPNs. Previous functional studies using RNAi-plants have provided experimental evidence that diverse nematode effectors, such as *Heterodera schachtii* 30D08 and Hs25A01 (Pogorelko et al. 2016; Verma et al. 2018), *Heterodera glycines* Hg16B09 (Hu et al. 2019), *Meloidogyne graminicola* Mg01965 (Zhuo et al. 2019) and MgMO237 (Chen et al. 2018), and *Meloidogyne enterolobii* MeTCTP (Zhuo et al. 2017) contribute significantly to nematodes parasitism. With respect to *M. incognita* effectors, it was demonstrated that transgenic *A. thaliana* plants that expressed a dsRNA targeting *MiMsp40* were less susceptible to *M. incognita*, as evidenced by decreased number of galls and eggs (Niu et al. 2016). Moreira et al. 2022 showed that downregulation of the *Minc03328* effector gene triggered by *in planta* RNAi strategy decreased the number of galls (85%), egg masses (90%), and the ratio [number of egg masses/number of galls] (87%) and consequently reduced the plant susceptibility to *M. incognita*.

The identification and characterization of the effectors employed by *M. incognita* to counteract plant defense responses and the mechanistic basis of effector activity in plants provide important insights into the biology of plant-nematode interactions (Vieira and Gleason 2019). In addition, this knowledge can be helpful in developing more effective control methods against *M. incognita*. An increasing number of putative nematode effectors have been described, but detailed information on the functional role of effectors involved in *M. incognita* parasitism is still lacking (Bellafiore et al. 2008; Gardner et al. 2018; Grynberg et al. 2020).

Here, we identified and functionally characterized a putative effector, named Minc16803. We found that *Minc16803* gene is transcriptionally expressed in all nematode stages, including pJ2, J3, J3/J4, adult females, and eggs. This gene encodes a protein with a predicted secretory N-terminal signal peptide and a motif characteristic of known effectors, reinforcing its potential as an effector protein. Furthermore, we demonstrated that transgenic *A. thaliana* lines overexpressing a dsRNA targeting the *Minc16803* transcripts significantly suppressed plant infection by *M. incognita*. Morphological analyses of *M. incognita*-induced galls in transgenic roots strongly suggest that the Minc16803 protein might contribute to the proper development of feeding sites in the host plant. Curiously, these analyses also revealed malformed maturing nematodes and ppJ2s near the female body, which hatched from eggs prior egg mass extrusion on root surface. Taken together, all data indicate that the putative effector protein Minc16803 plays a key role in *M. incognita* parasitism and may be a valuable target for plant-mediated RNAi control of nematodes.

Material and methods

Minc16803 gene sequence

The putative *Minc16803* effector gene was identified based on comparative genomic and transcriptomic analysis. Briefly, we searched for proteins having a predicted signal peptide for secretion, no transmembrane region, and harboring protein motifs characteristic of effector at the N-terminal region. In addition, we required the protein to be encoded by a gene expressed at all developmental stages of the *M. incognita* life cycles and being in maximum 3 copies, consistent with the triploid genome structure. The *Minc16803* (*Minc3s00746g16803*) sequence and its two paralogous *Minc3s00070g03473* and *Minc3s00200g07395* genes (Suppl. File S1) were retrieved from the BioProject ID PRJEB8714 (sample: ERS1696677) (Blanc-Mathieu et al. 2017) in the WormBase Parasite Database version WBPS16 (Lee et al. 2018). Subsequently, conserved domains in the *Minc16803* gene sequence were identified using CDD Database from NCBI (Marchler-Bauer et al. 2015), PFAM Database from EMBL-EBI (El-Gebali et al. 2019), and InterPro Scan (Blum et al. 2021), while the nuclear localization signal was predicted with a cutoff value of 0.5 using the NLStradamus online tool (Nguyen Ba et al. 2009). Secretory signal peptides were predicted using the MatureP tool (Orfanoudaki et al. 2017) and SignalP 5.0 program (Almagro Armenteros et al. 2019), whereas putative transmembrane domains were predicted using the TMHMM program (Möller et al. 2001). In addition, we used the MERCI software (Vens et al. 2011) to check whether protein motifs enriched at the N-terminal region of known effector proteins could be identified in *Minc16803*.

In silico expression level of the *Minc16803* gene

The expression levels of the *Minc16803* gene and its two paralogous genes *Minc3s00200g07395* and *Minc3s00070g03473* at different *M. incognita* life stages were retrieved from WormBase Parasite (Howe et al. 2017), in the 'Expression' section, sub-section 'Life Cycle' of gene-based displays. In short, in WormBase Parasite, RNA-seq data of five *M. incognita* developmental life stages (egg, J2, pJ2/J3, J4, and female), generated in triplicates (Choi et al. 2017), were aligned on the *M. incognita* annotated genome (Blanc-Mathieu et al. 2017) using TopHat2 (Kim et al. 2013). Expression values in Transcripts Per Million units (TPM) were determined from the aligned reads using HTSeq (Anders et al. 2015).

Meloidogyne incognita race 3 inoculum

Meloidogyne incognita race 3 inoculum was maintained on tomato plants (*Solanum lycopersicum* cv. Santa Cruz) under greenhouse conditions. Infected roots were collected at 90 days after infection (DAI), rinsed with water, and then grounded for 30 s in a 0.5% sodium hypochlorite solution using a blender. The suspension was sieved through a set of sieves (45, 100, and 500-mesh), while eggs were collected on the 500-mesh sieve. The collected eggs were submitted to the Baermann funnel technique, and hatched ppJ2s were transferred to a Becker with sterile distilled water and sequentially decanted at 4 °C for 7–14 days. For gene expression assays, eggs were collected as previously described, re-suspended in an inert suspension of kaolin substrate, and centrifuged at 2,500 rpm for 5 min. The precipitated material was re-suspended in a 30% (w/v) sucrose solution and centrifuged again at 2,500 rpm for 5 min. Finally, the supernatant was passed through a 500-mesh sieve, and the eggs retained on the sieve were rinsed in sterile water and immediately frozen in liquid nitrogen.

Meloidogyne incognita development in wild-type *Nicotiana tabacum* roots

The *N. tabacum* var. Petit Havana (SR1) plants were inoculated with 1,000 ppJ2s of *M. incognita* and maintained under greenhouse conditions. Infected roots were harvested during nematode parasitism at 5, 10, 15, and 22 DAI, washed with water, dried with paper towels, and stained with acid fuchsin according to Bybd et al. 1983. Then, root samples were immersed in 2.5% (v/v) sodium hypochlorite solution for clarification and washed with water for 10 min. Finally, the clarified roots were completely immersed in acid fuchsin

solution (1.25 g acid fuchsin solubilized in 1:3 v/v glacial acetic acid and distilled water). For better root staining, samples were slightly heated in a microwave for 1 min. After the staining step, the acid fuchsin solution was discarded; roots were rinsed and transferred to acidified glycerol solution (24:1 v/v glycerol and hydrochloric acid). Nematode stages were then visualized in galls under a stereomicroscope and imaged using a Zeiss Axiocam MR.

Minc16803 expression level during *M. incognita* parasitism in wild-type *N. tabacum*

Total RNA was extracted from *M. incognita* eggs, ppJ2, and infected *N. tabacum* galls at 5, 10, 15, and 22 DAI, using Quick-RNA™ Plant Mini-prep kit (Zymo Research, Irvine, CA, USA). RNA concentration was determined using a spectrophotometer (NanoDrop 2000, Thermo Scientific, Massachusetts, USA), and integrity was assessed in 1% agarose gel electrophoresis. RNA samples were treated with RNase-free RQ1 DNase I (Promega, Madison, Wisconsin, USA) according to the manufacturer's instructions. DNase-treated RNA was used as a template for cDNA synthesis using oligo-$(dT)_{20}$ primer (100 µM), random hexamers (50 µM), and SuperScript III RT (Life Technologies, Carlsbad, CA, USA) according to the manufacturer's instructions. RT-qPCR assays were performed in an Applied Biosystems 7500 Fast Real-Time PCR System (Applied Biosystems, Foster City, CA, USA) using 2 µl cDNA (diluted 1:20), 0.2 µM gene-specific primer (Suppl. Table S1), and GoTaq® qPCR Master Mix (Promega, Madison, Wisconsin, USA). Gene expression level was normalized using *Mi18S* and *MiGAPDH* as endogenous reference genes. Three biological replicates were used for each treatment. All cDNA samples were carried out in technical triplicate, while primer efficiencies were previously determined, and target-specific amplification was confirmed by a single and distinct peak in the melting curve analysis. The relative expression level was calculated using the $2^{-\Delta\Delta CT}$ method (Pfaffl 2001). Data were subjected to variance analysis (ANOVA) and, when significant, means were compared by Tukey test ($P < 0.05$) using the SASM-Agri statistical package (Canteri et al. 2001).

Binary vector construction, plant transformation, and selection of transgenic plants

The vector backbone used in this study was derived from the pPZP-201BK-EGFP binary cloning vector (Chu et al. 2014), in which the T-DNA sequence (*pUceS8.3::Minc16803-dsRNA*) was cloned. In this T-DNA, the interfering dsRNA targeting *Minc16803* gene transcripts was expressed under the control of the constitutive soybean *ubiquitin-conjugating 4* promoter (*pUceS8.3*) (patent: EP1953232B1). The nucleotide sequence of the *Minc16803* gene selected to target its transcripts by the RNAi strategy corresponded to the 200 bp sequence at nucleotide positions + 445 to + 644 relative to the start codon of the *Minc16803* coding sequence. Multiple sequence alignments were used to investigate whether this 200 bp sequence can also target the two paralogous genes (Suppl. File S2). In addition, the *Minc16803* nucleotide and protein sequences were previously subjected to a similarity search with the *A. thaliana* transcriptome to make sure that no homology was present and thus avoid possible off-target effects. The sense and antisense strands of the 200 bp dsRNA cloned between *Sal*I and *Spe*I restriction sites were separated by the *pdk* intron sequence of *pyruvate orthophosphate dikinase* (Smith et al. 2000). This full-length T-DNA was synthesized and assembled into the pPZP-201BK-EGFP backbone by the Epoch Life Science (Sugar Land, Texas, EUA). Subsequently, this resulting binary vector (named GS62658-4 vir*Minc16803*) was transfected into *Escherichia coli* and then, into *Agrobacterium tumefaciens* strain GV3101.

Arabidopsis thaliana ecotype Columbia (Col-0) plants were grown to the reproductive stage on a commercial substrate in a growth room (22 °C, 70–75% relative humidity, and photoperiod 16 h with ~ 200 µmol photons $m^{-2}.s^{-1}$ of light intensity). Transgenic plants were generated using the floral dip method as described previously by Clough and Bent (1998). Then, T_1 seeds from four independent transgenic lines (Line #1 to #4) and non-transgenic (wild-type or WT) *A. thaliana* were harvested. For generation advancement, seeds were surface-sterilized with 70% ethanol for 1 min and then, with 2% sodium hypochlorite solution supplemented with 0.5% Tween-20 for 10 min. After washing the seeds five times with sterile water, they were sowed on Petri plates containing Murashige-Skoog (MS) medium (Murashige and Skoog 1962) (2.2 g MS salts, 3 g phytagel, 10 g sucrose, pH 5.7) supplemented with 15 mg/L hygromycin B (Invitrogen, Carlsbad, CA, USA), except for seeds from wild-type control plants. Seed dormancy was broken by incubating the plates for 2 days at 4 °C in the dark. Posteriorly, these plates were transferred to a growth room, and 1-week-old seedlings were transplanted to pots containing sterile commercial substrate and maintained under the same conditions as described above.

Genomic DNA was isolated from young leaves collected from *A. thaliana* plants following the CTAB/chloroform extraction method (Allen et al. 2006). DNA concentration and purity were analyzed in a NanoDrop ND-1000 spectrophotometer (NanoDrop Technologies) and 1% agarose gel electrophoresis. The screening of T_1 lines and subsequent generations (T_2 and T_3) was carried out via PCR using specific primers for detection of the *eGFP* transgene (Suppl. Table S1). PCR was performed using GoTaq® DNA polymerase (Promega, Madison, WI, USA) with a final primer concentration of 10 mM and 100 ng of genomic DNA as

template in a PCR System 9700 (Life Technologies, Carlsbad, CA, USA). The PCR conditions included an initial denaturation step at 94 °C for 2 min; 35 cycles of denaturation at 94 °C for 30 s, annealing at 60 °C for 30 s, and extension at 72 °C for 60 s, followed by a final extension at 72 °C for 5 min using a PCR System 9700 (Life Technologies, Carlsbad, CA, USA). PCR products were then analyzed in 1% agarose gel electrophoresis. Additionally, the expression of the *eGFP* reporter gene was confirmed by visualization of the eGFP fluorescence protein in seedlings under the Axio Zoom macroscope v. 16, filter set 38 HE (Carl Zeiss, Jena, Germany). Segregation analyses of *A. thaliana* lines were performed based on inheritance patterns analyzed by germination of surface-sterilized seeds onto Petri plates containing MS medium supplemented with 15 mg/L hygromycin B up to the T_3 generation. Four independents transgenic T_3 lines were randomly selected to be used in nematode infection bioassays.

Meloidogyne incognita infection assay

For nematode infection bioassays of transgenic *A. thaliana* lines (Line #1 to #4) and wild-type control plants, 20-day-old plants were inoculated with 500 ppJ2s and maintained in a growth room at 22 °C. The *A. thaliana* plants were harvested at 60 DAI; roots were washed with water and stained with floxin B (Taylor and Sasser 1987). Then, galls and egg masses were counted and dissected under a binocular microscope, and the reproduction ratio [number of egg masses/number of galls] was evaluated. The bioassay was carried out with 10 plants per transgenic line or wild-type control *A. thaliana* in two biological repetitions.

Minc16803-RNAi transgene expression and *Minc16803* gene downregulation in *M. incognita* during parasitism in transgenic *A. thaliana* lines

Total RNA was extracted from transgenic and wild-type seedlings or galls at 10 DAI using TRIzol (Life Technologies, Carlsbad, CA, USA) according to the manufacturer's recommendations. RNAi transgene expression in transgenic *A. thaliana* lines was confirmed by RT-qPCR analysis using specific primers for the *pdk* intron sequence. Relative expression of the RNAi transgene was normalized using *AtActin 2*, *AtGAPDH*, and *AtEF1* as reference genes (Suppl. Table S1) and calibrated to the levels of the Line #1. On the other hand, *Minc16803* gene downregulation in *M. incognita* during its parasitism in transgenic *A. thaliana* lines was confirmed by RT-qPCR analysis using *MiGAPDH*, *MiActin* and *Miβ-tubulin* as reference genes (Suppl. Table S1). Primer efficiency was calculated using the Miner tool (http://www.miner.ewindup.info), and relative gene expression was analyzed using the $2^{-\Delta\Delta CT}$ method (Pfaffl 2001) through qBase + v.3.1 software (Biogazelle, Zwijnaarde, Belgium). The suitability of the *A. thaliana* and *M. incognita* reference genes was evaluated by geNorm analysis (Vandesompele et al. 2002), which showed *M-values* below 0.5. Each treatment consisted of three biological replicates and each biological replicate included three to five plants. All samples were evaluated in technical triplicates.

Gall morphology analysis of wild-type and transgenic *A. thaliana* lines

Galls of transgenic lines and wild-type control plants were collected at 7, 21 and 45 DAI, fixed in 2% glutaraldehyde in 50 mM PIPES buffer pH 6.9 for 15 days, dehydrated with an ethanol gradient (15, 30, 50, 70, 80, and 100%), embedded and polymerized in Technovit™ 7100 (Kulzer, Friedrichsdorf, Germany) as described by the manufacturer. Galls were then sectioned (3 µm), stained in 0.05% (w/v) toluidine blue, and mounted with Depex (Sigma-Aldrich, St. Louis, MO, USA). For morphological analyses, stained sections were observed under bright-field light microscopy, and the images were obtained with a digital camera (AxiocamHRc, Carl Zeiss, Oberkochen, Germany). At least 50 sections from 30 different galls of transgenic or wild-type control plants were analyzed. The mean diameter of galls and mean area of feeding sites were measured with ZEISS ZEN software. A total of 30 galls from two different experiments were examined per treatment.

Results

Bioinformatics analysis of *Minc16803* gene

Using different bioinformatics filters detailed in the methods section, we identified a putative effector gene in the *M. incognita* genome, referred here as *Minc16803* gene, located in the *Minc3s00746g16803* locus. The *Minc16803* gene is approximately 1.66 kb in size, divided into 10 exons and 9 intron sequences, and flanked by 5'- and 3'-UTR sequences. Its CDS sequence has 1,052 nucleotides encoding a protein of 343 amino acids, a predicted isoelectric point of 9.2, and a molecular weight of 40.25 kDa (Table 1; Suppl. File S1). The Minc16803 protein sequence showed the presence of a secretory signal peptide (from position 1 to 22 amino acid) at the N-terminal portion, a predicted non-cytoplasmatic domain, and the absence of transmembrane motifs, indicating that Minc16803 is likely a secreted protein (Table 1). In a previous analysis, four degenerate protein motifs had been identified enriched at the N-terminal region of known *M. incognita* effectors (Vens et al. 2011). We found three of

Table 1 Features of *Minc16803* (*Minc3s00746g16803*) gene, its two paralogous *Minc3s00200g07395* and *Minc3s00070g03473* genes, and its potential orthologous genes in other nematode species. The gene sequences were retrieved from WormBase database version WBPS16

Nematode species	Gene ID	Gene description	Nucleotide	Amino acid	Gene expression	Protein immunolocalization	CDD domain	PFAM domain	NLS motif	Signal peptide
M. incognita	*Minc3s00746g16803 Minc16803*	Putative effector involved in parasitism	1052	343	All nematode stages	Undefined	No	Non-cytoplasmatic domain	No	Yes
M. incognita	*Minc3s00200g07395*	*Minc16803* paralog	957	311	All nematode stages	Undefined	No	Non-cytoplasmatic and transmembrane domains	No	Yes
M. incognita	*Minc3s00070g03473*	*Minc16803* paralog	1099	292	All nematode stages	Undefined	No	Non-cytoplasmatic domain	No	Yes
M. floridensis	*scf7180000420581*	Orthologue of the *Minc16803*	937	312	Undefined	Undefined	No	No	No	No
M. javanica	*scaffold37606_cov431.g23340*	Orthologue of the *Minc16803*	804	267	Undefined	Undefined	No	Non-cytoplasmatic domain	No	Yes
M. hapla	*MhA1_Contig468.frz3.gene9*	Orthologue of the *Minc16803*	648	215	Undefined	Undefined	PLN02286	IPR001278	No	No
M. hapla	*MhA1_Contig468.frz3.gene5*	Orthologue of the *Minc16803*	870	289	Undefined	Undefined	No	Non-cytoplasmatic domain	No	Yes
G. rostochiensis	*GROS_g05191*	Orthologue of the *Minc16803*	1413	470	Undefined	Undefined	No	Non-cytoplasmatic domain	Yes	Yes
G. pallida	*GPLIN_000992700*	Orthologue of the *Minc16803*	1206	401	Undefined	Undefined	No	No	Yes	No
D. destructor	*Dd_04152*	Orthologue of the *Minc16803*	1548	515	Undefined	Undefined	No	No	Yes	No
B. xylophilus	*BXYJ5.050084300*	Orthologue of the *Minc16803*	1152	383	Undefined	Undefined	No	Non-cytoplasmatic domain	Yes	Yes
Bursaphelenchus okinawaensis	*BOKI.050088700*	Orthologue of the *Minc16803*	1170	389	Undefined	Undefined	No	Non-cytoplasmatic domain and signal peptide	Yes	Yes
Bursaphelenchus xylophilus	*BXY_0398000*	Orthologue of the *Minc16803*	1152	383	Undefined	Undefined	No	Non-cytoplasmatic domain and signal peptide	Yes	Yes
Ditylenchus dipsaci	*jg3035*	Orthologue of the *Minc16803*	795	264	Undefined	Undefined	No	No	Yes	No
Heterodera glycines	*Hetgly17661*	Orthologue of the *Minc16803*	1979	488	Undefined	Undefined	No	signal peptide	Yes	Yes

Table 1 (continued)

Nematode species	Gene ID	Gene description	Nucleotide	Amino acid	Gene expression	Protein immunolocalization	CDD domain	PFAM domain	NLS motif	Signal peptide
Heterodera schachtii	*Hsc_gene_10797*	Orthologue of the *Minc16803*	1470	489	Undefined	Undefined	No	Non-cytoplasmatic domain and signal peptide	Yes	Yes
Meloidogyne graminicola	*NXFT01001968.1.5091_g*	Orthologue of the *Minc16803*	600	199	Undefined	Undefined	No	No	No	No

PLN02286 Arginine-tRNA ligase, *IPR001278* Arginine-tRNA ligase

these four motifs at the N-terminal region of the encoded protein sequence of Minc16803 and Minc3s00070g03473, providing additional evidence that they might be putative *M. incognita* effectors. However, Minc3s00200g07395 did not show any of the degenerate motifs (Fig. 1A, Suppl. Table S2).

We also retrieved and analyzed the phylogenetic tree corresponding to gene entry 'Minc3s00746g16803' in WormBase Parasite (https://parasite.wormbase.org/Multi/GeneTree/Image?gt=WBGT00000000029539). All phylogenetic trees in WormBase Parasite have been generated using Ensembl Compara pipeline (Cunningham et al. 2022), which produces both nucleotide and amino acid-based phylogenies and then, compare to a reference species tree to infer duplication and speciation branches and thus, orthology and paralogy. The phylogenetic tree for *Minc16803* confirmed that *Minc3s00070g03473* and *Minc3s00200g07395* can be consistently considered its paralogs (Fig. 1B). In addition, orthologs were identified in several other species albeit all being plant-parasitic nematodes, including other root-knot nematodes (*Meloidogyne floridensis, Meloidogyne hapla, M. graminicola,* and *M. javanica*), cyst nematodes (*Globodera pallida*, *Globodera rostochiensis*, *H. glycines* and *Heterodera schachtii*), stem and bulb nematode (*Ditylenchus dipsaci*), and the pine wilt nematodes (*Bursaphelenchus xylophilus* and *Bursaphelenchus okinawaensis*). Therefore, *Minc16803* is widely conserved in several plant-parasitic nematodes, but specific to phytoparasites (Table 1, Fig. 1B). The high sequence identity between *Minc16803* and its two paralogous genes (95 to 99% amino acid identity) suggests that they may likely be the result of gene duplication, consistent with the triploid structure of the *M. incognita* genome (Blanc-Mathieu et al. 2017).

Minc16803 expression level at different *M. incognita* developmental stages

From transcriptome data mining, it was possible to identify the *Minc16803* gene expression profile, as well as its two paralogous *Minc3s00070g03473* and *Minc3s00200g07395* genes, at different *M. incognita* life stages (egg, ppJ2, pJ2/J3, J4, and female) during nematode parasitism in plants (Fig. 1C). Interestingly, the expression of all three genes was similar across the five different life stages of *M. incognita*; however, the *Minc3s00200g07395* gene had a higher expression level than the other genes at all developmental stages (Fig. 1C). Then, the in silico *Minc16803* gene expression data were confirmed by RT-qPCR analysis in different developmental stages of *M. incognita* during infection in *N. tabacum* plants. The different stages of the nematodes collected for the RT-qPCR analysis were identified through acid fuchsin staining of tobacco roots infected with *M. incognita*. Under our experimental conditions, penetration of ppJ2

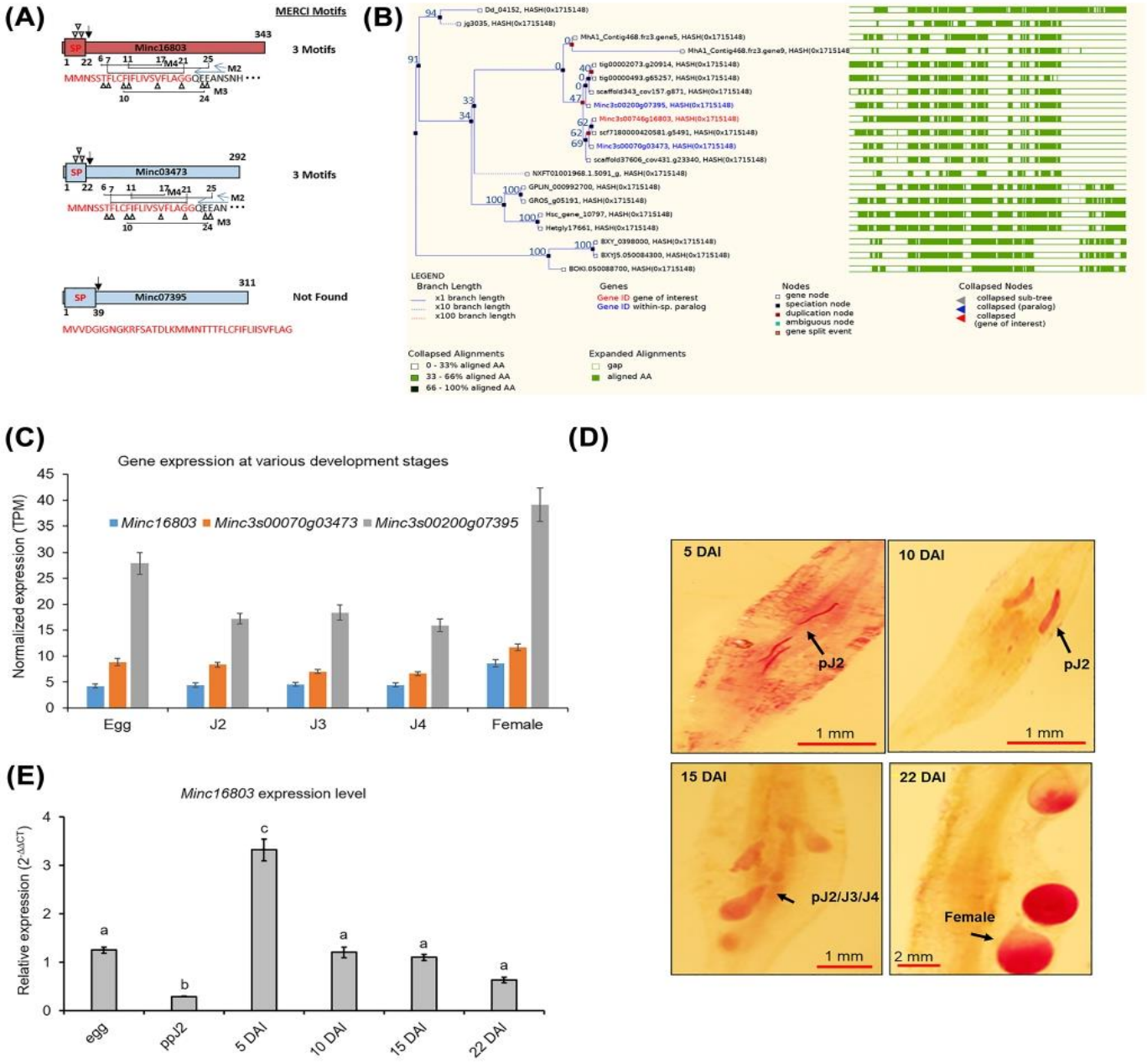

Fig. 1 Sequence analysis and gene expression profiles. **A** Schematic representation of MERCI motifs found at the N-terminal region of Minc16803 and Minc3s00070g03473 proteins. **B** Final merged phylogenetic tree (WBGT00000000029539), corresponding to *Minc16803* as well as its paralogs and orthologs retrieved from WormBase Parasite. **C** Gene expression profiles of the *Minc16803* and its paralogs *Minc3s00200g07395* and *Minc3s00070g03473* genes at different *M. incognita* life stages: egg, pJ2, J3, J4, and female, retrieved from WormBase Parasite and based on transcriptome datasets under BioProject number PRJNA390559 (Choi et al. 2017). Error bars represent confidence intervals corresponding to three libraries per nematode life stage. **D** Histological images of *M. incognita* pJ2, pJ2/J3/J4, and female during parasitism in *N. tabacum* roots at 5, 10, 15, and 22 days after inoculation (DAI). **E** *Minc16803* gene expression profile measured by RT-qPCR analysis in different *M. incognita* life stages (egg, ppJ2, and pJ2 to female) during its parasitism in *N. tabacum*. Relative expression levels were normalized with *Mi18S* and *MiGAPDH* as endogenous reference genes. Data are presented as means ± SE of three biological replicates. Different letters on the bars indicate significant differences based on Tukey's test ($P < 0.05$)

infectious juveniles into the root tissue starts within 1 DAI. Juvenile nematode migration toward the vascular cylinder is mainly visible around 5 DAI (Fig. 1D), and nematodes are characterized by a vermiform and slender body shape.

At 10 and 15 DAI, we verified that most tobacco roots were infected by *M. incognita,* presenting a more swollen body shape, and numerous nematodes were observed nearby the vascular tissue during the induction and establishment of feeding sites (Fig. 1D). The infected region shows clear changes in morphology, forming swellings and the typical fully developed galls around 15 DAI. However, it was not possible to precisely characterize the development stage of nematodes at 10 and 15 DAI based on their morphology due to the presence of pJ2 and non-feeding J3 and J4 nematodes. At 22 DAI, several adult females displaying a pear-shaped body were clearly observed in developed galls within the roots (Fig. 1D). We observed a significant decrease in the transcript levels of *Minc16803* in ppJ2 and at 22 DAI, while at 10 and 15 DAI, the *Minc16803* expression was similar to that observed in the eggs stage. The highest *Minc16803* expression was observed in pJ2 at 5 DAI, with an increase of 2.65-fold compared to the eggs, suggesting that the *Minc16803* plays a role at the early stages of parasitism (Fig. 1E).

Transgenic *A. thaliana* lines harboring *Minc16803*-dsRNA

To investigate the effect of *in planta* expression of dsRNA targeting *Minc16803* on *M. incognita* parasitism, several transgenic *A. thaliana* lines were generated. Then, we randomly selected only four lines (Line #1 to #4) for further analysis. The 200 bp sequence of the *Minc16803* transcript was cloned in sense and antisense separated by the *pdk* intron sequence in an expression cassette controlled by the strong and constitutive *pUceS8.3* promoter (Fig. 2A). In silico analysis using si-Fi software (Lück et al. 2019) revealed that the *Minc16803*-dsRNA designed based on 200 bp *Minc16803* sequence was predicted to generate 84 and 32 perfect matching 21 nucleotides small-interfering RNA (siRNA) molecules against its paralogous *Minc3s00070g03473* and *Minc3s00200g07395* genes, respectively. This data indicated that *Minc16803* and its two paralogous could be downregulated by the RNAi sequence used here, possibly resulting in the disruption of their biological function. After floral dip transformation, *A. thaliana* plants resistant to hygromycin were characterized by PCR to confirm the insertion of the T-DNA into the plant nuclear genome in T_1 to T_3 generations. Transgenic plants were also selected in MS medium supplemented with 15 mg/L hygromycin B up to T_3 generation, and an uniform population of resistant seedlings in the progenies was observed (Fig. S1A). Amplification by PCR of the *eGFP* fragment (423 bp) over the three generations demonstrated stable inheritance of the T-DNA (Fig. 2B). Additionally, the transgenic events were also confirmed by confocal analyses of eGFP fluorescence protein accumulation in the plant leaves (Fig. 2C). Phenotypic differences between the transgenic lines and wild-type control plants were not identified, indicating that the expression of *Minc16803*-dsRNA did not result in pleiotropic effects on plant architecture and development (Suppl. Fig. S1B).

Meloidogyne incognita infection assay on transgenic *A. thaliana* lines

To evaluate the efficacy of *in planta Minc16803*-dsRNA overexpression in reducing plant susceptibility to *M. incognita*, bioassays using *M. incognita* race 3 inoculum were performed with four transgenic lines and wild-type plants. Then, these plants were evaluated for galls/plant and egg masses/plant. Consistently, we observed a significant reduction of 66.3–84% in the number of galls and 79.3–93.3% in egg masses in transgenic *A. thaliana* lines compared with wild-type plants (Fig. 2D, E). Further, a significant decrease in the ratio [number of egg masses/number of galls] ranging from 54.7 to 64.1% was verified in the transgenic lines (Fig. 2F). Subsequently, RT-qPCR analyses were performed to confirm that the transgenic lines successfully overexpressed *Minc16803*-dsRNA and to examine whether the observed effects on nematode parasitism were due to *Minc16803* gene downregulation. Transgene expression analyses targeting the *pdk* intron showed that *Minc16803*-dsRNA was overexpressed in all four transgenic lines, whereas in the wild-type plants, gene expression was not detected (Fig. 2G). In addition, a significant decrease in *Minc16803* gene expression of 90–95% was observed in nematodes during parasitism in transgenic lines compared to those in wild-type control plants (Fig. 2H). However, our attempts to determine the silencing of *Minc3s00070g03473* and *Minc3s00200g07395* were unsuccessful. Due to the high identity among *Minc16803*, *Minc3s00070g03473,* and *Minc3s00200g07395*, it was not possible to design specific and efficient primers to detect *Minc3s00070g03473* and *Minc3s00200g07395* expression. We designed four pairs of primers for each gene (*Minc3s00070g03473* and *Minc3s00200g07395*), but all of them had poor performance. Primers that did not amplify the target sequence or primers that amplified the target sequence with efficiencies outside the acceptable range to be considered suitable for RT-qPCR analyses (90–110%) and/or showed more than one PCR amplification peak according to melting curve analysis were considered primers with poor performance.

Histological analysis of the galls in the transgenic *A. thaliana* lines

To further characterize the effects of *Minc16803* gene downregulation on nematode during plant parasitism, transgenic *A. thaliana* plants from Line #1 and wild-type control plants were infected with *M. incognita* ppJ2, and the roots were

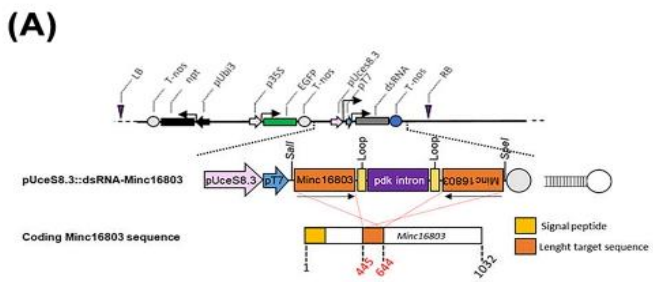
(A)
LB
T-nos
npt
pUbi3
pBSS
EGFP
T-nos
pUceS8.3
pT7
dsRNA
T-nos
RB
pUceS8.3::dsRNA-Minc16803
pUceS8.3
pT7
Minc16803
pdk intron
Minc16803
SalI
Loop
Loop
SacI
Coding Minc16803 sequence
Minc16803
Signal peptide
Lenght target sequence
1
445
644
1032

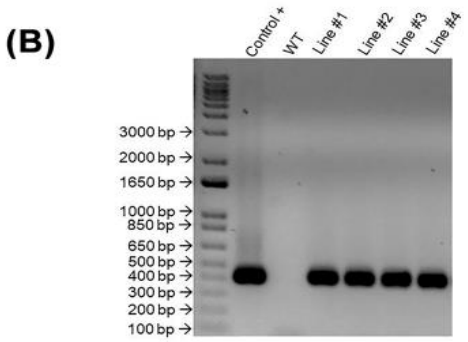
(B)
Control +
WT
Line #1
Line #2
Line #3
Line #4
3000 bp
2000 bp
1650 bp
1000 bp
850 bp
650 bp
500 bp
400 bp
300 bp
200 bp
100 bp

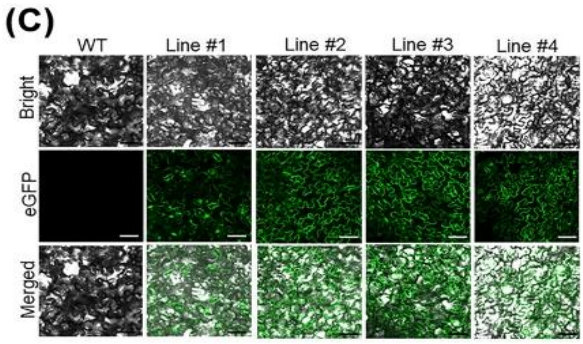
(C)
WT
Line #1
Line #2
Line #3
Line #4
Bright
eGFP
Merged

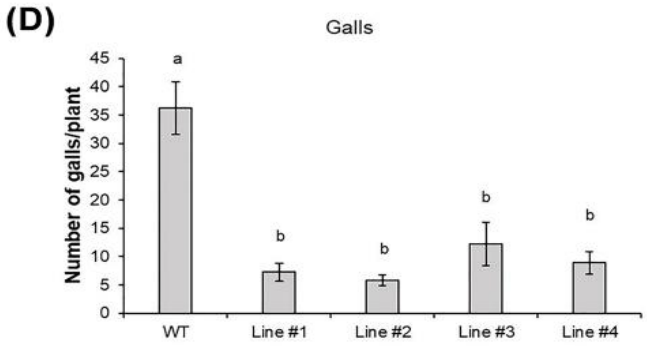
(D)
Galls
Number of galls/plant
WT
Line #1
Line #2
Line #3
Line #4

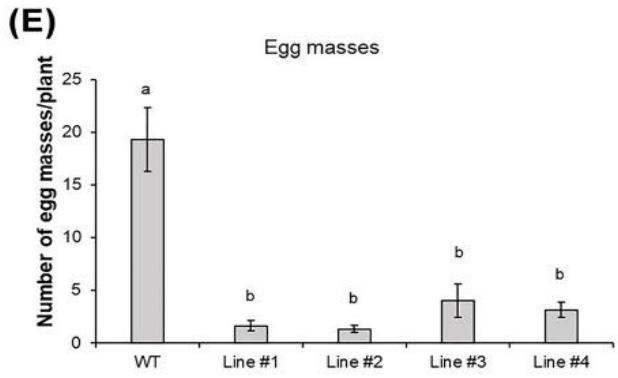
(E)
Egg masses
Number of egg masses/plant
WT
Line #1
Line #2
Line #3
Line #4

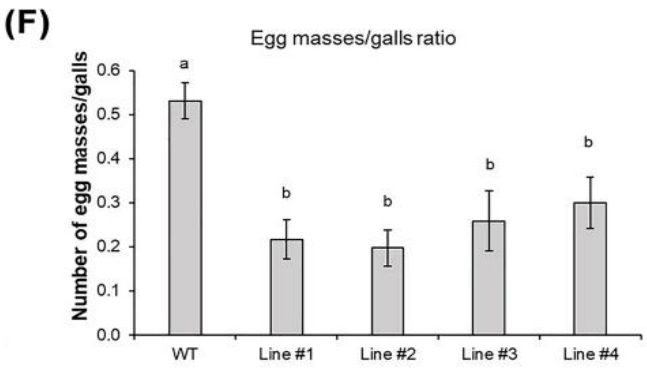
(F)
Egg masses/galls ratio
Number of egg masses/galls
WT
Line #1
Line #2
Line #3
Line #4

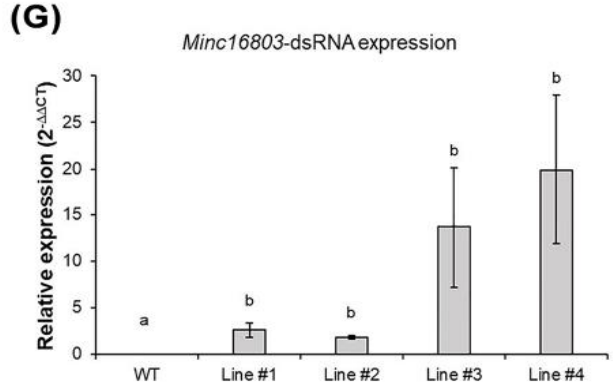
(G)
Minc16803-dsRNA expression
Relative expression (2-ΔΔCT)
WT
Line #1
Line #2
Line #3
Line #4

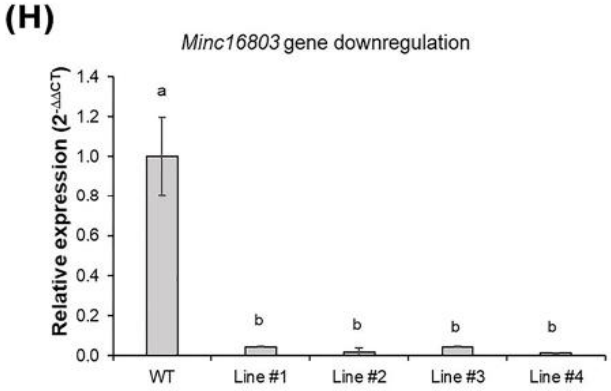
(H)
Minc16803 gene downregulation
Relative expression (2-ΔΔCT)
WT
Line #1
Line #2
Line #3
Line #4

◂**Fig. 2** *Agrobacterium*-mediated genetic transformation of *A. thaliana*, susceptibility level of transgenic *A. thaliana* lines to *M. incognita* race 3, and *Minc16803* gene expression in *M. incognita* during its parasitism in transgenic lines and wild-type control plants. **A** Overview of the T-DNA used into binary vector for genetic transformation of *A. thaliana* plants, targeting downregulation of *Minc16803* gene transcripts by the *in planta* RNAi strategy. **B** PCR detection of the *eGFP* transgene in *A. thaliana* lines, indicating the expected amplicon size of 400 bp. Marker: 1.0-kb DNA ladder (Invitrogen); positive control: binary vector; WT: wild-type control plant used as a negative control for PCR analysis and plant-nematode bioassays. **C** Fluorescence detection of eGFP protein in transgenic lines under a Zeiss inverted LSM510 META laser scanning microscope using 488-nm excitation line and the 500–530-nm band pass filter (Carl Zeiss). Scale bars: 10 mm. Plant susceptibility analysis based on **D** number of galls per plant, **E** number of egg masses per plant, and **F** ratio [number of egg masses/number of galls] in T_3 transgenic *A. thaliana* lines ($n = 10$ plants) at 60 DAI. Data are presented as means ± SE of 10 plants per transgenic line or wild-type control. Different letters on bars indicate statistically significant differences according to Tukey's test ($P < 0.05$). **G** Transgene expression level measured by RT-qPCR analysis in transgenic lines and wild-type control plants using the *pdk* intron fragment as the target. Relative expression levels were normalized using *AtActin 2*, *AtGAPDH,* and *AtEF1A* as endogenous reference genes. Transgene expression was undetected in WT plants, and transgene expression levels were relative to the expression of Line #1. **H** *Minc16803* gene expression measured by RT-qPCR analysis in *M. incognita* during parasitism in transgenic lines and wild-type control plants. Relative expression levels were normalized with *MiActin, MiTubulin* and *MiGAPDH* as endogenous reference genes. Data are presented as means ± SE of three biological replicates. Different letters on the bars indicate significant differences based on Tukey's test ($P < 0.05$)

collected at 7, 21, and 45 DAI for histological analysis. This analysis was focused only on Line #1 because it showed similar susceptibility levels to *Minc16803*-dsRNA Lines #2, #3, and #4 (Fig. 2D, F). We observed that the galls collected at 7 and 21 DAI in the wild-type plants showed maturing nematodes and multiple well-developed feeding sites with giant cells containing a dense cytoplasm, while upon *Minc16803* downregulation, giant cells were devoid of cytoplasm and nematodes showed morphological alterations (Fig. 3A, B).

The wild-type control roots at 45 DAI showed a large number of galls containing giant cells filled with cytoplasm and mature nematodes that developed normally. In addition, egg-laying females were often visible at 45 DAI (Fig. 4A). *Minc16803*-dsRNA (Line #1) infected roots showed fewer and smaller galls compared to wild-type roots. In *Minc16803*-dsRNA galls, we observed malformed nematodes without well-defined shapes, which stained more intensely than nematode sections in the wild-type plants (Fig. 4B). This suggests that induced downregulation of *Minc16803* within nematodes strongly affected their development and likely their maturation. However, some nematodes were capable of laying eggs that often hatched before egg mass extrusion (Fig. 4B). In addition, the gall diameters at 7 and 45 DAI, as well as the feeding site areas at 45 DAI from *Minc16803*-dsRNA (Line #1) roots, were significantly smaller compared to those from wild-type roots (Fig. 4C, D, E).

Discussion

Meloidogyne incognita is among the most devastating PPNs and has caused severe yield losses to several crops worldwide (Bernard et al. 2017). Currently, the control of *M. incognita* is mainly based on the use of chemical nematicides and resistant cultivars developed through conventional breeding (Koenning et al. 2001; Wheeler et al. 2014). However, *M. incognita* continues to overcome the limited number of resistant cultivars available, and several nematicides have been banned from use or are being phased out due to their negative impact on the environment and human health (Zhou et al. 2000; Silva et al. 2014; Oka 2020). Therefore, the development of innovative and environmentally friendly strategies for managing *M. incognita* is crucial to promote more sustainable agricultural systems.

Meloidogyne incognita has developed sophisticated mechanisms of parasitism to manipulate plant physiology and immunity signaling pathways that ultimately result in the establishment of permanent feeding structures, whereby nematodes take up nutrients needed for their development and reproduction (Kyndt et al. 2013; Ali et al. 2017). Among these, effector-dependent parasitism mechanisms are pivotal for successful infection during compatible plant-nematode interactions (Mejias et al. 2019). Identifying novel *M. incognita* target genes that encode effector proteins is an important step toward developing innovative biotechnological strategies that can be applied to the management of this devastating plant-parasite (Rutter et al. 2014). Herein, we described the identification of the *Minc16803* putative effector gene and demonstrated its contribution to the enhancement of *A. thaliana* resistance to *M. incognita* through the host-induced gene silencing system.

With rapid advances in sequencing technologies, genomic and transcriptomic information from an increasing number of nematodes is becoming available, which has facilitated the prediction and characterization of numerous effectors (Danchin et al. 2013; Pogorelko et al. 2020; Grynberg et al. 2020; Rocha et al. 2021). Prior to functional analyses, the prediction of putative effectors relies primarily on in silico analysis of genes encoding proteinaceous secretions that have a signal peptide for secretion and the absence of transmembrane domains (Xie et al. 2016; Chen et al. 2017). Taking advantage of published genomes for *M. incognita*, we identified the *Minc16803* gene. At a first step, an assessment of protein sequence using bioinformatic analyses was performed. As expected, we found that the predicted protein encoded by the *Minc16803* gene retrieved from the *M. incognita* genome contains a signal peptide and lacks

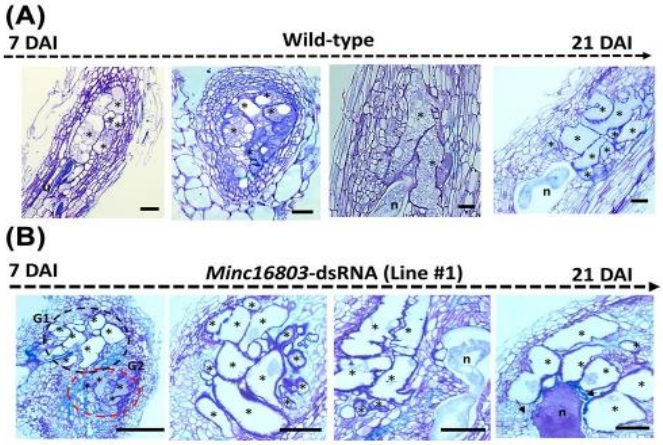

Fig. 3 Histological analysis of galls in wild-type and transgenic plants infected with *M. incognita*. Gall sections were stained with toluidine blue and imaged by bright-field microscopy. **A** Galls sections in the wild-type control roots showed well-developed feeding sites and nematodes. **B** *Minc16803*-dsRNA (Line #1) transgenic galls showed giant cells with low cytoplasmic content and apparent unstructured nematodes. Note that nematodes cuticle seems affected, and nematodes stained more strongly, suggesting morphological changes during their development (black arrows). *, giant cell; n, nematode; G1, gall 1 and G2, gall 2. Scale bars: 50 µm

transmembrane domains, which is structurally consistent with the potential secretory nature of the protein. The N-terminal signal peptide is important for directing the effector proteins from the cytoplasm to the endoplasmic reticulum of the nematode secretory esophageal gland cells, and then, the mature effector proteins are secreted into the root cells via the nematode stylet (Wang et al. 2010). Accordingly, the Minc16803 protein is presumably secreted. In addition, three motifs typical of known effectors (Vens et al. 2011; Grynberg et al. 2020; Rocha et al. 2021) were identified in the predicted Minc16803 protein sequence, suggesting that Minc16803 might be an effector protein secreted in plant tissue during parasitism. However, future in situ hybridization and/or antibody localization studies will be required to assess whether Minc16803 is expressed in the nematode esophageal gland cells and secreted in plant tissues in order to confirm that it is indeed an effector protein. Furthermore, putative orthologs of *Minc16803* gene were found in other *Meloidogyne* spp., as well as in other nematode genera, all being plant-parasitic species, suggesting that this gene may have a conserved role not only in the parasitism of *Meloidogyne* spp. but also in other phytoparasitic nematodes.

Subsequently, we analyzed the expression level of *Minc16803* gene throughout the life cycle of *M. incognita* during the compatible *M. incognita*-tobacco interaction. The peak of *Minc16803* gene expression at 5 DAI suggests that this putative effector acts at the early stages of infection by interfering with the initiation and/or establishment

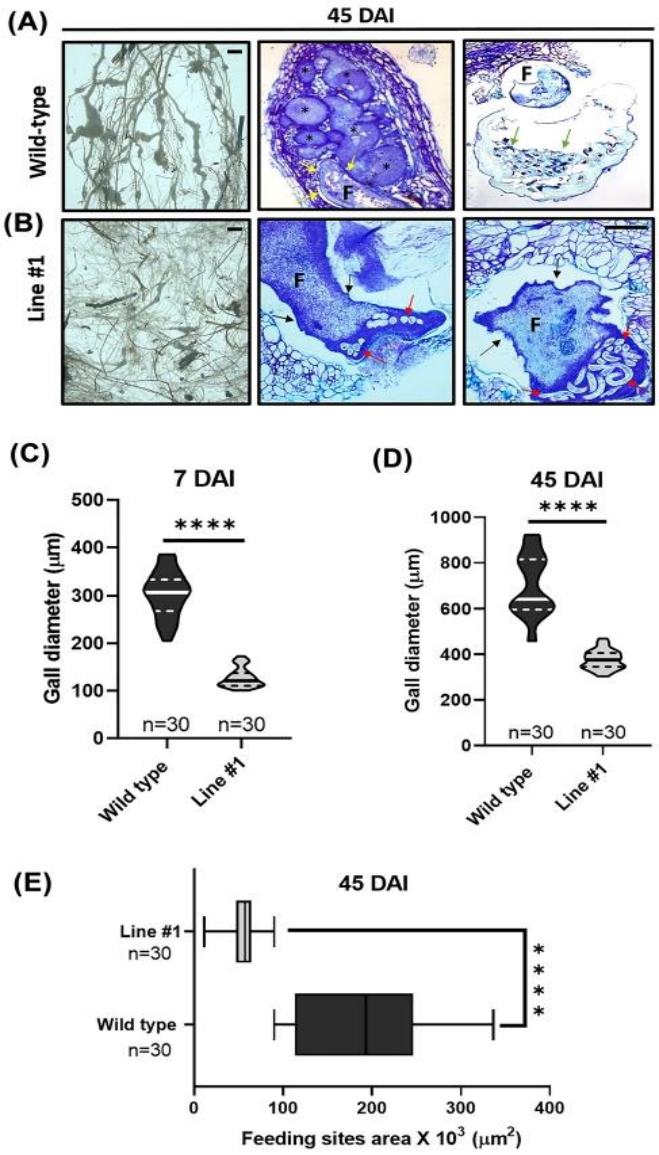

Fig. 4 Histological analysis of *M. incognita*-induced galls and measurement of the galls and feeding sites. Gall sections were stained with toluidine blue and imaged by bright-field microscopy. **A** Wild-type control roots illustrated a large number of galls at 45 DAI containing giant cells filled with cytoplasm. Nematodes had a rounded form and cuticles less stained (yellow arrows). Egg-laying females and egg masses (green arrows) were often visible at 45 DAI. **B** *Minc16803*-dsRNA (Line #1) infected roots showed fewer and smaller galls compared to wild-type roots. In *Minc16803*-dsRNA galls, the nematodes illustrated irregular forms and the cuticle seemed altered (black arrows), with no well-defined morphology and nematodes stained more strongly, suggesting structural body changes. Strikingly, the eggs in *Minc16803*-dsRNA (Line #1) apparently hatched prematurely (red arrows) compared to what was seen in wild-type plants (green arrows), and the gelatinous matrix containing the eggs colored more strongly. **C–D** Gall diameter measurements revealed significantly smaller galls in *Minc16803*-dsRNA (Line #1) compared to wild-type galls at 7 DAI and 45 DAI. **E** Feeding site area measurements revealed significantly smaller feeding sites in *Minc16803*-dsRNA (Line #1) compared to those in wild-type galls at 45 DAI. This analysis demonstrated that *Minc16803* down-regulation had a direct effect on gall and nematode development. Data are presented as means ± SD from two experiments with $n = 30$ galls examined per treatment. Statistical differences between treatments are based on Student`s t test (****$P < 0.0001$). *, giant cell; n, nematode; *F*, female. Scale bars: 50 µm

of feeding sites. However, *Minc16803* and its two paralogous genes were found to have considerable expression levels in all stages of nematode development. Suppression of plant defense at the early stages of nematode infection is extremely important to establish a successful infection. Thus, nematodes are expected to use some effectors at the early stages of parasitism, which is supported by the upregulation of the *Minc16803* gene at 5 DAI. Similar to our results, the *MjTTL5*, *MgGPP*, and *Mi-msp2* effector genes have been shown to be upregulated at early stages of *M. javanica*, *M. graminicola*, and *M. incognita* parasitism, respectively (Lin et al. 2016; Chen et al. 2017; Joshi et al. 2019).

In addition, an infection bioassay was performed to test whether the transgenic *A. thaliana* lines expressing *Minc16803*-dsRNA affect the infection and reproduction process of *M. incognita.* Indeed, the expression of *Minc16803*-dsRNA in transgenic *A. thaliana* lines downregulated *Minc16803* transcripts in the nematode, leading to reduced susceptibility of plants to *M. incognita*. We observed that the T_3 progeny of four independent transgenic lines showed a significant decrease of up to 84% and 93.3% in the number of galls and number of egg masses, respectively, indicating that *Minc16803* gene downregulation not only affected the ability of the nematode to infect the host plant but also compromised nematode reproduction. Furthermore, it was found that the ratio of number of egg masses/number of galls was significantly lower in the transgenic lines compared with the wild-type control plants. These data strongly suggest that the significant downregulation of *Minc16803* transcripts compromised the development of later-stage juveniles into female adults, as well as egg production that could ensure novel galls establishment. Thus, the reduced plant susceptibility to *M. incognita* among the four transgenic lines was most likely associated with the *Minc16803* gene expression downregulation in nematodes and potentially of its two paralogous genes.

In agreement with our findings that Minc16803 protein is critical for *M. incognita* infection and reproduction, a recent study showed that the number of galls in transgenic *A. thaliana* plants overexpressing dsRNA molecules against the effector genes *Mi-msp3*, *Mi-msp5*, *Mi-msp18,* and *Mi-msp24* of *M. incognita* was reduced by 89%, 78%, 86%, and 89%, respectively. In addition, the reproduction factor was significantly reduced in all dsRNA-overexpressing lines compared to the wild-type control plants (Joshi et al. 2020). Likewise, downregulation of the *Mi-msp2* effector gene by RNAi was shown to reduce *A. thaliana* susceptibility to *M. incognita*, as observed by the significant reduction in the number of galls, females, and egg masses by up to 54%, 66%, and 95%, respectively (Joshi et al. 2019). Furthermore, dsRNA molecules that target the *MiPDI1* effector gene were found to confer reduced susceptibility to *M. incognita* when overexpressed in *A. thaliana* (Zhao et al. 2020).

Unlike insects, nematodes are able to amplify the siRNA signal by RNA-dependent RNA polymerases (Pak and Fire 2007), and therefore, even a small amount of dsRNA produced by the plant may induce strong and prolonged gene downregulation in nematode cells. In addition, the siRNAs generated by the processing of dsRNA by the plant RNAi machinery can be efficiently taken up by nematode midgut cells and trigger an RNAi response (Steeves et al. 2006). Thus, the development of RNAi-based transgenic crops against highly effective target genes offers a valuable approach for conferring resistance to phytonematodes. Several studies have shown the efficacy of host-delivered RNAi silencing of effector and essential genes to control different nematode species, including *M. incognita* (Dinh et al. 2014; Dutta et al. 2015; Chaudhary et al. 2019; Zhao et al. 2019, 2020). Interestingly, Tian et al. 2019 reported that overexpression of dsRNA molecules targeting the *H. glycines HgY25* and *HgPrp17* genes in transgenic soybean plants resulted in a significant reduction in cyst and egg numbers. Similarly, it was recently shown that simultaneous downregulation of *cysteine protease*, *isocitrate lyase*, and *splicing factor* genes significantly impaired plant parasitism by *M. incognita* in transgenic cotton lines (Lisei-de-Sá et al. 2021).

To better understand how *Minc16803* gene downregulation might affect plant-nematode interactions, histological analyses of *M. incognita*-induced galls in the transgenic *A. thaliana* line and wild-type control plants were compared. Our results demonstrated that *Minc16803* plays a role in the induction and establishment of feeding sites as the transgenic galls exhibited giant cells lacking cytoplasm and surrounded by even more asymmetrically dividing neighboring cells. Interestingly, nematodes in the transgenic lines displayed irregular body shapes, suggesting cuticle damage and cytoplasmic degeneration. The morphological alterations in the nematode body might be attributed to the fact that giant cells did not support the full development of the nematodes. Intriguingly, numerous hatching *M. incognita* ppJ2s were frequently observed in the amorphous egg mass secreted by female nematodes that remained inside the root. These alterations indicate that some females, even with an aberrant phenotype, were able to lay the eggs that apparently hatched prematurely, perhaps in an effort to accelerate their infection cycle. Therefore, it is possible that the significant reduction in the number of egg masses found on the root surface of the transgenic lines is due to the unhealthy state of the maturing nematodes.

The molecular mechanisms by which nematode effector proteins overcome plant defense systems and facilitate plant parasitism are diverse. For instance, *M. javanica* MjTTL5 effector alters the plant's oxidative response through augmentation of the host's ROS-scavenging system by interacting with *A. thaliana* ferredoxin:thioredoxin reductase catalytic subunit (Lin et al. 2016). *M. incognita* MiMIF-2

interacts with *A. thaliana* annexins to suppress host immune responses and promote parasitism (Zhao et al. 2019). On the other hand, *M. incognita* MiEFF18 has been shown to target the plant core spliceosomal protein SmD1 to modulate the expression of critical genes required for giant cell ontogenesis (Mejias et al. 2021). However, the molecular mechanisms underlying the process by which the putative Minc16803 effector suppresses plant defenses to establish parasitism remain to be investigated. In addition, detailed studies will allow the precise identification of the tissues or cells in which the putative Minc16803 effector specifically acts, and the host target proteins that interact with Minc16803.

In summary, our findings indicate that transgenic *A. thaliana* lines overexpressing a *Minc16803*-dsRNA targeting *Minc16803* transcripts have reduced susceptibility to *M. incognita,* as observed by the remarkable reduction in the number of galls and egg masses. These results suggest that the putative *Minc16803* effector gene is an amenable target for improving the resistance of economically important crops to *M. incognita* using *in planta* RNAi technology. The *Minc16803* dsRNA can be pyramided with dsRNAs targeting other nematode genes or even with plant resistance genes to develop genetically engineered crops with improved and durable resistance to *M. incognita*. Furthermore, a major advantage of using RNAi technologies is that the dsRNA molecules can be rationally designed based on the gene sequence of interest to specifically target *M. incognita* or a wider range of closely related nematode species. Given that putative *Minc16803* orthologous have been found in other *Meloidogyne* spp. and the relative flexibility in selecting *Minc16803*-dsRNA target sites based on the gene sequence, the RNAi cassette could be adapted to downregulate not only *Minc16803* but also its orthologous genes. Therefore, it would be interesting to develop RNAi-based transgenic crops to suppress *Minc16803* gene expression in *M. incognita* and even its orthologous genes in other RKNs.

Author contributions

VJVM designed the experiments. VJVM and DHP analyzed the data, and DHP wrote the manuscript. EGJD, PMG, PG, and ACMB searched for nematode gene sequence and analyzed bioinformatics data. MFB performed sequence analysis and produced transgenic *A. thaliana* lines. VJVM performed generation advancements. VJVM, DHP, ITLT, and MELS performed the nematode bioassays. VJVM, ITLT, and JAE performed histological analyses. DHP and ITLT performed RT-qPCR analysis. MFGS, MFB, MCMS, CVM, EGJD, and JAE amended the manuscript. MFGS was the lead researcher, edited the manuscript, and provided financial support and intellectual input. All authors read and approved the final manuscript.

Supplementary Information The online version contains supplementary material available at https://doi.org/10.1007/s10340-023-01623-7.

Acknowledgements The authors acknowledge EMBRAPA, UCB, CNPq, CAPES, INCT PlantStress Biotech, and FAPDF for the scientific and financial support.

Funding This work was supported by grants from INCT PlantStress Biotech, EMBRAPA, CNPq, CAPES, and FAPDF. MFB is grateful to CNPq for a postdoctoral research fellowship (PDJ 150936/2018-4). ITLT is grateful to CAPES/Cofecub project Sv.922/18 for financial support in the researcher and students exchange program between institutions.

Data availability The data that support the findings of this study and any material presented in the manuscript are available from the corresponding author upon reasonable request.

Declarations

Conflict of interest The authors declare no conflict of interest.

References

Ali MA, Azeem F, Li H, Bohlmann H (2017) Smart parasitic nematodes use multifaceted strategies to parasitize plants. Front Plant Sci 8:1–21. https://doi.org/10.3389/fpls.2017.01699

Allen GC, Flores-Vergara MA, Krasynanski S et al (2006) A modified protocol for rapid DNA isolation from plant tissues using cetyltrimethylammonium bromide. Nat Protoc 1:2320–2325. https://doi.org/10.1038/nprot.2006.384

Almagro Armenteros JJ, Tsirigos KD, Sønderby CK et al (2019) SignalP 5.0 improves signal peptide predictions using deep neural networks. Nat Biotechnol 37:420–423. https://doi.org/10.1038/s41587-019-0036-z

Anders S, Pyl PT, Huber W (2015) HTSeq-a python framework to work with high-throughput sequencing data. Bioinformatics 31:166–169. https://doi.org/10.1093/BIOINFORMATICS/BTU638

Basso MF, Lourenço-Tessutti IT, Mendes RAG et al (2020) *MiDaf16-like* and *MiSkn1-like* gene families are reliable targets to develop biotechnological tools for the control and management of *Meloidogyne incognita*. Sci Rep 10:1–13. https://doi.org/10.1038/s41598-020-63968-8

Bauters L, Kyndt T, De Meyer T et al (2020) Chorismate mutase and isochorismatase, two potential effectors of the migratory nematode *Hirschmanniella oryzae*, increase host susceptibility by manipulating secondary metabolite content of rice. Mol Plant Pathol 21:1634–1646. https://doi.org/10.1111/MPP.13003

Bellafiore S, Shen Z, Rosso MN et al (2008) Direct identification of the *Meloidogyne incognita* secretome reveals proteins with host cell reprogramming potential. PLoS Pathog 4:e1000192. https://doi.org/10.1371/JOURNAL.PPAT.1000192

Bernard GC, Egnin M, Bonsi C (2017) The impact of plant-parasitic nematodes on agriculture and methods of control. In: Shah MM, Mahamood M (eds) Nematology–Concepts, Diagnosis and Control. InTech. https://doi.org/10.5772/intechopen.68958

Blanc-Mathieu R, Perfus-Barbeoch L, Aury J-M et al (2017) Hybridization and polyploidy enable genomic plasticity without sex in

the most devastating plant-parasitic nematodes. PLoS Genet 13:e1006777. https://doi.org/10.1371/journal.pgen.1006777
Blum M, Chang HY, Chuguransky S et al (2021) The InterPro protein families and domains database: 20 years on. Nucleic Acids Res 49:D344–D354. https://doi.org/10.1093/NAR/GKAA977
Bybd DW, Kirkpatrick T, Barker KR (1983) An improved technique for clearing and staining plant tissues for detection of nematodes. J Nematol 15:142–143. https://doi.org/10.1079/9781845930561.0059
Canteri MG, Althaus RA, Filho das JSV et al (2001) SASM-AGRI-Sistema para análise e separação de médias em experimentos agrícolas pelos métodos Scott-knott, Tukey e Duncan. Rev Bras Agrocomputação 1:18–24
Castagnone-Sereno P, Danchin EGJ, Perfus-Barbeoch L, Abad P (2013) Diversity and evolution of Root-Knot nematodes, genus Meloidogyne: new insights from the genomic era. Annu Rev Phytopathol 51:203–220. https://doi.org/10.1146/annurev-phyto-082712-102300
Chaudhary S, Dutta TK, Tyagi N et al (2019) Host-induced silencing of *Mi-msp-1* confers resistance to root-knot nematode *Meloidogyne incognita* in eggplant. Transgenic Res 28:327–340. https://doi.org/10.1007/S11248-019-00126-5/FIGURES/6
Chen J, Lin B, Huang Q et al (2017) A novel *Meloidogyne graminicola* effector, MgGPP, is secreted into host cells and undergoes glycosylation in concert with proteolysis to suppress plant defenses and promote parasitism. PLoS Pathog 13:e1006301. https://doi.org/10.1371/journal.ppat.1006301
Chen J, Hu L, Sun L et al (2018) A novel *Meloidogyne graminicola* effector, MgMO237, interacts with multiple host defence-related proteins to manipulate plant basal immunity and promote parasitism. Mol Plant Pathol 19:1942–1955. https://doi.org/10.1111/MPP.12671
Choi I, Subramanian P, Shim D et al (2017) RNA-Seq of plant-parasitic nematode *Meloidogyne incognita* at various stages of its development. Front Genet 8:190. https://doi.org/10.3389/FGENE.2017.00190/BIBTEX
Chu Y, Guimarães LA, Wu CL et al (2014) A technique to study *Meloidogyne arenaria* resistance in *Agrobacterium rhizogenes*-transformed peanut. Research 98:1292–1299. https://doi.org/10.1094/PDIS-12-13-1241-RE
Clough SJ, Bent AF (1998) Floral dip: a simplified method for *Agrobacterium*-mediated transformation of *Arabidopsis thaliana*. Plant J 16:735–743. https://doi.org/10.1046/J.1365-313X.1998.00343.X
Coke MC, Mantelin S, Thorpe P, Lilley CJ, Wright KM, Shaw DS, Chande A, Jones JT, Urwin PE (2021) The GpIA7 effector from the potato cyst nematode *Globodera pallida* targets potato EBP1 and interferes with the plant cell cycle. J Exp Bot 72(20):7301–7315. https://doi.org/10.1093/jxb/erab353
Cunningham F, Allen JE, Allen J et al (2022) Ensembl 2022. Nucleic Acids Res 50:D988–D995. https://doi.org/10.1093/NAR/GKAB1049
Da RM, Bournaud C, Dazenière J et al (2021) Genome expression dynamics reveal the parasitism regulatory landscape of the root-knot nematode *Meloidogyne incognita* and a promoter motif associated with effector genes. Genes (basel) 12:771. https://doi.org/10.3390/GENES12050771
da Silva EH, da Mattos VS, Furlaneto C et al (2014) Genetic variability and virulence of *Meloidogyne incognita* populations from Brazil to resistant cotton genotypes. Eur J Plant Pathol 139:195–204. https://doi.org/10.1007/s10658-014-0381-1
Danchin EGJ, Arguel M-J, Campan-Fournier A et al (2013) Identification of novel target genes for safer and more specific control of root-knot nematodes from a pan-genome mining. PLoS Pathog 9:e1003745. https://doi.org/10.1371/journal.ppat.1003745
Diaz-Granados A, Sterken MG, Overmars H et al (2020) The effector GpRbp-1 of *Globodera pallida* targets a nuclear HECT E3 ubiquitin ligase to modulate gene expression in the host. Mol Plant Pathol 21:66–82. https://doi.org/10.1111/MPP.12880
Dinh PTY, Brown CR, Elling AA (2014) RNA interference of effector gene *Mc16D10L* confers resistance against *Meloidogyne chitwoodi* in *Arabidopsis* and potato. Phytopathology 104:1098–1106. https://doi.org/10.1094/PHYTO-03-14-0063-R
Dutta TK, Papolu PK, Banakar P et al (2015) Tomato transgenic plants expressing hairpin construct of a nematode protease gene conferred enhanced resistance to root-knot nematodes. Front Microbiol 6:260. https://doi.org/10.3389/FMICB.2015.00260
El-Gebali S, Mistry J, Bateman A et al (2019) The Pfam protein families database. Nucleic Acids Res 47:D427–D432. https://doi.org/10.1093/NAR/GKY995
Gardner M, Dhroso A, Johnson N et al (2018) Novel global effector mining from the transcriptome of early life stages of the soybean cyst nematode *Heterodera glycines*. Sci Rep 8:1–15. https://doi.org/10.1038/s41598-018-20536-5
Grynberg P, Togawa RC, de Freitas LD et al (2020) Comparative genomics reveals novel target genes towards specific control of plant-parasitic nematodes. Genes (basel) 11:1–25. https://doi.org/10.3390/genes11111347
Habash SS, Radakovic ZS, Vankova R et al (2017) *Heterodera schachtii* tyrosinase-like protein—a novel nematode effector modulating plant hormone homeostasis. Sci Rep 7:1–10. https://doi.org/10.1038/s41598-017-07269-7
Howe KL, Bolt BJ, Shafie M et al (2017) WormBase ParaSite – a comprehensive resource for helminth genomics. Mol Biochem Parasitol 215:2. https://doi.org/10.1016/J.MOLBIOPARA.2016.11.005
Hu Y, You J, Li C et al (2019) The *Heterodera glycines* effector Hg16B09 is required for nematode parasitism and suppresses plant defense response. Plant Sci 289:110271. https://doi.org/10.1016/J.PLANTSCI.2019.110271
Huang G, Allen R, Davis EL et al (2006) Engineering broad root-knot resistance in transgenic plants by RNAi silencing of a conserved and essential root-knot nematode parasitism gene. Proc Natl Acad Sci U S A 103:14302–14306. https://doi.org/10.1073/pnas.0604698103
Jagdale S, Rao U, Giri AP (2021) Effectors of root-knot nematodes: an arsenal for successful parasitism. Front Plant Sci 12:800030. https://doi.org/10.3389/FPLS.2021.800030
Joshi I, Kumar A, Singh AK et al (2019) Development of nematode resistance in arabidopsis by HD-RNAi-mediated silencing of the effector gene Mi-msp2. Sci Rep 9:17404. https://doi.org/10.1038/s41598-019-53485-8
Joshi I, Kumar A, Kohli D et al (2020) Conferring root-knot nematode resistance via host-delivered RNAi-mediated silencing of four *Mi-msp* genes in *Arabidopsis*. Plant Sci 298:110592. https://doi.org/10.1016/j.plantsci.2020.110592
Kim D, Pertea G, Trapnell C et al (2013) TopHat2: accurate alignment of transcriptomes in the presence of insertions, deletions and gene fusions. Genome Biol 14:1–13. https://doi.org/10.1186/GB-2013-14-4-R36/FIGURES/6
Koenning SR, Barker KR, Bowman DT (2001) Resistance as a tactic for management of *Meloidogyne incognita* on cotton in North Carolina. J Nematol 33:126
Kyndt T, Vieira P, Gheysen G, de Almeida-Engler J (2013) Nematode feeding sites: unique organs in plant roots. Planta 238:807–818. https://doi.org/10.1007/s00425-013-1923-z
Lee RYN, Howe KL, Harris TW et al (2018) WormBase 2017: molting into a new stage. Nucleic Acids Res 46:D869–D874. https://doi.org/10.1093/NAR/GKX998
Leelarasamee N, Zhang L, Gleason C (2018) The root-knot nematode effector MiPFN3 disrupts plant actin filaments and promotes parasitism. PLoS Pathog 14:e1006947. https://doi.org/10.1371/journal.ppat.1006947

Lin B, Zhuo K, Chen S et al (2016) A novel nematode effector suppresses plant immunity by activating host reactive oxygen species-scavenging system. New Phytol 209:1159–1173. https://doi.org/10.1111/nph.13701

Lisei-de-Sá ME, Rodrigues-Silva PL, Morgante CV et al (2021) Pyramiding dsRNAs increases phytonematode tolerance in cotton plants. Planta 254:254–121. https://doi.org/10.1007/S00425-021-03776-0

Lourenço-Tessutti IT, Souza JDA, Martins-de-Sa D et al (2015) Knock-down of heat-shock protein 90 and isocitrate lyase gene expression reduced root-knot nematode reproduction. Phytopathology 105:628–637. https://doi.org/10.1094/PHYTO-09-14-0237-R

Lück S, Kreszies T, Strickert M et al (2019) siRNA-Finder (si-Fi) software for RNAi-target design and off-target prediction. Front Plant Sci 10:1023. https://doi.org/10.3389/fpls.2019.01023

Marchler-Bauer A, Derbyshire MK, Gonzales NR et al (2015) CDD: NCBI's conserved domain database. Nucleic Acids Res 43:D222–D226. https://doi.org/10.1093/NAR/GKU1221

Mejias J, Truong NM, Abad P et al (2019) Plant proteins and processes targeted by parasitic nematode effectors. Front Plant Sci 10:970. https://doi.org/10.3389/fpls.2019.00970

Mejias J, Bazin J, Truong NM et al (2021) The root-knot nematode effector MiEFF18 interacts with the plant core spliceosomal protein SmD1 required for giant cell formation. New Phytol 229:3408–3423. https://doi.org/10.1111/nph.17089

Mendes RAG, Basso MF, Fernandes J et al (2021a) Minc00344 and Mj-NULG1a effectors interact with GmHub10 protein to promote the soybean parasitism by *Meloidogyne incognita* and *M. javanica*. Exp Parasitol 229:108153. https://doi.org/10.1016/j.exppara.2021.108153

Mendes RAG, Basso MF, Paes-de-Melo B et al (2021b) The Mi-EFF1/Minc17998 effector interacts with the soybean GmHub6 protein to promote host plant parasitism by *Meloidogyne incognita*. Physiol Mol Plant Pathol 114:1–11. https://doi.org/10.1016/j.pmpp.2021.101630

Möller S, Croning MDR, Apweiler R (2001) Evaluation of methods for the prediction of membrane spanning regions. Bioinformatics 17:646–653. https://doi.org/10.1093/BIOINFORMATICS/17.7.646

Moreira VJV, Lourenço-Tessutti IT, Basso MF et al (2022) *Minc03328* effector gene downregulation severely affects *Meloidogyne incognita* parasitism in transgenic *Arabidopsis thaliana*. Planta 255:1–16. https://doi.org/10.1007/S00425-022-03823-4

Murashige T, Skoog F (1962) A revised medium for rapid growth and bio assays with tobacco tissue cultures. Physiol Plant 15:473–497. https://doi.org/10.1111/j.1399-3054.1962.tb08052.x

Nguyen Ba AN, Pogoutse A, Provart N, Moses AM (2009) NLStradamus: a simple hidden markov model for nuclear localization signal prediction. BMC Bioinform 10:1–11. https://doi.org/10.1186/1471-2105-10-202/FIGURES/7

Niu J, Liu P, Liu Q et al (2016) Msp40 effector of root-knot nematode manipulates plant immunity to facilitate parasitism. Sci Rep 6:1–13. https://doi.org/10.1038/srep19443

Oka Y (2020) From old-generation to next-generation nematicides. Agronomy 10:1387. https://doi.org/10.3390/agronomy10091387

Orfanoudaki G, Markaki M, Chatzi K et al (2017) MatureP: prediction of secreted proteins with exclusive information from their mature regions. Sci Rep 7:3263. https://doi.org/10.1038/s41598-017-03557-4

Pak J, Fire A (2007) Distinct populations of primary and secondary effectors during RNAi in *C. elegans*. Science 315(5809):241–244. https://doi.org/10.1126/science.1132839

Pfaffl MW (2001) A new mathematical model for relative quantification in real-time RT-PCR. Nucleic Acids Res 29:e45. https://doi.org/10.1093/nar/29.9.e45

Pogorelko G, Juvale PS, Rutter WB et al (2016) A cyst nematode effector binds to diverse plant proteins, increases nematode susceptibility and affects root morphology. Mol Plant Pathol 17:832–844. https://doi.org/10.1111/MPP.12330

Pogorelko G, Wang J, Juvale PS et al (2020) Screening soybean cyst nematode effectors for their ability to suppress plant immunity. Mol Plant Pathol 21:1240–1247. https://doi.org/10.1111/MPP.12972

Qin X, Xue B, Tian H et al (2021) An unconventionally secreted effector from the root knot nematode *Meloidogyne incognita*, Mi-ISC-1, promotes parasitism by disrupting salicylic acid biosynthesis in host plants. Mol Plant Pathol 00:1–14. https://doi.org/10.1111/MPP.13175

Rutter WB, Hewezi T, Abubucker S et al (2014) Mining novel effector proteins from the eMining novel effector proteins from the esophageal gland cells of *Meloidogyne incognita*. Mol Plant-Microbe Interact 27:965–974. https://doi.org/10.1094/MPMI-03-14-0076-R

Siddique S, Grundler FM (2018) Parasitic nematodes manipulate plant development to establish feeding sites. Curr Opin Microbiol 46:102–108. https://doi.org/10.1016/j.mib.2018.09.004

Sindhu AS, Maier TR, Mitchum MG et al (2009) Effective and specific *in planta* RNAi in cyst nematodes: expression interference of four parasitism genes reduces parasitic success. J Exp Bot 60:315–324. https://doi.org/10.1093/jxb/ern289

Smith NA, Singh SP, Wang MB et al (2000) Total silencing by intronspliced hairpin RNAs. Nature 407:319–320. https://doi.org/10.1038/35030305

Song H, Lin B, Huang Q et al (2021) The *Meloidogyne javanica* effector Mj2G02 interferes with jasmonic acid signalling to suppress cell death and promote parasitism in *Arabidopsis*. Mol Plant Pathol 22:1288–1301. https://doi.org/10.1111/MPP.13111

Souza Júnior JDA, Coelho RR, Lourenço IT et al (2013) Knocking-down *Meloidogyne incognita* proteases by plant-delivered dsRNA has negative pleiotropic effect on nematode vigor. PLoS ONE 8:85364. https://doi.org/10.1371/journal.pone.0085364

Steeves RM, Todd TC, Essig JS, Trick HN (2006) Transgenic soybeans expressing siRNAs specific to a major sperm protein gene suppress *Heterodera glycines* reproduction. Funct Plant Biol 33:991–999. https://doi.org/10.1071/FP06130

Taylor AL, Sasser JN (1978) Biology, identification and control of root-knot nematodes. North Carolina State University Graphics, 111

Tian B, Li J, Vodkin LO et al (2019) Host-derived gene silencing of parasite fitness genes improves resistance to soybean cyst nematodes in stable transgenic soybean. Theor Appl Genet 132:2651–2662. https://doi.org/10.1007/S00122-019-03379-0/FIGURES/7

Triantaphyllou AC, Hirschmann H (1960) Post infection development of *Meloidogyne incognita* chitwood 1949 (nematoda-heteroderidae). Ann L'institut Phytopathol Benaki 3:1–11

Truong NM, Chen Y, Mejias J et al (2021) The *Meloidogyne incognita* nuclear effector MiEFF1 interacts with *Arabidopsis* cytosolic glyceraldehyde-3-phosphate dehydrogenases to promote parasitism. Front Plant Sci 12:641480. https://doi.org/10.3389/fpls.2021.641480

Vandesompele J, De Preter K, Pattyn F et al (2002) Accurate normalization of real-time quantitative RT-PCR data by geometric averaging of multiple internal control genes. Genome Biol 3(7):research0034.1. https://doi.org/10.1186/gb-2002-3-7-research0034

Vens C, Rosso MN, Danchin EGJ (2011) Identifying discriminative classification-based motifs in biological sequences. Bioinformatics 27:1231–1238. https://doi.org/10.1093/BIOINFORMATICS/BTR110

Verma A, Lee C, Morriss S et al (2018) The novel cyst nematode effector protein 30D08 targets host nuclear functions to alter gene

expression in feeding sites. New Phytol 219:697–713. https://doi.org/10.1111/NPH.15179
Vieira P, Gleason C (2019) Plant-parasitic nematode effectors — insights into their diversity and new tools for their identification. Curr Opin Plant Biol 50:37–43. https://doi.org/10.1016/j.pbi.2019.02.007
Wang J, Lee C, Replogle A et al (2010) Dual roles for the variable domain in protein trafficking and host-specific recognition of *Heterodera glycines* CLE effector proteins. New Phytol 187:1003–1017. https://doi.org/10.1111/j.1469-8137.2010.03300.x
Wheeler TA, Siders KT, Anderson MG et al (2014) Management of *Meloidogyne incognita* with chemicals and cultivars in cotton in a semi-arid environment. J Nematol 46:101
Xie J, Li S, Mo C et al (2016) A novel *Meloidogyne incognita* effector Misp12 suppresses plant defense response at latter stages of nematode parasitism. Front Plant Sci 7:964. https://doi.org/10.3389/fpls.2016.00964
Zhang J, Coaker G, Zhou JM, Dong X (2020) Plant immune mechanisms: from reductionistic to holistic points of view. Mol Plant 13:1358–1378. https://doi.org/10.1016/J.MOLP.2020.09.007
Zhao J, Li L, Liu Q et al (2019) A MIF-like effector suppresses plant immunity and facilitates nematode parasitism by interacting with plant annexins. J Exp Bot 70:5943–5958. https://doi.org/10.1093/jxb/erz348
Zhao J, Mejias J, Quentin M et al (2020) The root-knot nematode effector MiPDI1 targets a stress-associated protein (SAP) to establish disease in Solanaceae and *Arabidopsis*. New Phytol 228:1417–1430. https://doi.org/10.1111/nph.16745
Zhou E, Wheeler TA, Starr JL (2000) Root galling and reproduction of *Meloidogyne incognita* isolates from Texas on resistant cotton genotypes. J Nematol 32:513–518
Zhuo K, Chen J, Lin B et al (2017) A novel *Meloidogyne enterolobii* effector MeTCTP promotes parasitism by suppressing programmed cell death in host plants. Mol Plant Pathol 18:45–54. https://doi.org/10.1111/MPP.12374
Zhuo K, Naalden D, Nowak S et al (2019) A *Meloidogyne graminicola* C-type lectin, Mg01965, is secreted into the host apoplast to suppress plant defence and promote parasitism. Mol Plant Pathol 20:346–355. https://doi.org/10.1111/MPP.12759

INFOGRÁFICO DO CAPÍTULO IV

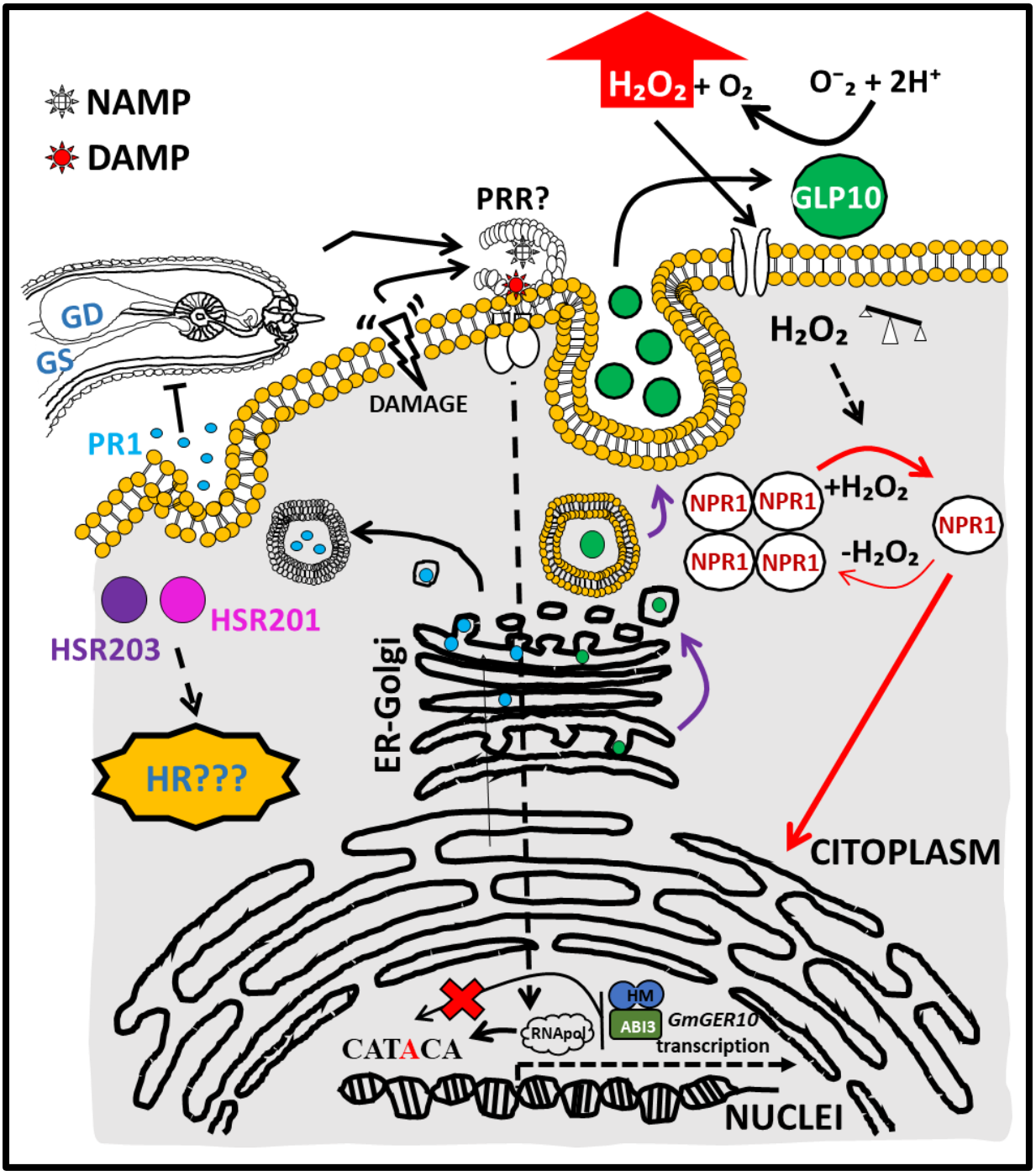

Neste estudo, demonstramos que a superexpressão de *GmGLP10 – Germin-like protein subfamily 10* – proveniente do genótipo de soja PI 595099, em plantas de tabaco, reduziram as suas susceptibilidades em mais de 49% com relação ao parâmetro número de galhas examinadas. Análises de microscopia confocal revelaram que GmGLP10 é exportada ao apoplasto das células vegetais onde fará emprego do íon superóxido, gerando H_2O_2 como resultado de sua catálise. Caso como o coativador transcricional NPR1, importante sensor ao

incremento de H_2O_2 *in planta*, é também aqui defendido como fator determinante da ativação transcricional de vários genes sensíveis ao estresse biótico. Desse modo, o incremento deste produto no citoplasma da célula vegetal foi mensurado via análises de RT-qPCR para vários marcadores sensíveis ao incremento de H_2O_2, relacionadas às vias: etileno (ET), ácido abscísico (ABA), jasmônico (JA) e salicílico (SA), espécies reativas de oxigênio (ERO) e resposta de hipersensibilidade (HR). Particularmente a este último caso, evidenciamos o apoio síncrono entre os genes *NtHSR201* e *NtHSR203* – relacionadas à resposta de hipersensibilidade – aos principais danos morfológicos observados na formação das CG, sendo eles, aqui defendidos, como mais um elemento integrante da ativação multifacetada dos eventos associados à morte celular programa (PCD) em plantas terrestres. Por fim, evidenciamos o papel-chave do (SNP)-908 como razão crucial da extinção do *cis*-elemento RYPE (consenso CATGCA) na sequência promotora de $GmGLP10_{pro}$ do genótipo PI 595099, justificando a sua alta expressão nesse genótipo em relação a cultivar susceptível BRS 133. Há indícios de que o fator de transcrição ABI3 aja na repressão promotora de $GmGLP10_{pro}$ da cultivar BRS 133, após sua ligação ao consenso RYPE e recrutamento de modificadores de histonas (HM) com atividades de metilação e/ou desacetilação.

CAPÍTULO IV

***GmGLP10*-overexpressing transgenic plants triggers defense response in *Meloidogyne incognita*-induced giant cells by up-regulation of H_2O_2-sensitive genes**

To be submitted

Valdeir Junio Vaz Moreira, Daniele Heloísa Pinheiro, Thuanne Pires Ribeiro, Harald Keller, Janice de Almeida Engler, Maria Fatima Grossi-de-Sa. *GmGLP10*-overexpressing transgenic plants triggers defense response in *Meloidogyne incognita*-induced giant cells by up-regulation of H_2O_2-sensitive genes. **New Phytologist**. (2024). To be submitted

Pages 99 to 166

SUMMARY

- *Meloidogyne incognita* is a widespread plant-parasitic nematode that causes substantial economic losses to soybean crops. Nonetheless, the mechanisms of soybean resistance to *M. incognita* remain poorly understood.
- Previously, we showed that *Germin-like protein subfamily 1 member 10* (*GmGLP10*) is upregulated at the transcriptional and translational levels in *M. incognita*-induced galls of the resistant soybean genotype PI 595099 but not in the susceptible soybean genotype BRS133, suggesting that GmGLP10 plays a role in soybean resistance to *M. incognita*.
- Here, we demonstrated that the absence of the *cis*-regulatory element RYREPEATBNNAPA in the *GmGLP10* promoter isolated from the soybean genotype PI 595099 may be responsible for the differential expression of *GmGLP10* in the *M. incognita*-induced galls of PI 595099 roots.
- Transgenic soybean hairy roots and tobacco plants overexpressing *GmGLP10* showed increased resistance to *M. incognita* compared to wild type. Furthermore, histological examination of *M. incognita*-induced galls showed a significant delay in female development and reproduction, as well as a reduction in gall size. In addition, upregulation of hormonal-, ROS- and defense-related genes was observed in the tobacco *GmGLP10*^{OE} lines, suggesting that GmGLP10 functions as a positive regulator of defense-induced responses by promoting dynamic transcriptional alterations in the *M. incognita*-induced galls.
- In contrast, *Arabidopsis thaliana glp10* mutant lines were less resistant to nematodes. Moreover, loss-of-function of GLP10 dramatically affected seed germination and *A. thaliana* development.
- Taken together, our results provide functional evidence that GmGLP10 contributes to plant resistance against *M. incognita* by interfering with a ROS pathway to reprogram gene expression for activating multiple downstream immunity responses.

RESUMO

- *Meloidogyne incognita* é um nematoide parasita de plantas que causa perdas econômicas substanciais as culturas de soja. No entanto, os mecanismos de resistência da soja ao *M. incognita* permanecem pouco compreendidos.
- Anteriormente, mostramos que o membro *Germin-like protein subfamily 1 member 10* (*GmGLP10*) é regulado positivamente tanto a níveis transcricionais quanto traducionais em galhas induzidas por *M. incognita* no genótipo de soja resistente PI 595099, mas não no genótipo de soja suscetível BRS133, sugerindo que *GmGLP10* desempenha um papel na resistência da soja ao *M. incognita*.
- Neste estudo, demonstramos que a ausência do *cis*-elemento RYREPEATBNNAPA no promotor GmGLP10 isolado do genótipo de soja PI 595099 pode ser responsável pela expressão diferencial de *GmGLP10* em galhas induzidas por *M. incognita* em raízes PI 595099.
- Raízes induzidas em folhas destacada de soja e plantas de tabaco superexpressando $GmGER10^{OE}$ mostraram maior resistência ao *M. incognita* em comparação com o controle experimental. Exames histológicos de galhas induzidas pelo *M. incognita* mostraram um atraso significativo no desenvolvimento e reprodução de fêmeas, bem como uma redução no tamanho das galhas. Além disso, a regulação positiva de genes relacionados a hormônios, ERO e defesa foi observada nas linhagens $GmGLP10^{OE}$ de tabaco transgênicos, sugerindo que *GmGLP10* funciona como um regulador positivo das respostas induzidas pela defesa, promovendo alterações de transcritos substanciais em galhas induzidas pelo *M. incognita*.
- Em contraste, linhagens *glp10-/-* mutantes de *Arabidopsis thaliana* foram menos resistentes aos nematoides. A perda de função de *glp10* afetou dramaticamente a germinação de sementes e o desenvolvimento de *A. thaliana*.
- Coletivamente, nossos resultados fornecem evidências funcionais de que o *GmGLP10* contribui para a resistência de plantas contra *M. incognita*, interferindo com uma via de ERO, cujo resultado possibilita reprogramar a expressão de genes intricados na defesa de plantas contra o nematoide formador de galha.

GmGLP10-overexpressing transgenic plants triggers defense response in *Meloidogyne incognita*-induced giant cells by up-regulation of H_2O_2-sensitive genes

Valdeir Junio Vaz Moreira[1,2,3], Daniele Heloísa Pinheiro[1,3], Thuanne Pires Ribeiro[1,3], Harald Keller[4], Janice de Almeida Engler[4] and Maria Fátima Grossi de Sá[1,3,5]

[1] Embrapa Recursos Genéticos e Biotecnologia (Embrapa Cenargen), Brasília, DF, Brazil
[2] Federal University of Brasília, UNB, Brasília, DF 70910-900, Brazil
[3] National Institute of Science and Technology, INCT PlantStress Biotech, Embrapa 70297-400, Brazil
[4] INRAE, Université Côte d'Azur, CNRS, ISA, 06903 Sophia Antipolis, France
[5] Catholic University of Brasília, Brasília, DF 71966-700, Brazil

[*]**Corresponding Authors**

Maria Fatima Grossi-de-Sa: fatima.grossi@embrapa.br

Summary

- *Meloidogyne incognita* is a widespread plant-parasitic nematode that causes substantial economic losses to soybean crops. Nonetheless, the mechanisms of soybean resistance to *M. incognita* remain poorly understood.
- Previously, we showed that *Germin-like protein subfamily 1 member 10* (*GmGLP10*) is upregulated at the transcriptional and translational levels in *M. incognita*-induced galls of the resistant soybean genotype PI 595099 but not in the susceptible soybean genotype BRS133, suggesting that GmGLP10 plays a role in soybean resistance to *M. incognita*.
- Here, we demonstrated that the absence of the *cis*-regulatory element RYREPEATBNNAPA in the *GmGLP10* promoter isolated from the soybean genotype PI 595099 may be responsible for the differential expression of *GmGLP10* in the *M. incognita*-induced galls of PI 595099 roots.
- Transgenic soybean hairy roots and tobacco plants overexpressing *GmGLP10* showed increased resistance to *M. incognita* compared to wild type. Furthermore, histological examination of *M. incognita*-induced galls showed a significant delay in female development and reproduction, as well as a reduction in gall size. In

addition, upregulation of hormonal-, ROS- and defense-related genes was observed in the tobacco *GmGLP10*^{OE} lines, suggesting that GmGLP10 functions as a positive regulator of defense-induced responses by promoting dynamic transcriptional alterations in the *M. incognita*-induced galls.

- In contrast, *Arabidopsis thaliana glp10* mutant lines were less resistant to nematodes. Moreover, loss-of-function of GLP10 dramatically affected seed germination and *A. thaliana* development.
- Taken together, our results provide functional evidence that GmGLP10 contributes to plant resistance against *M. incognita* by interfering with a ROS pathway to reprogram gene expression for activating multiple downstream immunity responses.

Introduction

The genus *Meloidogyne* (NEMATODA: HETERODERIDAE) consists of 98 species, with *M. incognita* being the largest endemic representative in the Americas (Jones *et al.,* 2013). In Brazil, *M. incognita, M. javanica* and *M. enterolobii* are responsible for losses in the soybean sector of more than US$6.5 billion per year, reaching 10 to 14% of the damage caused by plant-parasitic nematodes (PPNs) in agriculture worldwide (Barros *et al.,* 2022). Due to the increase in temperatures resulting from climate change, recent studies revealed the early embryogenic development of *M. incognita* (stage J1), inducing its premature hatching (Calderón-Urrea *et al.,* 2016). Pre-parasitic stage 2 juveniles (ppJ2s) are guided by plant metabolites released by the roots to establish feeding sites (Kihika *et al.,* 2017; Tsai *et al.,* 2021). Stage 2 parasitics juveniles (pJ2) complete their migratory endocytic cycle in two anterograde directions intracellularly. First, they migrate towards the root tip; and then, in an acropetal direction until vascular cylinder's cells where the nematodes will induce dedifferentiation into giant cells (GCs) (Bartlem *et al.,* 2014; Goverse & Smant 2014). At this point, their compatible interaction is stablished and the exchange of nematode's cuticles for the third (J3) and fourth (J4) stages give rise to adult females that will oviposit a glycoprotein matrix containing hundreds to thousands of eggs (Castagnone-Sereno *et al.,* 2013).

However, there are significant exceptions of non-compatible hosts, which during co-evolution, resulted in delayed PPNs development (Goverse & Smant 2014). Over the past decades, the domesticated soybean (*Glycine max* (L.) Merr.) PI 595099 [germplasm line G93-9223 (G83-559 x (G80-1515[2] x PI 230977)], has been the center for omics investigations, given

the genetic background responsible for the high resistance against cyst (CNs) and root-knot nematodes (RKNs) (Davis *et al.*, 1998; Lisei-de-Sá *et al.*, 2012). Recently, the combined transcriptome and proteome analyses revealed new insights involving the cross-talk between plant hormonal and some metabolic pathways as the main reasons attributed for the high tolerance of PI 595099 against *Meloidogyne* spp. (Beneventi *et al.*, 2013; Arraes *et al.*, 2022). To try to explain this phenotype, a model for resistance was proposed relating the phytohormones auxin (AUX), ethylene (ET), salicylic acid (SA) and jasmonic acid (JA) as the major agonists to enhance reactive oxygen species (ROS) levels in *M. javanica*-induced GCs (Beneventi *et al.*, 2013).

Through an integrated multi-omics analysis, Arraes *et al.*, (2022) found a large number of genes positively regulated in soybean upon *M. incognita* parasitism. The authors suggested that genes related to plant immune response and phenylpropanoid pathway could be responsible for PI 595099 resistance to *M. incognita*. Furthermore, genes involved in metabolism of carbohydrates and lipids, response to stimulus, signal transduction, and oxidation-reduction have also been implicated in plant defense against RKNs (Beneventi *et al.*, 2013; Arraes *et al.*, 2022). Transgenic approaches have further proven that the overexpression of *glutathione S-transferase* (*GmGST*) and *pathogenesis-related protein 10* (*GmPR10*) genes, originally from the soybean PI 595099, decrease soybean susceptibility against *M. incognita* up to 39% - 41% (Freitas-Alves *et al.*, 2023). The high differential expression of *Germin-like protein subfamily 1 member 10* (*GmGLP10*) observed in *M. incognita*-induced galls through transcriptome and proteome analyses (Arraes *et al.*, 2022), and the documented role of *GmGLP10* in disease resistance in plants (Liu *et al.*, 2016; Zhang *et al.*, 2018) encouraged us to further examine the roles of *GmGLP10* in the resistance of soybean against *M. incognita.*

In addition to their diverse roles in development, germination, pollen formation and stress-related signaling, germin-like proteins (GLPs) participate in defense against a broad range of bacteria and fungi pathogens (Davidson *et al.*, 2009; Manosalva *et al.*, 2009). Apoplastic GLPs are ubiquitous water-soluble glycoproteins located in the extracellular matrix, which contains a conserved β-barrel *core* that is involved in copper and manganese ion binding (Bernier & Berna 2001). To date, all GLPs contain at least one N-glycosylation site, while the high abundance of several short β-structures in C-terminal half gives them the possibility to mediate oligomer formation (Carter & Thornburg 1999). Due to their conserved motifs (namely germin boxes), which include Box-A (QDFCVAD), Box-B (G--P-H-HPRATEXXXX-G) and Box-C (GXXHFQ-N-G), GLPs belong to the “Cupin” subfamily, whose domain allows

catalysis of the dismutation of superoxide radicals into oxygen and hydrogen peroxide (Hu *et al.*, 2003).

In this study, a functional investigation revealed that transgenic soybean hairy roots and tobacco plants overexpressing *GmGLP10*^{OE} significantly increased resistance against *M. incognita*. The nucleotide polymorphism (SNP)-908 found into *cis*-regulatory repression motif RYREPEATBNNAPA [DNA motif CATGCA] in the *GmGLP10* promoter showed another important role by altering *GmGLP10* expression patterns in PI 595099 transgenic plants. As a result, *GmGLP10*-mediated anti-nematode signaling triggered phytohormone (ET, SA, JA) and defense (ROS and HR) genes expression, likely leading to a hypersensitive response in *M. incognita*-induced GCs. Conversely, the loss of *glp10* function inhibited *A. thaliana* development and increased susceptibility to nematode infection. These data highlight *GmGLP10*^{OE} as a new valuable target for crop improvement against RKNs.

Materials and Methods

Plasmid constructs

A CDS fragment covering 699 bp of the *GmGLP10* gene (*Glyma.20G220800.1*), was amplified via Q5® High-Fidelity DNA Polymerase (New England BioLabs, MA, USA) from the 30 DAI galls cDNA, containing the 5' (5'-GTCGAC-3; *SalI* restriction site) and 3' (5'-ACTAGT-3'; *SpeI* restriction site) in the forward (Fwd) and reverse primers (Rvs), respectively (Table S2), followed by ligation using T4 ligase (Promega, Madison, WI) in the binary vector pPZP201-BK-EGFP and sequencing (Moreira *et al.*, 2022; Moreira *et al.*, 2023). The final clone (pPZP201-BK-EGFP-GmGLP10) was subsequently used as a template for a second amplification containing the *attb1* and *attb2* sites in the Fwd and Rvs primers, followed by recombination in the pDONR entry vectors. To obtain the GmGLP10 clones fused to EGFP at both ends (C- and N-terminals), the GmGLP10-NS clone (without stop codon - NS) was cloned into the pDONR207 vector, while EGFP-ST (with stop codon - ST) was recombined into pDONR221, using BP clonase (Invitrogen, USA). After the second sequencing, both clones were recombined, via LR clonase (Invitrogen, USA), into the pK7FWG2 and pK7WGF2 vectors, respectively, followed by their introduction into *Agrobacterium tumefaciens* (strain GV3101) and agroinfiltration in *Nicotiana benthamiana* leaves. Likewise, around -2037 bp DNA fragment upstream of the translation start codon (ATG) from the soybean genotypes BRS

133 (susceptible) and PI 595099 (high tolerance) was first PCR-amplified using specific primers (Table S2) and cloned into the entry vector pDONR221. After sequencing, the fragments were subcloned into the destination vector pKGWFS7.

Agrobacterium-mediated plants transformation and plant growth conditions

Tobacco plants (*Nicotiana tabacum* cv. Petit Havana SR1) were grown under aseptic conditions on phytagel-solidified MS medium supplemented with 10 g/L sucrose and hygromycin (50 mg/L) (Murashige & Skoog 1962). Plants were grown in a climate control room at 22°C, 70 – 75% relative humidity and ~100 µmol photons m^{-2} s^{-1} light intensity with a 16-h-light/8-h-dark photoperiod and used for *Agrobacterium tumefaciens*-mediated nuclear transformation. Transgenic soybean cv. Williams 82 hairy roots was generated using *Agrobacterium rhizogenes* (strain K599), previously transformed with pPZP201-BK-EGFP-GmGLP10, according to Freitas-Alves *et al.*, (2023). Mutants *A. thaliana* lines, *glp10_1* (SALK_038626) and *glp10_2* (SALK_062879C), were obtained from the European Arabidopsis Stock Centre. Homozygous seeds of the both T-DNA insertion *glp10-/-* mutants and wild type control (ecotype Columbia, Col-0), were sown on a soil/sand mixture, stratified for 3 days at 4°C, and then grown under a 12 h photoperiod in a growth chamber at 21°C.

Histochemical GUS and histopathological analysis

Promoter activity of pGmGLP10::eGFP-GUS fusion lines were monitored at 4, 12 and 30 days after inoculation (DAI) with *M. incognita* (race 3) as described by de Almeida Engler *et al.*, (1999). Galls were collected at 30 DAI for morphological analysis and at 4, 12 and 30 DAI for GUS assays. Galls were fixed in 2% glutaraldehyde in 50 mM PIPES buffer (pH 6.9) during 2 weeks. After GUS assays, galls were imaged with and Axio Zoom. V16 (Zeiss) under bright-field optics using an Axiocam digital camera (Zeiss). For morphological analyses and GUS expression localization, galls were subsequently dehydrated using a gradient ethanol dilution series (10, 30, 50, 70, 90 and 100 v/v), embedded in Technovit 7100 (Heraeus Kulzer, Wehrheim, Germany) according to the manufacturer, and then sectioned to 5 µm. Sections were placed onto poly-L-lysine coated glass slides, stained in 0.05% toluidine blue, mounted in DPX (Sigma-Aldrich) and imaged with a digital Axiocam (Zeiss) under dark- or bright-field optics.

For BABB analysis, galls were fixed in 3% glutaraldehyde (in PBS pH 7.4) under vacuum during 15 min at 4°C, rinsed 3 times for 20 min in PBS (pH 7.4), and then dehydrated in a gradient ethanol. Samples were transferred to ethanol:BABB solution 1:1 (v/v) for 1 h, and finally maintained for 1 h in 100 % BABB [benzyl alcohol:benzyl benzoate 1:2 (v/v)] (Cabrera *et al*., 2018). Cleared samples were mounted in BABB and imaged using a Confocal Laser Scanning Microscopy system (LSM880; Zeiss).

For acid fuchsin staining, infested roots were stained according to Bybd *et al*. (1983). First, plant roots were washed under running water and then dried with paper towels. Samples were then immersed in 2.5% sodium hypochlorite solution for clarification, for 10 minutes and then washed for 5 minutes in running water. Infected roots were submerged in an acid fuchsin solution containing [1.25g of acid fuchsin solubilized in glacial acetic acid and distilled water (1:3 v/v)], and then heated for 1 minute in the microwave. After boiling the solution was discarded, roots were then washed under running water for 1 minute, and transferred to acidified glycerol solution. Samples were then mounted in glycerol, coversliped, and imaged using a differential interference contrast microscopy (Zeiss AxioCam MR).

Nematode infection tests

Due to their incompatibility with hosts, two races of *M. incognita* were used in this study (race 1 and race 3). The race 1 was used to infect the soybean genotypes, while the race 3 was used in the nematode infection tests with tobacco and *A. thaliana* plants. Both populations were previously characterized using SCAR markers and propagated in tomato plants (*Solanum lycopersicum* L., cv. Santa Cruz). 3-week-old soybean plants of genotypes BRS 133 and PI 595099, and transgenic tobacco plants were inoculated with 1.000 ppJ2s and examined after 60 DAI by counting gall and egg mass numbers.

For *A. thaliana* lines, plants were infected with 500 ppJ2s and examined under the same conditions as described above at 45 DAI. To normalize the data, all fresh roots had their weights examined and relativized by the final count obtained from the number of galls and egg masses. All parameters were analyzed using Microsoft Excel to calculate means and Standard deviation of the mean (SD). For each independently transformed line, we used at least 10 plants, in a completely randomized design, and all data referring to the bioassay represent mean ±

SD. Significant differences between treatments and wild type control plants were evaluated through variance analysis (ANOVA one-way) and Student-Newman-Keuls test ($P < 0.05$).

Data were tested for normality and homogeneity of variances using the Shapiro-Wilk and Bartlett tests, respectively. All counting data were transformed using the Box-Cox method. Analyses were performed in R Program (v. 3.6.1), using the easy anova (v. 7.0) and fpp (v.3.0-7) packages.

Gall diameter and giant cell area measurements

Gall diameter and giant cell area were measured to investigate differences in gall development in each transgenic line compared with the control wild type. The AxioVisionLE (Zeiss) software was used to measure both parameters in galls collected from soybean hairy roots ($n \geq 10$) at 14 DAI and 30 DAI, and galls from transgenic tobacco roots ($n = 30$) at 45 DAI. Feeding site development was evaluated in transgenic tobacco galls (30 DAI) by the BABB clearing method as described above. Data were analyzed by Wilcoxon test (significance level of 0.05). Vertical lines indicate mean values plus standard deviations determined for each technical replicate.

Microscopy analysis

For subcellular localization of fluorescent EGFP fusion at N- and C-terminals of GmGLP10, *N. benthamiana* leaves were used for agroinfiltration with *A. tumefaciens* previously transformed with the constructs described above. Fluorescence was visualized in epidermal cell layers 2 days after infiltration using a Confocal Laser Scanning Microscopy system (LSM880; Zeiss). For imaging GFP, the 488-nm excitation line, and the 500–530-nm bandpass filter were used. The same wavelength was used for BABB analysis and the green autofluorescence generated by glutaraldehyde was recovered. The images were then analyzed using the ZEN 2010 software (Zeiss).

RNA extraction and RT-qPCR analysis

Total RNA was extracted from 150 mg of galls (30 DAI) using TRIzol® (Invitrogen), followed by quantification in NanoDrop ND-1000 spectrophotometer (NanoDrop Technologies), and its quality and integrity were checked in 1 % (w/v) agarose gel stained with 0.1 μg/mL ethidium bromide. Each sample was treated with 2U RNase-Free DNase (Invitrogen, USA) and the cDNA synthesis was performed using SuperScript II (Invitrogen, Carlsbad, CA, USA) and Oligo-$(dT)_{20}$ primer, according to manufacturer's protocol.

The heterologous expression profile of *GmGLP10* and marker genes related to hormonal defense pathways (ET, HR, JA, SA and ROS), was performed with the real-time quantitative PCR (RT-qPCR) in optical 96-well plates in a 7.500 Fast Real-Time PCR System (Applied Biosystems), using the GoTaq® qPCR Master Mix (Promega, USA) to 1 X Master Mix final concentration. All genes were carried out in technical triplicate reactions for each biological sample (Table S2). The amplifications conditions were 95 °C during 10 minutes, followed by 40 cycles (15 seconds at 95 °C and 1 minute at 60 °C). *NtActin* and *NtL25* were chosen as endogenous control genes, and relative gene expression was calculated by the $2^{-\Delta\Delta Ct}$ comparative method.

Cis-regulatory elements annotation, phylogenetic analysis and genomic locations of Cupin domains

The *cis*-regulatory elements in each GmGLP10 promoter (-2037 bp upstream of the translation start codon) were identified by "Plant *Cis*-acting Regulatory DNA Elements" database (PLACE, https://www.dna.afrc.go.jp/PLACE /place seq. shtml). For the phylogenetic reconstruction of the soybean Cupin superfamily, the *Glycine max* deduced Cupin domain sequences, available in Phytozome, were used in a global alignment with all soybean Cupin sequences identified by InterProScan program (Quevillon *et al.*, 2005). Cupin domain sequence (code: IPR006045) was used as a guide to determine the distribution of the Cupin genes along 20 soybean chromosomes via PLAZA 3.0 (https://bioinformatics.psb.ugent.be/plaza/versions/plaza_v3_dicots/genome_mapping/index). All full-length domain sequences were aligned using Clustal X software and used as input to construct a phylogenetic tree using the MEGA 5.0 by Neighbor Joining (NJ) method with 1000 replicates of bootstrap analysis, according to the same parameters adopted by Wang *et al.*, (2014). WebLogo was used to create the distribution of Germin BOX amino-acid residues at the corresponding Cupin domain of all GmGLPs retrieved from phytozome

Results

The soybean genotype PI 595099 is highly resistant to *M. incognita* (race 1)

We re-evaluated the soybean genotype PI 595099 for resistance to the *M. incognita* isolate (race 1) by inoculation of plant roots with ppJ2s. Plant were kept under standard greenhouse conditions and evaluated at 60 DAI. The level of resistance of soybean genotype PI 595099 was compared to the *M. incognita*-susceptible soybean genotype BRS 133, which was used as a control (Fig. 1a). There was no significant difference in the fresh weight of infected roots at 60 DAI of both genotypes (Fig. 1b). The soybean genotype PI 595099 proved to be highly resistant to *M. incognita* infection. Observation of disease symptoms revealed that the amount of galls and egg masses in PI 595099 roots were notably less abundant than those in BRS 133 roots (Fig. 1c). Detailed analysis showed a significant reduction in the number of galls and egg masses in the soybean genotype PI 595099 compared to the soybean genotype BRS 133 (Fig. 1d-g). A reduction of over 57.24% in the number of galls/g of root and 54.68% in the number of egg masses/g of root was observed (Fig. 1e, 1g). Overall, we observed in both soybean genotypes that each *M. incognita*-induced gall had only one adult female producing egg mass and often more than one feeding site occurs in each gall (Fig. S1).

Changes in the *cis*-regulatory elements of the *GmGLP10* promoter likely confer high gene expression in the soybean genotype PI 595099

Previously, we showed that *GmGLP10* is significantly overexpressed at the transcriptomic and proteomic level in *M. incognita*-induced galls of soybean genotype PI 595099 compared to uninfected roots (Arraes *et al.*, 2022), but changes in its expression were not observed in the soybean genotype BRS 133. The expression profile of *GmGLP10* suggests that it might be involved in PI 595099 response to *M. incognita*. To further investigate the possible reasons that led to the contrasting *GmGLP10* expression patterns in both soybean genotypes, the -2.037-bp promoter fragments upstream of translation start sites of *GmGLP10* genes from soybean genotypes PI 595099 and BRS 133 were cloned and analyzed (Fig. S2a-b). In total, 494 and 491 *cis*-regulatory elements were predicted in the sequences of *GmGLP10* promoter from the soybean genotypes BRS 133 and PI 595099, respectively (Fig. 2a). According to the promoter sequence analyses, seven *cis*-regulatory elements were present in

higher number in the *GmGLP10* promoter from soybean genotype BRS 133, including CAATBOX1 (CAAT), GATABOX (CCAAT), MYBST1 (GGATA), GT1CONSENSUS (GRWAAW), IBOXCORE (GATAA), RYREPEATBNNAPA (CATGCA), and SREATMSD (TTATCC). On the other hand, four *cis*-regulatory elements were more frequent in the *GmGLP10* promoter from soybean genotype PI 595099, including MARTBOX (TTWTWTTWTT), POLASIG3 (AATAAT), TATABOX2 (TATAAAT), -10PEHVPSBD (TATTCT) (Fig. 2a). However, comparative analysis between the *GmGLP10* promoter sequences of soybean genotype BRS 133 relative to PI 595099 revealed two single nucleotide polymorphisms at (SNP)-458 (C nucleotide was mutated to T) and (SNP)-908 (G nucleotide was mutated to A) positions, which resulted in the addition of -10PEHVPSBD and the complete deletion of *cis*-regulatory element RYREPEATBNNAPA in PI 595099 (Fig. 2a-b).

To confirm that *GmGLP10* is expressed within *M. incognita*-induced galls, the *pGmGLP10::GUS* cassette harboring the *GmGLP10* promoter from PI 595099 was used to transform tobacco plants. At least three independent transgenic tobacco lines were generated using the *pGmGLP10::GUS* construct to investigate promoter activity driving GUS expression at different time points of infection (Fig. S2a-c). Our analysis of GUS staining assays revealed promoter activity (blue) in UR, and young (4-12 DAI) and mature (30 DAI) galls (Fig. 2c). Observations of sectioned galls under dark-field-optics revealed that GUS staining (red) was present in the GCs as well as in neighboring cells during early and late gall developmental stages, indicating that GmGLP10 is expressed during nematode parasitism (Fig. 2d). Promoter activity in UR was more restricted to the vascular tissue, revealing the same expression pattern seen in the vascular tissue of the galls (Fig. 2d).

Cloning and sequence analysis of *GmGLP10*

Molecular cloning and sequence analysis of the full-length coding sequence revealed that *GmGLP10* encodes a protein with a predict size of 24.94 kDa, one N-glycosylation site at the Asn-34, and high conserved germin box (-A, -B and -C) motifs (Table S1). In addition, GmGLP10 harbors a predicted signal peptide (SP) in the N-terminal region, which is likely responsible for the extracellular matrix (EM) localization of GmGLP10. We show here that all GLPs belongs to the Cupin_1 subfamily, with *GmGLP10* on chromosome 20 (Fig. S3a).

A total of 60 putative members of Cupin superfamily genes have previously been identified in the *G. max* soybean genome (version G. max v1.1) (Wang *et al.*, 2014). In this

study, we identified 23 new members of Cupin superfamily through Blasp searches against the recently available genome sequence of soybean (version G. max v11.0), updating the Cupin superfamily to 83 genes members (Fig. S3a). GLPs were organized into 14 phylogenetic groups, with GmGLP10 belonging to monophyletic group 1, (Fig. S3b).

Subcellular localization of GmGER10

We used transient expression assays to examine the subcellular localization of GmGLP10. Confocal images of *N. benthamiana* leaf cells harboring the GFP-ΔSP-GmGER10 or ΔSP-GmGER10-GFP constructs showed the transient subcellular localization of ΔSP-GmGER10 protein in the cytoplasmic region, while cells expressing the full GmGER10 protein revealed GFP signals at the cytoplasmic bridges as well as plasmatic membrane periphery (Fig 3). GFP signals in the nucleus were observed only with the GFP construct and the ΔSP-GmGER10 mutant, suggesting its passive diffusion restricted to its size. In addition, the co-localization between RFP-HDEL (ER marker) with GmGER10 demonstrates its clear involvement with the extrinsic secretion pathway in the ER before being exported to EM (Fig. 3).

Overexpression of *GmGLP10* in soybean hairy roots leads to increased resistance to *M. incognita*

To examine the possible involvement of *GmGLP10* in plant defense against *M. incognita,* we introduced the entire coding sequence of *GmGLP10* into the hairy roots of soybean. Overexpression of *GmGLP10* in soybean hairy roots resulted in reduced number of gall compared to control roots transformed with the empty vector. We observed a significant decrease of 54.50% in the number galls/plant and 30% in the number of galls/gram of root at 30 DAI (Fig. 4a-b). Histological analyses revealed an apparent inhibition in nematode development at 14 DAI and 30 DAI and apparently changed in GCs cytoplasm in view of low TB staining (Fig 4c). In addition, the galls and GCs of *GmGLP10* overexpression hairy roots displayed reduced sizes compared to the control at 14 DAI and 30 DAI (Fig. 4d-g). The inhibition in nematode development is likely due to the inhibited gall expansion seen during gall ontogenesis. Morphological and diameter size changes were not observed in uninfected

roots (UR) of *GmGLP10* overexpression roots compared to control, suggesting a specific effect of *GmGLP10* overexpression in galls (Fig. 4h-i).

Overexpression of *GmGLP10* in tobacco plants increases resistance to *M. incognita* and inhibits gall development

To further investigate the function of *GmGLP10* in plant defense against *M. incognita*, we generated three independent transgenic tobacco lines overexpressing *GmGLP10* (Fig. 5a, S4a-c, S5a). Transgenic lines were analyzed by PCR and EGFP reporter gene activity (Fig. S5b-c), and T4 homozygous progenies were obtained via hygromycin selection (Fig. S6a). *GmGLP10* overexpression in transgenic lines was confirmed by RT-qPCR analysis (Fig. 5b).

The phenotypic traits of *GmGLP10*^{OE} lines and wild type plants were evaluated throughout their development. The roots of *GmGLP10*^{OE} lines and wild type plants showed a similar weight at 60 DAI, while plant weight and length of *GmGLP10*^{OE} line#1 were significantly higher compared to control (Fig. 5c-d). A delay in the development was observed in *GmGLP10*^{OE} lines compared to control plants, as indicated by the size of young tobacco plants and the size of their leaves (Fig. S6b-c). However, their development increased throughout plant development, reaching a similar size as those of the wild type. Analysis of young tobacco leaf blade anatomy revealed that leaf thickness and mesophyll area of *GmGLP10*^{OE} lines were significantly decreased compared to those of wild type leaves (Fig. S6d-f).

Morphological examination of transgenic tobacco roots infected with *M. incognita* revealed a significant delay in female development and egg masses oviposition at 30 DAI compared to wild type (Fig. 5f). BABB analysis of *M. incognita*-induced galls from *GmGLP10*^{OE} lines demonstrated apparent smaller feeding sites as well as decreased nuclear density (red arrows) compared to wild type (Fig. 5g). Nuclear morphology of UR was normal, suggesting that *GmGLP10* overexpression affected mitotic activity only in GCs (Fig. S7a). The *GmGLP10*^{OE} lines exhibit significantly smaller gall size and GC area compared to wild type at 30 DAI (Fig. 5h-i). At 60 DAI, a significant decrease in the number of galls and egg masses was observed in *GmGLP10*^{OE} lines compared to control, with reductions in galls/g of root ranging from 40.52% - 41.94% and egg masses/g of root ranging from 49.1% - 62.83% (Fig. 5j-m).

Despite the resistance found in relation to the experimental control, the ratio (egg masses/galls) point to transgenic tobacco lines that are less susceptible in relation to the genetic background, concluding the participation of *GmGLP10* in its resistance when heterologous express (Fig. S7b).

Overexpression of *GmGLP10* in tobacco plants increases the expression of defense-related genes and hypersensitive response-related genes in *M. incognita*-induced galls

To better understand *GmGLP10* function during galls ontogeny, mature galls (30 DAI) of *GmGLP10*^{OE} lines were analyzed (Fig. 6a). Delay in nematode development (Line #2), apparent decreased xylem proliferation around GCs (arrows in Line #1) and lack of cytoplasm in GCs (Lines #1 and #2) were observed (Fig. 6a). To gain insights into the mechanisms underlying *GmGLP10*-mediated defense in transgenic tobacco plants, the expression of several marker genes related to defense signaling pathways was evaluated in the *M. incognita*-induced gall of *GmGLP10*^{OE} lines and wild type plants. RT-qPCR analysis revealed that among 24 marker genes evaluated, 11 genes were induced in the galls of *GmGLP10*^{OE} lines. Overexpression of *GmGLP10* in tobacco resulted in the upregulation of some genes implicated in HR (*NtHSR201* and *NtHSR203*), SA pathway (*NtPR-2* and *NtPR-5*), ET pathway (*NtERF1*, *NtACS6* and *NtEIN3*), JA pathway (*NtMYC2*, *NtAOC* and *NtAOS*), and ROS burst (*NtRBOHD* and *NtAPX*) (Fig. 6b-l). These analyses imply that key genes involved in defense signalling pathways are probably directly or indirectly subject to regulation by *GmGLP10* in *M. incognita*-induced galls.

The loss-of-function of the *Arabidopsis glp10* increases plant susceptibility to *M. incognita*

We screened homozygous Arabidopsis T-DNA insertional mutants of genes encoding germin-like proteins and found the locus At3g05950.1 with 64.6% of amino acid similarity with soybean GmGLP10 (Fig. 7a). Two mutant alleles [*glp10_1* (*SALK_038626*) and *glp10_2* (*SALK_062879*)] were selected and their homozygous (HM) *ger-/-* state was confirmed by PCR analysis (Fig. 7b). Observation of the seedlings grown in soil revealed that *Atglp10* loss-of-function led to inefficient and delayed germination, and retarded seedling development (Fig.

S8a). Following 22 days of growth, *glp10_1* and *glp10_2* mutants displayed decreased rosette diameter, leaf number, leaf length, leaf width and fresh weight (Fig 7 c-o, S8b-d).

To determine whether the stress caused by *M. incognita* parasitism interfere with plant development and flowering, wild type and mutant plants were challenged with *M. incognita* and compared to mock treatment. We observed that the rosette diameter of knockout plants was affected by *M. incognita* parasitism at 48 hours after inoculation; however, this difference of rosette diameter between non-inoculated and inoculated plants was less pronounced throughout plant development and from 15 DAI no difference was observed (Figs. 7f-J, S9). Considering the number of leafs per plant, we observed an increase in the number of leaves of inoculated wild type and *glp10_2* mutant at 15 DAI and 22 DAI (Figs. 7k-o). The same correlation was investigated by the number of plants with emerged tassels at different time points of infection, but no information could be obtained between root stress and plant height (Fig. S10).

Overall, a large number of females within the galls were seen in the roots of *glp10_1* and *glp10_2* mutant lines, while in the wild type roots usually only one female was observed in each gall, indicating that these mutants were highly susceptible to *M. incognita* (Fig. 8a). We phenotyped the plant roots by measuring the root weight at 45 DAI. We found that *glp10_1* and *glp10_2* mutant lines had significantly lower fresh weight relative to wild type roots, likely due to *Atglp10* loss-of-function (Fig 8b). Interestingly, *glp10_1* and *glp10_2* mutant lines showed an increased susceptibility to *M. incognita*, further demonstrating the involvement of *Atglp10* in plant defense against nematodes (Fig. 8c-g). *Glp10* loss-of-function had a significant impact on the plant susceptibility to *M. incognita*. The *glp10_2* mutant had significantly more galls/g of root, while both *glp10_1* and *glp10_2* showed an increase of 87% and 95% in number of egg masses/g of root (Fig. 8f-g).

Discussion

In the present study, we found that the roots of soybean genotype PI 595099 presented the typical disease symptoms caused by *M. incognita* parasitism (galls and egg masses) to a much lesser degree than in the known *M. incognita*-susceptible soybean genotype BRS 133, confirming that PI 595099 is resistant to this nematode. Among the many soybean genotypes available, the genotype PI 595099 is a recognized source of desirable traits for nematode resistance (de Sá *et al.*, 2012; Lopes-Caitar *et al.*, 2013; Vieira *et al.*, 2016; Alekcevetch *et al.*,

2019); however, many aspects of the mechanisms that govern *M. incognita*–soybean interactions are still not well understood. Therefore, mining resistance resources and understanding the genetic and molecular mechanisms of soybean resistance to *M. incognita* is an important step towards the development of novel soybean varieties based on precision breeding and biotechnological approaches.

We recently demonstrated through comparative multi-omics analysis that the expression of *GmGLP10* gene and its encoded protein is induced by *M. incognita* infection in the resistant soybean genotype PI 595099, but the same gene induction is not triggered in the susceptible soybean genotype BRS 133, suggesting that *GmGLP10* might be directly involved in a key pathway driving nematode resistance in soybean (Arraes *et al.*, 2022). Given that promoters play an important role in controlling the spatiotemporal gene expression, we next asked whether *GmGLP10* promoter has experienced structural divergence within the soybean genotypes and whether their sequence composition supports the differential *GmGLP10* expression in *M. incognita*-induced galls. Sequence variation in the soybean *GmGLP10* promoter was then investigated in genotypes BRS 133 and PI 595099. Even though there was a relatively small natural sequence variation in terms of sequence identity, such sequence variation resulted in considerable changes in the composition of *cis*-regulatory elements of both genotypes. We identified 494 *cis*-regulatory elements in BRS 133 and 491 *cis*-regulatory elements in PI 595099. The frequency of MARTBOX, POLASIG3, TATABOX2, and -10PEHVPSBD was increased in one unit in the genotype PI 595099 compared to BRS133, while CAATBOX1, GATABOX, MYBST1, GT1CONSENSUS, IBOXCORE, RYREPEATBNNAPA, and SREATMSD showed the opposite trend, decreasing their frequency. Interestingly, we further found that the (SNP)-458 caused the addition of -10PEHVPSBD and the (SNP)-908 led to the deletion of RYREPEATBNNAPA in PI 595099 relative to GmGLP10 promoter from BRS 133.

Little is known about the *cis*-regulatory element -10PEHVPSBD, which has been associated with plastid genes (Thum *et al.*, 2001). RYREPEATBNNAPA has been described as an ABA-responsive *cis*-regulatory element as it is an essential target site for ABSCISIC ACID INSENSITIVE3 (ABI3) transcription factor (Ezcurra *et al.*, 2000; Nambara & Marion-Poll, 2003), a major component of ABA signaling pathway that regulates seed germination, plant development, growth, abiotic and biotic stress responses (Chen *et al.*, 2020). ABI3 directly induces or represses the transcription of many target genes (Tian *et al.*, 2020). For instance, during the plant dehydration stress, ABI3 negatively regulates the expression of *RAV1*

transcription factor by binding to the RYREPEATBNNAPA of its promoter and decreasing the content of histones H3K4me3 and H3K27ac associated with its transcription activation (Sengupta *et al.*, 2020). In another study, ABI3 negatively affects the DNA-binding activity of ERF1 to the *cis*-element present in the promoters of *ABI5*, *ARF7*, *AUX1* and *PIN1* genes implicated in lateral root development (Zhang *et al.*, 2023). Based on these findings, the (SNP)-908 found in the *GmGLP10* promoter appears to be important to avoid the repressive effects on gene expression caused by ABI3. Therefore, it is possible that the distinct number of *cis*-regulatory elements and the absence of the RYREPEATBNNAPA in the *GmGLP10* promoter isolated from the soybean genotype PI 595099 might be responsible for the differential expression of *GmGLP10* in the *M. incognita*-induced galls of PI 595099 roots. Even though it is known that ABI3 interacts with RYREPEATBNNAPA in the nucleus to repress the expression of diverse genes (Tian *et al.*, 2020), further studies are required to elucidate how is the regulation of *GmGLP10* expression in both soybean genotypes. It would be interesting to test through chromatin immunoprecipitation (ChIP) assays if ABI3 transcript factor indeed can bind directly to the *GmGLP10* promoter that contain the *cis*-regulatory element RYREPEATBNNAPA and if the lack of RYREPEATBNNAPA sequence prevent ABI3 from binding to the *GmGLP10* promoter.

Like other isolated GLPs, which are usually localized in the apoplast and its extracellular matrix, GmGLP10 was observed at the cytoplasmic bridges and plasmatic membrane periphery, suggesting that it is likely an apoplastic protein. The presence of a N-terminal signal peptide in GmGLP10 protein supports its apoplastic localization. Our functional experiments revealed that *GmGLP10* overexpression in soybean hair roots and tobacco plants results in increased resistance to *M. incognita*, whereas knockout of *AtGLP10* in Arabidopsis led to reduced resistance, indicating that GmGLP10 functions as a positive regulator in *M. incognita* resistance. Consistent with these observations, several studies have shown that GLPs play a key role in plant resistance against fungal, bacterial and virus pathogens (Banerjee & Maiti, 2010; Knecht *et al.*, 2010; Banerjee *et al.*, 2010; Guevara-Olvera *et al.*, 2012; Rietz *et al.*, 2012; Mejía-Teniente *et al.*, 2015; Beracochea *et al.*, 2015; Liu *et al.*, 2016). For instance, *GmGLP10* overexpression in transgenic tobacco significantly enhanced resistance to *Sclerotinia sclerotiorum*. In addition, H_2O_2 levels and expression of plant defense-related genes and HR-associated genes were increased in the transgenic plants (Zhang *et al.*, 2018). Similarly, *GhGLP2*-overexpressing Arabidopsis showed increased resistance against *Verticillium dahlia* and *Fusarium oxysporum* pathogens. Moreover, induction of defense- and oxidative stress-

related genes, increased callose deposition and cell wall lignification at infection sites were observed in transgenic plants (Pei *et al.*, 2020). A recent study showed that overexpression of *OsGLP3-7* increased rice resistance to *Pyricularia oryzae*, *Magnaporthe oryzae*, and *Xanthomonas oryzae*, which was accompanied by enhanced expression of genes involved in JA and phytoalexin pathways. Further, higher levels of H_2O_2, JA and phytoalexin were detected in transgenic plants. By contrast, RNAi suppression of *OsGLP3-7* increased disease symptoms, as well as H_2O_2, JA and phytoalexin levels (Sun *et al.*, 2023). Additionally, functional analysis of a cotton *GLP* gene using *GhABP19*-overexpressing and *GhABP19*-RNAi transgenic lines demonstrated that GhABP19 modulates cotton defense response against *Verticillium dahliae* and *Fusarium oxysporum* through its SOD activity and activation of JA pathway (Pei *et al.*, 2019).

Multiple and coordinated plant immune responses are triggered upon pathogen perception and infection, including reactive oxygen species (ROS) production, defense gene expression, defense hormone production (jasmonates, salicylates, auxins, gibberellins and abscisic acid), mitogen-activated protein kinase (MAPK) activation and intracellular Ca^{2+} influx (Zhang *et al.*, 2020; Rutter *et al.*, 2022; Zou *et al.*, 2024). It is generally believed that GLP-mediated plant resistance against pathogens is partially due to their superoxide dismutase activity, which is intrinsically linked with ROS. SOD catalyzes the dismutation of the superoxide radical (O_2^-) into hydrogen peroxide (H_2O_2) and molecular oxygen (O_2), which are less reactive products, thereby protecting plant cells from oxidative burst. H_2O_2 in turn has a direct antimicrobial effect. Furthermore, the H_2O_2 acts as a local and systemic signaling molecule activating downstream signal transduction pathways of hypersensitive response and systemic acquired resistance (Waszczak *et al.*, 2018) and regulates SA and/or JA signaling pathways (Myers *et al.*, 2023). Therefore, it is tempting to speculate that H_2O_2 produced by the activity of GmGLP10 might contribute to plant immune responses against *M. incognita*.

To better understand how GmGLP10 improves plant resistance to *M. incognita*, we conducted RT-qPCR analysis on a subset of genes with known roles in the plant hormonal, ROS and defense pathways. Consistent with previous studies (Liu *et al.*, 2016; Zhang *et al.*, 2018; Pei *et al.*, 2019, 2020), our gene expression analysis of *GmGLP10*^{OE} lines and wild type plants indicates that GmGLP10 mediates host resistance to *M. incognita* through the regulation of hormonal-, ROS- and defense-related genes. Remarkably, two HR-related genes (*NtHSR201* and *NtHSR203*), two SA-related genes (*NtPR2* and *NtPR5*), three ET-related genes (*NtERF1*

and *NtACS6*, *NtEN3*), three JA-related genes (*NtMYC2*, *NtAOC* and *NtAOS*) and one ROS-related gene (*NtRBOHD*) were transcriptionally upregulated by *GmGLP10* overexpression.

Nonexpressor of pathogenesis-related genes 1 (NPR1) is an SA receptor that plays a key role in plant defense responses. In its inactive form, NPR1 is present in the cytoplasm as an oligomer. When the ROS burst is triggered, the reduction of the cytoplasm is induced by SA resulting in the activation of the thioredoxin TRXh5 that promotes the release of NPR1 (Tada *et al.*, 2008). In the nucleus, monomeric NPR1 binds to transcription factors to induce the expression of defense genes (Zhang *et al.*, 1999; Zhou *et al.*, 2000). Thus, it is possible that H_2O_2 signaling molecules induced by *M. incognita* infection and those produced by GmGLP10 activity function synergistically with SA to activate NPR1, which in turn may lead to the coordinated induction of a large number of defense genes in soybean. It is worthwhile to investigate whether the cellular redox changes caused by *GmGLP10* overexpression are involved in SA/NPR1-mediated transcriptional reprogramming in the *GmGLP10*^{OE} lines since NPR1 has the ability to sense the redox state of the cell.

Interestingly, we observed that the seed germination of *glp10-1* and *glp10-2* mutants was dramatically decreased compared to wild type, providing strong evidence that GmGLP10 also play a role in seed dormancy and/or germination. However, the seed germination was not affected by *GmGLP10* overexpression. Previous findings suggest that GLPs can positively or negatively regulate different aspects of seed physiology, including dormancy, germination and vigour. For instance, the germination potential and seedling percentage of rice *Oscdp3.10* mutants were significantly lower than those of wild type plants, but the germination percentage of mutant were not significantly affected by *Oscdp3.10* loss-of-function. In addition, it was shown that the seed vigour of *Oscdp3.10* overexpressing lines was similar to the control (Peng *et al.*, 2022). Nonetheless, another study showed an inverse correlation between *OsGLP2-1* expression levels and seed germination rate, indicating that *OsGLP2-1* negatively regulates seed dormancy and germination. It was demonstrated that *OsGLP2-1* overexpression in rice led to deep dormancy and decreased germination rate, while suppression of *OsGLP2-1* resulted in the release of dormancy (Wang *et al.*, 2020). On the other hand, Arabidopsis loss-of-function *AtPirin1* mutants display reduced germination levels in the absence of stratification (Lapik & Kaufman, 2003).

Based on our findings and those reported on the literature, we suggest a model to describe the molecular function of GmGLP10 in mediating resistance to *M. incognita* in the soybean genotype PI 595099 (Figure 9). In the soybean genotype BRS 133, the *GmGLP10*

expression is likely repressed transcriptionally by the transcription factor ABI3 due to the presence of the *cis*-regulatory element RYREPEATBNNAPA in its promoter, consequently limiting the expression levels of *GmGLP10* during *M. incognita* parasitism. Conversely, the absence of *cis*-regulatory element RYREPEATBNNAPA in the *GmGLP10* promoter of genotype PI 595099 may impair its interaction with ABI3 and the transcription factor may not exert its repressive transcriptional regulation on *GmGLP10*. As a result, *GmGLP10* is induced during *M. incognita* infection and contributes to soybean resistance through the increase of H_2O_2 in the apoplast, which in turn promotes changes in the redox cellular environment and release of the NPR1 monomers that translocate into the nucleus to activate the transcription of several defense genes. Further investigation is required to elucidate the underlying molecular mechanisms governing the role of *GmGLP10* in plant resistance to *M. incognita*.

Acknowledgements

This present study was supported by Coordenação de Aperfeiçoamento de Pessoal de Nível Superior (CAPES), Conselho Nacional de Desenvolvimento Científico e Tecnológico (CNPq), Fundação de Apoio à Pesquisa do Distrito Federal (FAP-DF), and INCT-Plant Stress Biotech. VJVM and DHP was supported by CAPES-COFECUB Sv.622/18. We thank Olivier Pierre & for technical assistance confocal assays and Olivier Magliore for supplying us with pre-parasitic nematodes. MFGS, who is the group leader, is grateful to CAPES/Cofecub project for financial support in the researcher and students exchange program between institutions. HK and JAE proof read the article and provide scientific English language assistance.

Competing interests

None declared.

Author contributions

VJVM & MFGS conceived the project. VJVM designed all experiments, performed most of the experiments and wrote the first draft of the manuscript. DHP performed the GUS staining analysis. TPR performed the real time RT-qPCR assays. HK provided intellectual inputs for T-

DNA mutants analysis. VJVM, HK & JAE amended the manuscript. MFGS was the lead researcher of all this work, edited this manuscript and also provided financial support and intellectual input. All authors read this present study and approved the final version.

ORCID

Valdeir Junio Vaz Moreira – https://orcid.org/0000-0002-8908-6028

Daniele Heloísa Pinheiro – https://orcid.org/0000-0002-7804-1537

Thuanne Pires Ribeiro - https://orcid.org/0000-0002-5335-3139

Harald Keller - https://orcid.org/0000-0003-1243-8467

Janice de Almeida Engler - https://orcid.org/0000-0002-8312- 672X

Maria Fatima Grossi de Sá - https://orcid.org/0000-0001- 8184-9599

Data availability

All relevant data that support the findings of this study can be found within the article and its supporting information.

References

Alekcevetch JC, de Lima Passianotto AL, Ferreira EGC, Dos Santos AB, da Silva DCG, Dias WP, Belzile F, Abdelnoor RV, Marcelino-Guimarães FC. (2021). Genome-wide association study for resistance to the *Meloidogyne javanica* causing root-knot nematode in soybean. **Theoretical and Applied Genetics**. Mar; 134(3):777-792. doi: 10.1007/s00122-020-03723-9.

Almeida Engler J, De Vleesschauwer V, Burssens S, Celenza JL Jr, Inze D, Van Montagu M, Engler G, Gheysen G. (1999). Molecular markers and cell cycle inhibitors show the importance of cell cycle progression in nematode induced galls and syncytia. **The Plant Cell**. 11: 793–808

Arraes FBM, Vasquez DDN, Tahir M, Pinheiro DH, Faheem M, Freitas-Alves NS, Moreira-Pinto CE, Moreira VJV, Paes-de-Melo B, Lisei-de-Sa ME, Morgante CV, Mota APZ, Lourenço-Tessutti IT, Togawa RC, Grynberg P, Fragoso RR, de Almeida-Engler J, Larsen MR,

Grossi-de-Sa MF. (2022). Integrated Omic Approaches Reveal Molecular Mechanisms of Tolerance during Soybean and *Meloidogyne incognita* Interactions. **Plants (Basel)**. Oct 17; 11(20):2744. doi: 10.3390/plants11202744.

Banerjee J, Maiti MK. (2010). Functional role of rice germin-like protein1 in regulation of plant height and disease resistance. **Biochemical and biophysical research communications**. 394: 178–183.

Barros FMDR, Pedrinho A, Mendes LW, Freitas CCG, Andreote FD. Interactions between Soil Bacterial Diversity and Plant-Parasitic Nematodes in Soybean Plants. (2022). **Applied and Environmental Microbiology**. Sep 13; 88(17):e0096322. doi: 10.1128/aem.00963-22.

Bartlem DG, Jones MG, Hammes UZ. (2014). Vascularization and nutrient delivery at root-knot nematode feeding sites in host roots. **Journal of Experimental Botany**. Apr; 65(7):1789-98. doi: 10.1093/jxb/ert415.

Beneventi MA, da Silva OB Jr, de Sá ME, Firmino AA, de Amorim RM, Albuquerque EV, da Silva MC, da Silva JP, Campos Mde A, Lopes MJ, Togawa RC, Pappas GJ Jr, Grossi-de-Sa MF. (2013). Transcription profile of soybean-root-knot nematode interaction reveals a key role of phythormones in the resistance reaction. **BMC Genomics**. May 10; 14:322. doi: 10.1186/1471-2164-14-322.

Beracochea VC, Almasia NI, Peluffo L, Nahirñak V, Hopp EH, Paniego N, Heinz RA, Vazquez-Rovere C, Lia VV. (2015). Sunflower germin-like protein HaGLP1 promotes ROS accumulation and enhances protection against fungal pathogens in transgenic *Arabidopsis thaliana*. **Plant Cell Reports**. Oct; 34(10):1717-33. doi: 10.1007/s00299-015-1819-4.

Bernier F. O., Berna A. (2001). Germins and germin-like proteins: plant do-all proteins. But what do they do exactly? **Plant Physiology and Biochemistry**. 39; 545–554. 10.1016/s0981-9428(01)01285-2

Bybd DW, Kirkpatrick T, Barker KR. (1983). An improved technique for clearing and staining plant tissues for detection of nematodes. **Journal of Nematology**. 15:142–143.

Cabrera J, Olmo R, Ruiz-Ferrer V, Abreu I, Hermans C, Martinez-Argudo I, Fenoll C, Escobar C. A. (2018). Phenotyping Method of Giant Cells from Root-Knot Nematode Feeding Sites by Confocal Microscopy Highlights a Role for CHITINASE-LIKE 1 in Arabidopsis. **International Journal of Molecular Sciences**. Feb 1; 19(2):429. doi: 10.3390/ijms19020429.

Calderón-Urrea A, Vanholme B, Vangestel S, Kane SM, Bahaji A, Pha K, Garcia M, Snider A, Gheysen G. (2016). Early development of the root-knot nematode *Meloidogyne incognita*. **BMC Developmental Biology**. Apr 28; 16:10. doi: 10.1186/s12861-016-0109-x.

Carter C, Thornburg RW. (1999). Germin-like proteins: structure, phylogeny, and function. **Journal of Plant Biology**. 42, 97–108.

Castagnone-Sereno, P., Danchin, E. G., Perfus-Barbeoch, L. & Abad, P. (2013). Diversity and evolution of root-knot nematodes, genus *Meloidogyne*: new insights from the genomic era. **Annual Review of Phytopathology**. 51, 203–220.

Castro B, Citterico M, Kimura S, Stevens DM, Wrzaczek M, Coaker G. (2021). Stress-induced reactive oxygen species compartmentalization, perception and signaling. **Nature Plants**. Apr; 7(4):403-412. doi: 10.1038/s41477-021-00887-0.

Chi YH, Paeng SK, Kim MJ, Hwang GY, Melencion SM, Oh HT, Lee SY. (2013). Redox-dependent functional switching of plant proteins accompanying with their structural changes. **Frontiers in Plant Science**. Jul 26; 4:277. doi: 10.3389/fpls.2013.00277.

Davidson RM, Reeves PA, Manosalva PM, Leach JE. (2009). Germins: a diverse protein family important for crop improvement. **Plant Science**. 177:499–510. doi:10.1016/j.plantsci.2009.08.012

Davis EL, Meyers DM, Burton JW, Barker KR. (1998). Resistance to Root-knot, Reniform, and Soybean Cyst Nematodes in Selected Soybean Breeding Lines. **Journal of Nematology**. Dec; 30(4S):530-41.

de Sá MEL, Lopes MJC, de Araújo Campos M, Paiva LV, dos Santos RMA, Beneventi MA, Firmino AAP, de Sá MFG. (2012). Transcriptome analysis of resistant soybean roots infected by *Meloidogyne javanica*. **Genetics and Molecular Biology**. 35: 272–282.

Ezcurra I, Wycliffe P, Nehlin L, Ellerström M, Rask L. (2000). Transactivation of the Brassica napus napin promoter by ABI3 requires interaction of the conserved B2 and B3 domains of ABI3 with different cis-elements: B2 mediates activation through an ABRE, whereas B3 interacts with an RY/G-box. **The Plant journal**. 24: 57–66.

Freitas-Alves NS, Moreira-Pinto CE, Arraes FBM, Costa LSL, de Abreu RA, Moreira VJV, Lourenço-Tessutti IT, Pinheiro DH, Lisei-de-Sa ME, Paes-de-Melo B, Pereira BM, Guimaraes PM, Brasileiro ACM, de Almeida-Engler J, Soccol CR, Morgante CV, Basso MF, Grossi-de-Sa MF. (2023). An *ex-vitro* hairy root system from petioles of detached soybean leaves for *in*

planta screening of target genes and CRISPR strategies associated with nematode bioassays. **Planta**. Dec 18; 259(1):23. doi: 10.1007/s00425-023-04286-x.

Goverse A, Smant G. (2014). The activation and suppression of plant innate immunity by parasitic nematodes. **Annual Review of Phytopathology**. 52:243-65. doi: 10.1146/annurev-phyto-102313-050118.

Guevara-Olvera L, Ruíz-Nito ML, Rangel-Cano RM, Torres-Pacheco I, Rivera-Bustamante RF, Muñoz-Sánchez CI, González-Chavira MM, Cruz-Hernandez A, Guevara-González RG. (2012). Expression of a germin-like protein gene (*CchGLP*) from a geminivirus-resistant pepper (*Capsicum chinense* Jacq.) enhances tolerance to geminivirus infection in transgenic tobacco. **Physiological and Molecular Plant Pathology**. 78: 45–50.

Hu X, Bidney DL, Yalpani N, Duvick JP, Crasta O, Folkerts O, Lu G. (2003). Overexpression of a gene encoding hydrogen peroxide-generating oxalate oxidase evokes defense responses in sunflower. **Plant Physiology**. Sep; 133(1):170-81. doi: 10.1104/pp.103.024026.

Jones JT, Haegeman A, Danchin EG, Gaur HS, Helder J, Jones MG, Kikuchi T, Manzanilla-López R, Palomares-Rius JE, Wesemael WM, Perry RN. (2013). Top 10 plant-parasitic nematodes in molecular plant pathology. **Molecular Plant Pathology**. Dec; 14(9):946-61. doi: 10.1111/mpp.12057.

Kihika R, Murungi LK, Coyne D, Ng'ang'a M, Hassanali A, Teal PEA, Torto B. (2017). Parasitic nematode *Meloidogyne incognita* interactions with different *Capsicum annum* cultivars reveal the chemical constituents modulating root herbivory. **Scientific Reports**. Jun 6; 7(1):2903. doi: 10.1038/s41598-017-02379-8.

Knecht K, Seyffarth M, Desel C, Thurau T, Sherameti I, Lou B, Oelmüller R, Cai D. (2010). Expression of *BvGLP-1* encoding a germin-like protein from sugar beet in *Arabidopsis thaliana* leads to resistance against phytopathogenic fungi. **Molecular plant-microbe interactions**. 23: 446–457.

Lapik YR, Kaufman LS. 2003. The Arabidopsis Cupin Domain Protein AtPirin1 Interacts with the G Protein α-Subunit GPA1 and Regulates Seed Germination and Early Seedling Development. **The Plant Cell**. 15: 1578–1590.

Lisei-de-Sá ME, Conceição Lopes MJ, de Araújo Campos M, Paiva LV, Dos Santos RM, Beneventi MA, Firmino AA, de Sá MF. (2012). Transcriptome analysis of resistant soybean

roots infected by *Meloidogyne javanica*. **Genetics and Molecular Biology**. Jun; 35(1 (suppl)):272-82. doi: 10.1590/S1415-47572012000200008.

Liu Q, Yang J, Yan S, Zhang S, Zhao J, Wang W, Yang T, Wang X, Mao X, Dong J, Zhu X, Liu B. (2016). The germin-like protein OsGLP2-1 enhances resistance to fungal blast and bacterial blight in rice. **Plant Molecular Biology**. Nov; 92(4-5):411-423. doi: 10.1007/s11103-016-0521-4.

Lopes-Caitar VS, Ccg De Carvalho M, Darben LM, Kuwahara MK, Nepomuceno AL, Dias WP, Abdelnoor R V, Marcelino-Guimarães FC. (2013). Genome-wide analysis of the Hsp20 gene family in soybean: comprehensive sequence, genomic organization and expression profile analysis under abiotic and biotic stresses. **BMC Genomics**. 14: 577.

Lopes NDS, Santos AS, de Novais DPS, Pirovani CP, Micheli F. (2023). Pathogenesis-related protein 10 in resistance to biotic stress: progress in elucidating functions, regulation and modes of action. **Frontiers in Plant Science**. Jul 4; 14:1193873. doi: 10.3389/fpls.2023.1193873.

Manosalva PM, Davidson RM, Liu B, Zhu X, Hulbert SH, Leung H, Leach JE. (2009). A germin-like protein gene family functions as a complex quantitative trait locus conferring broad-spectrum disease resistance in rice. **Plant Physiology**. Jan; 149(1):286-96. doi: 10.1104/pp.108.128348.

Mejía-Teniente L, de Jesús Joaquin-Ramos A, Torres-Pacheco I, Rivera-Bustamante RF, Guevara-Olvera L, Rico-García E, Guevara-Gonzalez RG. (2015). Silencing of a Germin-Like Protein Gene (CchGLP) in Geminivirus-Resistant Pepper (Capsicum chinense Jacq.) BG-3821 Increases Susceptibility to Single and Mixed Infections by Geminiviruses PHYVV and PepGMV. **Viruses**. 7: 6141–6151.

Moreira VJV, Lourenço-Tessutti IT, Basso MF, *et al.* (2022). *Minc03328* effector gene downregulation severely affects *Meloidogyne incognita* parasitism in transgenic *Arabidopsis thaliana*. **Planta**. 255:1–16. https://doi.org/10.1007/S00425-022-03823-4

Moreira VJV, Pinheiro DH, Lourenço-Tessutti IT, Basso MF, Lisei-deSa ME, Silva MCM, Danchin EGJ, Guimaraes PM, Grynberg P, Brasileiro ACM, Macedo LLP, Morgante CV, Almeida-Engler J, Grossi-de-Sa MF. (2023). *In planta* RNAi targeting *Meloidogyne incognita* Minc16803 gene perturbs nematode parasitism and reduces plant susceptibility. **Journal of Pest Science**. https://doi.org/10.1007/ s10340-023-01623-7

Murashige T; Skoog, F. (1962). A revised medium for rapid growth and bioassays with tobacco tissue cultures. **Physiologia Plantarum**. 15, 473–497. doi:10.1111/j.1399-3054.1962.tb08052.x

Myers RJ, Fichman Y, Zandalinas SI, Mittler R. (2023). Jasmonic acid and salicylic acid modulate systemic reactive oxygen species signaling during stress responses. **Plant Physiology**. 191: 862–873.

Nambara E, Marion-Poll A. (2003). ABA action and interactions in seeds. **Trends in plant science**. 8: 213–217.

Pei Y, Zhu Y, Jia Y, Ge X, Li X, Li F, Hou Y. (2020). Molecular evidence for the involvement of cotton GhGLP2, in enhanced resistance to *Verticillium* and *Fusarium* Wilts and oxidative stress. **Scientific Reports**. Jul 27; 10(1):12510. doi: 10.1038/s41598-020-68943-x.

Pei Y, Li X, Zhu Y, Ge X, Sun Y, Liu N, Jia Y, Li F, Hou Y. (2019). GhABP19, a Novel Germin-Like Protein From *Gossypium hirsutum*, Plays an Important Role in the Regulation of Resistance to Verticillium and Fusarium Wilt Pathogens. **Frontiers in Plant Science**. May 8; 10:583. doi: 10.3389/fpls.2019.00583.

Peng L, Sun S, Yang B, Zhao J, Li W, Huang Z, Li Z, He Y, Wang Z. (2022). Genome-wide association study reveals that the cupin domain protein OsCDP3 10. **Plant Biotechnology Journal**. 20: 485–498.

Ribeiro C, de Melo BP, Lourenço-Tessutti IT, Ballesteros HF, Ribeiro KVG, Menuet K, Heyman J, Hemerly A, de Sá MFG, De Veylder L, de Almeida Engler J. (2024). The regeneration conferring transcription factor complex ERF115-PAT1 coordinates a wound-induced response in root-knot nematode induced galls. **New Phytologist**. Jan; 241(2):878-895. doi: 10.1111/nph.19399.

Rietz S, Bernsdorff FEM, Cai D. (2012). Members of the germin-like protein family in *Brassica napus* are candidates for the initiation of an oxidative burst that impedes pathogenesis of *Sclerotinia sclerotiorum*. **Journal of Experimental Botany**. 63: 5507–5519.

Rutter WB, Franco J, Gleason C. (2022). Rooting Out the Mechanisms of Root-Knot Nematode-Plant Interactions. **Annual Review of Phytopathology**. 60: 43–76.

Sengupta S, Ray A, Mandal D, Nag Chaudhuri R. (2020). ABI3 mediated repression of RAV1 gene expression promotes efficient dehydration stress response in *Arabidopsis thaliana*.

Biochimica et Biophysica Acta-Gene Regulatory Mechanisms. Sep; 1863(9):194582. doi: 10.1016/j.bbagrm.2020.194582.

Sun B, Li W, Ma Y, Yu T, Huang W, Ding J, Yu H, Jiang L, Zhang J, Lv S, Yang J, Yan S, Liu B, Liu Q. (2023). OsGLP3-7 positively regulates rice immune response by activating hydrogen peroxide, jasmonic acid, and phytoalexin metabolic pathways. **Molecular Plant Pathology**. Mar; 24(3):248-261. doi: 10.1111/mpp.13294.

Tada Y, Spoel SH, Pajerowska-Mukhtar K, Mou Z, Song J, Wang C, Zuo J, Dong X. (2008). Plant Immunity Requires Conformational Charges of NPR1 via S-Nitrosylation and Thioredoxins. **Science**. 321: 5891.

Thum KE, Kim M, Morishige DT, Eibl C, Koop HU, Mullet JE. (2001). Analysis of barley chloroplast psbD light-responsive promoter elements in transplastomic tobacco. **Plant Molecular Biology**. Oct; 47(3):353-66. doi: 10.1023/a:1011616400264.

Tian R, Wang F, Zheng Q, Niza VMAGE, Downie AB, Perry SE. (2020). Direct and indirect targets of the Arabidopsis seed transcription factor ABSCISIC ACID INSENSITIVE3. **The Plant Journal**. Aug; 103(5):1679-1694. doi: 10.1111/tpj.14854.

Tsai AY, Iwamoto Y, Tsumuraya Y, Oota M, Konishi T, Ito S, Kotake T, Ishikawa H, Sawa S. (2021). Root-knot nematode chemotaxis is positively regulated by l-galactose sidechains of mucilage carbohydrate rhamnogalacturonan-I. **Science Advances**. Jul 2; 7(27):eabh4182. doi: 10.1126/sciadv.abh4182.

Vieira, P.M.H.; Arêdes, F.A.S.; Ferreira, A.; Ferreira, M.F.S. (2016). Comparative analysis of soybean genotype resistance to *Heterodera glycines* and *Meloidogyne* species via resistance gene analogs. **Genetics and Molecular Research**. 15, 1–13.

Wang H, Sun S, Ge W, Zhao L, Hou B, Wang K, Lyu Z, Chen L, Xu S, Guo J, Li M, Su P, Li X, Wang G, Bo C, Fang X, Zhuang W, Cheng X, Wu J, Dong L, Chen W, Li W, Xiao G, Zhao J, Hao Y, Xu Y, Gao Y, Liu W, Liu Y, Yin H, Li J, Li X, Zhao Y, Wang X, Ni F, Ma X, Li A, Xu SS, Bai G, Nevo E, Gao C, Ohm H, Kong L. (2020). Horizontal gene transfer of *Fhb7* from fungus underlies *Fusarium* head blight resistance in wheat. **Science**. May 22; 368(6493):eaba5435. doi: 10.1126/science.aba5435.

Wang X, Zhang H, Gao Y, Sun G, Zhang W, Qiu L. (2014). A comprehensive analysis of the *Cupin* gene family in soybean (*Glycine max*). **PLoS One**. Oct 31; 9(10):e110092. doi: 10.1371/journal.pone.0110092.

Wang H, Zhang Y, Xiao N, Zhang G, Wang F, Chen X, Fang R. (2020). Rice GERMIN-LIKE PROTEIN 2-1 Functions in Seed Dormancy under the Control of Abscisic Acid and Gibberellic Acid Signaling Pathways. **Plant Physiology**. 183: 1157–1170.

Waszczak C, Carmody M, Kangasjärvi J. (2018). Reactive Oxygen Species in Plant Signaling. **Annual review of plant biology**. 69: 209–236.

Zhang J, Coaker G, Zhou JM, Dong X. (2020). Plant immune mechanisms: From reductionistic to holistic points of view. **Molecular Plant**. 13: 1358–1378.

Zhang Y, Fan W, Kinkema M, Li X, Dong X. (1999). Interaction of NPR1 with basic leucine zipper protein transcription factors that bind sequences required for salicylic acid induction of the PR-1 gene. **Proceedings of the National Academy of Sciences of the United States of America**. 96: 6523–6528.

Zhang J, Zhao P, Chen S, Sun L, Mao J, Tan S, Xiang C. (2023). The ABI3-ERF1 module mediates ABA-auxin crosstalk to regulate lateral root emergence. **Cell Reports: Cell Press**. Jul 25; 42(7):112809. doi: 10.1016/j.celrep.2023.112809.

Zhang Y, Wang X, Chang X, Sun M, Zhang Y, Li W, Li Y. (2018). Overexpression of germin-like protein *GmGLP10* enhances resistance to *Sclerotinia sclerotiorum* in transgenic tobacco. **Biochemical and Biophysical Research Communications**. Feb 26; 497(1):160-166. doi: 10.1016/j.bbrc.2018.02.046.

Zhao Q. (2016). Lignification: Flexibility, Biosynthesis and Regulation. **Trends in Plant Science**. Aug; 21(8):713-721. doi: 10.1016/j.tplants.2016.04.006.

Zhou JM, Trifa Y, Silva H, Pontier D, Lam E, Shah J, Klessig DF. (2000). NPR1 differentially interacts with members of the TGA/OBF family of transcription factors that bind an element of the PR-1 gene required for induction by salicylic acid. **Molecular plant-microbe interactions**. 13: 191–202.

Zou J, Kyndt T, Yu J, Zhou J. (2024). Plant–nematode battle: engagement of complex signaling network. **Trends in Parasitology**. 40: 846–857.

Figures and legends

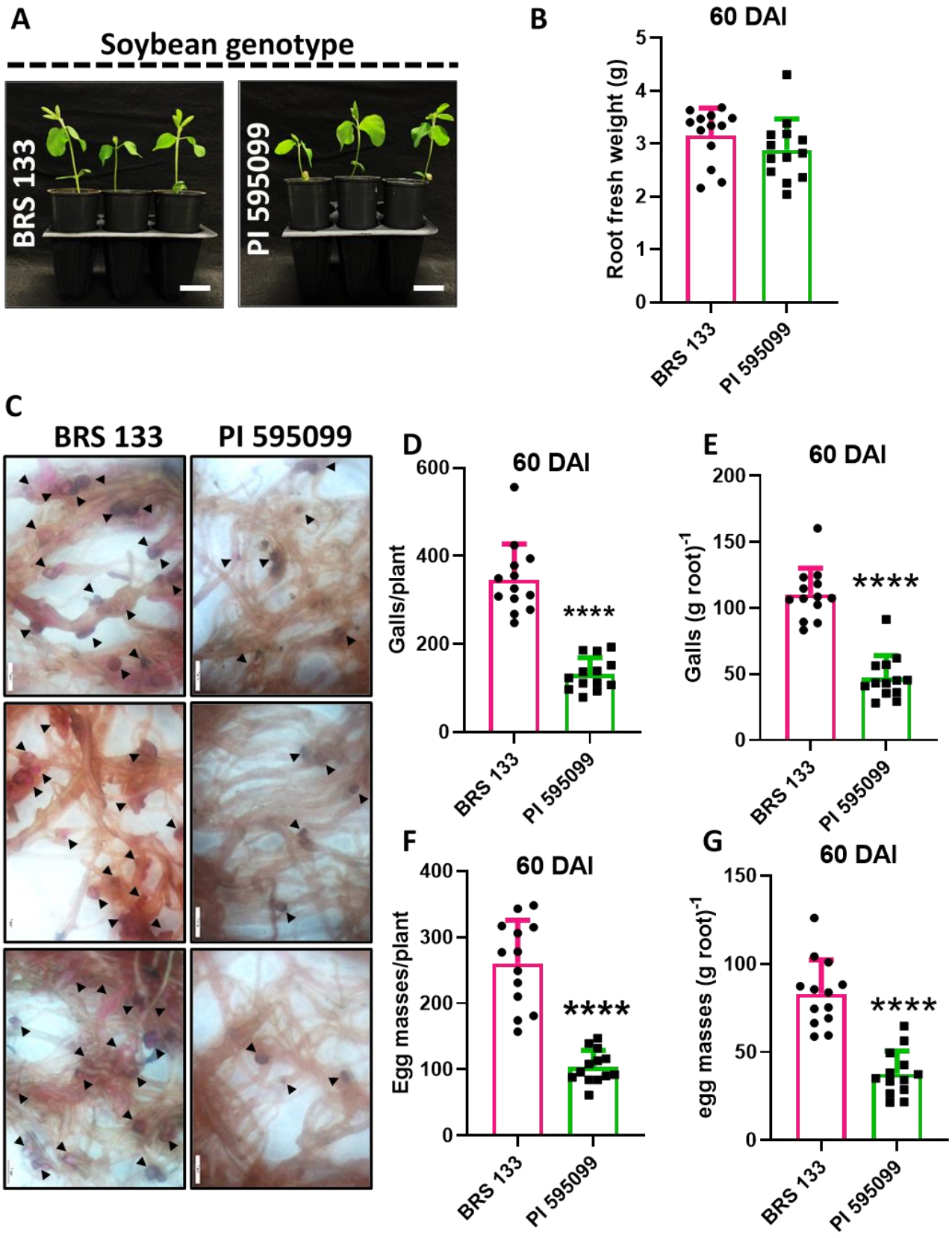

Figure 1. Performance of soybean genotypes BRS 133 and PI 595099 under *M. incognita* infection. (**A**) Soybean genotypes at V1 growth stage was the T0 point used in our study for *M. incognita* (race 1) inoculation. Scale bars: 10 cm. (**B**) Average value of root fresh weight (g) of soybean genotypes evaluated after 60 DAI. (**C**) Histological examination of infected roots under bright-field optics. Black arrows show egg masses staining with phloxine B. Scale bars: 100 µm. The resistance test was performed using the parameters (**D**, **E**) Galls/plant, galls/gram of roots, and (**F**, **G**) Egg masses/plant, egg masses/gram of roots. Significant differences were analyzed by Student's t test (n=13, ****P < 0.0001). Data are presented as means ± SD.

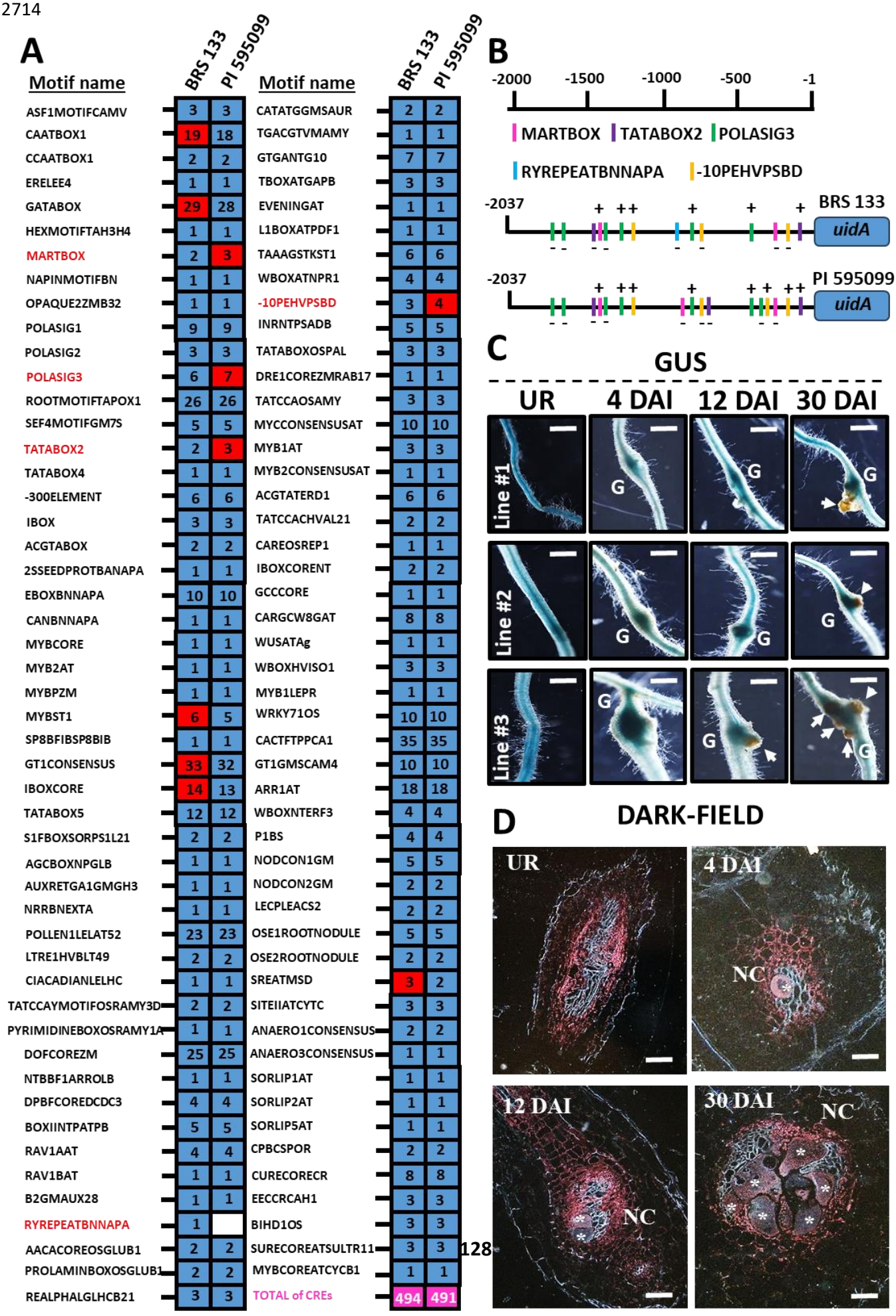
A
Motif name
BRS 133
PI 595099
ASF1MOTIFCAMV 3 3
CAATBOX1 19 18
CCAATBOX1 2 2
ERELEE4 1 1
GATABOX 29 28
HEXMOTIFTAH3H4 1 1
MARTBOX 2 3
NAPINMOTIFBN 1 1
OPAQUE2ZMB32 1 1
POLASIG1 9 9
POLASIG2 3 3
POLASIG3 6 7
ROOTMOTIFTAPOX1 26 26
SEF4MOTIFGM7S 5 5
TATABOX2 2 3
TATABOX4 1 1
-300ELEMENT 6 6
IBOX 3 3
ACGTABOX 2 2
2SSEEDPROTBANAPA 1 1
EBOXBNNAPA 10 10
CANBNNAPA 1 1
MYBCORE 1 1
MYB2AT 1 1
MYBPZM 1 1
MYBST1 6 5
SP8BFIBSP8BIB 1 1
GT1CONSENSUS 33 32
IBOXCORE 14 13
TATABOX5 12 12
S1FBOXSORPS1L21 2 2
AGCBOXNPGLB 1 1
AUXRETGA1GMGH3 1 1
NRRBNEXTA 1 1
POLLEN1LELAT52 23 23
LTRE1HVBLT49 2 2
CIACADIANLELHC 1 1
TATCCAYMOTIFOSRAMY3D 2 2
PYRIMIDINEBOXOSRAMY1A 1 1
DOFCOREZM 25 25
NTBBF1ARROLB 1 1
DPBFCOREDCDC3 4 4
BOXIINTPATPB 5 5
RAV1AAT 4 4
RAV1BAT 1 1
B2GMAUX28 1 1
RYREPEATBNNAPA 1
AACACOREOSGLUB1 2 2
PROLAMINBOXOSGLUB1 2 2
REALPHALGLHCB21 3 3
Motif name
BRS 133
PI 595099
CATATGGMSAUR 2 2
TGACGTVMAMY 1 1
GTGANTG10 7 7
TBOXATGAPB 3 3
EVENINGAT 1 1
L1BOXATPDF1 1 1
TAAAGSTKST1 6 6
WBOXATNPR1 4 4
-10PEHVPSBD 3 4
INRNTPSADB 5 5
TATABOXOSPAL 3 3
DRE1COREZMRAB17 1 1
TATCCAOSAMY 3 3
MYCCONSENSUSAT 10 10
MYB1AT 3 3
MYB2CONSENSUSAT 1 1
ACGTATERD1 6 6
TATCCACHVAL21 2 2
CAREOSREP1 1 1
IBOXCORENT 2 2
GCCCORE 1 1
CARGCW8GAT 8 8
WUSATAg 1 1
WBOXHVISO1 3 3
MYB1LEPR 1 1
WRKY71OS 10 10
CACTFTPPCA1 35 35
GT1GMSCAM4 10 10
ARR1AT 18 18
WBOXNTERF3 4 4
P1BS 4 4
NODCON1GM 5 5
NODCON2GM 2 2
LECPLEACS2 2 2
OSE1ROOTNODULE 5 5
OSE2ROOTNODULE 2 2
SREATMSD 3 2
SITEIIATCYTC 3 3
ANAERO1CONSENSUS 2 2
ANAERO3CONSENSUS 1 1
SORLIP1AT 1 1
SORLIP2AT 1 1
SORLIP5AT 1 1
CPBCSPOR 2 2
CURECORECR 8 8
EECCRCAH1 3 3
BIHD1OS 3 3
SURECOREATSULTR11 3 3
MYBCOREATCYCB1 1 1
TOTAL of CREs 494 491
B
-2000
-1500
-1000
-500
-1
MARTBOX
TATABOX2
POLASIG3
RYREPEATBNNAPA
-10PEHVPSBD
-2037
BRS 133
uidA
-2037
PI 595099
uidA
C
GUS
UR
4 DAI
12 DAI
30 DAI
Line #1
Line #2
Line #3
G
D
DARK-FIELD
UR
4 DAI
NC
12 DAI
NC
30 DAI
NC

Figure 2. *GmGLP10* promoters sequencing analysis and GUS activity under *pGmGLP10* (PI 595099) control. (**A**) *Cis*-regulatory elements of *pGmGLP10* from the soybean genotype BRS 133 (susceptible) and PI 595099 (resistance) predicted by PLACE database (**B**) Schematic diagram of the frequency of *cis*-regulatory elements found in *pGmGLP10* of both soybean genotypes. (**C**) GUS activity performed in transgenic tobacco plants under *pGmGLP10* (PI 595099) control. (**D**) Dark-field optics images of sectioned galls (4, 12 and 30 DAI) and URs illustrating GUS staining (red) in vascular tissues and GCs induced by *M. incognita*. G, Galls; White arrows, egg mass; NC, Neighbouring cells; UR, uninfected roots; Asterisk, giant cell; DAI, days after inoculation. Scale bars: 50 µm.

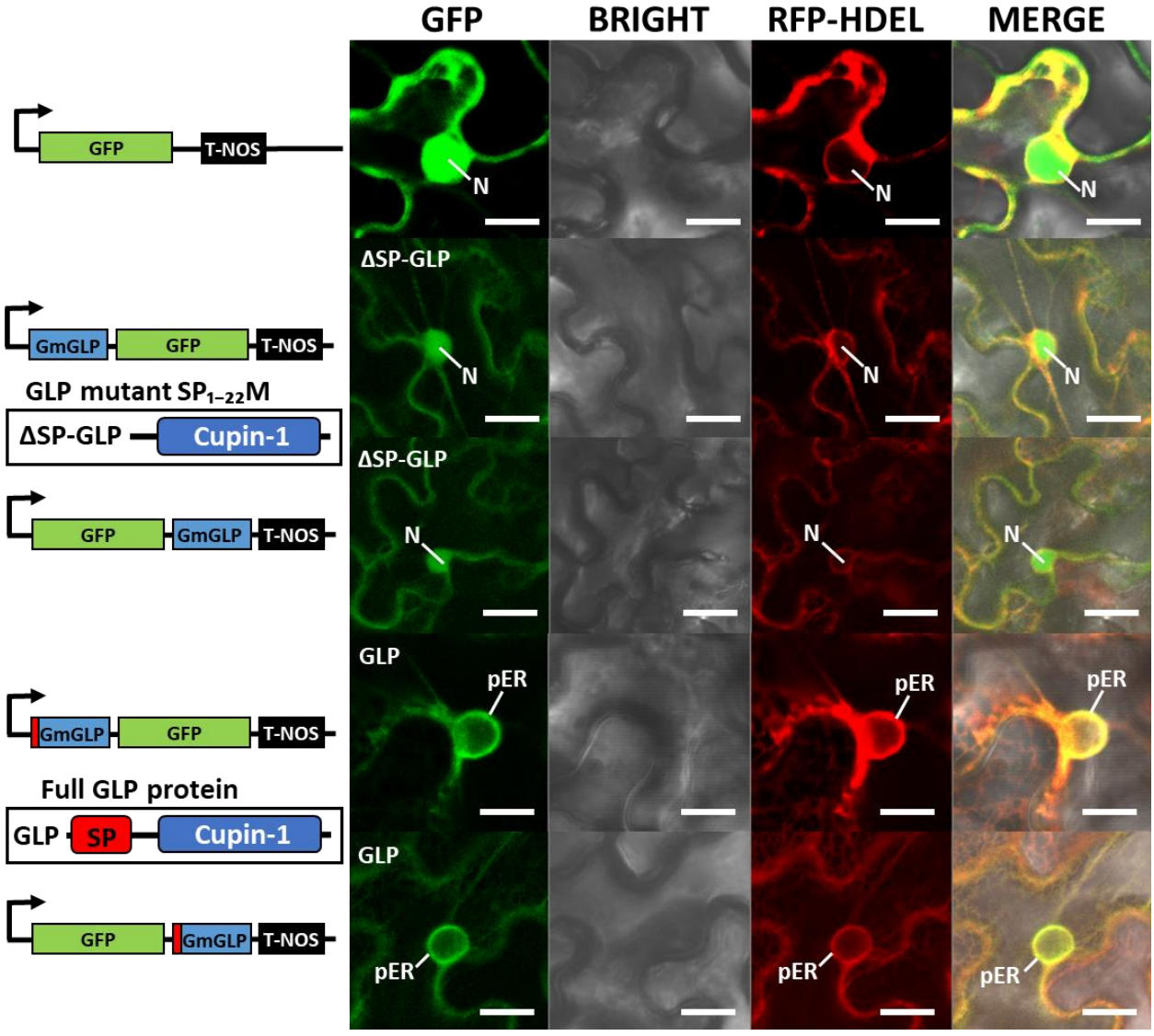

Figure 3. The soybean GmGLP10 is likely an apoplastic protein. The full GmGLP10 protein and ΔSP-GmGLP10 protein (without signal peptide - ΔSP) fused to GFP at N- and C-terminals were expressed in *N. benthamiana* leaves and examined under a confocal microscope 2 days after infiltration. In all experiments, more than 30 cells were examined. Confocal images show the transient subcellular localization of ΔSP-GmGLP10 protein in cytoplasmic region of *N. benthamiana* leaf cells transformed with both GFP terminals fused constructs, while the full GmGLP10 revealed GFP signals at cytoplasmic bridges as well as plasmatic membrane periphery. GFP signals in the nucleus were confirmed only for construct GFP and the ΔSP-GmGLP10 mutant indicating its passive diffusion restricted to its size. In turn, the co-localization between RFP-HDEL (ER marker) with GmGLP10 demonstrates its clear involvement with the extrinsic secretion pathway in the ER before being exported to EM (merged signals). Scale bars, 10 mm.

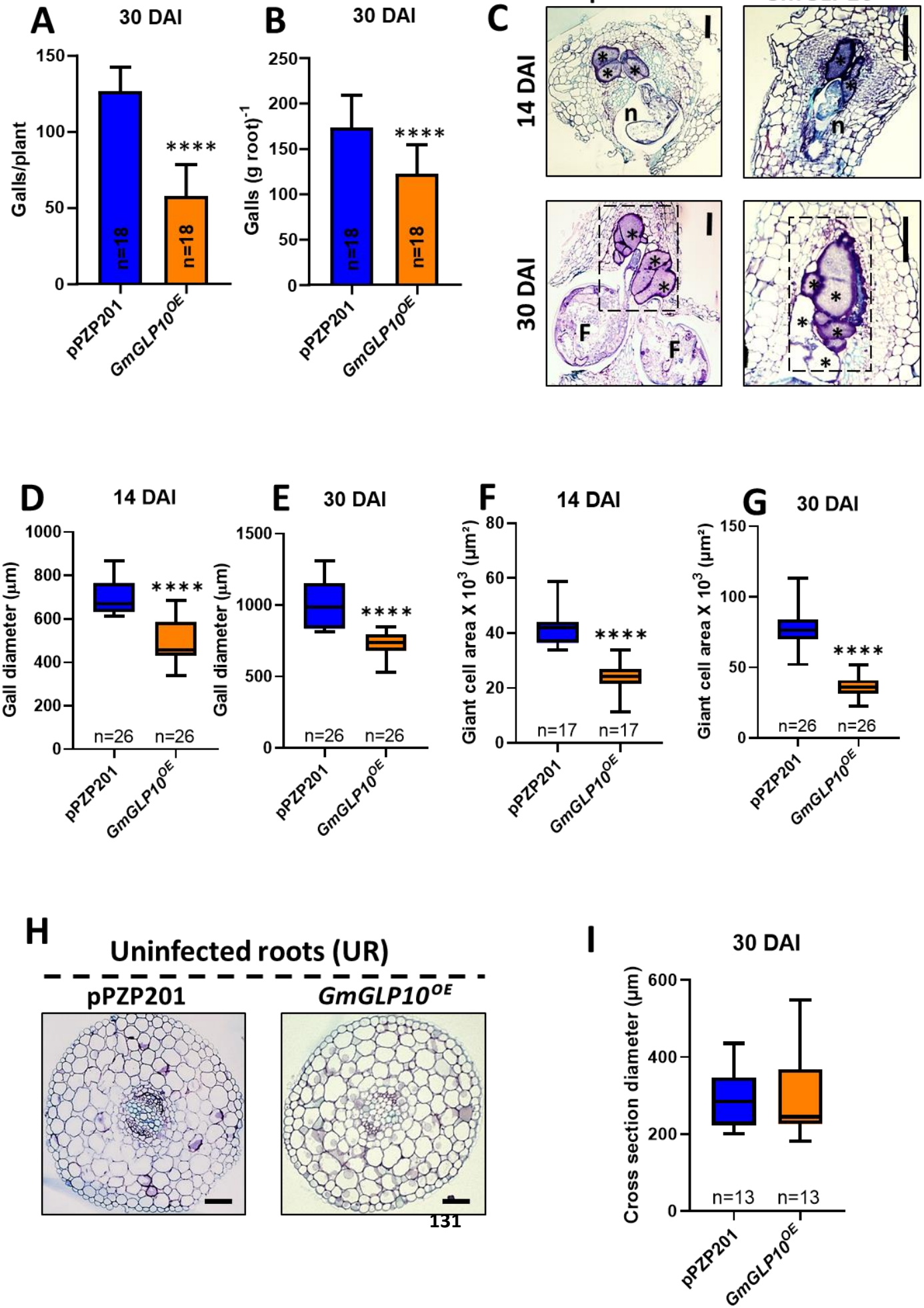
A
30 DAI
Galls/plant
150
100
50
0
****
n=18
n=18
pPZP201
GmGLP10OE
B
30 DAI
Galls (g root)-1
250
200
150
100
50
0
****
n=18
n=18
pPZP201
GmGLP10OE
C
pPZP201
GmGLP10OE
14 DAI
30 DAI
n
F
D
14 DAI
Gall diameter (µm)
1000
800
600
400
200
0
****
n=26
n=26
pPZP201
GmGLP10OE
E
30 DAI
Gall diameter (µm)
1500
1000
500
0
****
n=26
n=26
pPZP201
GmGLP10OE
F
14 DAI
Giant cell area X 10³ (µm²)
80
60
40
20
0
****
n=17
n=17
pPZP201
GmGLP10OE
G
30 DAI
Giant cell area X 10³ (µm²)
150
100
50
0
****
n=26
n=26
pPZP201
GmGLP10OE
H
Uninfected roots (UR)
pPZP201
GmGLP10OE
I
30 DAI
Cross section diameter (µm)
600
400
200
0
n=13
n=13
pPZP201
GmGLP10OE

Figure 4. Nematode bioassay and histological analysis of *M. incognita*-induced galls of soybean hairy roots overexpressing *GmGLP10*. Infection tests showed a significant reduction (****P < 0.0001) in (**A**) galls/plant and (**B**) galls (g root)$^{-1}$ evaluated in soybean hairy roots at 30 DAI. Histological examination was performed in galls induced at (**C**) 14 DAI and 30 DAI (n=18) revealing a big delayed in nematode development and possible damaged in GCs in view of the low TB staining observed. The same cross-section images showed a significant reduction in gall diameters evaluated at (**D**) 14 DAI and (**E**) 30 DAI (n=26) as well as GC area measurements at (**F**) 14 DAI and (**G**) 30 DAI (n=17). Histological analysis was also used to evaluated possible morphological changes in (**H**) uninfected roots (UR) by (**I**) cross section diameter measurements, indicating no alteration in roots anatomy (n=13). Significant differences were analyzed by Student's t test (****P < 0.0001). Data are presented as means ± SD. Scale bars: 50 µm.

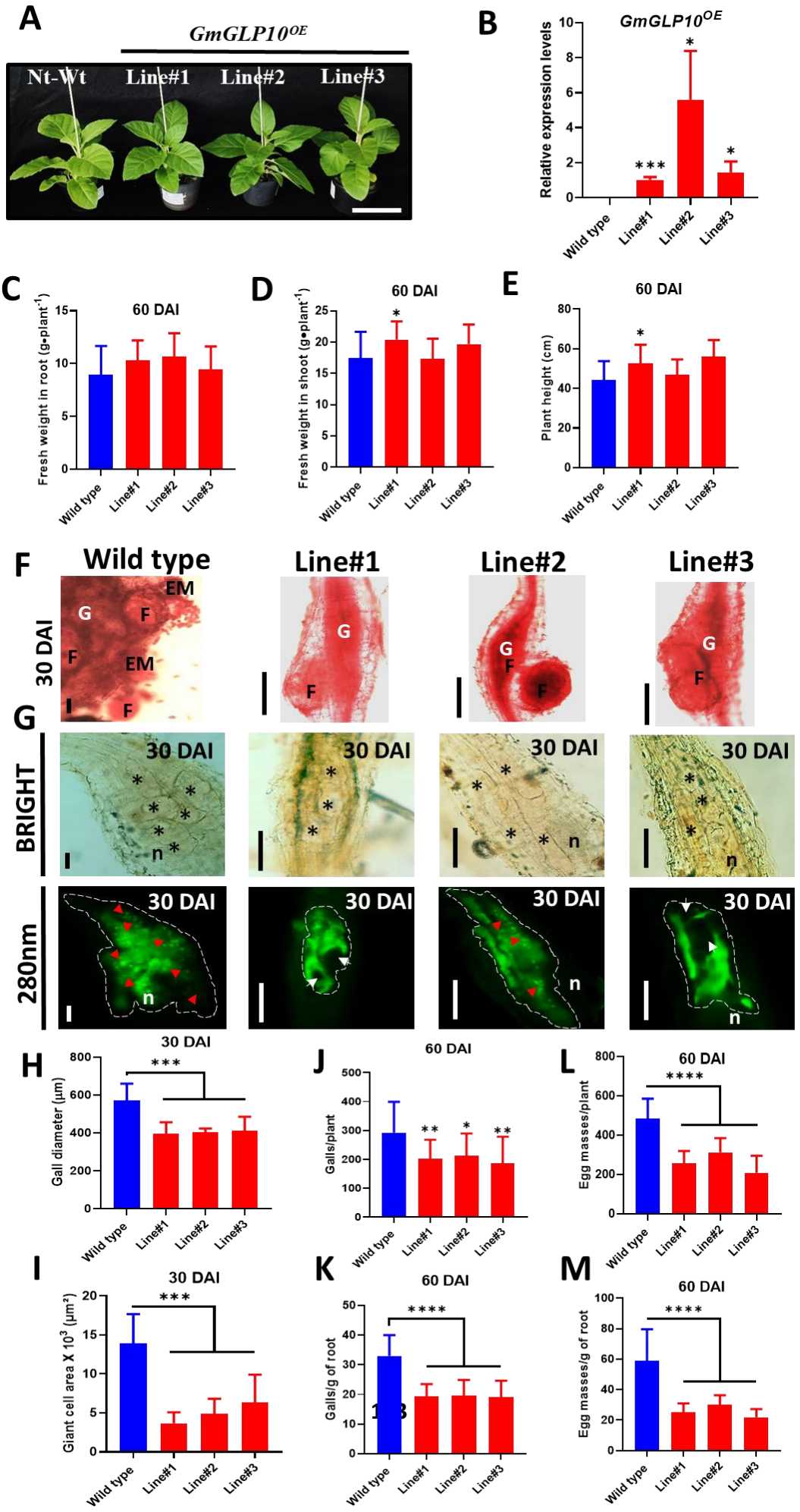
A
GmGLP10OE
Nt-Wt
Line#1
Line#2
Line#3
B
GmGLP10OE
Relative expression levels
Wild type
Line#1
Line#2
Line#3
C
60 DAI
Fresh weight in root (g•plant-1)
D
60 DAI
Fresh weight in shoot (g•plant-1)
E
60 DAI
Plant height (cm)
F
Wild type
Line#1
Line#2
Line#3
30 DAI
EM
G
F
G
BRIGHT
280nm
n
H
30 DAI
Gall diameter (µm)
J
60 DAI
Galls/plant
L
60 DAI
Egg masses/plant
I
30 DAI
Giant cell area X 10³ (µm²)
K
60 DAI
Galls/g of root
M
60 DAI
Egg masses/g of root

Figure 5. Transgenic tobacco plants overexpressing *GmGLP10* reduce susceptibility against *M. incognita* by interfering in GCs formation and nematode development. (**A**) Phenotypic analysis of *GmGLP10*^{OE} transgenic tobacco plants at 30 DAI. Scale bars: 10 cm. (**B**) *GmGLP10* transcript abundance in transgenic tobacco lines. Relative expression levels were calculated relative to the Line #1 (lowest expression level). Fresh weight measurements of (**C**) roots, (**D**) shoots and (**E**) plant height. Significant differences were analyzed by Student's t test (*P < 0.01). (**F**) Acid fuchsin staining of galls at 30 DAI revealed a delay in nematode reproduction compared to wild-type control. (**G**) Whole cleared galls of *GmGLP10*^{OE} lines showed low nuclei cluster content (red arrows) and empty spaces into GCs (white arrows). Scale bars: 50 µm. (**H**) Galls diameters and (**I**) giant cells area measurements were performed on galls collected at 30 DAI. Significant differences were analyzed by Student's t test (n=15, ***P < 0.001). The parameters (**J**) galls/plant, (**K**) galls (g root)$^{-1}$, (**L**) egg masses/plant and (**M**) egg masses (g root)$^{-1}$ were evaluated at 60 DAI. Significant differences were analyzed by Student's t test (n>13, *P < 0.05, **P < 0.01, ****P < 0.0001). Data are presented as means ± SD.

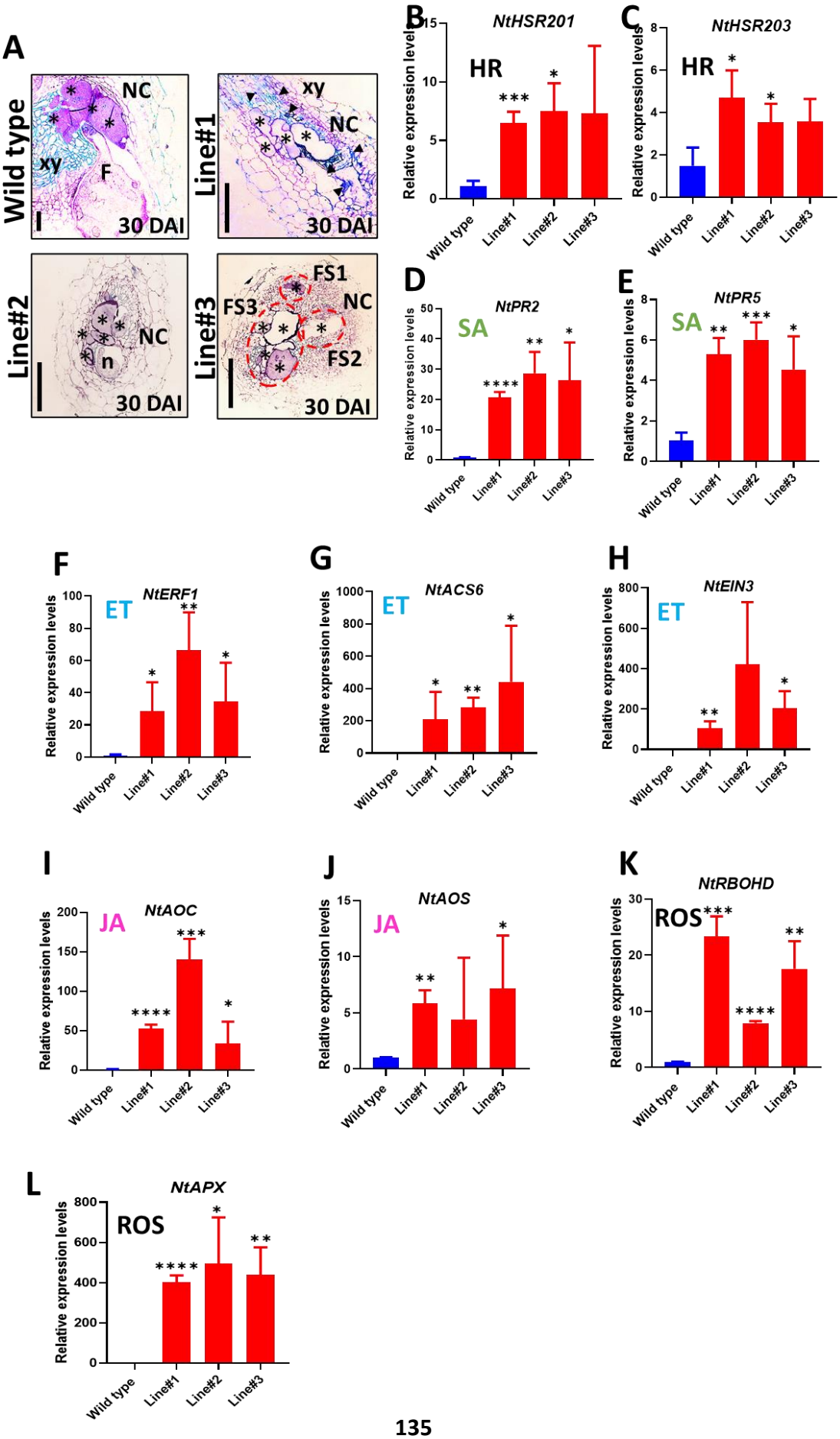
A
Wild type
Line#1
Line#2
Line#3
NC
xy
F
n
FS1
FS2
FS3
30 DAI
B
NtHSR201
HR
C
NtHSR203
HR
D
NtPR2
SA
E
NtPR5
SA
F
NtERF1
ET
G
NtACS6
ET
H
NtEIN3
ET
I
NtAOC
JA
J
NtAOS
JA
K
NtRBOHD
ROS
L
NtAPX
ROS
Relative expression levels
Wild type
Line#1
Line#2
Line#3

Figure 6. Transgenic tobacco plants overexpressing *GmGLP10* reduce susceptibility against *M. incognita* by interfering in GCs formation and defense gene expression. (**A**) Histological examination of *M. incognita*-induced galls at 30 DAI. Scale bars: 50 µm. Several defense genes related to Hypersensitive Response – HR: (**B**) *NtHSR201*, (**C**) *NtHSR203*; Salicylic Acid – SA: (**D**) *NtPR2*, (**E**) *NtPR5*; Ethylene – ET: (**F**) *NtERF1*, (**G**) *NtACS6*, (**H**) *NtEIN3*; Jasmonic Acid – JA: (**I**) *NtAOC*, (**J**) *NtAOS*; and Reactive Oxygen Species – ROS: (**K**) *NtRBOHD* and (**L**) *NtAPX* were examined by RT-qPCR analysis showing up-regulation in the transgenic plants. Relative expression levels were calculated by $2^{-\Delta\Delta Ct}$ and expressed as means of technical triplicates of the three biological replicates. All target genes levels were normalized using the *NtL25* and *NtActin* as reference genes. Significant differences were analyzed by Student's t test (*P < 0.05, **P < 0.01, ***P < 0.001, ****P < 0.0001). Data are presented as means ± SD.

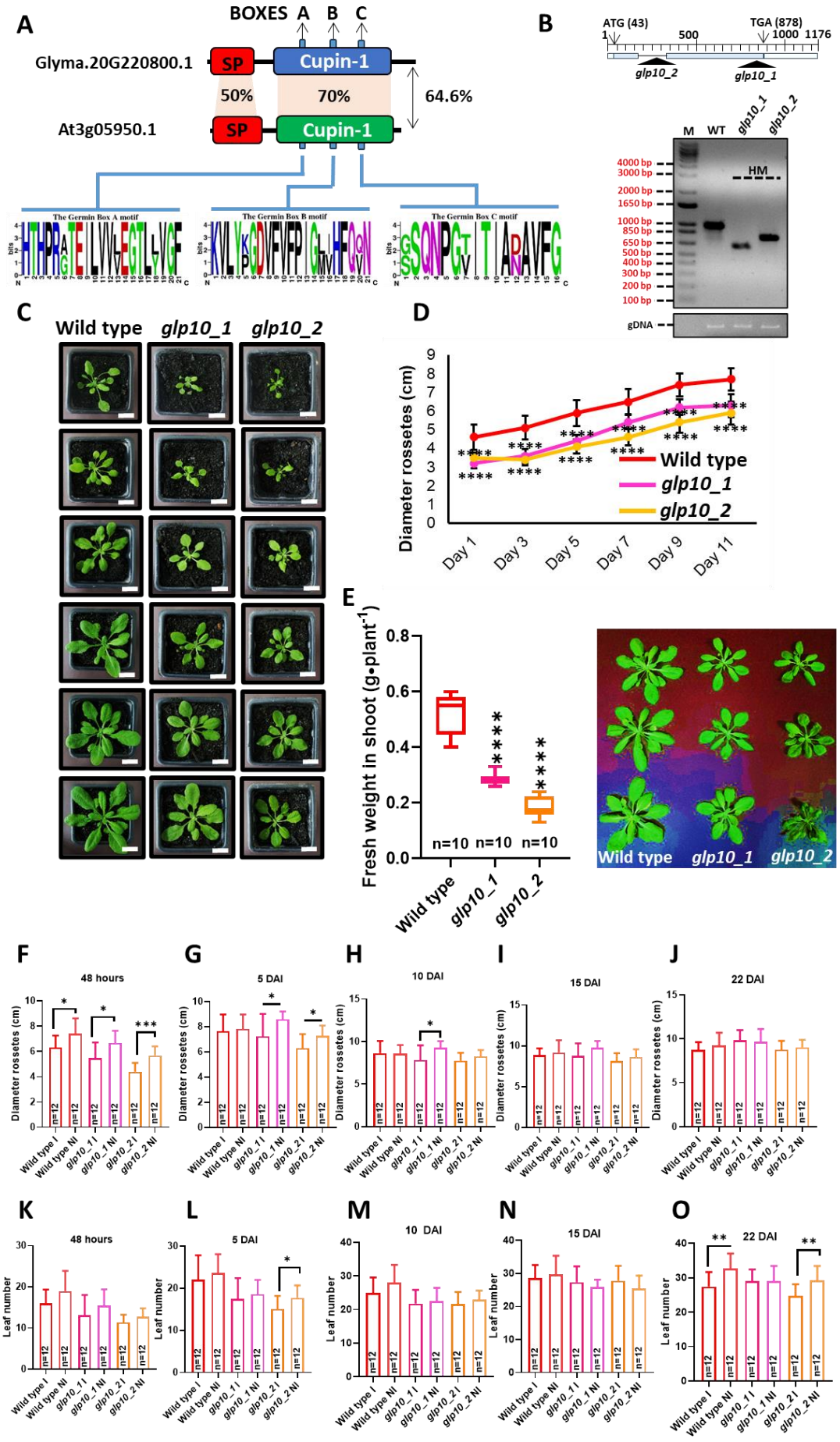
A
BOXES A B C
Glyma.20G220800.1
SP
Cupin-1
50%
70%
64.6%
At3g05950.1
SP
Cupin-1
The Germin Box A motif
The Germin Box B motif
The Germin Box C motif
B
ATG (43)
TGA (878)
1
500
1000
1176
glp10_2
glp10_1
M
WT
glp10_1
glp10_2
4000 bp
3000 bp
2000 bp
1650 bp
1000 bp
850 bp
650 bp
500 bp
400 bp
300 bp
200 bp
100 bp
HM
gDNA
C
Wild type
glp10_1
glp10_2
D
Diameter rossetes (cm)
Wild type
glp10_1
glp10_2
Day 1
Day 3
Day 5
Day 7
Day 9
Day 11
E
Fresh weight in shoot (g•plant-1)
n=10 n=10 n=10
Wild type
glp10_1
glp10_2
Wild type
glp10_1
glp10_2
F
48 hours
G
5 DAI
H
10 DAI
I
15 DAI
J
22 DAI
Diameter rossetes (cm)
n=12
Wild type I
Wild type NI
glp10_1 I
glp10_1 NI
glp10_2 I
glp10_2 NI
K
48 hours
L
5 DAI
M
10 DAI
N
15 DAI
O
22 DAI
Leaf number

Figure 7. Molecular characterization of *Arabidopsis thaliana glp10-/-* mutant lines. (**A**) *A. thaliana At3g05950.1* is a functional ortholog of soybean *GmGLP10* (*Glyma.20G220800.1*) and they share 64.6% of amino acid sequence identity, while their signal peptide (SP) and *Cupin_1* domain share 50 and 70% of identity, respectively. The germin boxes A, B and C are presented by WebLogo. (**B**) Structure of the *glp10* gene with the mutations studied in this work are indicated by *glp10_1* (SALK_038626) and *glp10_2* (SALK_062879). 5'- and 3'-UTR are indicated by white boxes, exons are indicated by blue boxes, and introns by black line. Homozygous *glp10-/-* plants for each knockout line were confirmed by PCR analysis. M, marker; WT, Wild type; gDNA, genomic DNA. (**C**) Phenotypic analysis of Arabidopsis *glp10-/-* mutant lines in different times points after germination (DAG). Scale bars: 3 cm. (**D**) Diameter rosettes measurements analysis at different DAGs. (**E**) Fresh weight measurements in shoots were analyzed at Day 11. Significant differences were analyzed by Student's test (n=10, ****P < 0.0001). Data are presented as means ± SD. (**F-J**) Diameter rosettes analysis in plants infected (I) and non-infected (NI) with *M. incognita* (race 3) at different times points. (**K-O**) Number of leaves analysis at different time points after *M. incognita* infection. In both cases were adopted the times points 48h, 5, 10, 15 and 22 DAI as intervals of analysis. Significant differences were analyzed by Student's test (n=12, *P < 0.02, **P < 0.006, ***P < 0.0002). Data are presented as means ± SD.

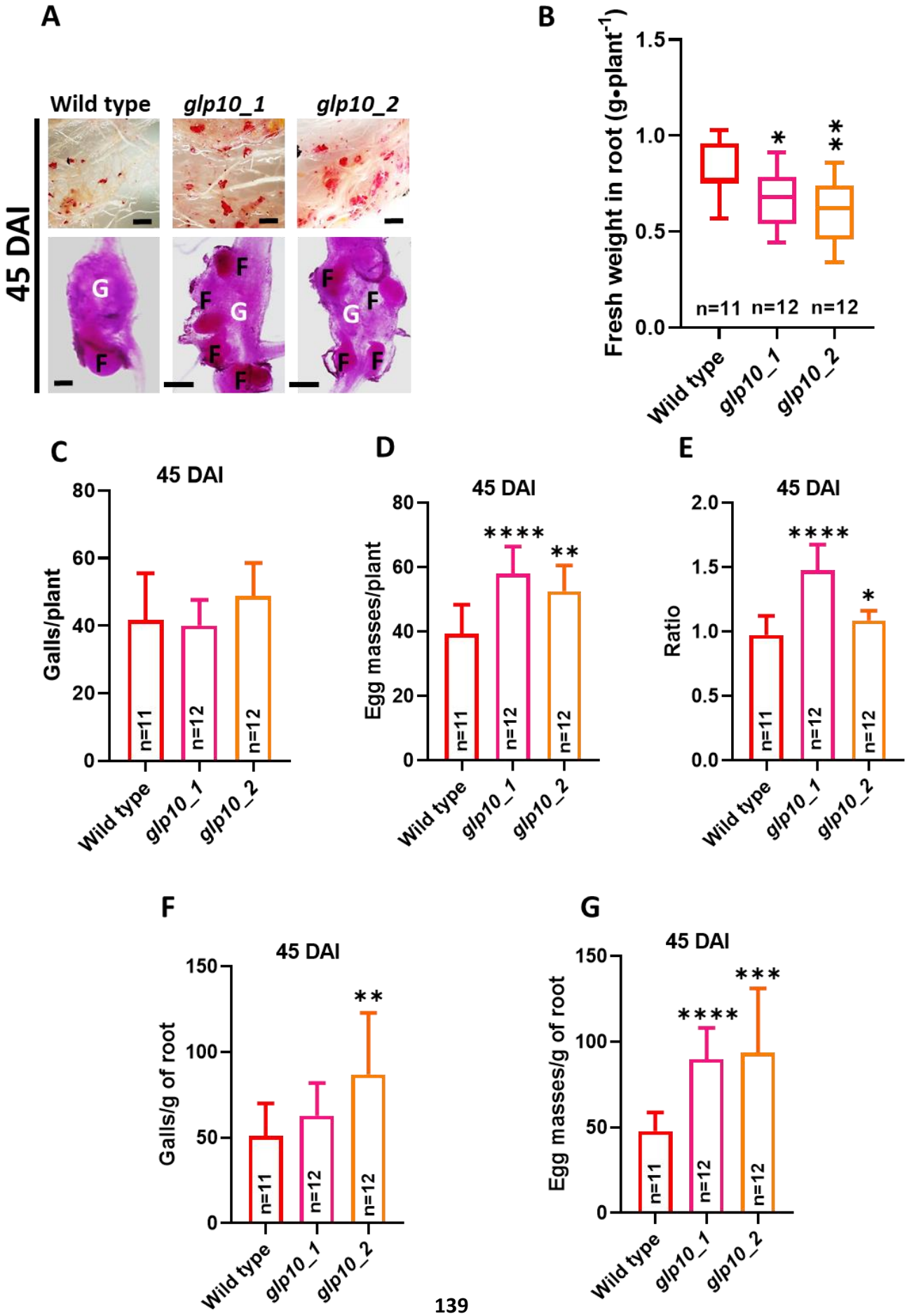
A
Wild type
glp10_1
glp10_2
45 DAI
G
F
B
Fresh weight in root (g•plant-1)
1.5
1.0
0.5
0.0
n=11 n=12 n=12
Wild type
glp10_1
glp10_2
C
45 DAI
Galls/plant
80
60
40
20
0
n=11
n=12
n=12
D
45 DAI
Egg masses/plant
****
**
E
45 DAI
Ratio
2.0
1.5
1.0
0.5
0.0
****
*
F
45 DAI
Galls/g of root
150
100
50
0
**
G
45 DAI
Egg masses/g of root
***
****

Figure 8. Arabidopsis *glp10-/-* mutant lines increase the susceptibility to *M. incognita*. (**A**) Acid fuchsin staining of galls at 45 DAI revealed multiple nematodes in a single root knot gall in mutant *glp10-/-* lines. Scale bars: 50 µm. (**B**) Fresh weight of infected roots. The parameters (**C**) galls/plant, (**D**) egg masses/plant, (**E**) Ratio (egg masses/plant), (**F**) galls (g root)$^{-1}$, and (**G**) egg masses (g root)$^{-1}$ were evaluated at 45 DAI. Significant differences were analyzed by Student's tests (n>10, *P < 0.05, **P < 0.01, ***P < 0.001, ****P < 0.0001). Data are presented as means ± SD. G, Galls; F, female nematodes.

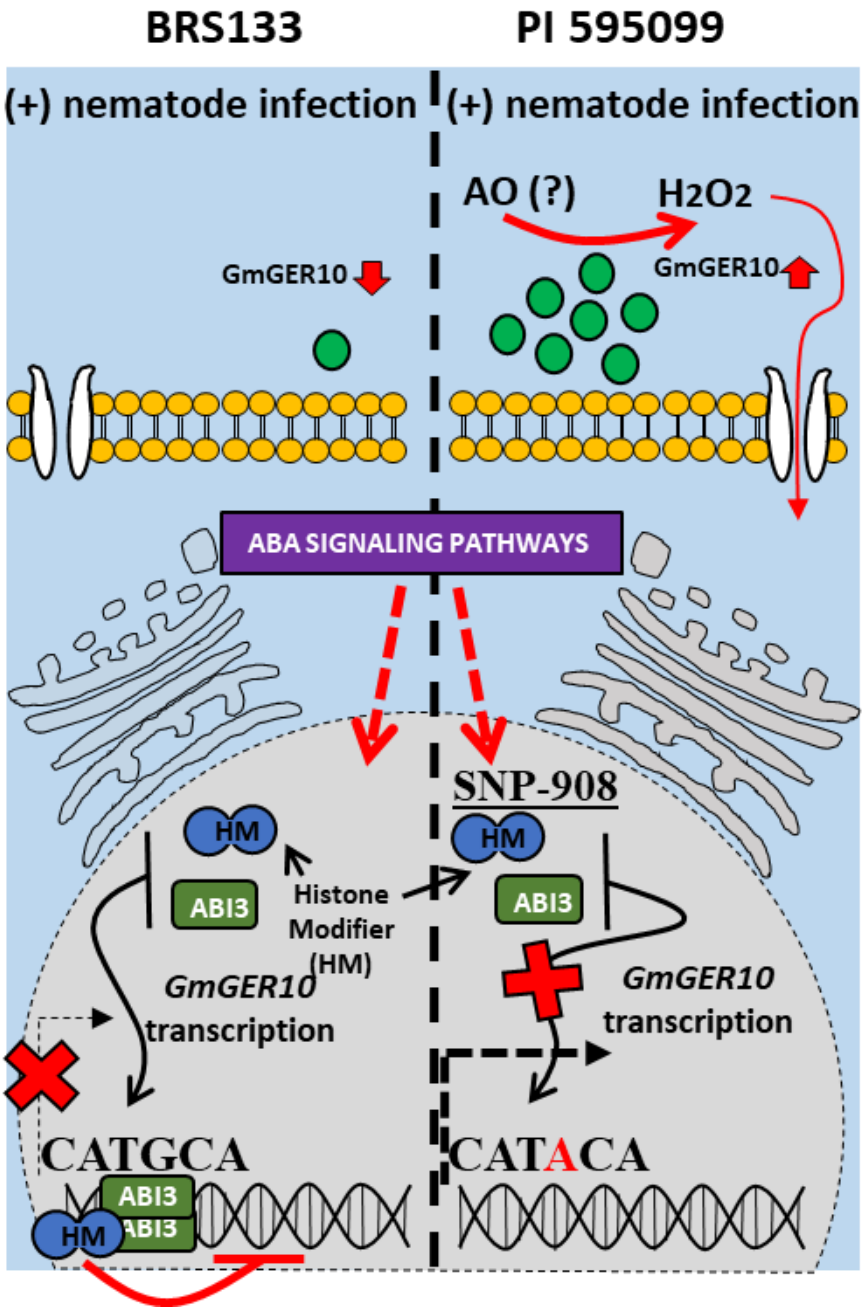

Figure 9: Model proposed to explain the difference of the *GmGLP10* expression between soybean genotypes (PI 595099 and BRS 133) based on the extinction of the RYREPEATBNNAPA (CATGCA) motif. Under *M. incognita* infection, the elevation of ABA mobilizes the transcription factor ABI3 to the nucleus, acting in the recognition of the CATGCA motif and repression of *GmGLP10* expression via deacetylating and/or methylating histones (HM) (Sengupta *et al.*, 2020). Through this indication, there is strong evidence that *GmGLP10* remains in an inactive transcriptional stage in the susceptible genotype, due to the new heterochromatin stage formed; while (SNP)-908, identified by the G908A exchange in the PI 595099 genotype, refers to a new resistance to the ABI3/HM module. Although these

indications provide circumstantial evidence of the negative role of the RYREPEATBNNAPA motif in the susceptible context, additional studies will be conducted in the BRS 133 cultivar in order to determine whether gene depletion of this motif can circumvent the repressive activity of the ABI3/HM module.

Supporting Information

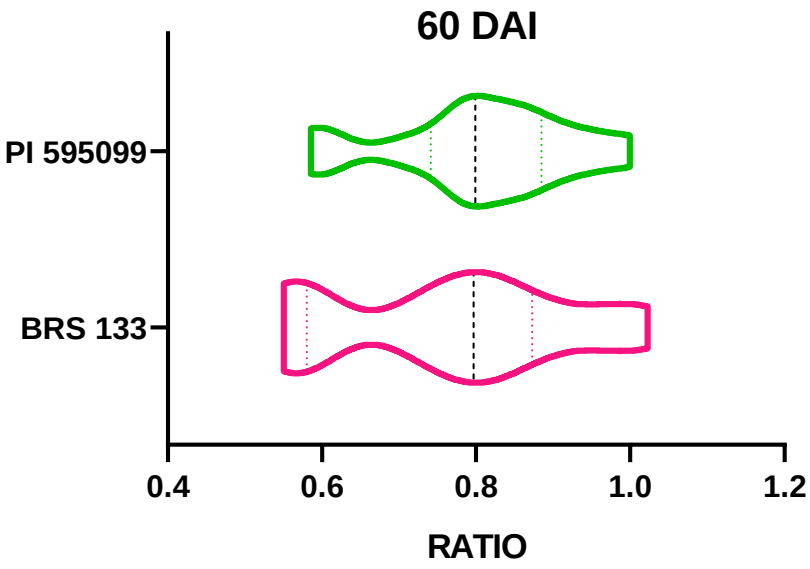

Fig. S1. The ratio (egg masses/galls) was determined according to the relation between egg masses/galls analyzed after 60 DAI. Data represent mean ± SD (n=13). Statistical differences are marked with *($P < 0.05$) based on Student's t-test analysis.

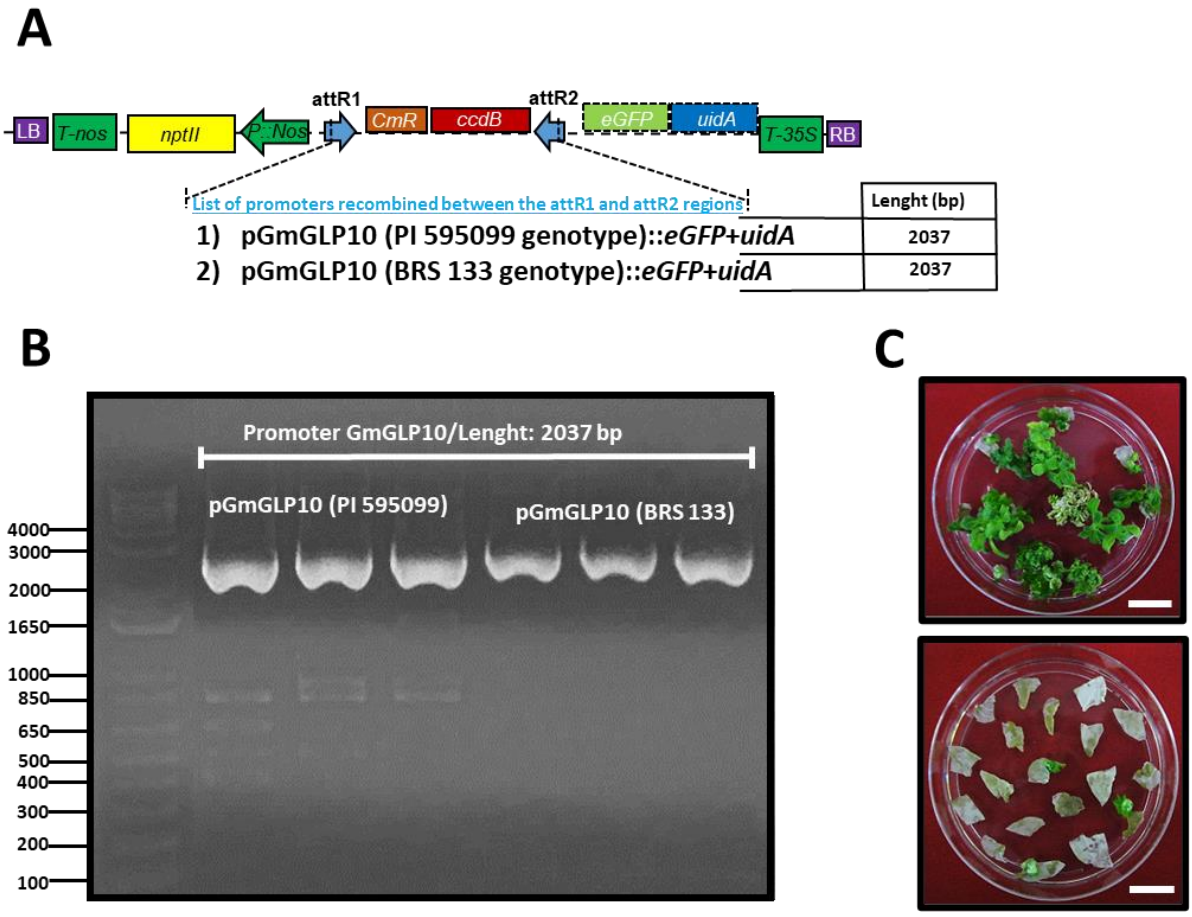

Fig. S2. Physical map used for cloning GmGLP10 promoters from soybean genotype and transformation of tobacco plants. (**A**) pKGWFS7 map used as destination vector for GmGLP10 promoters cloning. In this study, a -2.037-bp region upstream from the transcription initiation site was selected to examine GUS activity. (**B**) PCR fragments from soybean pGmGLP10 promoters isolated to cloning and sequencing by Sanger methods. (**C**) Transgenic tobacco explants generated by *A. tumefaciens*-mediated transformation previously transfected with recombinant pKGWFS7 plasmids. Scale bars: 2 cm.

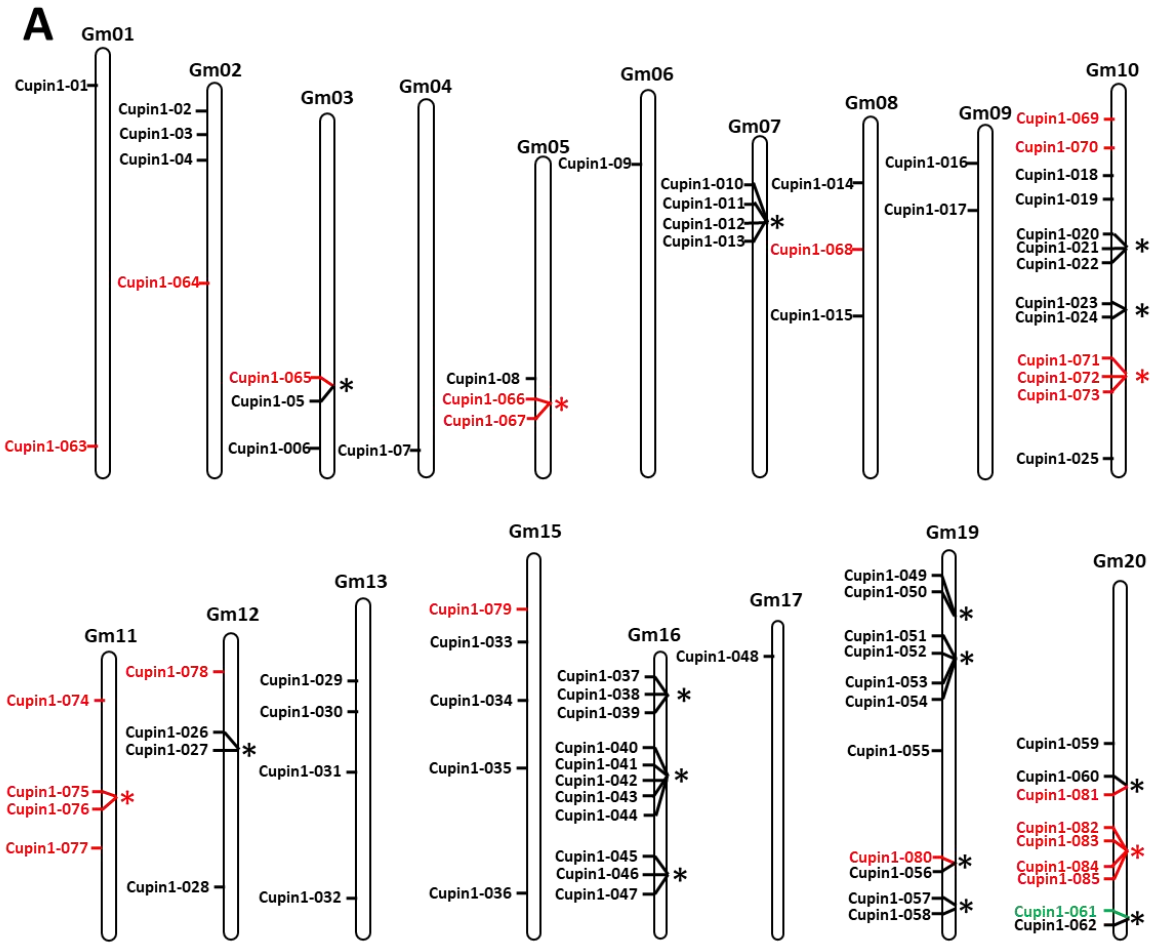
A
Gm01
Cupin1-01
Cupin1-063
Gm02
Cupin1-02
Cupin1-03
Cupin1-04
Cupin1-064
Gm03
Cupin1-065
Cupin1-05
Cupin1-006
Gm04
Cupin1-07
Gm05
Cupin1-08
Cupin1-066
Cupin1-067
Gm06
Cupin1-09
Gm07
Cupin1-010
Cupin1-011
Cupin1-012
Cupin1-013
Cupin1-014
Cupin1-068
Cupin1-015
Gm08
Cupin1-016
Cupin1-017
Gm09
Gm10
Cupin1-069
Cupin1-070
Cupin1-018
Cupin1-019
Cupin1-020
Cupin1-021
Cupin1-022
Cupin1-023
Cupin1-024
Cupin1-071
Cupin1-072
Cupin1-073
Cupin1-025
Gm11
Cupin1-074
Cupin1-075
Cupin1-076
Cupin1-077
Cupin1-078
Gm12
Cupin1-026
Cupin1-027
Cupin1-028
Gm13
Cupin1-029
Cupin1-030
Cupin1-031
Cupin1-032
Gm15
Cupin1-079
Cupin1-033
Cupin1-034
Cupin1-035
Cupin1-036
Gm16
Cupin1-037
Cupin1-038
Cupin1-039
Cupin1-040
Cupin1-041
Cupin1-042
Cupin1-043
Cupin1-044
Cupin1-045
Cupin1-046
Cupin1-047
Gm17
Cupin1-048
Gm19
Cupin1-049
Cupin1-050
Cupin1-051
Cupin1-052
Cupin1-053
Cupin1-054
Cupin1-055
Cupin1-080
Cupin1-056
Cupin1-057
Cupin1-058
Gm20
Cupin1-059
Cupin1-060
Cupin1-081
Cupin1-082
Cupin1-083
Cupin1-084
Cupin1-085
Cupin1-061
Cupin1-062
B
Tree scale: 1
bootstrap
0.2
0.4
0.6
0.8
1
I
II
III
IV
V
VI
VII
VIII
IX
X
XI
XII
XIII
XIV

Fig. S3. Graphical representation and phylogenetic reconstruction of soybean GmGLP superfamily. (**A**) Graphical representation of the location for the GmGLP superfamily on the soybean chromosomes. Only *GmGLP10* containing the *Cupin_1* domain (code: IPR006045) is predicted in this analysis. The new identified *GmGLP* genes are in red, while the previously described *GmGLP* by Wang *et al.*, 2014 are indicated in black. The *GmGLP10* (Cupin1-061), used in this study is located in chromosome Gm20 and is represent in green color. The asterisks indicate tandem duplicated genes. (**B**) All GmGLP amino acid sequences from the soybean genome were used to perform the phylogenetic analysis by using the Maximum Likelihood method and JTT matrix-based model (Jones *et al.*, 1992). The final *GmGLP* phylogenetic tree conducted in MEGA X and curated using the online tool Interactive Tree Of Life – iTOL was grouped into 14 groups in view of previously function described for some members in literature. The bootstrap values are indicated by blue circles (minimum 70).

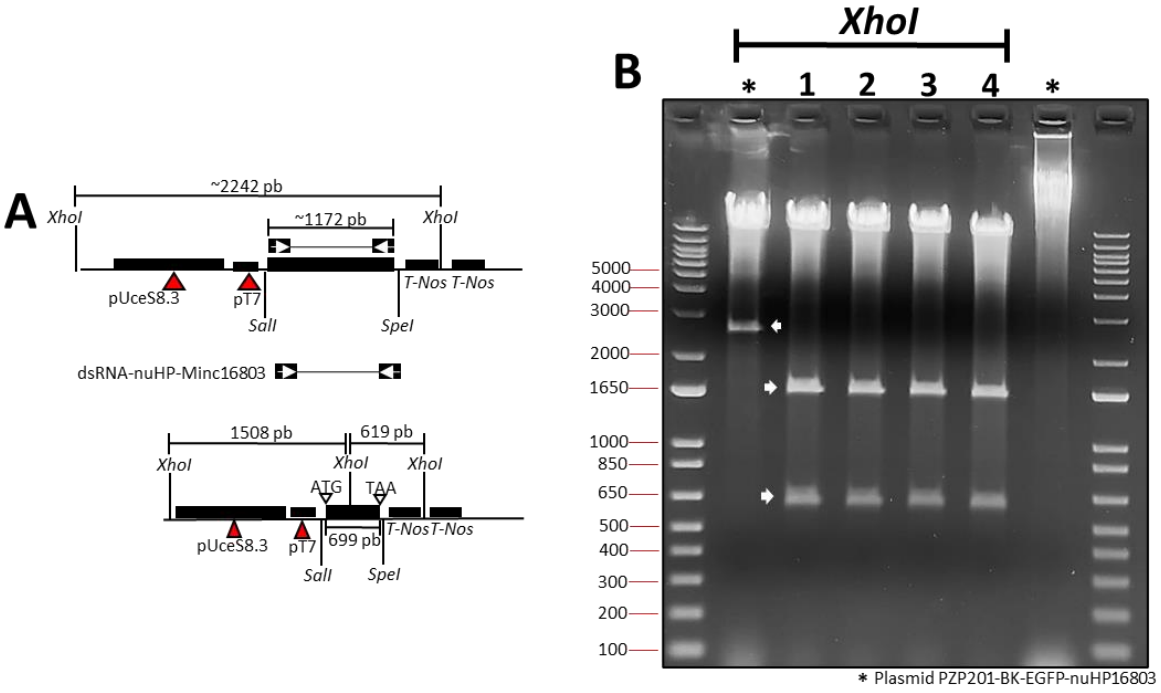
A
~2242 pb
XhoI
~1172 pb
XhoI
pUceS8.3
pT7
T-Nos T-Nos
SalI
SpeI
dsRNA-nuHP-Minc16803
1508 pb
619 pb
XhoI
XhoI
XhoI
ATG
TAA
pUceS8.3
pT7
699 pb
T-NosT-Nos
SalI
SpeI
B
XhoI
* 1 2 3 4 *
5000
4000
3000
2000
1650
1000
850
650
500
400
300
200
100
* Plasmid PZP201-BK-EGFP-nuHP16803

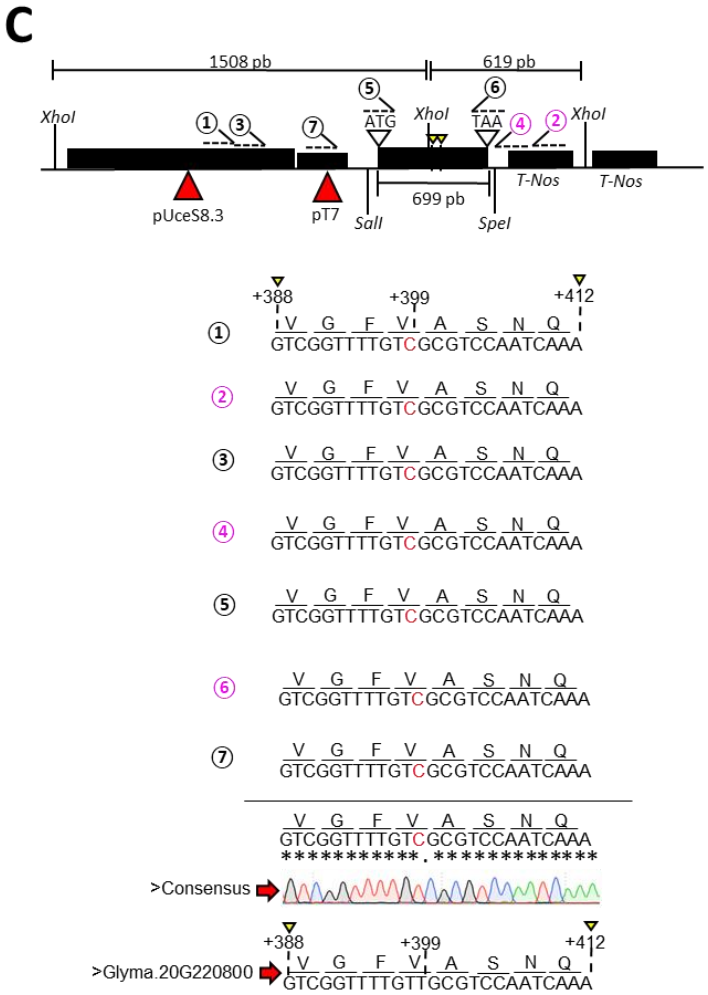
C
1508 pb
619 pb
XhoI
ATG
XhoI
TAA
XhoI
T-Nos
T-Nos
pUceS8.3
pT7
699 pb
SalI
SpeI
+388
+399
+412
① V G F V A S N Q GTCGGTTTTGTCGCGTCCAATCAAA
② V G F V A S N Q GTCGGTTTTGTCGCGTCCAATCAAA
③ V G F V A S N Q GTCGGTTTTGTCGCGTCCAATCAAA
④ V G F V A S N Q GTCGGTTTTGTCGCGTCCAATCAAA
⑤ V G F V A S N Q GTCGGTTTTGTCGCGTCCAATCAAA
⑥ V G F V A S N Q GTCGGTTTTGTCGCGTCCAATCAAA
⑦ V G F V A S N Q GTCGGTTTTGTCGCGTCCAATCAAA
V G F V A S N Q
GTCGGTTTTGTCGCGTCCAATCAAA
**********.**********
>Consensus
+388
+399
+412
>Glyma.20G220800
V G F V A S N Q
GTCGGTTTTGTTGCGTCCAATCAAA

2997

Fig. S4. Cloning and sequencing of expression cassettes aiming *GmGLP10*^{OE} ectopic expression in GCs. (**A**) Statistically significant values of log2(FC; fold-change) given by differential *GmGLP10* expression levels at transcriptome and proteomes analysis performed in soybean genotype PI 595099 (Arraes *et al.*, 2022). (**B**) Physical maps of the expression cassettes used in this study to ectopic expression of *GmGLP10* under *pUceS8.3* soybean promoter (Moreira *et al.*, 2023). The *dsRNA-nuHP-Minc16803* transgene from PZP201-BK-EGFP-nuHP16803 vector was replaced by *GmGLP10* using *SalI* and *SpeI* enzymes. (**C**) Confirmation of *GmGLP10* cloning into PZP201-BK-EGFP-nuHP16803 plasmids using *XhoI* restriction enzymes. The cleavage DNA products (white arrows) is consistent with the three *XhoI* sites presents inside and outside of *GmGLP10* DNA sequences. (**D**) The *GmGLP10* cloning was confirmed by Sanger sequencing. A single synonymous mutation was found, but it was irrelevant for amino acid exchange.

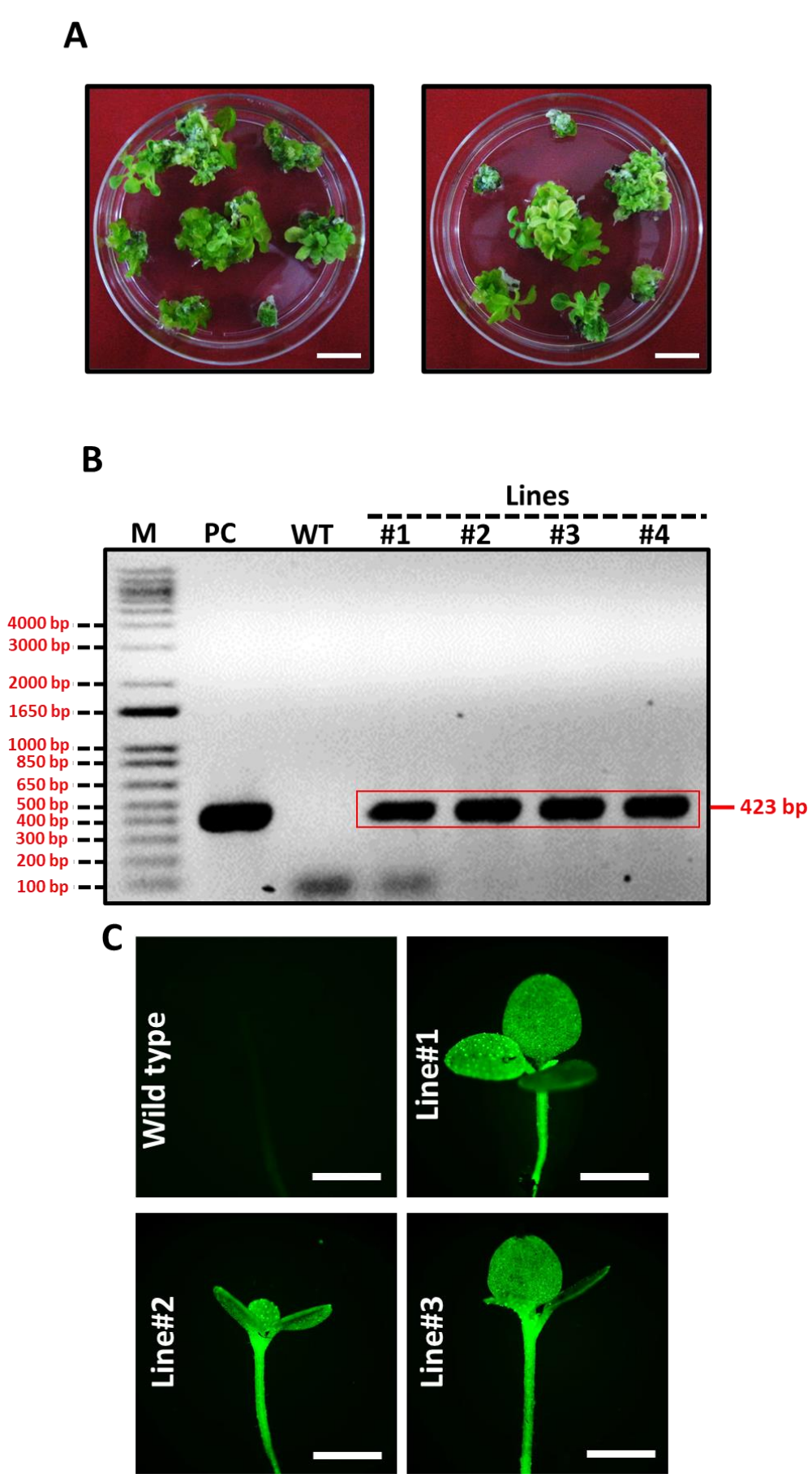
A
B
Lines
M
PC
WT
#1
#2
#3
#4
4000 bp
3000 bp
2000 bp
1650 bp
1000 bp
850 bp
650 bp
500 bp
400 bp
300 bp
200 bp
100 bp
423 bp
C
Wild type
Line#1
Line#2
Line#3

Fig. S5. Generation of transgenic tobacco plants overexpressing *GmGLP10^{OE}*. (**A**) Regeneration of primary hygromycin-resistant explants lines transformed by *A. tumefaciens* previously transfected with pPZP201-BK-EGFP-GmGLP10 generated in this study. Scale bars: 2 cm. (**B**) PCR analysis from four independent transgenic lines (T0). Primers were designed to *eGFP* target whose expected amplicon size is 423 bp. The transgenics lines#1, #2 and #3 were used in this study. (**C**) T4 transgenic seedlings expressing eGFP under a stereo fluorescence macroscope (Leica, Wetzlar, Germany). Scale bars: 1 cm. M, marker; PC, positive control (pPZP201-BK-EGFP-GmGLP10 – 50ng/µL); WT, Wild-type (Negative control).

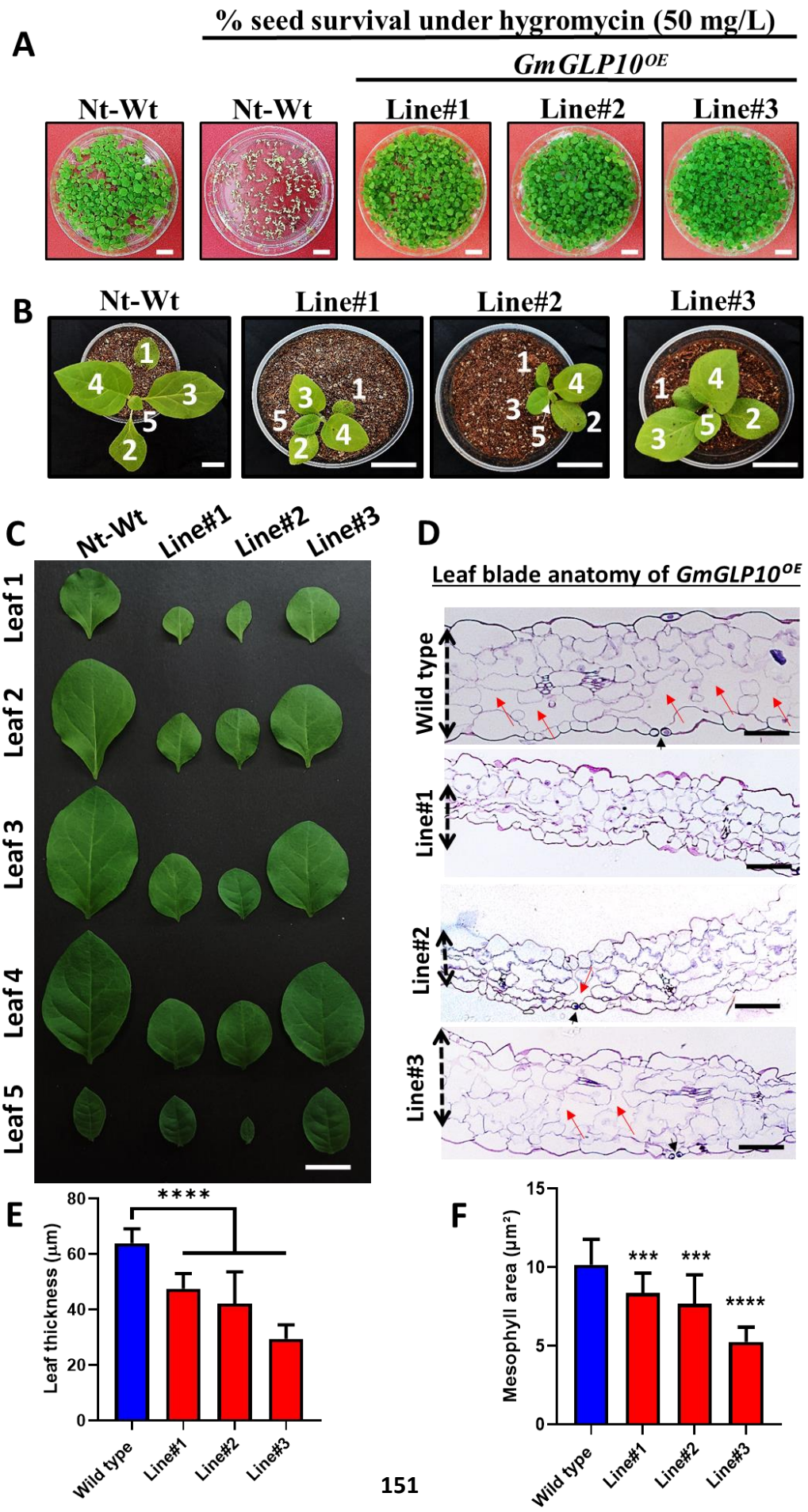
A
% seed survival under hygromycin (50 mg/L)
GmGLP10OE
Nt-Wt
Nt-Wt
Line#1
Line#2
Line#3
B
Nt-Wt
Line#1
Line#2
Line#3
C
Nt-Wt
Line#1
Line#2
Line#3
Leaf 1
Leaf 2
Leaf 3
Leaf 4
Leaf 5
D
Leaf blade anatomy of GmGLP10OE
Wild type
Line#1
Line#2
Line#3
E
Leaf thickness (µm)
****
Wild type
Line#1
Line#2
Line#3
F
Mesophyll area (µm²)
***
***
****
Wild type
Line#1
Line#2
Line#3

Fig. S6. Generation of transgenic tobacco plants overexpressing *GmGLP10^{OE}*. (**A**) Seed assays to confirm transgenic tobacco plants. T4 transgenic *GmGLP10^{OE}* tobacco and Wild-type (Wt) seeds were germinated under synthetic medium supplemented with hygromycin antibiotics (50 mg/L). Scale bars: 2 cm. (**B**) Phenotypes of soil-grown transgenic tobacco lines after 2 weeks in greenhouse. Consecutive numbers on tobacco leaves (from the bottom to the top of the plant) represent measurement points for morphological analyses. Scale bars: 5 cm. (**C**) Tobacco leaves phenotype from transgenic *GmGLP10^{OE}* plants and Wild-type control. Scale bars: 2 cm. (**D**) Anatomical structure of the leaf blade from transgenic *GmGLP10^{OE}* tobacco (Line#1, #2 and #3) and Wild type. The upper and lower epidermis and the mesophyll region were apparently disorganized, containing restricted aerenchyma tissue in a small volume. Red arrows and Blak arrows represent aerenchyma tissue and stomata, respectively. Scale bars: 50 µm. (**E**) Leaf thickness and (**F**) Mesophyll area measurements. Data represent mean ± SD (n=16). Statistical differences are marked with ****($P < 0.0001$) based on Student's t-test analysis.

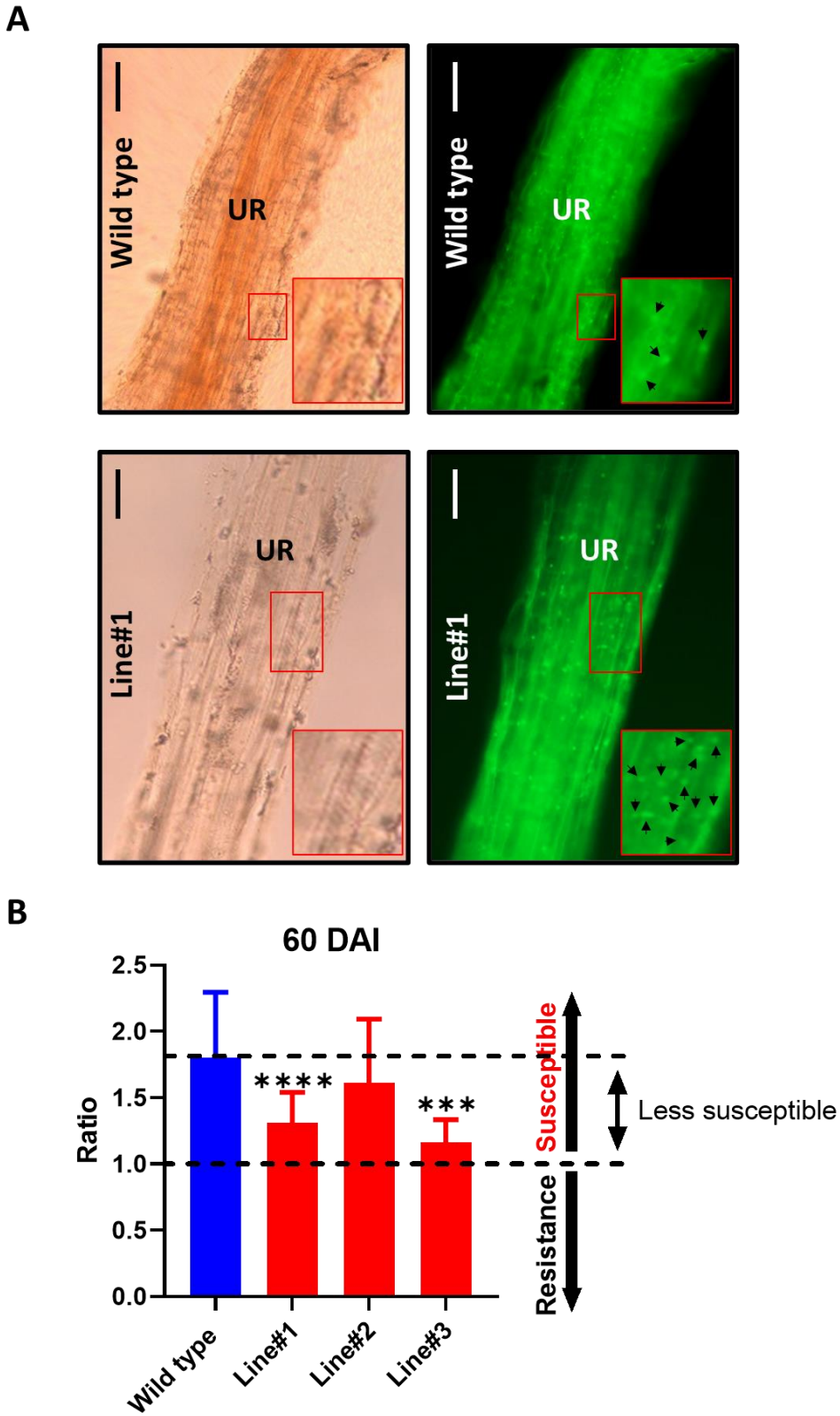

Fig. S7. Control BABB analysis in Uninfected roots (URs) and examination of infection test by ratio (egg masses/galls). (**A**) Whole cleared URs from Wild-type and transgenic *GmGLP10*^{OE} tobacco (Line#1). Red line on images is magnified to show nuclei (black arrows). Scale bars: 50 µm. (**B**) Ratio (egg masses/plant). In sum, Ratio > 1 denotes more than one egg

masses per *M. incognita*-induced galls, while Ratio < 1 indicate that the nematodes fail in their ability to develop in adult females and reproduction. Compared with Wild-type control (R = 1.8), Line#1 (R = 1.3) and Line#3 (R = 1.1) are less susceptible, while no difference was obtained by Line#2 (R = 1.6). Data represent mean ± SD (n=16). Statistical differences are marked with ****($P < 0.0001$ and $n>13$) based on Student's t-test analysis.

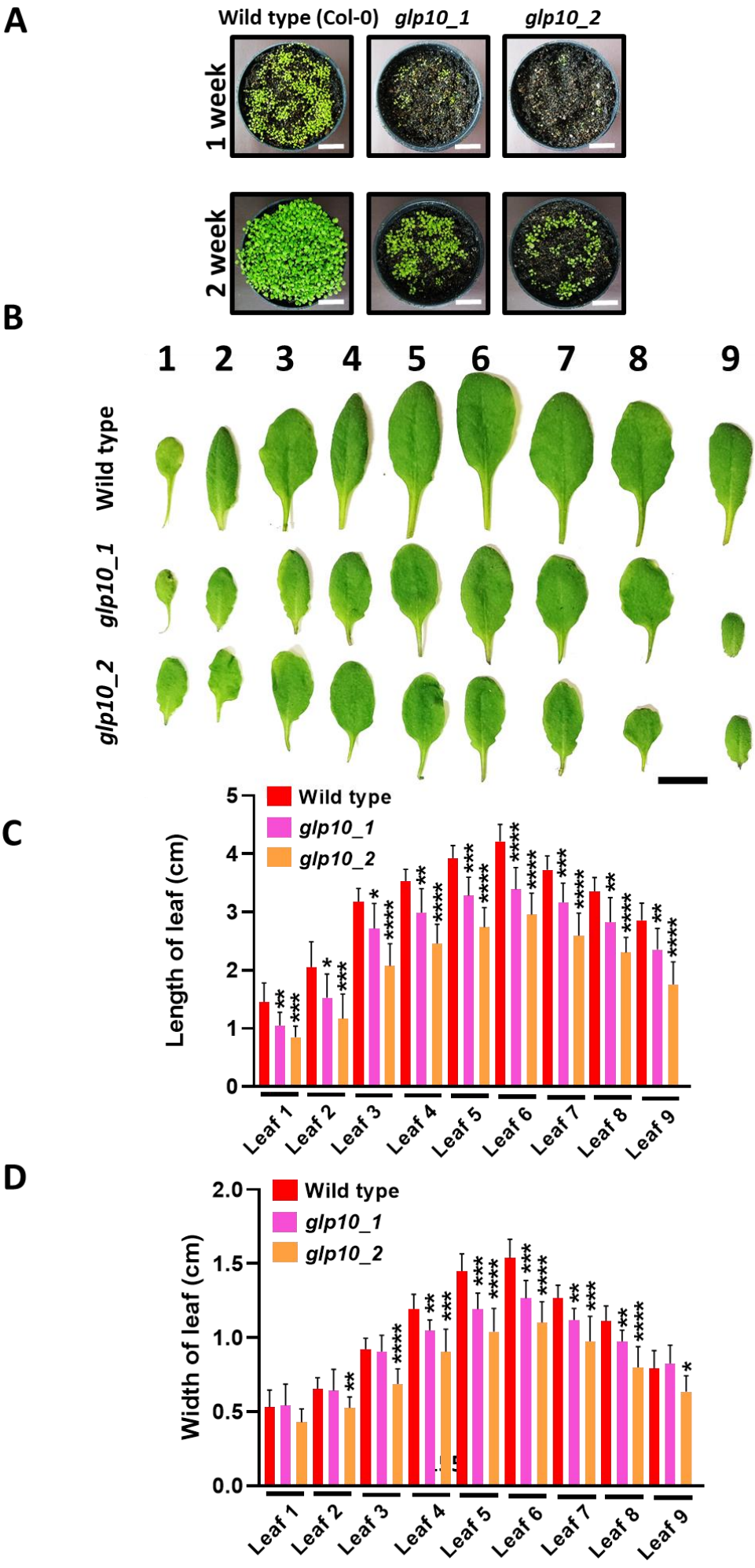
A
Wild type (Col-0)
glp10_1
glp10_2
1 week
2 week
B
1
2
3
4
5
6
7
8
9
Wild type
glp10_1
glp10_2
C
Length of leaf (cm)
Wild type
glp10_1
glp10_2
Leaf 1
Leaf 2
Leaf 3
Leaf 4
Leaf 5
Leaf 6
Leaf 7
Leaf 8
Leaf 9
D
Width of leaf (cm)
Wild type
glp10_1
glp10_2
Leaf 1
Leaf 2
Leaf 3
Leaf 4
Leaf 5
Leaf 6
Leaf 7
Leaf 8
Leaf 9

Fig. S8. Germination and above-ground Arabidopsis growth is compromised in the *glp10-/-* mutants. (**A**) Wild-type (Col-0) and HM *glp10-/-* Arabidopsis seeds were germinated in soils and representative germinated seedlings images presented show a delay in *glp10-/-* mutants development compared with control. Representative photos were taken at 1 and 2 weeks after germination. Scale bars: 2 cm. (**B**) Rosette leaves of 3-week-old of *A. thaliana* plants grown in grown-chamber at 16-h-light/8-h-dark photoperiod at 21°C. Scale bars: 0.5 cm. (**C**) Length of leaf and (**D**) Width of leaf measurements. In total was used 9 plants per genotype. Data represent mean ± SD (n=9). Statistical differences are marked with ****($P < 0.0001$ and $n>13$) based on Student's t-test analysis. Experiment was performed once.

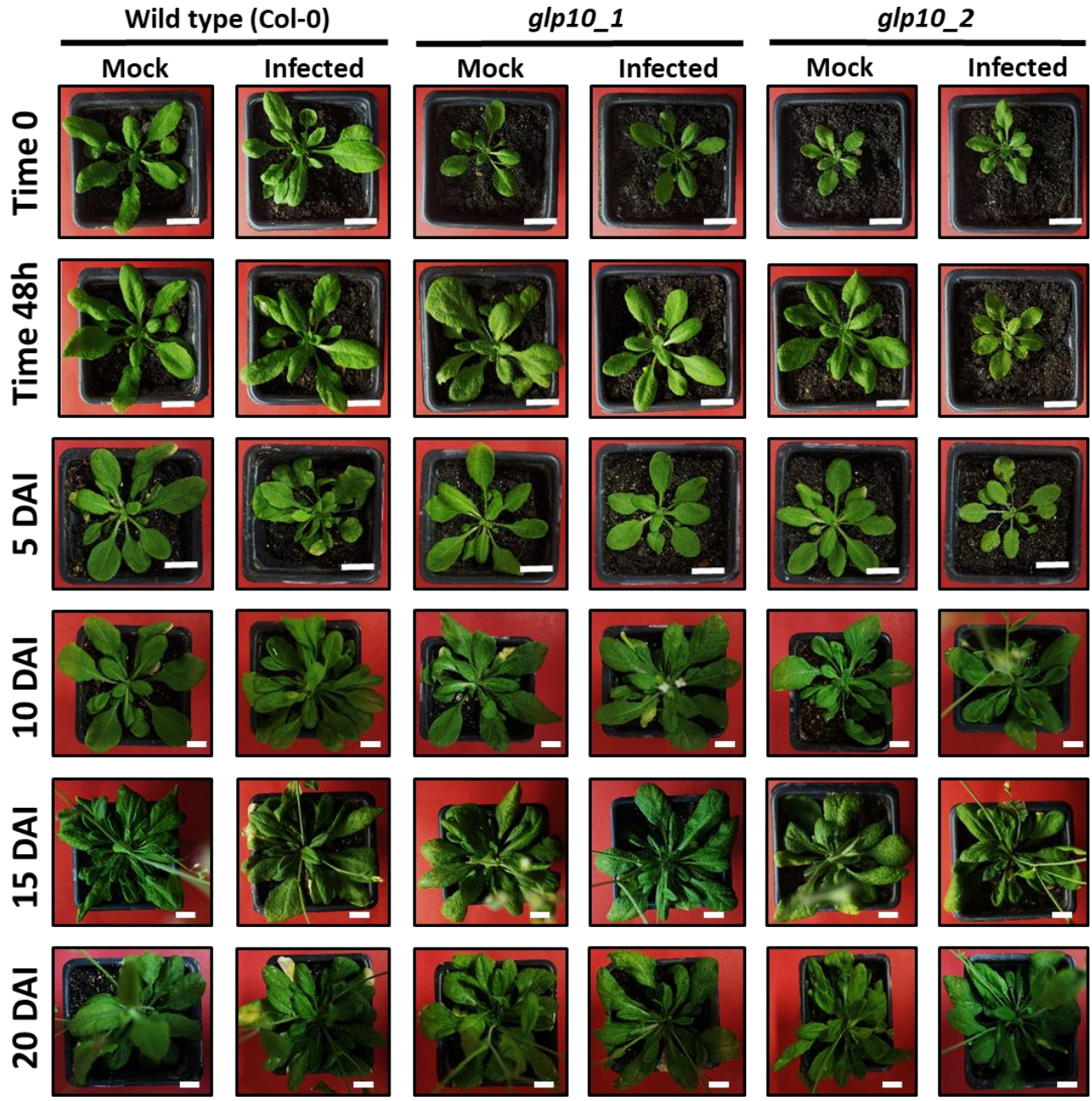

Fig. S9. Phenotypical characterization of HM *glp10-/-* mutant lines under *M. incognita* infections at different times points. The plants were infected with *M. incognita* (Time 0) and the diameter rosettes and number of leaves parameters evaluated in 0, 48h, 5, 10, 15 and 22 DAI. Each treatment was subdivided in two subgroups (Mock and Infected) containing n=12 plants. 10 DAI was considered the onset of the reproductive stage in view of the precocious inflorescence's emergence. Scale bars: 3 cm.

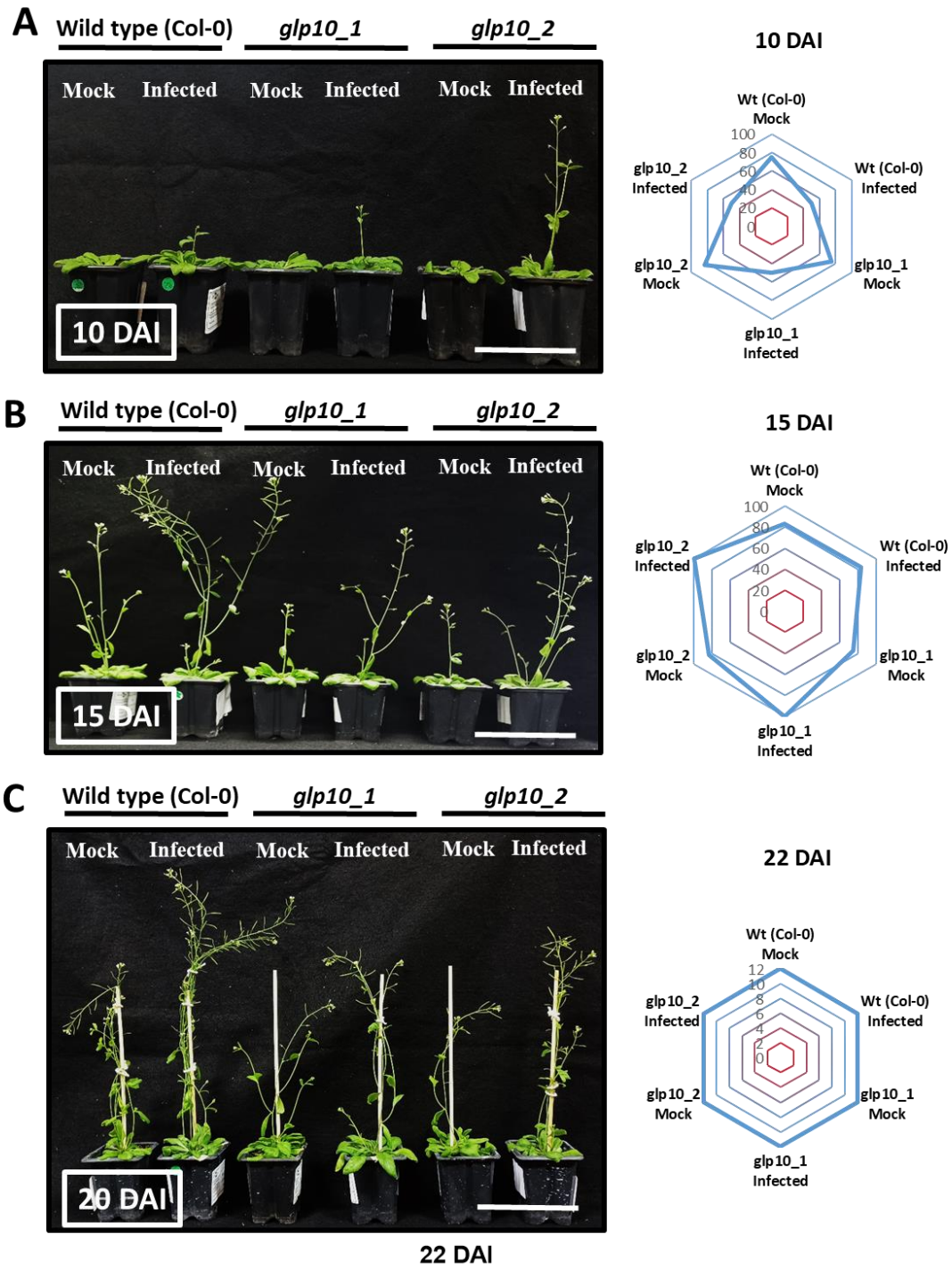
A
Wild type (Col-0)
glp10_1
glp10_2
Mock
Infected
Mock
Infected
Mock
Infected
10 DAI
10 DAI
Wt (Col-0) Mock
Wt (Col-0) Infected
glp10_1 Mock
glp10_1 Infected
glp10_2 Mock
glp10_2 Infected
100
80
60
40
20
0
B
Wild type (Col-0)
glp10_1
glp10_2
Mock
Infected
Mock
Infected
Mock
Infected
15 DAI
15 DAI
Wt (Col-0) Mock
Wt (Col-0) Infected
glp10_1 Mock
glp10_1 Infected
glp10_2 Mock
glp10_2 Infected
100
80
60
40
20
0
C
Wild type (Col-0)
glp10_1
glp10_2
Mock
Infected
Mock
Infected
Mock
Infected
20 DAI
22 DAI
Wt (Col-0) Mock
Wt (Col-0) Infected
glp10_1 Mock
glp10_1 Infected
glp10_2 Mock
glp10_2 Infected
12
10
8
6
4
2
0
D
Plant height (cm)
40
30
20
10
0
n=10
n=10
n=12
n=10
n=12
n=10
*
Wild type I
Wild type NI
ger_1 I
ger_1 NI
ger_2 I
ger_2 NI

Fig. S10. The effect of root stress and plant height. The emerged tassels were accounted in (**A**) 10 DAI, (**B**) 15 DAI and (**C**) 22 DAI and the data presents in radar plot (blue lines). No direct correlation was found between plants infected with *M. incognita* and the reproductive stage advances (hallmarked by the inflorescence's emergence). Scale bars: 8 cm. (**D**) Plant height measurements. All treatments and subgroups (I, infected and NI, non-infected) was cultivated in a growth chamber with standard settings and measured at 22 DAI. Statistical analysis was examined by Student's tests. The asterisks above each bar indicate the significative (*$P \leq 0.05$ and $n>10$). All results are present as means ± standard deviation.

3177 # Tables

Table S1: Complete inventory of the GmGER superfamily in soybean genomes.

	Glyma v11.0	Name	Length	Cupin 1-domain	TM	SP	Molecular weight (kDa)	pI
1	Glyma01g38340.2	GLP070	614	239 - 394	---------	1 to 22	71.74	5.42
2	Glyma01g04450.1	GLP001	220	63 - 212	---------	1 to 25	23.6	8.49
3	Glyma02g16440.1	GLP071	506	116 - 275 and 316 - 480	---------	1 to 43	57.81	6.16
4	Glyma02g03100.1	GLP002	220	63 - 212	---------	1 to 25	23.7	8.88
5	Glyma02g05010.1	GLP003	205	54 - 196	5 to 27	1 to 26	22.3	8.81
6	Glyma02g01085.1	GLP004	147	14 - 136	---------	---------	15.79	6.26
7	Glyma03g38630.1	GLP005	218	59 - 208	---------	1 to 21	22.84	9.06
8	Glyma03g32030.1	GLP006	495	36 - 241 and 323 - 472	---------	1 to 19	55.70	5.89
9	Glyma03g32020.3	GLP072	390	33 - 238 and 324 - 385	---------	1 to 18	44.17	5.33
10	Glyma04g39040.2	GLP007	199	52 - 175	---------	1 to 29	22.43	8.67
11	Glyma05g30300.1	GLP073	381	26 - 182 and 215 - 364	---------	---------	41.33	5.23
12	Glyma05g30290.1	GLP074	358	3 - 159 and 192 - 341	---------	---------	38.87	5.22
13	Glyma05g25620.1	GLP008	215	59 - 209	---------	1 to 21	23.03	6.27
14	Glyma06g15930.1	GLP009	228	76 - 206	---------	1 to 27	24.84	7.05
15	Glyma07g04310.1	GLP010	209	53 - 199	---------	1 to 18	22.01	6.57
16	Glyma07g04320.1	GLP011	208	54 - 198	---------	1 to 19	21.61	9.15
17	Glyma07g04330.1	GLP012	208	54 - 198	---------	1 to 19	21.93	6.95
18	Glyma07g04340.1	GLP013	225	71 - 215	21 to 38	1 to 20	23.85	8.55
19	Glyma07g04400.1	GLP014	208	54 - 198	---------	1 to 19	21.93	6.95
20	Glyma08g13440.1	GLP075	361	3 - 161 and 196 - 343	---------	---------	39.01	5.12
21	Glyma08g08600.1	GLP015	215	59 - 209	---------	1 to 20	22.84	7.05
22	Glyma08g24320.1	GLP016	211	65 - 202	---------	1 to 18	23.25	5.90
23	Glyma09g03010.1	GLP017	217	60 - 210	---------	1 to 21	22.98	6.02
24	Glyma09g08030.1	GLP018	135	73 - 121	4 to 26	1 to 20	15.30	10.71
25	Glyma10g28190.1	GLP019	223	65 - 213	---------	1 to 26	23.58	9.42
26	Glyma10g28020.1	GLP020	220	61 - 209	---------	1 to 22	23.20	8.32
27	Glyma10g28010.1	GLP021	221	62 - 210	7 to 24	1 to 23	23.38	7.64
28	Glyma10g04280.1	GLP076	563	37 - 250 and 391 - 537	---------	1 to 23	63.79	5.17
29	Glyma10g31200.2	GLP022	198	61 - 187	2 to 21	1 to 20	21.61	5.84
30	Glyma10g31210.1	GLP023	232	62 - 215	---------	1 to 20	24.98	6.89
31	Glyma10g11935.1	GLP024	125	1 - 113	15 to 34	---------	13.60	6.25
32	Glyma10g39170.1	GLP077	584	193 - 351 and 399 - 555	5 to 27	1 to 26	68.20	5.94
33	Glyma10g39150.1	GLP078	621	212 - 370 and 422 - 583	7 to 29	1 to 24	72.22	5.50
34	Glyma10g39161.1	GLP079	337	33 - 165	7 to 24	1 to 26	38.89	8.40
35	Glyma10g08360.1	GLP025	226	68 - 214	---------	1 to 23	24.68	7.06
36	Glyma10g03390.1	GLP080	504	110 - 271 and 312 - 478	7 to 26	1 to 26	57.99	6.08
37	Glyma10g42611.1	GLP026	177	55 - 168	5 to 22	1 to 20	19.05	7.71
38	Glyma11g07020.1	GLP081	696	240 - 395	7 to 24	1 to 23	81.76	5.32
39	Glyma11g15870.1	GLP082	476	40 - 194 and 279 - 429	7 to 26	1 to 24	52.91	5.73
40	Glyma11g15360.1	GLP083	356	3 - 157 and 195 - 339	---------	---------	38.37	5.53
41	Glyma11g15290.1	GLP084	356	3 - 157 and 195 - 339	---------	---------	38.43	5.68
42	Glyma12g31110.1	GLP027	207	56 - 197	---------	1 to 24	22.20	5.72

43	Glyma12g09760.2	GLP028	207	53 - 199	7 to 25	1 to 25	21.94	6.90
44	Glyma12g09630.2	GLP029	207	53 - 199	7 to 25	1 to 25	21.94	6.90
45	Glyma12g09640.2	GLP030	212	67 - 204	5 to 27	1 to 27	23.02	6.96
46	Glyma12g07180.1	GLP085	356	3 - 157 and 195 - 339	---------	---------	38.30	5.31
47	Glyma13g16960.2	GLP031	199	45 - 189	---------	---------	20.73	8.60
48	Glyma13g22050.1	GLP032	226	68 - 214	---------	1 to 23	24.40	6.05
49	Glyma13g40360.1	GLP033	483	43 - 197 and 289 - 438	---------	1 to 23	54.58	5.98
50	Glyma13g18450.2	GLP034	491	38 - 249 and 357 - 491	---------	1 to 24	55.37	5.46
51	Glyma15g05040.2	GLP035	351	176 - 327	---------	---------	39.62	5.38
52	Glyma15g19510.1	GLP036	213	57 - 203	---------	1 to 22	22.24	6.03
53	Glyma15g04710.1	GLP086	356	3 - 157 and 195 - 339	---------	---------	38.31	5.82
54	Glyma15g35130.1	GLP037	231	65 - 201	---------	1 to 18	25.67	5.54
55	Glyma15g13960.1	GLP038	215	59 - 209	---------	1 to 20	22.87	6.02
56	Glyma16g00980.1	GLP039	209	53 - 199	---------	1 to 18	21.91	7.01
57	Glyma16g00990.1	GLP040	181	27 - 171	---------	1 to 19	19.18	7.90
58	Glyma16g07580.1	GLP041	214	57 - 204	---------	1 to 22	22.95	5.58
59	Glyma16g07560.2	GLP042	188	31 - 178	---------	---------	20.10	5.02
60	Glyma16g07550.1	GLP043	210	56 - 200	---------	1 to 21	22.59	9.17
61	Glyma16g01000.1	GLP044	206	52 - 196	---------	1 to 17	21.97	6.49
62	Glyma16g06520.1	GLP045	221	58 - 209	---------	1 to 20	23.94	6.90
63	Glyma16g06530.1	GLP046	220	60 - 209	---------	1 to 20	23.78	6.41
64	Glyma16g06500.1	GLP047	221	57 - 209	---------	1 to 20	23.99	6.90
65	Glyma16g06630.1	GLP048	221	59 - 210	---------	1 to 20	24.03	8.82
66	Glyma16g06640.1	GLP049	215	59 - 209	---------	1 to 20	23.45	6.83
67	Glyma17g05760.1	GLP050	208	52 - 198	---------	1 to 17	21.32	8.53
68	Glyma19g27580.1	GLP051	212	58 - 209	---------	1 to 20	22.78	6.50
69	Glyma19g34770.2	GLP087	536	36 - 220 and 360 - 509	---------	1 to 21	60.48	6.49
70	Glyma19g34780.1	GLP052	481	36 - 240 and 309 - 458	---------	1 to 19	54.24	5.73
71	Glyma19g09370.2	GLP053	181	49 - 169	---------	1 to 20	19.84	8.49
72	Glyma19g09990.1	GLP054	221	58 - 209	---------	1 to 20	23.99	6.90
73	Glyma19g09810.1	GLP055	221	58 - 209	---------	1 to 20	23.99	6.90
74	Glyma19g09830.1	GLP056	221	58 - 209	---------	1 to 20	23.99	6.90
75	Glyma19g09840.1	GLP057	221	58 - 209	---------	1 to 20	23.99	6.90
76	Glyma19g09860.1	GLP058	221	58 - 209	---------	1 to 20	23.99	6.90
77	Glyma19g24840.1	GLP059	212	50 - 201	---------	1 to 19	22.86	5.49
78	Glyma19g24850.1	GLP060	221	58 - 209	---------	1 to 20	23.98	6.90
79	Glyma19g24870.2	GLP061	221	58 - 209	---------	1 to 20	23.95	6.90
80	Glyma19g24910.1	GLP062	219	59 - 208	---------	1 to 19	23.64	5.76
81	Glyma19g24900.1	GLP063	221	58 - 209	---------	1 to 20	23.98	6.90
82	Glyma19g41220.1	GLP064	219	60 - 209	---------	1 to 22	22.99	9.23
83	Glyma19g41070.2	GLP065	184	41 - 177	---------	---------	19.62	4.69
84	Glyma20g25461.1	GLP088	137	22 - 127	---------	---------	14.53	6.81
85	Glyma20g25430.1	GLP066	207	55 - 197	---------	1 to 24	22.12	6.90
86	Glyma20g22180.1	GLP067	224	65 - 214	---------	1 to 27	23.73	9.52
87	Glyma20g28640.1	GLP089	439	34 - 193 and 240 - 401	---------	1 to 23	50.44	5.88
88	Glyma20g28650.1	GLP090	605	196 - 354 and 406 - 567	7 to 29	1 to 24	70.30	5.12

89	Glyma20g28660.1	GLP091	605	196 - 354 and 406 - 567	7 to 29	1 to 24	70.30	5.12
90	Glyma20g36320.1	GLP068	222	61 - 211	3 to 21	1 to 20	23.91	8.48
91	Glyma20g28466.1	GLP092	383	178 - 350	---------	---------	43.97	9.01
92	Glyma20g28460.1	GLP093	439	34 - 193 and 240 - 401	---------	1 to 23	50.47	5.88
93	Glyma20g36300.1	GLP069	232	62 - 215	---------	1 to 20	24.97	8.43

TM, transmebrane; SP, signal peptide; pI, point isoeletric. New GmGER members is identified in red colors.

Supplemental Table S2: List of primers used in this study.

Gene cloning and eGFP tags fusions (N- and C-terminals)				
Primer name	**Sequence (5'-3')**	**Purpose**	**Tm (°C)**	**Reference**
SalI-GmGLP10_Fwd	gcgcgc*GTCGAC*ATGAAGGTTTTTTACTTCTTCG	GmGLP10 gene 3' flanking region PCR amplification	60.0	In this study
SpeI-GmGLP10_Rvs	ataaat*ACTAGT*TTAATTATGTTTCCCGTTAACT	GmGLP10 gene 5' flanking region PCR amplification	60.0	In this study
attB1-GFP-GmGLP10_Fwd	GGGGACAAGTTTGTACAAAAAAGCAGGCTtcATGAAGGTTTTTTACTTCTTCG	To generate GFP fusions at GmGLP10 N-terminals	60.0	In this study
attB2-GFP-GmGLP10_Rvs	GGGGACCACTTTGTACAAGAAAGCTGGGTtTTAATTATGTTTCCCGTTAACT	To generate GFP fusions at GmGLP10 N-terminals	60.0	In this study
attB1-GmGLP10-GFP_Fwd	GGGGACAAGTTTGTACAAAAAAGCAGGCTtcACCATGAAGGTTTTTTACTTCTTCG	To generate GFP fusions at GmGLP10 C-terminals	60.0	In this study
attB2-GmGLP10-GFP_Rvs	GGGGACCACTTTGTACAAGAAAGCTGGGTtATTATGTTTCCCGTTAACTTTGTTG	To generate GFP fusions at GmGLP10 C-terminals	60.0	In this study
ΔSP$_{1-22}$M-GmGLP10-GFP_Fwd	GGGGACAAGTTTGTACAAAAAAGCAGGCTTCACCATGTATGATCCAAGCCCCTTGCAAGAC	To generate GFP fusions at ΔSP$_{1-22}$M- GmGLP10 C-terminals	60.0	In this study
attB2-GmGLP10-GFP_Rvs	GGGGACCACTTTGTACAAGAAAGCTGGGTtATTATGTTTCCCGTTAACTTTGTTG	To generate GFP fusions at ΔSP$_{1-22}$M- GmGLP10 C-terminals	60.0	In this study
GFP-ΔSP$_{1-22}$M-GmGLP10_Fwd	GGGGACAAGTTTGTACAAAAAAGCAGGCTTCATGTATGATCCAAGCCCCTTGCAAGAC	To generate GFP fusions at ΔSP$_{1-22}$M- GmGLP10 N-terminals	60.0	In this study
attB2-GFP-GmGLP10_Rvs	GGGGACCACTTTGTACAAGAAAGCTGGGTtTTAATTATGTTTCCCGTTAACT	To generate GFP fusions at ΔSP$_{1-22}$M- GmGLP10 N-terminals	60.0	In this study
attB1_p::GmGLP10_Fwd	GGGGACAAGTTTGTACAAAAAAGCAGGCTGTATATGAGATTTGAACAGCCAAGA	GmGLP10 promoter cloning	60.0	In this study
attB2_p::GmGLP10_Rvs	GGGGACCACTTTGTACAAGAAAGCTGGGTTTTTCTCCCTCTCGCTACTAAC	GmGLP10 promoter cloning	60.0	In this study
Primers for GmGLP10 promoter sequencing by Sanger methods.				
SEQ1_p::GmGLP10_Rvs1	GTGTACCGAATAACTTGGCAAATATAA	GmGLP10 promoter sequencing	60.0	In this study
SEQ2_p::GmGLP10_Fwd2	GCTAAATCTTGACTCTCCCAGACA	GmGLP10 promoter sequencing	60.0	In this study
SEQ2_p::GmGLP10_Rvs2	GTGATCCTTCTCCACCCCTG	GmGLP10 promoter sequencing	60.0	In this study
SEQ3_p::GmGLP10_Fwd3	GCACTTTCTGTTTTCCCGAATACC	GmGLP10 promoter sequencing	60.0	In this study
SEQ3_p::GmGLP10_Rvs3	CGAGTGTCCACTATTGCATATTTATC	GmGLP10 promoter sequencing	60.0	In this study

SEQ4_p::GmGLP10_Fwd4	GGAACCATTCATTTACGTCACTTGT	GmGLP10 promoter sequencing	60.0	In this study
SEQ4_p::GmGLP10_Rvs4	CCCCACATCATCGTCATGATG	GmGLP10 promoter sequencing	60.0	In this study
SEQ5_p::GmGLP10_Fwd5	GCCGCCAGGTCTCAAAACAAA	GmGLP10 promoter sequencing	60.0	In this study
SEQ5_p::GmGLP10_Rvs5	TTTTCTCCCTCTCGCTACTAACTTAATT	GmGLP10 promoter sequencing	60.0	In this study
Primers for characterization of T-DNA insertion sites in *A. thaliana glp10-/-* mutant lines.				
LP_glp10_1_Fwd	TTAAAAATGATGTCGGCCATC	T-DNA for Salk mutants	56.1	
RP_glp10_1_Rvs	TAACGTTGACAAAATCCCTGG	T-DNA for Salk mutants	56.1	
LP_glp10_2_Fwd	ACGTTCACATCCAGCTGAAAC	T-DNA for Salk mutants	56.1	
RP_glp10_2_Rvs	TTCTTTCTTTGTTCATTCGCC	T-DNA for Salk mutants	56.1	
LBb1.3_NEW_Rvs	ATTTTGCCGATTTCGGAAC	T-DNA for Salk mutants	56.1	
Primers for characterization of transgene insertion in tobacco plants (T0).				
eGFP_Fwd	GACGTAAACGGCCACAAGTT	Transgenic tobacco lines selection	60.0	Moreira *et al.*, (2022)
eGFP_Rvs	GATGCCGTTCTTCTGCTTGT	Transgenic tobacco lines selection	60.0	Moreira *et al.*, (2022)
Primers used for RT-qPCR analysis.				
NtAOS_Fwd	GCCAAACGCGACCTTATGAT	Marker genes for JA signaling	60.0	Guimaraes *et al.*, (2022)
NtAOS_Rvs	CCACAAAATCCTTTCCGGCA	Marker genes for JA signaling	60.0	Guimaraes *et al.*, (2022)
NtAOC_Fwd	CCTGCTTATCTTCGCTTGAG	Marker genes for JA signaling	60.0	Guimaraes *et al.*, (2022)
NtAOC_Rvs	ATGCAGAGTCCAGCCGTTAT	Marker genes for JA signaling	60.0	Guimaraes *et al.*, (2022)
NtMYC2_Fwd	CCTCATTGATGGTGCTCGTG	Marker genes for JA signaling	60.0	Guimaraes *et al.*, (2022)
NtMYC2_Rvs	TTTCGGTGTTCTTGCTCAGC	Marker genes for JA signaling	60.0	Guimaraes *et al.*, (2022)
NtACS6_Fwd	ATGCCAAGGAAAGGGATTCTACA	Marker genes for ET signaling	60.0	Guimaraes *et al.*, (2022)
NtACS6_Rvs	TGGGAGGTTTGGGCGAAGA	Marker genes for ET signaling	60.0	Guimaraes *et al.*, (2022)
NtACO_Fwd	GACAAAGGGACATTACAAGAAGT	Marker genes for ET signaling	60.0	Guimaraes *et al.*, (2022)
NtACO_Rvs	GAGAAGGATTATGCCACCAG	Marker genes for ET signaling	60.0	Guimaraes *et al.*, (2022)
NtEFE26_Fwd	CGGACGCTGGTGGCATAAT	Marker genes for ET signaling	60.0	Guimaraes *et al.*, (2022)
NtEFE26_Rvs	CAACAAGAGCTGGTGCTGGATA	Marker genes for ET signaling	60.0	Guimaraes *et al.*, (2022)
NtEIN3_Fwd	AAATGGACCTGCAGCCATAG	Marker genes for ET signaling	60.0	Guimaraes *et al.*, (2022)
NtEIN3_Rvs	TGAAGCTCCTGCAAAGTGTG	Marker genes for ET signaling	60.0	Guimaraes *et al.*, (2022)

NtERF1_Fwd	TTAACGTCGGATGGTCGCCG	Marker genes for ET signaling	60.0	Guimaraes *et al.*, (2022)
NtERF1_Rvs	ACACCTCTGTAATGCCTTCC	Marker genes for ET signaling	60.0	Guimaraes *et al.*, (2022)
NtPR3_Fwd	CAGGAGGGTATTGCTTTGTTAGG	Marker genes for ET signaling	60.0	Guimaraes *et al.*, (2022)
NtPR3_Rvs	CGTGGGAAGATGGCTTGTTGTC	Marker genes for ET signaling	60.0	Guimaraes *et al.*, (2022)
NtEDS1_Fwd	TGATGACTTCAATGCTAATGTGAG	Marker genes for SA signaling	60.0	Guimaraes *et al.*, (2022)
NtEDS1_Rvs	GATCATGTAAGGTCCTGTATCTTC	Marker genes for SA signaling	60.0	Guimaraes *et al.*, (2022)
NtNPR1_Fwd	GAATGATACGGCAGAAGA	Marker genes for SA signaling	60.0	Guimaraes *et al.*, (2022)
NtNPR1_Rvs	AGATGAGGAGATGTTGTTAG	Marker genes for SA signaling	60.0	Guimaraes *et al.*, (2022)
NtHIN1_Fwd	CGACCTAACAAAGTCAAGTTCTACG	Marker genes for HR signaling	60.0	Guimaraes *et al.*, (2022)
NtHIN1_Rvs	CTCTATCTCCCAATAAAACCAAGC	Marker genes for HR signaling	60.0	Guimaraes *et al.*, (2022)
NtHSR515_Fwd	TTGGGCAGAATAGATGGGTA	Marker genes for HR signaling	60.0	Guimaraes *et al.*, (2022)
NtHSR515_Rvs	TTTGGTGAAAGTCTTGGCTC	Marker genes for HR signaling	60.0	Guimaraes *et al.*, (2022)
NtLOX_Fwd	GGACTTGAAGGATGTTGGTGC	Marker genes for JA signaling	60.0	Guimaraes *et al.*, (2022)
NtLOX_Rvs	TCACATTAAACGTAGCATCTCCT	Marker genes for JA signaling	60.0	Guimaraes *et al.*, (2022)
NtCA_Fwd	CGCCTGTGGAGGTATCAAA	Marker genes for ROS signaling	60.0	Guimaraes *et al.*, (2022)
NtCA_Rvs	GAGAAGGAGAAAGACCGAACT	Marker genes for ROS signaling	60.0	Guimaraes *et al.*, (2022)
NtACC_Fwd	TCTGAGGTTACTGATTTGGATTGG	Marker genes for ET signaling	60.0	Guimaraes *et al.*, (2022)
NtACC_Rvs	TGGACATGGTGGATAGTTGCT	Marker genes for ET signaling	60.0	Guimaraes *et al.*, (2022)
NtCAT1_Fwd	TGGACTTCATACTGGTCTCA	Marker genes for ROS signaling	60.0	Guimaraes *et al.*, (2022)
NtCAT1_Rvs	TTCCCATTGTTTCAGTCATTCA	Marker genes for ROS signaling	60.0	Guimaraes *et al.*, (2022)
NtAPX1_Fwd	GAGAAATATGCTGCGGATGA	Marker genes for ROS signaling	60.0	Guimaraes *et al.*, (2022)
NtAPX1_Rvs	CGTCTAATAACAGCTGCCAA	Marker genes for ROS signaling	60.0	Guimaraes *et al.*, (2022)
NtRbohD_Fwd	ACCAGCACTGACCAAAGAA	Marker genes for ROS signaling	60.0	Guimaraes *et al.*, (2022)
NtRbohD_Rvs	TAGCATCACAACCACAACTA	Marker genes for ROS signaling	60.0	Guimaraes *et al.*, (2022)
NtPR1_Fwd	AACCCATCCATACTATTCCTTG	Marker genes for SA signaling	60.0	Zhang *et al.*, (2018)

NtPR1_Rvs	GCCGCTAACCTATTGTCCC	Marker genes for SA signaling	60.0	Zhang *et al.*, (2018)
NtPR2_Fwd	TGATGCCCTTTTGGATTCTATG	Marker genes for SA signaling	60.0	Zhang *et al.*, (2018)
NtPR2_Rvs	AGTTCCTGCCCCGCTTT	Marker genes for SA signaling	60.0	Zhang *et al.*, (2018)
NtPR4_Fwd	GGAAAACGGAAAGGTAAGAAG AGG	Marker genes for SA signaling	60.0	Zhang *et al.*, (2018)
NtPR4_Rvs	GGACACGAGGTAGGTATCACAA CAA	Marker genes for SA signaling	60.0	Zhang *et al.*, (2018)
NtPR5_Fwd	TTCAATGCTGCTGGTAGGGG	Marker genes for SA signaling	60.0	Zhang *et al.*, (2018)
NtPR5_Rvs	GGTTAGTCGGGGCGAAAGTC	Marker genes for SA signaling	60.0	Zhang *et al.*, (2018)
NtHSR201_Fwd	CAGCAGTCCTTTGGCGTTGTC	Marker genes for HR signaling	60.0	Zhang *et al.*, (2018)
NtHSR201_Rvs	GCTCAGTTTAGCCGCAGTTGTG	Marker genes for HR signaling	60.0	Zhang *et al.*, (2018)
NtHSR203_Fwd	TGGCTCAACGATTACGCA	Marker genes for HR signaling	60.0	Zhang *et al.*, (2018)
NtHSR203_Rvs	GCACGAAACCTGGATGG	Marker genes for HR signaling	60.0	Zhang *et al.*, (2018)
NtL25_Fwd	GCTAAGGTTGCCAAGGCTGTCA AG	Reference genes	60.0	Guimaraes *et al.*, (2022)
NtL25_Rvs	GCACTAATACGAGGGTACTTGG GGTTT	Reference genes	60.0	Guimaraes *et al.*, (2022)
NtActin_Fwd	CATTGGCGCTGAGAGATTCC	Reference genes	60.0	Guimaraes *et al.*, (2022)
NtActin_Rvs	GCAGCTTCCATTCCGATCA	Reference genes	60.0	Guimaraes *et al.*, (2022)
GmGLP10_Fwd1	TGGCCATTGCTGGTCTTAGT	To confirme *GmGLP10* overexpression	60.0	In this work
GmGLP10_Rvs1	AAGCTTTGGCGAGAACTTCA	To confirme *GmGLP10* overexpression	60.0	In this work

Restriction enzyme sequences (italic format), attB sequence (underlined). Start codon and stop codon are in yellow and green, respectively. The deletion of signal peptide (ΔSP_{1-22}) was replaced by start codon to encode methionine (M) at begin of coding sequence.

CONCLUSÕES GERAIS

A presente investigação teve por objetivo validar o silenciamento gênico pós-transcricional dos genes efetores *Minc03328* e *Minc16803* e a superexpressão do gene *Germin-like protein subfamily 1 member 10* (*GmGLP10*), proveniente do genótipo de soja PI 595099, cujos resultados permitiram traçar novas medidas protetivas em cultivares de interesse agronômico contra o ataque do NFG *M. incognita*.

Baseado em nossos dados, verificamos que os alvos *Minc03328* e *Minc16803* podem ser utilizados como alternativa preventiva pelo uso da tecnologia do RNA de interferência, sendo os seus silenciamentos capazes de reduzir a susceptibilidade de linhagens transgênicas de *A. thaliana* em mais de 84%. Apesar dos seus aspectos elusivos *in planta*, certificamos dos seus usos na manutenção de células gigantes, uma vez que a regulação negativa de ambos transcritos foi capaz de infringir na integridade dos sítios de alimentação os quais representam a sua única medida de sobrevivência em plantas terrestres.

Além do elevado grau de similaridade compartilhada com outras espécies *Meloidogyne* substanciar um mecanismo preservado de ação desses efetores, análises de homologias de sequências aos níveis de ambas sequências codantes também evidenciaram a exclusividade legítima dos genes *Minc03328* e *Minc16803* reclusa a grande parte das espécies nocivas formadores de galhas. Tomando como relevância a utilização de sequências específicas como mecanismo da depleção do transcrito, via ação das proteínas Argonautas, as possibilidades de *off-targets* foram também investigadas nos genomas de outros organismos pertencentes ao reino *Metazoa* confirmando o mínimo de interferência possível que o uso da tecnologia do RNAi poderá proporcionar no meio ambiente. Este dado permitiu o estabelecimento do uso dos cassetes gênicos em plantas de soja e algodão. Os primeiros transformantes independentes gerados (T0) encontram em fase de caracterização molecular (estudos em andamento).

Neste estudo, o papel funcional do gene *Germin-like protein subfamily 1 member 10* (*GmGLP10*) foi também explorado, revelando uma terceira medida a ser perseguida tanto pela sua expressão heteróloga em plantas de interesse comerciais, quanto por técnicas de edição de genomas. A princípio, os indícios ômicos revelavam alta expressão diferencial de *GmGLP10* no genótipo resistente de soja PI 595099 como indicadores do seu fenótipo de resistência contra *M. incognita*, sendo o apoio deste último fim confirmado em linhagens transgênicas de tabaco superexpressando *GmGLP10*. Nossos dados demonstraram uma redução da susceptibilidade de plantas de tabaco em mais de 49%, enquanto que os testes de resistência realizados em raízes

transgênicas pilosas, induzidas a partir do pecíolo de folhas da soja, indicaram uma redução em mais de 55% do número de galhas.

A partir desses dados, revelamos o papel funcional da proteína apoplástica GmGLP10 na geração de peróxido de hidrogênio, sendo a sua atividade averiguada por meio do monitoramento transcricional de vários marcadores gênicos, sensíveis ao incremento das ERO no citoplasma da célula vegetal. Dentre suas identidades, destacam-se as vias do etileno (ET), ácido abscísico (ABA), jasmônico (JA) e salicílico (SA), espécies reativas de oxigênio (ERO) e resposta de hipersensibilidade (HR). Particularmente ao último caso, evidenciamos o apoio síncrono entre os genes relacionadas à resposta de hipersensibilidade *NtHSR201* e *NtHSR203* aos principais danos morfológicos observados na formação das CG. Ademais, casos como o atraso do desenvolvimento de nematoides e a desorganização do xilema foram também observados nos exames histológicos, remetendo como outros indícios correlatos à HR como resultado final da expressão ectópica de *GmGLP10* em CG.

Por fim, evidenciamos o papel chave do (SNP)-908 como razão crucial da extinção do *cis*-elemento RYPE (consenso CATGCA) na sequência promotora de $GmGLP10_{pro}$ do genótipo PI 595099, justificando a sua alta expressão nesse genótipo em relação a cultivar susceptível BRS 133. Há indícios de que o fator de transcrição ABI3 aja na repressão promotora de $GmGLP10_{pro}$ da cultivar BRS 133, após sua ligação ao consenso RYPE e recrutamento de modificadores de histonas (HM) com atividades de metilação e/ou desacetilação. Por meio desse indicativo, existe uma forte evidência de que *GmGLP10* permaneça em estádio transcricional inativo no genótipo susceptível, devido ao novo estádio de heterocromatina formado; enquanto o (SNP)-908, identificado pela troca G908A no genótipo PI 595099, remete para uma nova resistência ao módulo ABI3/HM. Apesar desses indícios fornecerem evidências circunstanciais do papel negativo do motivo RYPE no contexto susceptível, estudos adicionais serão conduzidos na cultivar BRS 133 a fim de averiguar se a depleção gênica deste motivo, via sistema CRISPR-Cas9, poderá contornar a atividade repressiva do módulo ABI3/HM.

CURRÍCULO

Valdeir Junio Vaz Moreira possui graduação em Bioquímica pela Universidade Federal de Viçosa (2016) e mestrado em Biologia Celular e Molecular pela Universidade Federal do Rio Grande do Sul (2019). Atualmente é estudante de doutorado pelo Programa de Biologia Molecular da Universidade de Brasília e membro da *International Society for Molecular Plant-Microbe Interactions* (*IS-MPMI*). Desde 2017 trabalha como pesquisador no laboratório de Interação Molecular Planta-Praga (LIMPP-I) na Embrapa Recursos Genéticos e Biotecnologia (CENARGEN) sob supervisão da Prof(a). Dra. Maria Fátima Grossi de Sá. Em 2021 foi contemplado com uma bolsa de doutorado sanduíche pelo projeto CAPES-COFECUB para exercer suas atividades de pesquisas no *Institute de la Rechérche Agronomique - INRAE*, em Sophia Antipolis, França, sob supervisão da Dra. Janice de Almeida Engler. Em seus trabalhos de pesquisa, visa compreender quais genes de patógenos de plantas podem ser alvos pela técnica de RNA de interferência (RNAi) para ser aplicado na agricultura brasileira. Foi bolsista destaque pela CAPES em 2022 pela descoberta dos genes de parasitismo *Minc03328* e *Minc16803* como alvos promissores pelo RNAi para o controle do nematoide formador de galha - *Meloidogyne incognita*. Também atua na prospecção e caracterização de genes de resistência e promotores vegetais para o desenvolvimento de cassetes gênicos para a geração de plantas geneticamente modificadas (soja e algodão) para o controle de nematoides parasitas formadores de cisto e galhas. Além disso, visa entender quais vias de sinalização relacionadas à imunidade de plantas estão envolvidas com a resistência contra esses mesmos patógenos para o desenvolvimento de circuitos genéticos em cultivares elite no campo. Possui ampla experiência em Biologia Molecular (clonagem por restrição gênica, GATEWAY, Golden Gate Cloning, PCR, RT-qPCR, BiFC, imunoprecipitação de cromatina e proteína, western blot, EMSA, mono e duplo híbrido de leveduras, expressão transiente de proteínas e RNAs em células vegetais, atividade enzimática e fisiologia vegetal); em Biologia Celular (microscopia de luz, confocal Z-stack, técnicas de coloração utilizando corante ácidos e básicos) e também na geração de produto. Devido a sua grande motivação e determinação pela ciência recebeu o prêmio na Embrapa Recursos Genéticos e Biotecnologia em 1° lugar no Concurso Talento Estudantil, o 1° lugar no XX Simpósio de Biologia Molecular da Universidade de Brasília e 1° lugar no Seventh International Congress of Nematology, França.

LISTA DE PUBLICAÇÕES

As publicações listadas abaixo correspondem à produção científica do estudante Valdeir Junio Vaz Moreira durante o período que desenvolveu seu doutorado pelo Programa de Pós-Graduação em Biologia Molecular (PPGBIOMOL) da Universidade de Brasília em parceria com as Instituições Embrapa Recursos Genéticos e Biotecnologia - Brasília, DF (CENARGEN) e o *Institute Nacional de la Recherche Agronomique* (*INRAE*), Sophia-Antipolis, França (CAPES-COFECUB Sv.622/18).

PUBLICAÇÕES ACEITAS

- Freitas-Alves NS, Moreira-Pinto CE, Arraes FBM, Costa LSL, de Abreu RA, **Moreira VJV**, Lourenço-Tessutti IT, Pinheiro DH, Lisei-de-Sa ME, Paes-de-Melo B, Pereira BM, Guimaraes PM, Brasileiro ACM, de Almeida-Engler J, Soccol CR, Morgante CV, Basso MF, Grossi-de-Sa MF. (2023). An *ex-vitro* hairy root system from petioles of detached soybean leaves for *in planta* screening of target genes and CRISPR strategies associated with nematode bioassays. **Planta**. Dec 18; 259(1):23. doi: 10.1007/s00425-023-04286-x.
- **Moreira VJV**, Pinheiro DH, Lourenço-Tessutti IT, Basso MF, Lisei-deSa ME, Silva MCM, Danchin EGJ, Guimaraes PM, Grynberg P, Brasileiro ACM, Macedo LLP, Morgante CV, Almeida-Engler J, Grossi-de-Sa MF. (2023). *In planta* RNAi targeting *Meloidogyne incognita* Minc16803 gene perturbs nematode parasitism and reduces plant susceptibility. **Journal of Pest Science**. https://doi.org/10.1007/s10340-023-01623-7
- **Moreira VJV**, Lourenço-Tessutti IT, Basso MF, Lisei-de-Sa ME, Morgante CV, Paes-de-Melo B, Arraes FBM, Martins-de-Sa D, Silva MCM, de Almeida Engler J, Grossi-de-Sa MF. (2022). Minc03328 effector gene downregulation severely affects *Meloidogyne incognita* parasitism in transgenic *Arabidopsis thaliana*. **Planta**. Jan 20; 255(2):44. doi: 10.1007/s00425-022-03823-4.
- Arraes FBM, Vasquez DDN, Tahir M, Pinheiro DH, Faheem M, Freitas-Alves NS, Moreira-Pinto CE, **Moreira VJV**, Paes-de-Melo B, Lisei-de-Sa ME, Morgante CV, Mota APZ, Lourenço-Tessutti IT, Togawa RC, Grynberg P, Fragoso RR, de Almeida-Engler J, Larsen MR, Grossi-de-Sa MF. (2022). Integrated Omic Approaches Reveal Molecular Mechanisms of Tolerance during Soybean and *Meloidogyne*

incognita Interactions. **Plants (Basel)**. Oct 17; 11(20):2744. doi: 10.3390/plants11202744.

- Arraes FBM, Martins-de-Sa D, Noriega Vasquez DD, Melo BP, Faheem M, de Macedo LLP, Morgante CV, Barbosa JARG, Togawa RC, **Moreira VJV**, Danchin EGJ, Grossi-de-Sa MF. (2021). Dissecting protein domain variability in the core RNA interference machinery of five insect orders. **RNA Biology**. Nov; 18(11):1653-1681. doi: 10.1080/15476286.2020.1861816.
- Lisei-de-Sá ME, Rodrigues-Silva PL, Morgante CV, de Melo BP, Lourenço-Tessutti IT, Arraes FBM, Sousa JPA, Galbieri R, Amorim RMS, de Lins CBJ, Macedo LLP, **Moreira VJV**, Ferreira GF, Ribeiro TP, Fragoso RR, Silva MCM, de Almeida-Engler J, Grossi-de-Sa MF. (2021). Pyramiding dsRNAs increases phytonematode tolerance in cotton plants. **Planta**. Nov 15; 254(6):121. doi: 10.1007/s00425-021-03776-0.
- Basso MF, Arraes FBM, Grossi-de-Sa M, **Moreira VJV**, Alves-Ferreira M, Grossi-de-Sa MF. (2020). Insights Into Genetic and Molecular Elements for Transgenic Crop Development. **Frontiers in Plant Science**. May 15; 11:509. doi: 10.3389/fpls.2020.00509.

PUBLICAÇÕES PRONTAS PARA SUBMISSÃO

- **Moreira VJV**, Pinheiro DH, Ribeiro TP, Engler, JDA; Keller H, Grossi-de-Sá MF. (2024). *GmGLP10*-overexpressing transgenic plants triggers defense response in *Meloidogyne incognita*-induced giant cells by up-regulation of H_2O_2-sensitive genes. **NEW PHYTOLOGIST**. (To be submitted)
- Souza-Junior, JDA, **Moreira, VJV**, Pinheiro, DH, Coelho RR, Cabral D, Veylder LD, Grossi-de-Sá MF, Engler JDA. (2024). The involvement of plant SIM/SMR inhibitors on the cell cycle regulation of galls induced by root-knot nematodes. **PLANT CELL AND ENVIRONMENT**. (Under revision)
- **Moreira VJV**, Grossi-de-Sá MF. (2024). An update in RNAi effector diversity underpinning root-knot nematodes control. **BioEssays**. (To be submitted)
- Abreu-Souza JP, Ribeiro TP, **Moreira VJV**, Almeida-Engler JD, Grossi-de-Sá MF. *In planta* RNAi targeting the putative effector *Minc3s00280g09294* gene reduces plant susceptibility to *Meloidogyne incognita*. **PLANTA**. (To be submitted)

PRÊMIOS

- 1° Lugar no XII Simpósio do Programa de Pós-graduação em Biologia Molecular - Categoria Biologia Celular e Molecular de Microrganismos, Programa de Biologia Molecular da Universidade de Brasília. (2023).
- 1° Place in the Student Poster Competition of the Seventh International Congress of Nematology in the category of Nematode Management, Seventh International Congress of Nematology (ICN2022). (2023).
- Bolsista em Destaque pela CAPES, Coordenação de Aperfeiçoamento de Pessoal de Nível Superior. (2022).
- 1° Lugar no XXVI Talento Estudantil com o trabalho intitulado: Explorando a via de sinalização mediada pela proteína Germin de soja visando o controle de nematoides de galha, Embrapa Recursos Genéticos e Biotecnologia - Brasília/DF (2022).
- Menção honrosa ao trabalho "Silenciamento dos genes *Minc16803* e *Minc03328* de *Meloidogyne incognita* afeta o parasitismo do nematoide e reduz a susceptibilidade em *Arabidopsis thaliana*", Embrapa Recursos Genéticos e Biotecnologia - Brasília/DF, Concurso Minha Tese em 3 Minutos (3MT) (2022).
- 1° Lugar no X Simpósio do Programa de Pós-graduação em Biologia Molecular - Categoria Biologia Celular e Molecular de Microrganismos, Programa de Biologia Molecular da Universidade de Brasília. (2021).
- 1° Lugar no XXV Talento Estudantil, Embrapa Recursos Genéticos e Biotecnologia - Brasília/DF. (2020).

ANEXOS

Supporting information - Figures S1-S4

Minc03328 EFFECTOR GENE DOWNREGULATION SEVERELY AFFECTS *Meloidogyne incognita* PARASITISM IN TRANSGENIC *ARABIDOPSIS THALIANA*

Valdeir Junio Vaz Moreira[1,2,3], Isabela Tristan Lourenço-Tessutti[1,4], Marcos Fernando Basso[1,4], Maria Eugênia Lisei-de-Sá[1,3,5], Carolina Vianna Morgante[1,4,6], Bruno Paes-de-Melo[1,7], Fabrício Barbosa Monteiro Arraes[1,2,4], Diogo Martins-de-Sá[1,3], Maria Cristina Mattar Silva[1,4], Janice de Almeida-Engler[4,8], Maria Fatima Grossi-de-Sa[1,4,9]. *Minc03328* effector gene downregulation severely afects *Meloidogyne incognita* parasitism in transgenic *Arabidopsis thaliana*. PLANTA. Planta (2022) 255:44. doi.org/10.1007/s00425-022-03823-4

[1]Embrapa Genetic Resources and Biotechnology, Brasilia, DF 70770-917, Brazil

[2]Biotechnology Center, PPGBCM, UFRGS, Porto Alegre, RS 90040-060, Brazil

[3]Federal University of Brasilia, UNB, Brasilia, DF 70910-900, Brazil

[4]National Institute of Science and Technology, INCT PlantStress Biotech, Embrapa 70297-400, Brazil

[5]Agriculture Research Company of Minas Gerais State, Uberaba, MG 31170-495, Brazil

[6]Embrapa Semiarid, Petrolina, PE 56302-970, Brazil

[7]Federal University of Viçosa, Viçosa, MG 36570-900, Brazil

[8]INRAE, Université Côte d'Azur, CNRS, ISA, 06903 Sophia Antipolis, France 9 Catholic University of Brasilia, Brasilia, DF 71966-700, Brazil

[*]**Corresponding Authors**

Maria Fatima Grossi-de-Sa: fatima.grossi@embrapa.br

Pages 182 to 192

SUPPLEMENTAL FIGURES AND LEGENDS

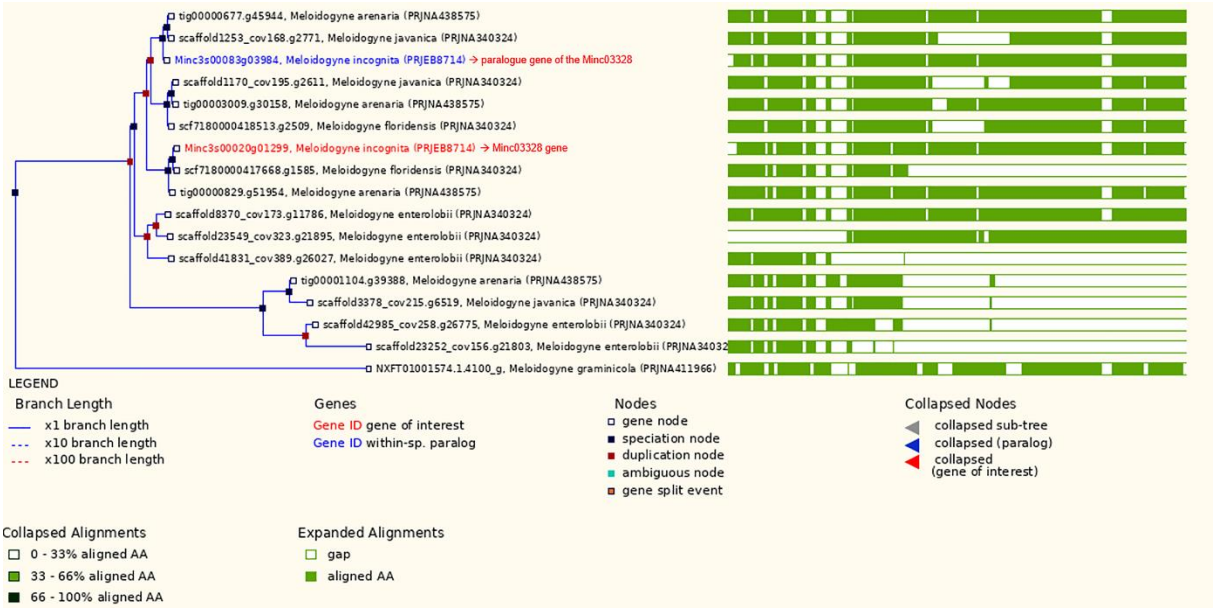

Suppl. Fig. S1 Comparative genomic tree of the *Minc3s00020g01299* (*Minc03328*) gene generated from BioProject PRJEB8714 and retrieved from WormBase database version WBPS14. The comparative genomic tree was automatically generated by the WormBase ParaSite using the Ensembl Compara tools using default parameters. The alignments on the right of the gene tree show the regions of synteny between gene sequences.

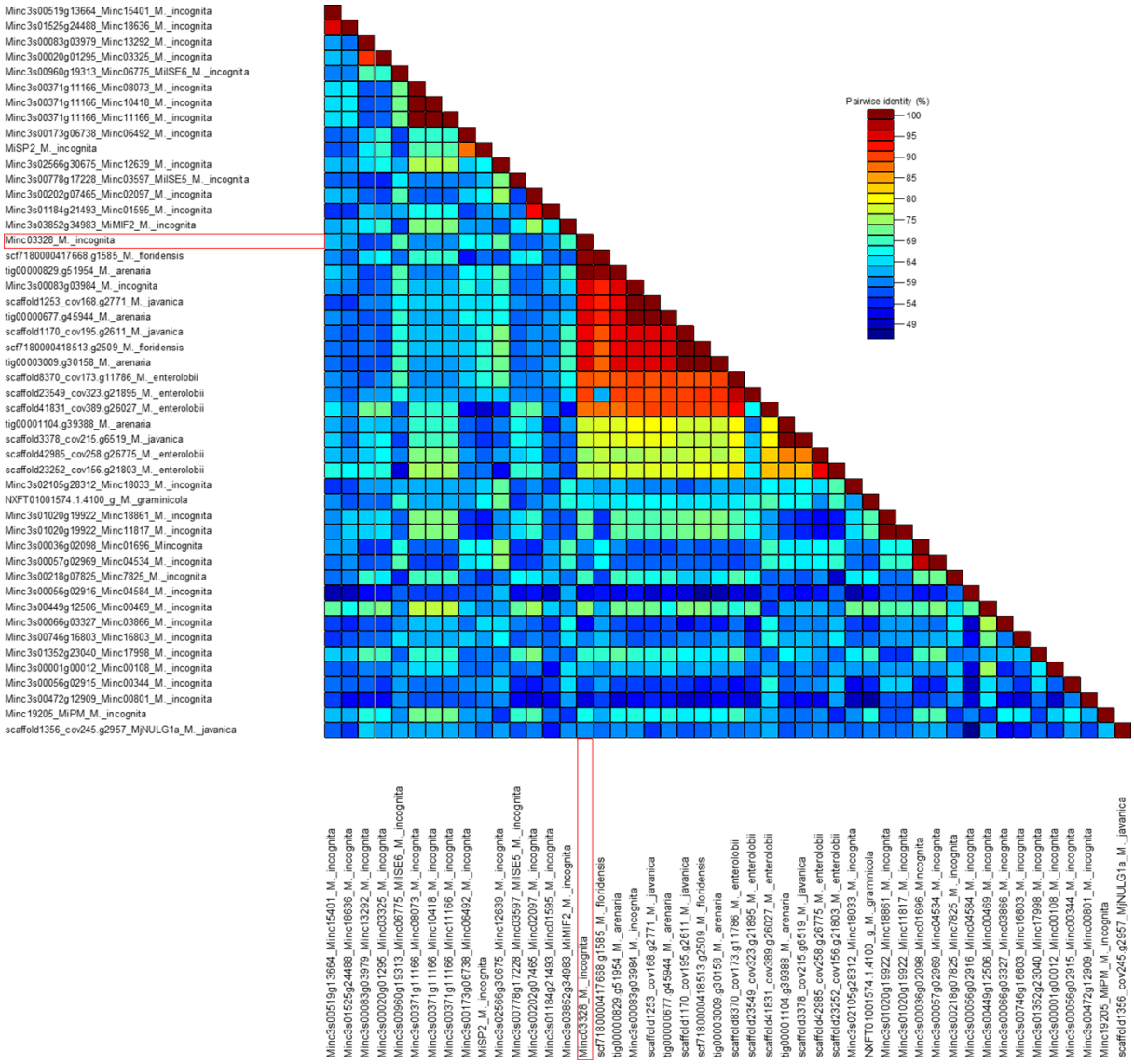

Suppl. Fig. S2 *In silico* sequence analysis of the *M. incognita* effector genes, highlighting in red boxes the *Minc3s00020g01299* (*Minc03328*) gene studied in this work. Pairwise sequence identity matrices of nucleotide sequences were generated using Sequence Demarcation Tool version 1.2 software. Gene sequences were retrieved from WormBase Parasite Database version WBPS13.

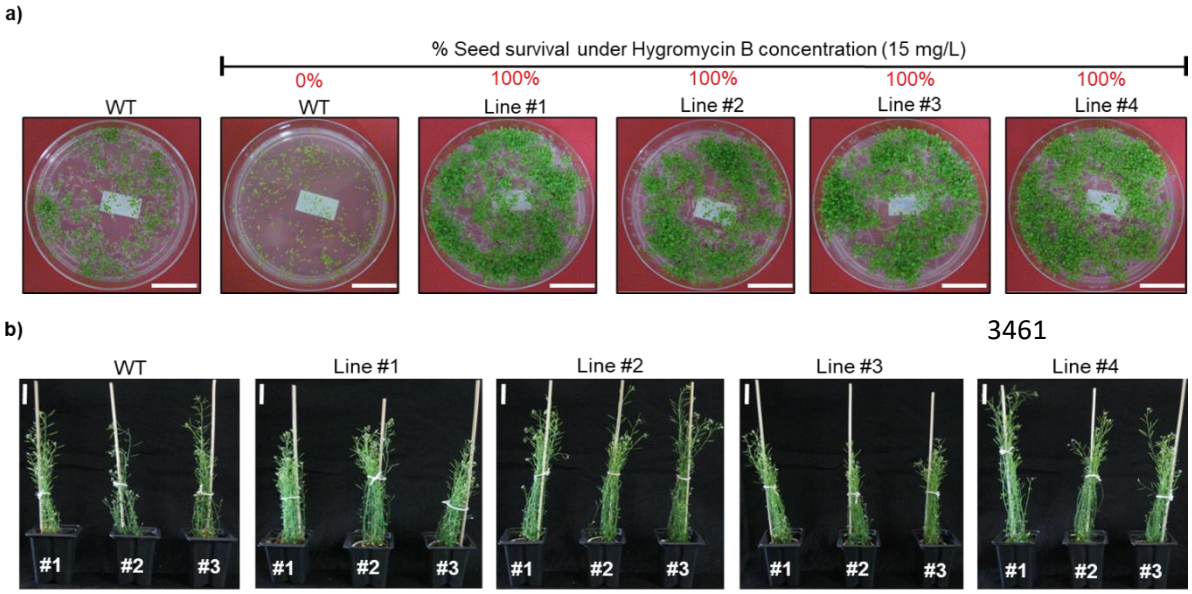

Suppl. Fig. S3 Phenotype of the transgenic *A. thaliana* lines and wild-type control plants during screening in Petri plates containing MS-agar and 15 mg/L hygromycin, and after acclimatization and cultivation under growth room. **a** *A. thaliana* T_3 transgenic lines selected *in vitro* under half-strength (0.5X) MS medium containing 15 mg/L hygromycin B. **b** Transgenic *A. thaliana* lines during advancement of generations (T_1 to T_3). Scale bars: 1 cm.

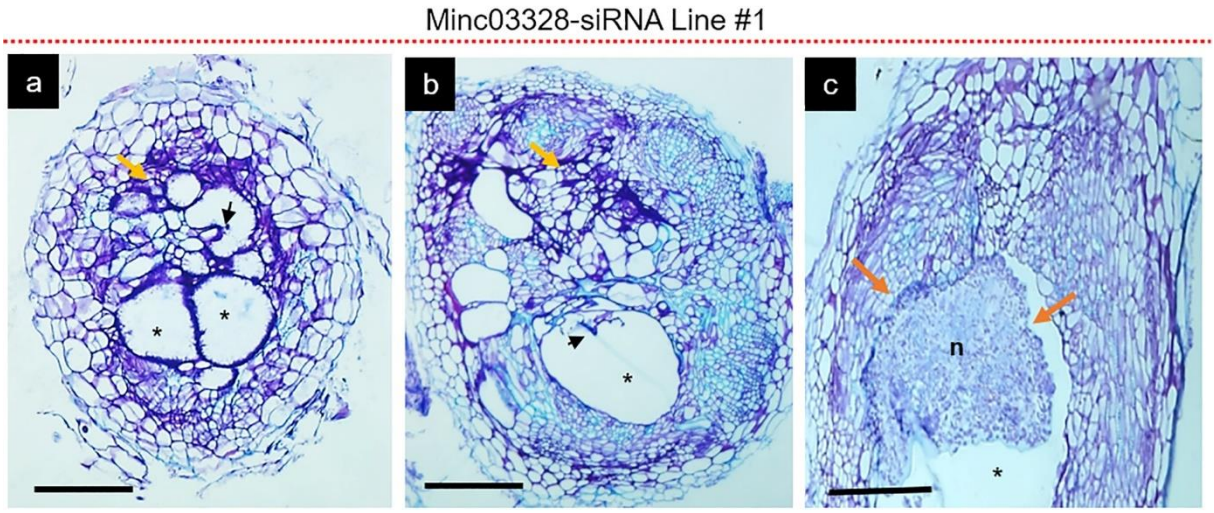

Suppl. Fig. S4 Histopathological morphology of *M. incognita*-induced galls in the Minc03328-siRNA line of *A. thaliana*. Plants from transgenic Line #1 and wild-type control plants were submitted to *M. incognita* infection, and gall and nematode morphology was evaluated at 45 DAI. Sectioned galls were stained with toluidine blue. **a** and **b** Transgenic galls presented giant cells with few cytoplasmic contents and often contained regular cell walls (black arrows). Neighboring cells from transgenic galls showed more irregular sizes and shapes (yellow arrows) than wild-type control galls suggesting altered giant cell ontogenesis. **c** Nematode cuticle was apparently disintegrating (orange arrow) and not well defined. This analysis demonstrated that *Minc03328* gene silencing caused a direct effect on nematode morphology as well indirectly in gall structure. Abbreviations: asterisks, giant cell; n, nematode. Scale bars = 50 µm.

Table S1: Primer sequences used in this study.

Primer name	Gene	Gene ID	Sequence 5'– 3'	Purpose	References
GFP-F	*eGFP* transgene	transgene	GACGTAAACGGCCACAAGTT	PCR	This work
GFP-R			GATGCCGTTCTTCTGCTTGT	PCR	This work
Minc03328-F	*Minc03328*	Minc3s00020g01299	TGATAAGCGCCCTAGGAAATGA	qPCR	This work
Minc03328-R			GACTAGGATCGTATCGGGTGC	qPCR	This work
Mi18S-F	*Mi18S*	Minc3s02085g28182	ACCGTGGCCAGACAAACTAC	qPCR	This work
Mi18S-R			GATCGCTAGTTGGCATCGTT	qPCR	This work
MiGAPDH-F	*MiGAPDH*	Minc3s07075g40689	GCTTCCTGCACTACTAATTGTCTTG	qPCR	Lourenço-Tessutti *et al.* (2015)
MiGAPDH-R			CAGTAACAGCGTGTACAGTAGTCAT	qPCR	Lourenço-Tessutti *et al.* (2015)
miActin-F	*MiActin*	Minc3s00730g16611	GATTCGTATGTGGGAGATGAGG	qPCR	This work
miActin-R			TTAGCCTTTGGGTTGAGAGG	qPCR	This work
miβ-tubulin-F	*Miβ-tubulin*	Minc3s00001g00047	TGGAAAGTATGTCCCAAGAGC	qPCR	Lourenço-Tessutti *et al.* (2015)
miβ-tubulin-R			CACCACCAAGCGAGTGAGT	qPCR	Lourenço-Tessutti *et al.* (2015)
Pdk intron-F	*Pdk intron*	transgene	TGCTAATATAACAAAGCGCAAGA	qPCR	This work
Pdk intron-R			ACCTTGTTTATTCATGTTCGACT	qPCR	This work
Actin 2-F	*AtActin 2*	AT3G18780	CTTGCACCAAGCAGCATGAA	qPCR	Che *et al.* (2010)
Actin 2-R			CCGATCCAGACACTGTACTTCCTT	qPCR	Che *et al.* (2010)
GAPDH-F	*AtGAPDH*	AT1G13440	TTGGTGACAACAGGTCAAGCA	qPCR	Ogneva *et al.* (2021)
GAPDH-R			AAACTTGTCGCTCAATGCAATC	qPCR	Ogneva *et al.* (2021)
EF1-F	*AtEF1*	AT5G60390	TGAGCACGCTCTTGCTTTCA	qPCR	This work
EF1-R			GGTGGTGGCATCCATCTTGTTACA	qPCR	This work

References: Lourenço-Tessutti IT, Souza Junior JDA, Martins-de-Sa D, Viana AAB, Carneiro RMDG, Togawa RC, de Almeida-Engler J, Batista JAN, Silva MCM, Fragoso RR, Grossi-de-Sa MF (2015) Knock-down of heat-shock protein 90 and isocitrate lyase gene expression reduced root-knot nematode reproduction. Phytopathology 105:628-637.

Che P, Bussell JD, Zhou W, Estavillo GM, Pogson BJ, Smith SM (2010) Signaling from the endoplasmic reticulum activates brassinosteroid signaling and promotes acclimation to stress in Arabidopsis. Science Signal 3(141):ra69.

Ogneva ZV, Volkonskaia VV, Dubrovina AS, Suprun AR, Aleynova OA, Kiselev KV (2021) Exogenous stilbenes improved tolerance of Arabidopsis thaliana to a shock of ultraviolet B radiation. Plants 10(7):1282.

Suppl. Table S2: Effector *Minc03328* (*Minc3s00020g01299*) coding sequence organized in 6 exons and 5 introns, selected as a target sequence for *in planta* RNAi strategy to downregulate *Minc03328* gene.

Length	**Sequence**
Gene structure	
5'-UTR 30 bp	tataaagatatacttttagATGCTTAAAGCGGCATCAATGTTTTACTCA
CDS 1.428 bp	ATGATTCCTTTCCTTATTCTGTTGTGCTCCTTATTTGAAAATTGCGGTGCTGGCGTTCCACATGCAGCTGTAAGCAGTTCGCA GGGAGTCAACATTCCGCATAAAATTAGTGCATCAATGACAAAATTGGGCAATCCTCGTGTGACTCATGTTACTTTCCCAGTAAAACA AAATTCAAGCAAATCTGGCATCAGTTTGACTGTAAGTGACCCAAAACAGCCCGTTCTTCGTGCTTCTGCAAAACACGATAATCAGGA TTTGTTTAGCAATGACGAAAACAACGATGATGATATATTAGATGAATTACAATATTACATCAAGAAATATGAAGAAAAGGAAAGA GACGAGGTTGCAAGAATTAATCTTGAAGATGTTGAAGAGCACAACAAATACATGGAAGAACAAGAAAAGTTATATGAACAAACAAA AGGAAAAGAAGGCCTTGATAAAATTTCCAAGAATCTTCTTGATAGAAAACATGCTAGTTACAGTAAAATAAGTTCATATGAACTTAT CAAAGAATTTTATGGAATTGATCTGGAATATAAAATTCCGAAAACAATTGAACAACGAAAAAATCTCGTAACAAAATTACTTGAAGG TTTTATAAAGATGATAAATAAAAGGAACAAGGAAAAATTTGATATAATGATAAGCGCCCTAGGAAATGAAAATCATAAAGAAAAAA AGGGAGAATTTGATGAATTTTTACAGTATCTAGAACTGTTCGCACCCGATACGATCCTAGTCTCCTTTCTTCAAATTCCTGATGAAGGT CGACAACTTTTGTTTGAAACTTTCGATGAGATATTAACAGATTTGAAAAAAAGTAAAAACAAAAAAGATGAACACGGAAAAATAATT AAAGGCAGTTCTCAACATCCAGCTGTCCATTTGAAAAAATATCACGACAAATTAAACAACAGCGATCTCGATGCTGATACAAAAGAA CGAATTGATCAATTCTTCACAATTGTTCAAAATGACTTCAATCAATTGCCAATATATTTAACAGAAAATTTTGCCAGTCTCTTCAGAA AAATTGCAACATTAGGACTCCCGGGATTAAAAGAAGCATTAATCCGTTACTTAGAAGTATGGAATCATGCAGATCCTCAGGATCAGC AAATGATGGCAAACGCATTTCCTAAATTGGCTTTCTTCTACAACGATTCAAAATCAATGAAAATGAATGATTGGGCTTATCGTTCAGT AAAAGGAAATTTCTTTTTTAAAATTCCACTTTTGATATTGCTTAAAATGATTTTCTTGAACAAGCCAAAATTGGAGAATGATAGTGCTT TATATAAAGAATTGCGTGAAAAATTAACAAAAGATTTTGAAGCTAACAAGGAGCTTATTGATGAAATTGGAAAGTTCTTTAAACCCG CAAAACCCCTTGTTGGTTCAGTAAAAATTTTGAATTGA
First start codon 10 aa	MLKAASMFYS
Second start codon 475 aa 54.99 kDa pI 6.67	MIPFLILLCSLFENCGAGVPHAAVSSSQGVNIPHKISASMTKLGNPRVTHVTFPVKQNSSKSGISLTVSDPKQPVLRASAKHDNQDLFSNDEN NDDDILDELQYYIKKYEEKERDEVARINLEDVEEHNKYMEEQEKLYEQTKGKEGLDKISKNLLDRKHASYSKISSYELIKEFYGIDLEYKIP KTIEQRKNLVTKLLEGFIKMINKRNKEKFDIMISALGNENHKEKKGEFDEFLQYLELFAPDTILVSFLQIPDEGRQLLFETFDEILTDLKKSKN KKDEHGKIIKGSSQHPAVHLKKYHDKLNNSDLDADTKERIDQFFTIVQNDFNQLPIYLTENFASLFRKIATLGLPGLKEALIRYLEVWNHAD PQDQQMMANAFPKLAFFYNDSKSMKMNDWAYRSVKGNFFFKIPLLILLKMIFLNKPKLENDSALYKELREKLTKDFEANKELIDEIGKFFK PAKPLVGSVKILN*
3'-UTR 50 bp	tatgcgagaaaaaatgaaagaagtgatatgtaaaaaaagtgaaggaagat

Nucleotide and amino acid sequence in blue letters: 5'-UTR with a putative premature start codon. Nucleotide and amino acid sequence in yellow letters: predicted importation peptide signal (22 aa length). Underline nucleotide sequence: sequence target (200 bp length) used in RNAi strategy. Nucleotide sequence in red: peptide sequence (14 aa length) used as a reference to synthesis of the anti-Minc03328 polyclonal antibody.

Suppl. Table S3: Literature review about *M. incognita* effector genes already validated by *in planta* RNAi strategy in different plant species.

Effector gene	In situ localization	Host plant	Promoter	Phenotype	References
MiMSP40	subventral esophageal	*A. thaliana*	*CaMV35S*	35 to 50% reduction in galls number 13 to 18% reduction in egg masses	Niu *et al.* (2016)
Mi16D10	subventral esophageal	*A. thaliana*	*CaMV35S*	63 to 90% reduction in galls number and gall size	Huang *et al.* (2006a) and Huang *et al.* (2006b)
Mi16D10	subventral esophageal	Grape hairy roots	*CaMV35S*	-	Yang *et al.* (2013)
Mi16D10	subventral esophageal	Potato	*CaMV35S*	-	Dinh *et al.* (2015)
Mi8D05	subventral esophageal	*A. thaliana*	*CaMV35S*	90% reduction in gall formation	Xue *et al.* (2013)
Mi-msp3	subventral esophageal	*A. thaliana*	*CaMV35S*	89% reduction in galls number	Joshi *et al.* (2020)
MiISE5	subventral esophageal	Pepper	(**)	31% reduction in galls number 44% reduction in egg masses	Shi *et al.* (2018)
Mi-CRT	subventral esophageal	*A. thaliana*	*CaMV35S*	High reduction in galls number	Jaubert *et al.* (2005); Jaouannet *et al.* (2013)
msp-20	subventral esophageal	*S. melongena* (eggplant)	*CaMV35S*	41 to 67% reduction in multiplication factor	Shivakumara *et al.* (2017)
Mi-CM-3	subventral esophageal	*N. benthamiana*	(**)	51% reduction in females number	Wang *et al.* (2018)
Mi-msp-1 or Mi-vap-1	subventral esophageal	*S. melongena* (eggplant)	*CaMV35S*	33 to 46% reduction in galls number 41 to 51% reduction in egg masses 62 to 70% reduction in multiplication factor	Chaudhary *et al.* (2019a) and Chaudhary *et al.* (2019b)
Minc03328	Subventral esophageal	*A. thaliana*	*pUceS8.3*	85% reduction in galls number 90% reduction in egg masses 64 to 87% reduction in [galls/egg masses] ratio	Rutter *et al.* (2014) This work
Mi-msp5	dorsal oesophageal glands cells	*A. thaliana*	*CaMV35S*	78% reduction in galls number	Joshi *et al.* (2020)
Mi-msp18	dorsal oesophageal glands cells	*A. thaliana*	*CaMV35S*	86% reduction in galls number	Joshi *et al.* (2020)
Mi-msp24	dorsal oesophageal glands cells	*A. thaliana*	*CaMV35S*	89% reduction in galls number	Joshi *et al.* (2020)
Misp12	dorsal oesophageal glands cells	*N. benthamiana*	(**)	63% reduction in egg number	Xie *et al.* (2016)
msp-18	dorsal oesophageal glands cells	*S. melongena*	*CaMV35S*	43 to 69% reduction in multiplication factor	Shivakumara *et al.* (2017)
MiMIF-2 (MIF-like)	hypodermis cuticle	*A. thaliana*	*CaMV35S*	60% reduction in galls number	Zhao *et al.* (2019)
Mi-msp2	(*)	*A. thaliana*	*CaMV35S*	52 to 54%, 60 to 66%, and 84 to 95% reduction respectively in galls numbers, females, and egg masses	Joshi *et al.* (2019)
MiIDL1	-	*A. thaliana*	*CaMV35S*	40% reduction in galls number	Kim *et al.* (2018)
Minc01696 *Minc00344* *Minc00801*	Subventral esophageal Subventral esophageal Rectal glands	*N. tabacum* and soybean hairy roots	*pUceS8.3*	80 to 90% reduction in egg, J2, galls number, and nematode reproduction factor	Grossi-de-Sa, MF (personal communication)

Mi-cpl *Mi-icl* *Mi-sf*	cysteine protease isocitrate lyase splicing factor	Cotton	*pUceS8.3*	reduction in gall formation (57-64%) and egg masses production (58-67%), as well as in the estimated reproduction factor (60-78%)	Lisei-de-Sa *et al.* (2021)

(*) upregulated during early parasitic stages; (**) virus-mediated RNAi; (-) not described so far.

References in the Supplemental Table S3

Dinh PT, Zhang L, Mojtahedi H, Brown CR, Elling AA (2015) Broad *Meloidogyne* resistance in potato based on RNA interference of effector gene 16D10. J Nemal 47:71-78.

Huang G, Allen R, Davis EL, Baum TJ, Hussey RS (2006a) Engineering broad root-knot resistance in transgenic plants by RNAi silencing of a conserved and essential root-knot nematode parasitism gene. PNAS 103:14302-14306. https://doi.org/10.1073/pnas.0604698103

Huang G, Dong R, Allen R, Davis EL, Baum TJ, Hussey RS (2006b) A root-knot nematode secretory peptide functions as a ligand for a plant transcription factor. Mol Plant Microbe Interact 19:463-470. https://doi.org/10.1094/MPMI-19-0463

Jaouannet M, Magliano M, Arguel MJ, Evangelisti E, Abad P, Rosso MN (2013) The root-knot nematode calreticulin Mi-CRT is a key effector in plant defense suppression. Mol Plant Microbe Interact 26:97-105. https://doi.org/10.1094/MPMI-05-12-0130-R

Jaubert S, Milac AL, Petrescu AJ, de Almeida-Engler J, Abad P, Rosso MN (2005) *In planta* secretion of a calreticulin by migratory and sedentary stages of root-knot nematode. Mol Plant Microbe Interact 18:1277-1284. https://doi.org/10.1094/MPMI-18-1277

Joshi I, Kumar A, Kohli D, Singh AK, Sirohi A, Subramaniam K, Chaudhury A, Jain PK (2020) Conferring root-knot nematode resistance via host-delivered RNAi-mediated silencing of four *Mi-msp* genes in Arabidopsis. Plant Sci 298:110592. https://doi.org/10.1016/j.plantsci.2020.110592

Niu J, Liu P, Liu Q, Chen C, Guo Q, Yin J, Yang G, Jian H (2016) Msp40 effector of root-knot nematode manipulates plant immunity to facilitate parasitism. Sci Rep 6:19443. https://doi.org/10.1038/srep19443

Shi Q, Mao Z, Zhang X, Zhang X, Wang Y, Ling J, Lin R, Li D, Kang X, Sun W, Xie B (2018) A *Meloidogyne incognita* effector MiISE5 suppresses programmed cell death to promote parasitism in host plant. Sci Rep 8:7256. https://doi.org/10.1038/s41598-018-24999-4

Shivakumara TN, Chaudhary S, Kamaraju D, Dutta TK, Papolu PK, Banakar P, Sreevathsa R, Singh B, Manjaiah KM, Rao U (2017) Host-induced silencing of two pharyngeal gland genes conferred transcriptional alteration of cell wall-modifying enzymes of *Meloidogyne incognita* vis-à-vis perturbed nematode infectivity in eggplant. Front Plant Sci 8:473. https://doi.org/10.3389/fpls.2017.00473

Wang X, Xue B, Dai J, Qin X, Liu L, Chi Y, Jones JT, Li H (2018) A novel *Meloidogyne incognita* chorismate mutase effector suppresses plant immunity by manipulating the salicylic acid pathway and functions mainly during the early stages of nematode parasitism. Plant Pathol 67:1436–1448. https://doi.org/10.1111/ppa.12841

Xue B, Hamamouch N, Li C, Huang G, Hussey RS, Baum TJ, Davis EL (2013) The *8D05* parasitism gene of *Meloidogyne incognita* is required for successful infection of host roots. Phytopathology 103:175-181. https://doi.org/10.1094/PHYTO-07-12-0173-R

Yang Y, Jittayasothorn Y, Chronis D, Wang X, Cousins P, Zhong G-Y (2013) Molecular characteristics and efficacy of 16D10 siRNAs in inhibiting root-knot nematode infection in transgenic grape hairy roots. PLoS ONE 8:e69463. https://doi.org/10.1371/journal.pone.0069463

Suppl. File S1. Amino acid sequence analysis for polyclonal antibody production against Minc03328 effector protein.

a Amino acid sequence alignment between Minc03328 (target gene used in this study) protein, its orthologous gene, and peptide sequence used for polyclonal antibody production.

```
Minc3s00083g03984       PIKQSSSNSGISLTVSGPKQPVLRASAKHDHQDLFSNDENNDDDLLDELQYYIKKLHEKE
Minc03328               PVKQNSSKSGISLTVSDPKQPVLRASAKHDNQDLFSNDENNDDDILDELQYYIKKYEEKE
Antibody peptide        ----------------------------KHDNQDLFSNDENN------------------
                                                    ***:**********
```

b BLASTP analysis (WormBase) against *Meloidogyne incognita* PRJEB8714 dataset (Blanc-Mathieu *et al*. 2017), allowing found only 2 hits: *Minc3s00020g01299* (Minc03328 target gene used in this study) and *Minc3s00083g03984* (orthologous gene of the *Minc03328*).

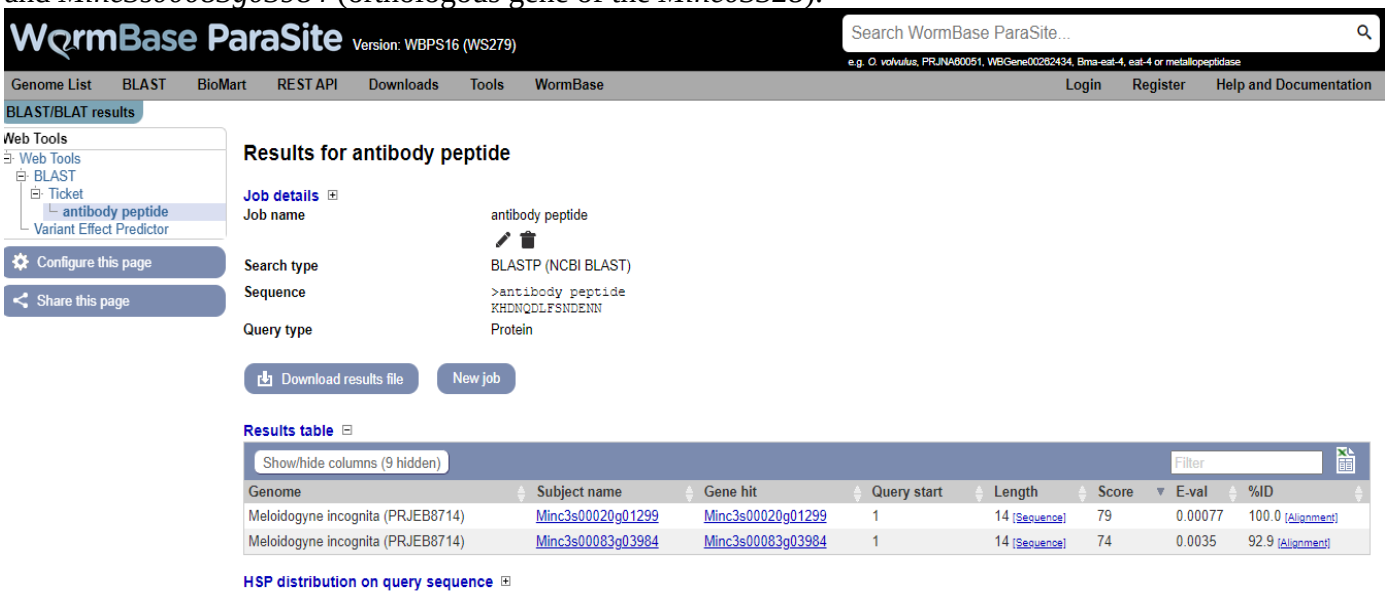

c BLASTP analysis (NCBI) against the *Meloidogyne incognita* taxid:6306 dataset. Two top hits: *Minc3s00497g13327* (query cover: 92% and percentage identity: 75%) and *Minc3s01544g24587* (query cover: 35% and percentage identity: 100%).

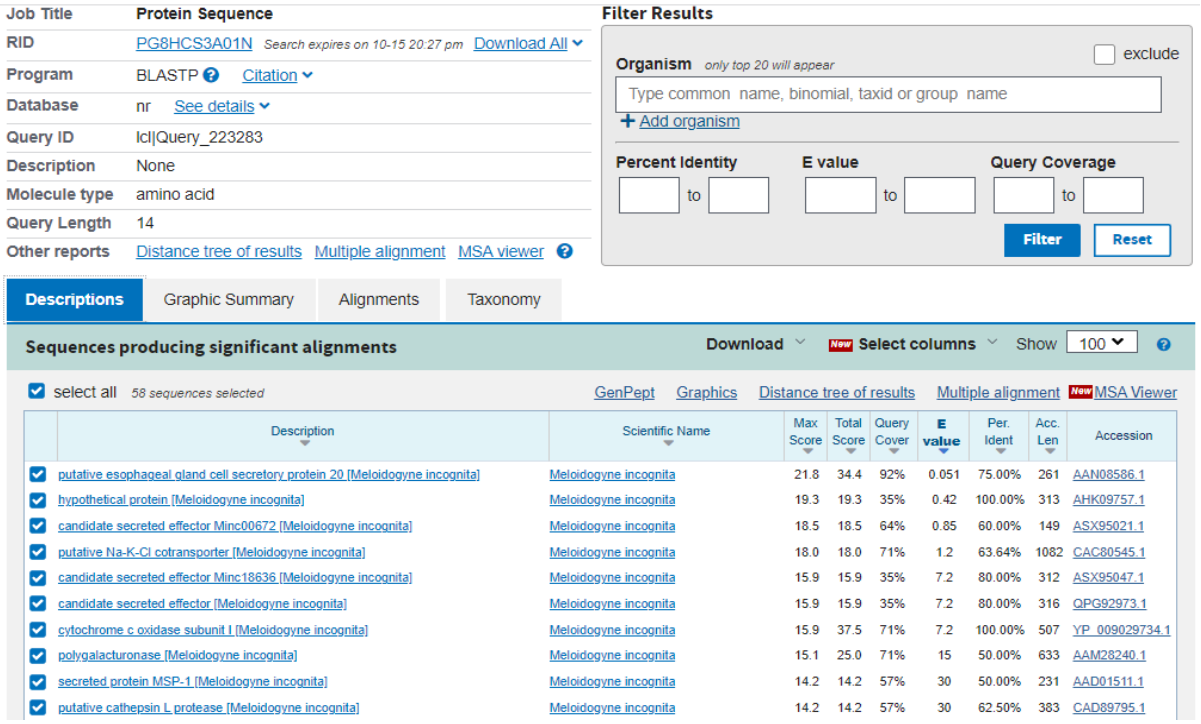

Suppl. File S2. Sequence alignment of nucleotide between Minc03328 and its homologous gene Minc3s00083g03984. Letters with yellow background are highlighted 200-bp RNAi sequence and in green are highlighted primer set used in RT-PCR assays for gene expression.

ANEXOS

Supporting information - Figures S1-S2

IN PLANTA RNAi TARGETING *Meloidogyne incognita* Minc16803 GENE PERTURBS NEMATODE PARASITISM AND REDUCES PLANT SUSCEPTIBILITY

Valdeir Junio Vaz Moreira[1,2,5§], Daniele Heloísa Pinheiro[1,7§], Isabela Tristan Lourenço-Tessutti[1,7], Marcos F Basso[1,7], Maria E Lisei-de-Sa[1,3,7], Carolina V Morgante[1,4,7], Maria C M Silva[1,7], Etienne G J Danchin[6,7], Patrícia M Guimarães[1,7], Priscila Grynberg[1,7], Ana C M Brasileiro[1,7], Leonardo L P Macedo[1,7], Janice de Almeida Engler[6,7], Maria Fatima Grossi-de-Sa[1,7,8 *]. *In planta* RNAi targeting *Meloidogyne incognita* Minc16803 gene perturbs nematode parasitism and reduces plant susceptibility. Journal of Pest Science. (2023). doi.org/10.1007/s10340-023-01623-7

[1]Embrapa Genetic Resources and Biotechnology, Brasilia, DF 70770-917, Brazil

[2]Biotechnology Center, PPGBCM, UFRGS, Porto Alegre, RS 90040-060, Brazil

[3]Federal University of Brasilia, UNB, Brasilia, DF 70910-900, Brazil

[4]National Institute of Science and Technology, INCT PlantStress Biotech, Embrapa 70297-400, Brazil

[5]Agriculture Research Company of Minas Gerais State, Uberaba, MG 31170-495, Brazil

[6]Embrapa Semiarid, Petrolina, PE 56302-970, Brazil

[7]Federal University of Viçosa, Viçosa, MG 36570-900, Brazil

[8]INRAE, Université Côte d'Azur, CNRS, ISA, 06903 Sophia Antipolis, France 9 Catholic University of Brasilia, Brasilia, DF 71966-700, Brazil

§ These authors contributed equally to this work.

[*]**Corresponding Authors** Maria Fatima Grossi-de-Sa: fatima.grossi@embrapa.br

Pages 194 to 201

SUPPLEMENTAL FIGURES AND LEGENDS

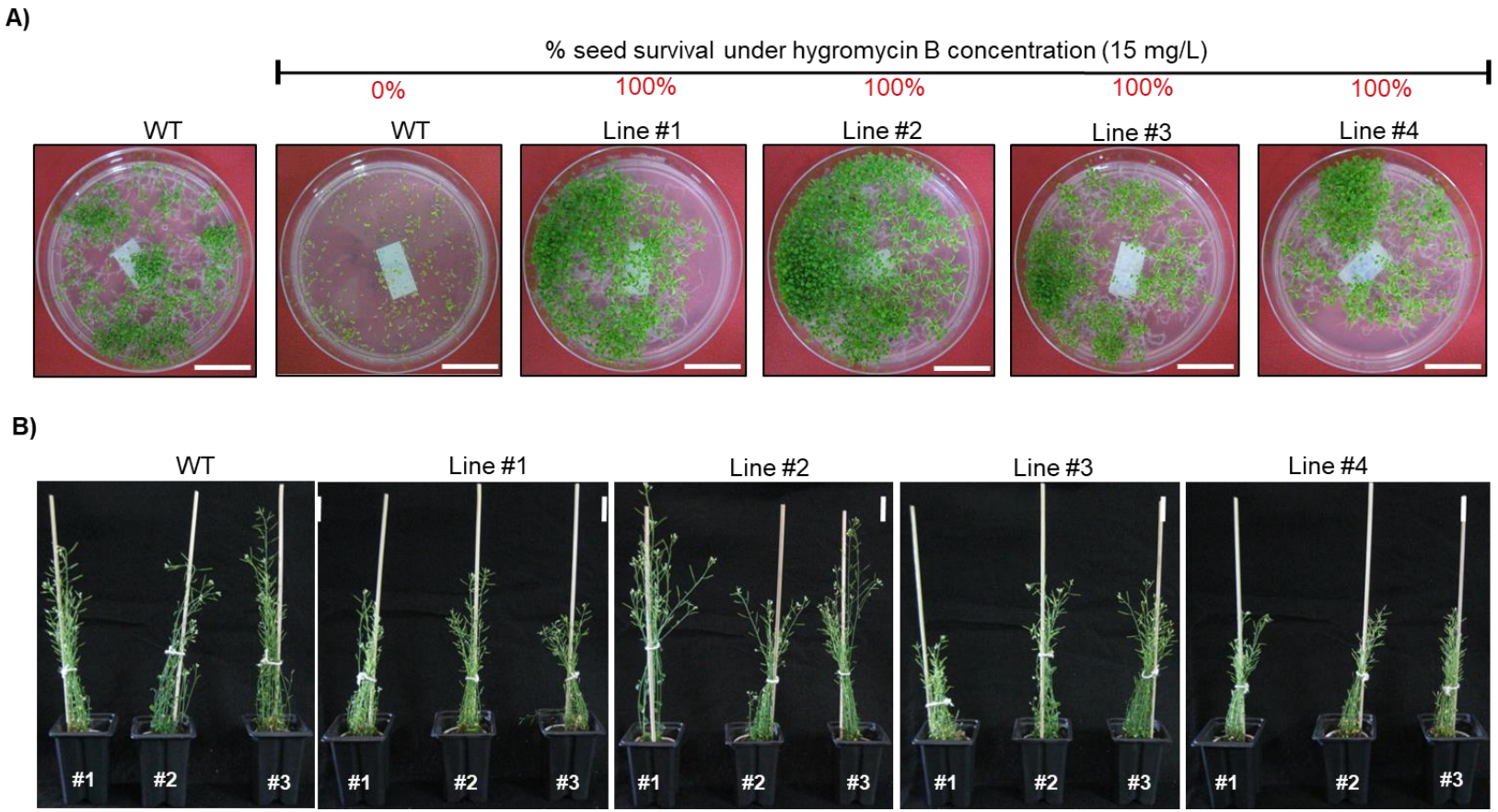

Supplemental Fig. S1. Phenotype of the transgenic *A. thaliana* lines and wild-type control plants during screening in Petri plates containing MS-agar and 15 mg/L hygromycin, and after plant acclimatization and cultivation under growth room. **(A)** *A. thaliana* T_3 transgenic lines selected *in vitro* under half-strength (0.5X) MS medium containing 15 mg/L hygromycin B. (**B)** Transgenic *A. thaliana* lines in the T_3 generation. Scale bars: 1 cm.

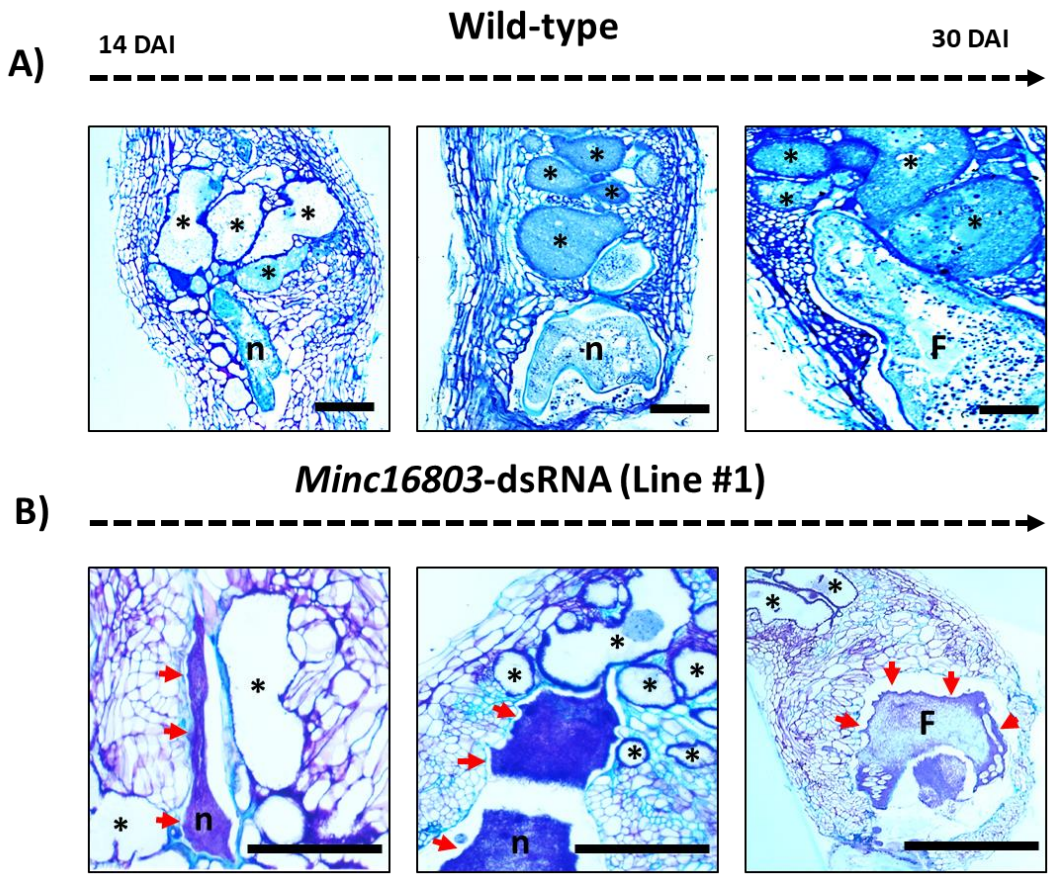

Supplemental Fig. S2: Histological analysis of toluidine stained galls of wild-type and *Minc16803*-dsRNA (Line #1) plants. (A) Gall sections in wild-type lines showed typical morphology of sectioned root-knot nematodes during parasitism throughout gall development. (B) Gall morphology in the *Minc16803*-dsRNA (Line #1) illustrates nematodes with aberrant morphology (red arrows) and often strongly blue stained compared to nematodes in wild-type sections. *Minc16803* silencing not only perturbs feeding sites development but also leaded to dark blue stained and abnormal nematode morphology compared to the wild-type. Asterisk, giant cell; n, nematode; F, adult female. Scale bars = 50 µm

Supplemental Table S1. Primer sequences used in this study.

Primer	Gene ID	Sequence (5`-3`)	Purpose	Reference
GFP-F	Transgene	GACGTAAACGGCCACAAGTT	PCR	Moreira et al. (2022)
GFP-R		GATGCCGTTCTTCTGCTTGT		
Minc16803-F	*Minc3s00746g16803*	CAGTCAACTTATTAAGCAACACATTG	RT-qPCR	This study
Minc16803-R		TCTTAACTGAAGAGCATTGCCA		
MiActin-F		TGGTTATTCTTTCACCGCAAC	RT-qPCR	Lourenço-Tessutti et al. (2015)
MiActin-R		AAGACGAAGCAGCTGTAGCC		
MiTubulin-F		TGGAAAGTATGTCCCAAGAGC	RT-qPCR	Lourenço-Tessutti et al. (2015)
MiTubulin-R		CACCACCAAGCGAGTGAGT		
Mi18S-F	*Minc3s02085g28182*	ACCGTGGCCAGACAAACTAC	RT-qPCR	Júnior et al. (2013)
Mi18S-R		GATCGCTAGTTGGCATCGTT		
MiGAPDH-F	*Minc3s07075g40689*	GCTTCCTGCACTACTAATTGTCTTG	RT-qPCR	Lourenço-Tessutti et al. (2015)
MiGAPDH-R		CAGTAACAGCGTGTACAGTAGTCAT		
Pdk intron-F	Transgene	TGCTAATATAACAAAGCGCAAGA	RT-qPCR	Moreira et al. (2022)
Pdk intron-R		ACCTTGTTTATTCATGTTCGACT		
AtActin 2-F	*AT3G18780*	CTTGCACCAAGCAGCATGAA	RT-qPCR	Che et al. (2010)
AtActin 2-R		CCGATCCAGACACTGTACTTCCTT		
AtGAPDH-F	*AT1G13440*	TTGGTGACAACAGGTCAAGCA	RT-qPCR	Ogneva et al. (2021)
AtGAPDH-R		AAACTTGTCGCTCAATGCAATC		
AtEF1-F	*AT5G60390*	TGAGCACGCTCTTGCTTTCA	RT-qPCR	Moreira et al. (2022)
AtEF1-R		GGTGGTGGCATCCATCTTGTTACA		

Supplemental Table S2. Identification of MERCI motifs in the putatite effectors of *M. incognita.*

Candidate	MERCI motifs found at N-terminal	Motifs	Properties of MERCI motif at N-terminal portion of the proteins
Minc16803	Not found	M1	neutral buried neutral large buried neutral neutral neutral hydrophobic hydrophobic neutral acyclic acyclic acyclic buried
	start position(s): 7 FLCFIFLIVSVFLAG start position(s): 11 IFLIVSVFLAGGQEE	M2	large hydrophobic neutral buried neutral neutral buried buried neutral acyclic acyclic hydrophobic neutral acyclic acyclic
	start position(s): 10 FIFLIVSVFLAGGQE	M3	hydrophobic neutral buried acyclic neutral neutral neutral buried neutral large neutral acyclic neutral polar acyclic
	start position(s): 6 TFLCFIFLIVSV	M4	neutral neutral L buried hydrophobic buried neutral hydrophobic neutral neutral acyclic neutral
Minc3s00070g03473	Not found	M1	neutral buried neutral large buried neutral neutral neutral hydrophobic hydrophobic neutral acyclic acyclic acyclic buried
	start position(s): 7 FLCFIFLIVSVFLAG start position(s): 11 IFLIVSVFLAGGQEE	M2	large hydrophobic neutral buried neutral neutral buried buried neutral acyclic acyclic hydrophobic neutral acyclic acyclic
	start position(s): 10 FIFLIVSVFLAGGQE	M3	hydrophobic neutral buried acyclic neutral neutral neutral buried neutral large neutral acyclic neutral polar acyclic
	start position(s): 6 TFLCFIFLIVSV	M4	neutral neutral L buried hydrophobic buried neutral hydrophobic neutral neutral acyclic neutral
Minc3s00200g07395	Not found	M1	neutral buried neutral large buried neutral neutral neutral hydrophobic hydrophobic neutral acyclic acyclic acyclic buried
	Not found	M2	large hydrophobic neutral buried neutral neutral buried buried neutral acyclic acyclic hydrophobic neutral acyclic acyclic
	Not found	M3	hydrophobic neutral buried acyclic neutral neutral neutral buried neutral large neutral acyclic neutral polar acyclic
	Not found	M4	neutral neutral L buried hydrophobic buried neutral hydrophobic neutral neutral acyclic neutral

Supplemental File S1. Nucleotide and amino acid sequences of the *Minc16803* gene (*Minc3s00746g16803*) effector and its two paralogue genes (*Minc3s00070g03473* and *Minc3s00200g07395*).

>Minc3s00746g16803

ATGATGAACTCATCAACTTTTCTTTGTTTTATTTTCCTGATTGTTTCCGTATTTTTG
GCTGGTGGACAGGAAGAAGCTAATTCAAACCACGTTTACCGCGAAGAATATGAA
ACTTATGAGACGCTGCAAAGACGCAAAATTCCTCCTCCACAGACTTTTGAGTTTG
CCGAGACAGAATTTAGAAGACCTAGTTATTACTTGTCAGTGCCGTTTCGCTCACA
AAACAGGCTTCAGTGCCAAGTTATTGACTTCCAAAAATTCTCAAAANAATATGAA
ACTTATGAGACGCTGCAAAGACGCAAAATTCCTCCTCCACAGACTTTTGAGTTTG
CCGAGACAGAATTTAGAAGACCTAGTTATTACTTGTCAGTGCCGTTTCGCTCACA
AAACAGGCTTCAGACAATTCCTGAGGATATATTCAGTCAACTTATTAAGCAACAC
ATTGCTCGCAACCGTGCCAAGTTATTGACTTCCAAAAATTCTCAAAATGGCAATG
CTCTTCAGTTAAGACAAACACCGTTCCGTCGATGGTCACCAACTAATGGGAACTA
CAAGGAAAAATTGCGTCAATGGAAGGCAGAGCTTAAAAGTCGGCTTCGAGGTCT
GAAAATTCCAGAGCAAGTGGTTTCTCCGAACAATGGAAGCGATCAGGAAGGGAC
TTTCACAAAGGAGCTACCTTATTATGTGACATACAATCCACAGACTAATATGTAT
CAAATATCAAATCAGCCACCTCTAGTGTATACAGGAATAGCAAGTGAGAAGACG
GCTAAACCTAACCAACAAAATTCGACAATTAGAAAGGAGTCACACAAACCAACA
GTTTCTGACAAATTGAAAGAACCTCCCTTGCTAATTGTACTGCAAAAAGCACTTC
CCCTTGATAAAAGTATTCAAGAAGAACACAAAGCGATATCTCAAAATATTCTTGG
AAAGCAACTGAACATTCCAAATGCAAAACAAATTTTATTTTTGGACGATTATGAA
GAAAGTATGAACGAGGACGATTATAAAGCAAATGATGAAAATTAG ---- 1.032
nucleotides length

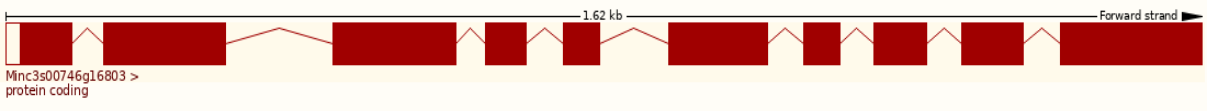

MMNSSTFLCFIFLIVSVFLAGGQEEANSNHVYREEYETYETLQRRKIPPPQTFEFAETE
FRRPSYYLSVPFRSQNRLQCQVIDFQKFSKXYETYETLQRRKIPPPQTFEFAETEFRRPS
YYLSVPFRSQNRLQTIPEDIFSQLIKQHIARNRAKLLTSKNSQNGNALQLRQTPFRRWS
PTNGNYKEKLRQWKAELKSRLRGLKIPEQVVSPNNGSDQEGTFTKELPYYVTYNPQT
NMYQISNQPPLVYTGIASEKTAKPNQQNSTIRKESHKPTVSDKLKEPPLLIVLQKALPL
DKSIQEEHKAISQNILGKQLNIPNAKQILFLDDYEESMNEDDYKANDEN ---- 343 amino acid length

Red letters: secretory signal peptide for protein importation (1 to 22 aa)

>Minc3s00070g03473

ATGATGAACTCATCAACTTTTCTTTGTTTTATTTTCCTGATTGTTTCCGTATTTTTG
GCTGGTGGACAGGAAGAAGCTAATTCAAACCACGTTTACCGCGAAGAATATGAA

ACTTATGAGACGCTGCAAAGACGCAAAATTCCTCCTCCACAGACTTTTGAGTTTG
CCGAGACAGAATTTAGAAGACCTAGTTATTACTTGTCAGTGCCGTTTCGCTCACA
AAACAGGCTTCAGACAATTCCTGAGGATATATTCAGTCAACTTATTAAGCAACAC
ATTGCTCGCAACCGTGCCAAGTTATTGACTTCCAAAAATTCTCAAAATGGCAATG
CTCTTCAGGGTGTAACTGAGTTAAGACAAACACCGTTCCGTCGATGGTCACCAAC
TAATGGGAACTACAAGGAAAAATTGCGTCAATGGAAGGCAGAGCTTAAAAGTCG
GCTTCGAGGTCTGAAAATTCCAGAGCAAGTGGTTTCTCCGAACAATGGAAGCGAT
CAGGAAGGGACTTTCACAAAGGAGCTACCTTATTATGTGACATACAATCCACAGA
CTAATATGTATCAAATATCAAATCAGCCACCTCTAGTGTATACAGGAATAGCAAG
TGAGAAGACGGCTAAACCTAACCAACAAAATTCGACAATTAGAAAGGAGTCACA
CAAACCAACAGTTTCTGACAAATTGAAAGAACCTCCCTTGCTAATTGTACTGCAA
AAAGCACTTCCCCTTGATAAAAATACTCAAGATGAACACAAAGCGATATCTCAAA
ATATTCTTGGAAAGCAACTGAACATTCCAAATGCAAAACAAATTTTATTTTTGGA
CGATTATGAAGAAAGTATGAACGAGGACGATTATAAAGCAAATGATGAAAATTA
G ------ 1.099 nucleotides length

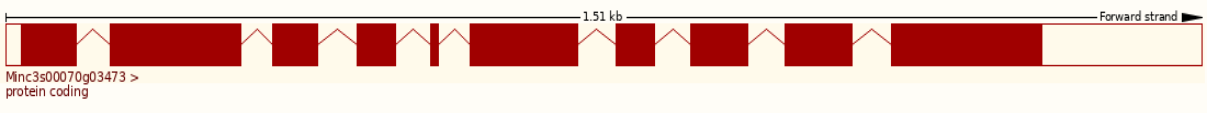

MMNSSTFLCFIFLIVSVFLAGGQEEANSNHVYREEYETYETLQRRKIPPPQTFEFAETE
FRRPSYYLSVPFRSQNRLQTIPEDIFSQLIKQHIARNRAKLLTSKNSQNGNALQGVTEL
RQTPFRRWSPTNGNYKEKLRQWKAELKSRLRGLKIPEQVVSPNNGSDQEGTFTKELP
YYVTYNPQTNMYQISNQPPLVYTGIASEKTAKPNQQNSTIRKESHKPTVSDKLKEPPL
LIVLQKALPLDKNTQDEHKAISQNILGKQLNIPNAKQILFLDDYEESMNEDDYKANDE
N ------ 292 amino acid length

Red letters: secretory signal peptide for protein importation

>Minc3s00200g07395

ATGGTGGTGGATGGAATTGGTAATGGAAAGCGTTTTTCAGCAACTGATCTCAAAA
TGATGAACACTACTACTTTTCTTTGTTTTATTTTCCTGATTATTTCCGTATTTCTGG
CTGGTGGACAGGAAGAAGCCAATTCAAACCACGTTTACCGGGAAGAATATGAAA
CTTATGAGACGCTGCAAAGACACAAAATTCCTCCTCCACAGACTTTCGAATTTGC
CGAGACAGAATTTAGAAGACCTAGTTATTACTTATCAGTGCCGTTTCGCTCACAA
AACAAGCTTCAGACAATTCCTGAGGATATATTCAGCCAACTTATTAAGCAACACA
TTGCTCGCAACCGTATGAAGTTATTGAATTCCAAAAATTCTCAAAATGGCAATGC
TCTTCAGGGTGTAACTGAGTTAAGGCAAACACCGTTCCGTCGATGGTCACCAACT
AATGGGAACTACAAAGAAAAATTGCGTCAATGGAAGGCAGAGCTTAAAAGTCGG
CTTAGAGGTCTGAAAATTCCAGAGCAAGTTTCTCCTCCGAGCAATGGAAGCGATC
ATGAAGGAACTTTCACAAAGGAGCTACCTTATTATGTGACATACAATCCACAGAC
AAATATGTATCAAATATCAAATCAGCCACCTCTAGTATATACAGGAATTGAGAGT

GAGAAGACGGCTAAACCTACTCAACAAAATTCGACTATTAGAAAGGAGTCACAC
AAACCTTCAACAGTTTCTGATAAATTAAAAGAACCTCCCTTGCTGATTGTACTGC
AAAAAGCACTTCCCCTGGATAAAAATACTCAAGAAGAACACAAAGCGATATCTC
AAAATATTCTTGGGAAACAACTGAACATTCCAAATGCAAAACAAATTTTATTTTT
GGACGATTATGAAGAAAGTGTAAACGAAGACGATTATAAAGAAAATGATGAAAA
TTAG ---- 957 nucleotides length

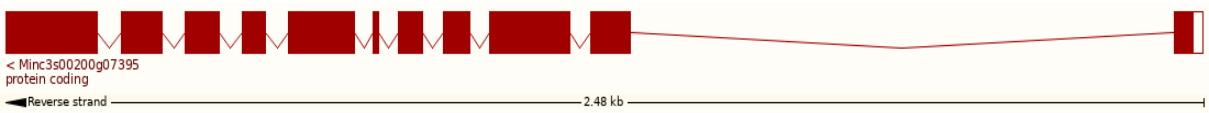

MVVDGIGNGKRFSATDLKMMNTTTFLCFIFLIISVFLAGGQEEANSNHVYREEYETYE
TLQRHKIPPPQTFEFAETEFRRPSYYLSVPFRSQNKLQTIPEDIFSQLIKQHIARNRMKL
LNSKNSQNGNALQGVTELRQTPFRRWSPTNGNYKEKLRQWKAELKSRLRGLKIPEQ
VSPPSNGSDHEGTFTKELPYYVTYNPQTNMYQISNQPPLVYTGIESEKTAKPTQQNSTI
RKESHKPSTVSDKLKEPPLLIVLQKALPLDKNTQEEHKAISQNILGKQLNIPNAKQILF
LDDYEESVNEDDYKENDEN ----- 311 amino acid length

Red letters: secretory signal peptide for protein importation

Supplemental File S2. Sequence aligment of the *Minc16803* (*Minc3s00746g16803*) effector gene and its two paralogue genes (*Minc3s00070g03473* and *Minc3s00200g07395*). In red letters are highlighted the 200 bp DNA region used in the RNAi strategy.

```
Minc3s00200g07395       ATG...CCACAGACTTTCGAATTTGCCGAGACAGAATTTAGAAGACCTAGTTATTACTTA
Minc3s00746g16803       ATG...CCACAGACTTTTGAGTTTGCCGAGACAGAATTTAGAAGACCTAGTTATTACTTG
Minc3s00070g03473       ATG...CCACAGACTTTTGAGTTTGCCGAGACAGAATTTAGAAGACCTAGTTATTACTTG
                        ***...*********** ** ************************************

Minc3s00200g07395       TCAGTGCCGTTTCGCTCACAAAACAAGCTTCAGACAATTCCTGAGGATATATTCAGCCAA
Minc3s00746g16803       TCAGTGCCGTTTCGCTCACAAAACAGGCTTCAGACAATTCCTGAGGATATATTCAGTCAA
Minc3s00070g03473       TCAGTGCCGTTTCGCTCACAAAACAGGCTTCAGACAATTCCTGAGGATATATTCAGTCAA
                        ************************* ****************************** ***

Minc3s00200g07395       CTTATTAAGCAACACATTGCTCGCAACCGTATGAAGTTATTGAATTCCAAAAATTCTCAA
Minc3s00746g16803       CTTATTAAGCAACACATTGCTCGCAACCGTGCCAAGTTATTGACTTCCAAAAATTCTCAA
Minc3s00070g03473       CTTATTAAGCAACACATTGCTCGCAACCGTGCCAAGTTATTGACTTCCAAAAATTCTCAA
                        ****************************   ********** ****************

Minc3s00200g07395       AATGGCAATGCTCTTCAGGGTGTAACTGAGTTAAGGCAAACACCGTTCCGTCGATGGTCA
Minc3s00746g16803       AATGGCAATGCTCTTC-----------AGTTAAGACAAACACCGTTCCGTCGATGGTCA
Minc3s00070g03473       AATGGCAATGCTCTTCAGGGTGTAACTGAGTTAAGACAAACACCGTTCCGTCGATGGTCA
                        ****************           ******* ************************

Minc3s00200g07395       CCAACTAATGGGAACTACAAAGAAAAATTGCGTCAATGGAAGGCAGAGCTTAAAAGTCGG
Minc3s00746g16803       CCAACTAATGGGAACTACAAGGAAAAATTGCGTCAATGGAAGGCAGAGCTTAAAAGTCGG
Minc3s00070g03473       CCAACTAATGGGAACTACAAGGAAAAATTGCGTCAATGGAAGGCAGAGCTTAAAAGTCGG
                        ******************** ****************************************

Minc3s00200g07395       CTTAGAGGTCTGAAAATTCCAGAGCAAGTTTCTCCTCCGAGCAATGGAAGCGATCATGAA
Minc3s00746g16803       CTTCGAGGTCTGAAAATTCCAGAGCAAGTGGTTTCTCCGAACAATGGAAGCGATCAGGAA
Minc3s00070g03473       CTTCGAGGTCTGAAAATTCCAGAGCAAGTGGTTTCTCCGAACAATGGAAGCGATCAGGAA
                        *** ************************   * ****** *************** ***

Minc3s00200g07395       GGAACTTTCACAAAGGAGCTACCTTATTATGTGACATACAATCCACAGACAAATATGTAT
Minc3s00746g16803       GGGACTTTCACAAAGGAGCTACCTTATTATGTGACATACAATCCACAGACTAATATGTAT
Minc3s00070g03473       GGGACTTTCACAAAGGAGCTACCTTATTATGTGACATACAATCCACAGACTAATATGTAT
                        ** ********************************************** *********

Minc3s00200g07395       CAAATATCAAATCAGCCACCTCTAGTATATACAGGAATTGAGAGTGAGAAGACGGCTAAA
Minc3s00746g16803       CAAATATCAAATCAGCCACCTCTAGTGTATACAGGAATAGCAAGTGAGAAGACGGCTAAA
Minc3s00070g03473       CAAATATCAAATCAGCCACCTCTAGTGTATACAGGAATAGCAAGTGAGAAGACGGCTAAA
                        ************************** *********** *  ******************

Minc3s00200g07395       CCTACTCAACAAAATTCGACTATTAGAAAGGAGTCACACAAACCTTCAACAGTTTCTGAT
Minc3s00746g16803       CCTAACCAACAAAATTCGACAATTAGAAAGGAGTCACACAAAC---CAACAGTTTCTGAC
Minc3s00070g03473       CCTAACCAACAAAATTCGACAATTAGAAAGGAGTCACACAAAC---CAACAGTTTCTGAC
                        ****  ************** ********************   *************

Minc3s00200g07395       AAATTAAAAGAACCTCCCTTGCTGATTGTACTGCAAAAAGCACTTCCCCTGGATAAAAAT
Minc3s00746g16803       AAATTGAAAGAACCTCCCTTGCTAATTGTACTGCAAAAAGCACTTCCCCTTGATAAAAGT
Minc3s00070g03473       AAATTGAAAGAACCTCCCTTGCTAATTGTACTGCAAAAAGCACTTCCCCTTGATAAAAAT
                        ***** ***************** ************************** ******* *

Minc3s00200g07395       ACTCAAGAAGAACACAAAGCGATATCTCAAAATATTCTTGGGAAACAACTGAAC...TAG
Minc3s00746g16803       ATTCAAGAAGAACACAAAGCGATATCTCAAAATATTCTTGGAAAGCAACTGAAC...TAG
Minc3s00070g03473       ACTCAAGATGAACACAAAGCGATATCTCAAAATATTCTTGGAAAGCAACTGAAC...TAG
                        * ****** ********************************** ** *********...***
```